THE EFFECTS OF CALCINEURIN INHIBITORS ON EPITHELIAL ELECTROLYTE TRANSPORT

BY

BARBARA ANN JENSEN

Thesis submitted for the degree of Doctor of Philosophy in the Division of Medicine

University College London
Centre for Nephrology
Royal Free Campus
Rowland Hill Street
London
NW3 2PF

2018

Declaration

I, Barbara Ann Jensen, confirm that the work presented in this thesis is my own. Where information has been derived from other sources, I confirm that this has been indicated in the thesis.

Abstract

Calcineurin inhibitor (CNI)-induced hypertension is common after renal transplantation, rendering patients susceptible to cardiovascular and kidney disease, graft failure and death. CNI-induced hypertension occurs as a result of enhanced sodium retention by activation, via phosphorylation, of the renal thiazide-sensitive NaCl cotransporter, NCC (SLC12A3). CNI-treated renal transplant patients also have increased NCC abundance in isolated urinary exosomes.

The studies described in this thesis were designed to investigate the effects of CNI treatment on mouse renal and intestinal sodium transport proteins, to determine whether alterations in proteins other than NCC may also contribute towards sodium retention. These changes were compared with those in an established mouse model of metabolic syndrome, comprising hypertension, insulin resistance, obesity and hypercholesterolemia which are also associated with CNI use. The abundance of NCC and phospho-NCC was also investigated in urinary exosomes from patients taking CNIs or with Gitelman syndrome.

There was a higher abundance of NCC and pNCC in urinary exosomes from CNI-treated renal transplant patients compared with patients with Gitelman syndrome. Both CNI-treated and metabolic syndrome rodent models displayed a significant increase in pNCC. No differences were observed for intestinal transport proteins with CNI-treatment, however, a lower abundance of PiT1 and SGLT1 in the small intestine was observed with high-fat feeding. Renal NHE3 and ENaC were down-regulated in CNI-treated mice, a response that could be compensatory to the upregulation of pNCC in the DCT.

These data provide evidence that CNIs influence a number of renal sodium transport proteins that may contribute towards the development of

hypertension following transplantation. These studies suggest an important role for calcineurin in the regulation of blood pressure and sodium transport in the kidney, and its possible involvement in the pathogenesis of hypertension and electrolyte disorders.

Acknowledgements

Firstly, I would like to express my gratitude to my supervisors, Doctor Stephen Walsh, Doctor Joanne Marks and Professor Robert Unwin for their support throughout my PhD. I am eternally grateful for all the invaluable guidance and knowledge you have provided me which has allowed me to mature as a scientist.

I would also like to thank my fellow lab colleagues and everyone at the Centre for Nephrology for providing a motivating and friendly environment.

Special thanks to Professor Joy Townsend, Mr John and Jean Woodcock, Mr Barry Sweetbaum and my close friend, Miss Chenchen Song, for their continuous support and encouragement throughout my entire educational life and for being there for me when I needed advice and direction.

Lastly and most importantly, a huge thanks to my parents, Ms Cristina Castro and Mr Edward Jensen, and my sisters, Miss Jessica and Mariah Jensen. You've all been my biggest supporters from the very start and have always pushed me to go further in my career and I would not be where I am right now if it weren't for all of you so thank you and I love you all.

Table of Contents

List of Figures

Chapter IV

Chapter V

Chapter VI

List of Tables

Appendix I

Abbreviations

1,25 $(OH)_2D_3$	1,25 dihydroxyvitamin D_3
ALIX	Apoptosis-linked gene-2-interacting protein X
AMPK	AMP-activated protein kinase
ATP	Adenosine triphosphate
BBM(V)	Brush border membrane (vesicle)
BLM	Basolateral membrane
BMI	Body mass index
CD	Collecting duct
cDNA	Complementary deoxyribonucleic acid
CNI	Calcineurin inhibitor
CsA	Cyclosporine A
CUL3	Cullin-3
CVD	Cardiovascular disease
DBP	Diastolic blood pressure
DCT	Distal convoluted tubule
DSI	Distal small intestine
DTT	Dithiothreitol
ENaC	Epithelial Sodium channel
FGF23	Fibroblast growth factor-23
FK506	Tacrolimus
FKBP12	FK506 binding protein-12
GFR	Glomerular filtration rate
GLUT	Facilitative glucose transporter
GS	Gitelman syndrome
HDLs	High-density lipoproteins
HS	High salt
HF	High fat
KLHL3	Kelch-like-3
LDLs	Low-density lipoproteins
LI	Large intestines

MAP	Mean arterial pressure
mRNA	Messenger ribonucleic acid
NaPi	Sodium phosphate cotransporter
(p)NCC	(Phospho) Sodium chloride cotransporter
NFAT	Nuclear factor of activated T cells
NHE3	Sodium hydrogen exchanger-3
NKCC	Sodium potassium chloride cotransporter
OSR1	Oxidative stress-responsive kinase-1
P(C)T	Proximal (convoluted) tubule
PHAII	Pseudohypoaldosteronism Type II
PNST	Post-nuclear supernatant
PSI	Proximal small intestine
PTDM	Post-transplant Diabetes Mellitus
PTH	Parathyroid hormone
RAAS	Renin-angiotensin-aldosterone system
RT-PCR	Reverse transcription polymerase chain reaction
SBP	Systolic blood pressure
SEM	Standard error of the mean
SGK1	Serum/glucocorticoid-regulated kinase-1
SGLT	Sodium-dependent glucose transporter
SLC	Solute carrier
SNS	Sympathetic nervous system
SPAK	STE20/SPS1-related proline/alanine-rich kinase
TAL	Thick ascending limb
TGF	Tubuloglomerular feedback
THP	Tamm-Horsfall protein
TSG101	Tumour susceptibility gene-101
WNK	With-no-lysine [K]

Chapter I
Introduction

1.1 Hypertension

Hypertension, or high blood pressure, continues to remain an important public health challenge and one of the world's leading risk factors for cardiovascular and chronic renal diseases. Hypertension is defined as blood pressures higher than normal blood pressure levels; systolic blood pressure (SBP) >120mmHg and diastolic blood pressure (DBP) >80mmHg, or the requirement for anti-hypertensive therapy. These can be further sub-categorised into three hypertensive groups; pre-hypertensive (120 – 139mmHg (SBP), 80 – 89mmHg (DBP)), stage I (140 – 159mmHg (SBP), 90 – 99mmHg (DBP)) or stage II (>160mmHg (SBP), >100mmHg (DBP)) hypertension (Chobanian et al., 2003). The risk for cardiovascular disease (CVD) mortality doubles for each 20mmHg increase in SBP and for each 10mmHg increase in DBP (Lewington et al., 2002). This is particularly critical in adults aged 40 – 69 years.

Many observational studies, including those dating back as far as the 1970's, have explored the direct relationship between increased blood pressure and the risks for cardiovascular and renal disease progression (Franklin et al., 1997; Kannel et al., 1971; Klag et al., 1996; Lakka et al., 1999; Stokes et al., 1989). One such study from the Framingham Heart Study has greatly contributed to our knowledge of hypertension and its association to CVD outcomes. With over half a century of work, their studies have shown associations with CVD through elevated SBP and pulse pressure, and hemodynamic changes, i.e., increased artery stiffness, with age (Franklin et al., 1997; Kannel et al., 1971). In relation to renal disease progression, in 1996, Klag *et al*, conducted a follow-up study over 16 years specifically monitoring the development of end-stage renal disease in 332,544 men, and

found that 814 of these subjects either died of end-stage renal disease or were undergoing treatment (Klag et al., 1996). Vasan *et al*, in 2001, looked at the cardiovascular event rates in 6859 hypertension-free subjects over an 11-year study and found 397 of these subjects had had a cardiovascular event that included death from CVD, myocardial infarction, stroke and congestive heart failure (Vasan et al., 2001).

A systematic report on the global burden of hypertension by Kearney *et al*., showed, in 2000, nearly 1 billion adults (26% of the adult population) had hypertension and that this was predicted to increase to 1.56 billion (60% of the adult population) by the year 2025 (Kearney et al., 2005). Additionally, recent data from the Global Burden of Disease study demonstrated hypertension to be the biggest leading risk factor for global disease and mortality, accounting for 9.4 million deaths each year, particularly for adults aged 50 – 60 years and older than 70 years (Lim et al., 2012).

Numerous worldwide studies have recorded information on hypertension prevalence, awareness, treatment and control, and have shown these rates to fluctuate over the recorded ~20-year period (as summarised in **Table.1.1** and **Appendix.I.Table.A.1**). For example, in the UK, over the past 15 years the prevalence of hypertension has significantly decreased among the population and both hypertension awareness and treatment has continued to rise (**Table.1.1**). However, control rates remain low with >68% of the population with uncontrolled hypertension and ~50% of the patients still not seeking treatment. While some studies have placed a bias on gender and location, i.e. lower prevalence of hypertension observed in women than men and a higher prevalence observed in urban areas than rural areas, other studies lean towards multifactorial factors; an interplay of genetic and environmental influences. Unfortunately, the point still stands that a large number of hypertensive subjects remain undetected, and prevention and control measures for hypertension continue to remain inadequate. Overall, the data collected from these studies underscores the urgent need to re-

emphasise hypertension awareness programs targeting the public in order to prevent a CVD epidemic.

Year of Data Collection	Age Range	Gender	Sample Size	Prevalence (%)	Awareness (%)	Treatment (%)	Control (%)	Reference
1991 - 1992	35 - 64	Male	812	45	30	13	31	(Antikainen et al., 2006)
		Female	797	32	36	17	39	
1995	35 - 64	Male	678	44	34	20	40	(Antikainen et al., 2006)
		Female	727	31	51	28	42	
1998	>16	Male	5222	41.5	40.3	25.7	31.1	(Primatesta et al., 2001)
		Female	6307	33.3	52.2	38	28.2	
2003	>16	Male	4279	33.1	59.7	43.1	47.8	(Primatesta and Poulter, 2006)
		Female	4555	30.1	63.9	52.4	43.9	
2006	20 - 79	Male	3555	32.9	60.6	45.1	23.9	(Joffres et al., 2013)
		Female	3826	27.3	70.7	58.2	31.1	

Table 1.1. Summary of the prevalence, awareness, treatment and control of hypertension in the UK. Hypertension prevalence rates were recorded according to the international definition of hypertension. Control rates show the proportion of control among treated hypertensive patients.

1.2 Renal post-transplant hypertension

Hypertension is very common following transplantation, affecting 80 – 85% of patients. The onset of post-transplant hypertension has been shown to occur between the first few months and the first year post-transplantation and, if left untreated and uncontrolled, its prevalence continues to increase over time (Campistol et al., 2004; Coles et al., 1972; Curtis et al., 1985a; Kasiske, 1987; Kasiske et al., 2004). Most importantly, post-transplant hypertension has been shown to be highly associated with long-term graft survival, CVD development and recipient mortality (Campistol et al., 2004; Fernandez-Fresnedo et al., 2001; Kasiske et al., 2004; Opelz et al., 1998). One of the most well cited studies by Opelz *et al*, in the Collaborative Transplant Study, was the first to analyse the negative outcomes of graft and patient survival in relation to blood pressure and observed a strikingly significant association between poor graft and patient survival and increased levels of systolic and diastolic blood pressure following transplantation (Opelz et al., 1998). Concluding that post-transplant blood pressure is a significant predictor of long-term graft outcome, a later supporting study demonstrated that patients with controlled SBP had significantly improved graft survival (Opelz et al., 2005), thereby highlighting the importance of monitoring and controlling blood pressure after transplantation to confer beneficial graft survival and function.

Extensive observational (both in clinical and laboratory settings) and statistical modelling analyses have identified numerous factors that may contribute to the development and persistence of post-transplant hypertension. These contributing factors include transplant-related factors (delayed graft function), age, gender, race, increased body weight, declining graft function, number of acute rejection episodes and, in particular, pre-transplant and donor-related factors (Campistol et al., 2004; Cosio et al., 1995; Kasiske, 1987).

1.2.1 Pre-transplant factors (pre-existing hypertension or diseased native kidneys)

Patients with poorly controlled high blood pressure before transplantation were shown to require additional and/or higher doses of anti-hypertensive medication after transplantation and displayed significantly poor graft survival (Cosio et al., 1997; Ponticelli et al., 1993). The presence of diseased native kidneys has also shown to have an effect on the function of the transplanted kidney, and that removal of these native kidneys can lower blood pressure, thereby prolonging graft function (Curtis et al., 1985b; Kasiske, 1987).

1.2.2 Donor-related factors (hypertensive donor – genetic influence)

Animal cross-transplantation studies of genetic hypertension have been previously performed to understand the mechanisms attributing to post-transplant hypertension. Previous studies have utilised renal transplant experiments on normotensive rat recipients of hypertensive donors from the Milan hypertensive strain (Bianchi et al., 1974), the Dahl salt-sensitive hypertensive strain (Dahl and Heine, 1975; Dahl et al., 1974) and the stroke-prone spontaneously hypertensive strain (Kopf et al., 1993; Rettig et al., 1990b, 1990a, 1989). Normotensive recipients of a hypertensive kidney developed hypertension while recipients of a normotensive kidney displayed lower blood pressure levels similar to that of the donors, implying that the genetic background of the donor kidney determines the blood pressure of the recipients. This ‘genetic transmission’ has also been observed in follow-up human renal transplant studies, whereby, over an 8-year period, patients with no family history of hypertension that were engrafted with a kidney from a donor with a hypertensive family history showed elevated blood pressure and the requirement for anti-hypertensive therapy (Guidi et al., 1996). In a follow-up study of the same patients, recipients from a normotensive family with a hypertensive kidney showed not only an increase in blood pressure but also

a greater degree of acute rejections (Guidi et al., 1998), supporting that not only can a 'genetically hypertensive' kidney cause hypertension in a normotensive recipient, it can also increase the susceptibility of the recipient to acute and chronic consequences.

It is evident that many factors contribute to post-transplant hypertension in these patients. However, one particularly important and widely known contributing factor is the immunosuppressive therapy received by these patients in the form of calcineurin inhibitors, which will be the main focus of this thesis.

1.3 Calcineurin inhibitors (CNI)

1.3.1 Post-transplant hypertension

Calcineurin inhibitors (CNIs), Cyclosporine A (CsA, or ciclosporin) and Tacrolimus (FK506), are the most widely used CNIs and are routinely administered to post-transplant recipients to prevent organ transplant rejection. The discovery of the immunosuppressive effects of CsA, in the 1970s (Borel, 1976; Borel et al., 1994), provided a major breakthrough in medicine and became the principal immunosuppressive drug for organ transplantation. FK506 was later discovered and approved (Kino et al., 1987a) as the main immunosuppressive drug alternative to CsA owing to its greater inhibitory potency (Kino et al., 1987b) and its association with a higher rate of patient/graft survival and lower rate of allograft rejection (Grimm et al., 2006; Krämer et al., 2005; Webster et al., 2005). This was demonstrated in a number of studies, whereby the incidence of acute rejection in FK506-treated patients were between 17.1 – 19.6% compared to 35.7 – 37.3% in CsA-treated patients, showing almost a two-fold decrease in rejection rates and prompting this transition (Kim et al., 2004; Krämer et al., 2005; Margreiter, 2002).

However, despite its clear benefits in improving graft survival and preventing organ rejection, CNIs are major risk factors for post-transplant hypertension. CsA, as it was discovered first, has been extensively demonstrated as an inducer of post-transplant hypertension in numerous follow up studies of renal transplant patients. For example, a study by Ponticelli *et al*, followed 212 CsA-treated renal transplant patients for 5 years, and showed the prevalence of hypertension was 81.6% at 1 year and 81.2% at 5 years post-transplantation (Ponticelli et al., 1993). This was similarly observed by Campistol *et al*, who showed more than 80% and 95% of renal transplant patients were hypertensive at 3 and 5 years post-transplantation, respectively (Campistol et al., 2004). In addition to these findings, patients are often diagnosed with elevated serum potassium levels (hyperkalemia) (Adu et al., 1983; Laine and Holmberg, 1995), reduced glomerular filtration rate (GFR) and increased vascular resistance (Kiberd, 1989), the reversal of which is achieved when CNIs are replaced with alternative immunosuppressants (Curtis et al., 1986).

The mechanisms by which CNIs induce hypertension are still not fully elucidated and although the administration of CNIs in these transplant patients is required, the consequential hypertensive side effects will continue to hamper long-term graft and patient survival and increase the rate of mortality. It is therefore essential to understand the molecular pathogenesis of CNI-induced hypertension to enable better control of hypertension following transplantation.

1.3.2 Calcineurin

CNIs act by inhibiting the calcium (Ca^{2+})-dependent calmodulin-activated serine/threonine phosphatase, calcineurin (Clipstone and Crabtree, 1992; Liu et al., 1991, 1992). Calcineurin acts as a major regulator of many biological pathways such as cell proliferation, B-cell function, cardiac development and,

most importantly, T-cell proliferation via interleukin-2 (IL-2) expression (Clipstone and Crabtree, 1992; Heit et al., 2006; Molkentin et al., 1998; Ranger et al., 1998).

Upon activation of the T-cell signalling cascade, intracellular release and binding of calcium to the regulatory B subunit of calcineurin (CnB) and calmodulin activates the phosphatase activity of calcineurin (**Fig.1.1**) (Stemmer and Klee, 1994). This associates with and dephosphorylates the conserved phosphoserines in the amino terminus of the cytoplasmic inactive subunits of the transcription factor, nuclear factor of activated T cells (NFAT) (Beals et al., 1997). This dephosphorylation promotes the translocation of NFAT into the nucleus, where persistent elevations of intracellular calcium concentration and calcineurin activity are required to maintain its nuclear localisation. From here, NFAT binds to DNA promoter regions to activate IL-2 transcription, and the transcription of early cytokine genes, promoting T-cell proliferation (Flanagan et al., 1991; Shaw et al., 1988; Timmerman et al., 1996).

However, in order to prevent organ rejection, CNIs suppress T-cell proliferation (**Fig.1.1**). Its mode of action has been defined by numerous studies. CsA and FK506 exert their inhibitory effects through binding to the immunophilins, cyclophilin and FK506-binding protein-12 (FKBP12), respectively (Handschumacher et al., 1984; Harding et al., 1989; Liu et al., 1991). These complexes then competitively bind to calcineurin, hindering substrate approach to the active site, and thereby disrupting calcineurin-mediated NFAT dephosphorylation. This permits its re-phosphorylation and reappearance in the cytoplasm and prevents IL-2 transcription/T-cell proliferation (Emmel et al., 1989; Flanagan et al., 1991; Griffith et al., 1995; Kissinger et al.; Loh et al., 1996; Shaw et al., 1995).

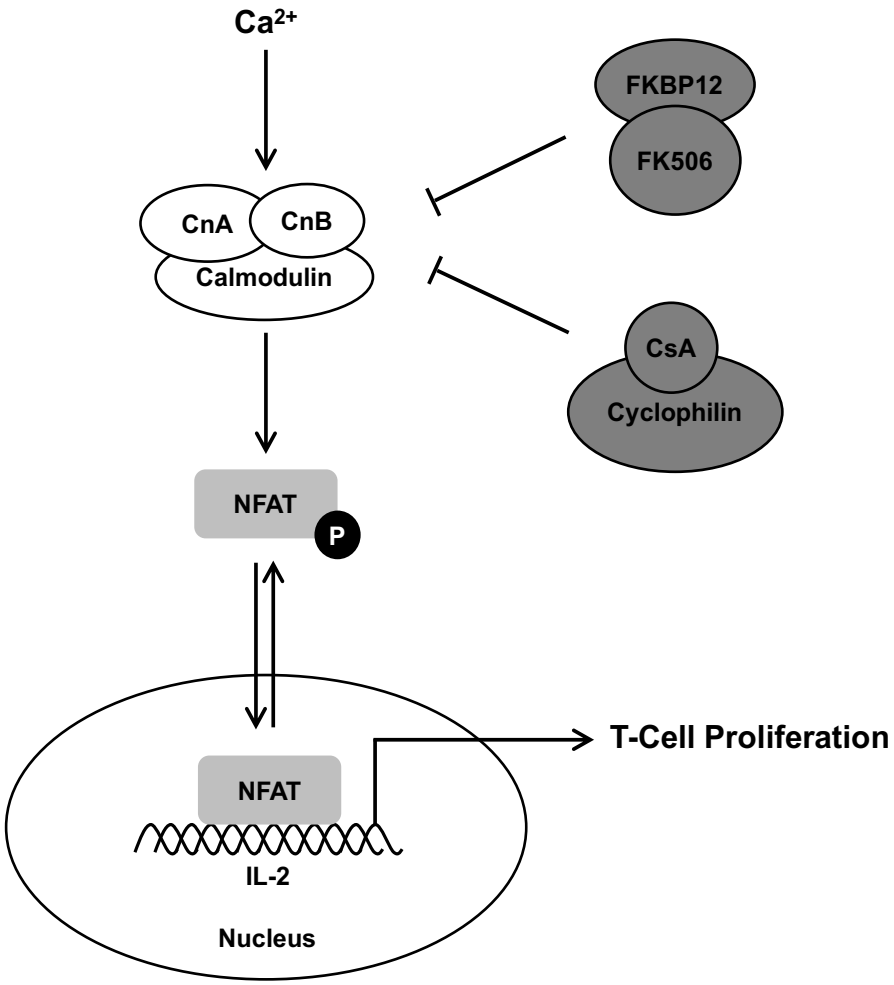

Figure 1.1. A schematic diagram of the calcineurin/NFAT-mediated pathway for T-cell activation. Calcineurin becomes activated in response to an increase in intracellular Ca^{2+}, dephosphorylates NFAT proteins which then facilitates its translocation into the nucleus. Here, the NFAT proteins bind to the regulatory sequences for target genes, such as IL-2, and activates gene expression. With the addition of CNIs, CsA and FK506, in complex with cyclophilin and FKBP12, respectively, bind to calcineurin which inhibits NFAT dephosphorylation, nuclear translocation and T-cell proliferation.

There are three proposed mechanisms contributing to CNI-induced hypertension; 1) increased renal sodium retention (which is the main focus of this thesis), 2) increased vasoconstriction and, 3) activation of the sympathetic nervous system. The next sub-sections aim to provide an overview into some of the sodium-dependent transporters present in the kidneys and gastrointestinal tract that were focused on in this research project.

1.4 CNI-induced hypertension: Sodium retention

1.4.1 Renal sodium transport

The kidneys are crucial organs in the regulation of sodium (Na^+) homeostasis and blood pressure. Mutations in renal Na^+-related transport have been associated with both hypertension and hypotension. The capability to regulate Na^+ excretion and reabsorption is accomplished through controlled expression of cotransporters, exchangers and ion channels within each segment of the nephron. This tightly controlled movement of ions across the cell into or out of the blood thereby allows the kidneys to adapt to dietary salt intake and regulate Na^+ transport (and thus, blood pressure) accordingly.

The proximal segment of the nephron, the proximal convoluted tubule (PCT), is involved in the majority of Na^+ reabsorption processes while the distal segments, the distal convoluted tubule (DCT) and collecting duct (CD), are involved in the fine tuning of Na^+ transport. The reabsorption processes in the proximal segment are regulated by the glomerular filtration rate (GFR) and tubuloglomerular feedback (TGF) mechanisms. Many hormones are also known to act on the tubule and affect electrolyte reabsorption. The GFR is the rate at which blood is filtered through the glomerulus and this is controlled by the TGF mechanism that stimulates compensatory effects on glomerular vascular resistance and reabsorption processes upon changes in filtrate salt content (Schnermann et al., 1970). As part of this feedback, Na^+

content is sensed by the macula densa, a region of specialised cells localised to the lining of the DCT and is in close proximity to the glomerulus (**Fig.1.2a**). These groups of cells monitor tubular sodium chloride (NaCl) concentration and adjust filtration accordingly through the GFR/TGF mechanism. For example, a decrease in GFR results in the decrease of NaCl delivery to the macula densa (as Na^+ reabsorption would have occurred in the PCT) which stimulates, not only the vasodilation of the afferent arteriole at the glomerulus to increase GFR, but also stimulates renin release and activation of the renin-angiotensin-aldosterone (RAA) system that will increase blood volume, blood pressure and GFR.

Electrolyte transport in the nephron can occur either by the paracellular (through the intercellular space between cells) or transcellular (through the cell) routes. Throughout the nephron, transcellular Na^+-coupled transport is the general mechanism for Na^+ reabsorption and movement across the apical membrane occurs down a chemical concentration and/or electrochemical gradient established by the basolateral Na^+-K^+-ATPase pump. The energy provided from this Na^+-K^+-ATPase pump is derived from adenosine triphosphate (ATP) hydrolysis resulting in the electrogenic transport of $3Na^+$ out and $2K^+$ into the cell (Skou, 1957, 1962). This creates a negative charge inside the cell, due to the low concentration of Na^+, providing energy for solute transport. This pump therefore provides the main driving force along the whole nephron to facilitate Na^+ and solute movement across the apical and basolateral membrane (BLM) (**Fig.1.2b-e**). In the following sections, Na^+ reabsorption at each segment of the nephron will be described.

1.4.1.1 Proximal convoluted tubule (PCT)

A majority of reabsorption occurs within the PCT with around 65-75% of ions including sodium (Na^+), potassium (K^+), chloride (Cl^-), phosphate (Pi or PO_4^{3-}

), calcium (Ca^{2+}), and bicarbonate (HCO_3^-), and 100% of organic solutes such as glucose and amino acids, being reabsorbed.

At the brush border membrane (BBM) of the PCT, the sodium-hydrogen antiporter 3, NHE3 (*SLC9A3*), is considered to be the main form of Na^+-coupled transport (Murer et al., 1976). Cloning, sequencing and expression analysis showed NHE3 to be specifically expressed in the kidney and small intestine (Tse et al., 1992). Studies in mice lacking NHE3 function were found to be mildly acidotic due to impaired HCO_3^- reabsorption (Schultheis et al., 1998a), indicating that NHE3, as well as playing a role in Na^+ homeostasis, is a regulator of acid-base balance. NHE3 acts by exporting H^+ in exchange for Na^+ import (**Fig.1.2b**). The exported H^+ can combine with filtered luminal HCO_3^- aided by carbonic anhydrase (CA) to generate carbon dioxide (CO_2) which can freely diffuse into the cell. Within the cell, CO_2 is rehydrated to form carbonic acid, which dissociates, allowing the H^+ to be exported back into the lumen for another cycle. The intracellularly generated HCO_3^- leaves the cell via the Na^+-coupled basolaterally localised NBCe1A (or NBC1, *SLC4A4*) transporter at a 3 HCO_3^-: 1 Na^+ stoichiometry (Boron and Boulpaep, 1983a, 1983b; Romero et al., 1997; Schmitt et al., 1999a; Yoshitomi et al., 1985).

Sodium transport is also coupled to glucose reabsorption by two distinct Na^+-dependent glucose cotransporters; SGLT2 and SGLT1 (*SLC5A2* and *SLC5A1*, respectively) (**Fig.1.2b**) (Hediger et al., 1987; Hummel et al., 2011; Kanai et al., 1994; You et al., 1995). SGLT2 is a low-affinity/high-capacity Na^+-dependent glucose cotransporter predominantly expressed at the BBM in the S1 and S2 segments of the PCT (Kanai et al., 1994; Turner and Moran, 1982; You et al., 1995). Previous genetic and biochemical analysis revealed this transporter as the main regulator of glucose transport, reabsorbing Na^+ and glucose at a 1:1 stoichiometry (Kanai et al., 1994; Turner and Moran, 1982). In addition, SGLT2 was found to work in

conjunction with SGLT1, a high-affinity/low-capacity Na^+-dependent glucose cotransporter expressed in the later S3 segment of the proximal tubule (PT), which transports Na^+ and glucose at a 2:1 stoichiometry (Lee et al., 1994; Turner and Moran, 1982). The concept of the sequential positioning and affinity/capacity properties of SGLT2 and SGLT1 transporters at the early and late segments of the PT, respectively, provides optimal reabsorption to ensure little glucose is lost in the urine. The major role for SGLT2 in glucose reabsorption has been shown in studies whereby mice deficient for SGLT2 displayed significantly lower fractional glucose reabsorption in the early segments of the PCT and limited reabsorption in the downstream segments, which was most likely mediated by SGLT1 (Vallon et al., 2011). Additionally, SGLT2-deficient mice and individuals with SGLT2 mutations, display persistent glycosuria due to the impairment of glucose reabsorption (Calado et al., 2004; Heuvel et al., 2002; Magen et al., 2005; Santer et al., 2003; Vallon et al., 2011). In further studies, SGLT2 and SGLT1 have been proposed to mediate 97% and 3% of glucose transport in the kidney, respectively, however, under SGLT2-deficient or inhibited conditions, renal glucose reabsorption is still maintained at ~36 - 44% (Rieg et al., 2014; Vallon et al., 2011). In studies with SGLT2 inhibitor-treated mice, SGLT1-mediated renal glucose transport was found to increase up to ~40%, suggesting compensation by SGLT1 when SGLT2 is absent (Rieg et al., 2014). This was also supported in comparisons between wild type and SGLT1-deficient mice treated with an SGLT2-inhibitor, which revealed a difference in fractional glucose reabsorption of ~45% (Rieg et al., 2014). Furthermore, a double knockout of SGLT2 and SGLT1 completely eliminated renal glucose reabsorption and displayed a significantly enhanced glycosuric effect, compared to SGLT2 knockout alone (Powell et al., 2013; Rieg et al., 2014). These studies demonstrate that, under euglycemic conditions, SGLT2 contributes to the bulk reabsorption of glucose in the PCT, whereas SGLT1 reabsorbs any residual glucose. In addition, under conditions of SGLT2 loss, compensatory SGLT1-mediated uptake is increased by up to ~40%.

Following Na^+-coupled glucose transport, glucose leaves the cell through the basolateral Na^+-independent GLUT glucose transporters (**Fig.1.2b**) (Chin et al., 1993).

Phosphate (Pi) reabsorption in the kidneys is Na^+-dependent and is also tightly regulated in the PT as it is the major site of extracellular phosphate homeostasis. Phosphate reabsorption is driven primarily by the Na^+-K^+-ATPase pump and regulated by three classes of Na^+/Pi cotransporters; type I, type II and type III, of which, based on ribonuclease protection assays, accounts for 15, 84 and 0.5% of total Na^+/Pi cotransporter mRNAs, respectively, (Tenenhouse et al., 1998). The type II Na^+/Pi cotransporters include two renal isoforms; NaPi-IIa (Npt2a, *SLC34A1*) and NaPi-IIc (Npt2c, *SLC34A3*) (**Fig.1.2b**). NaPi-IIa is thought to be the major regulator of Pi reabsorption. This conclusion was derived from previous cloning, immunohistochemical and expression analyses which revealed apical localisation of NaPi-IIa exclusively throughout the BBM of the PCT, with its highest levels in the early S1 segments (Collins and Ghishan, 1994; Custer et al., 1994; Magagnin et al., 1993). In addition, NaPi-IIa knockout mice display a significant reduction of Pi transport by ~70%, supporting that Pi transport is largely mediated by NaPi-IIa (Beck et al., 1998; Tenenhouse et al., 2003). Pi transport by NaPi-IIa is electrogenic, transporting Na^+ and Pi at a 3:1 stoichiometry (Forster et al., 1999), and its expression is regulated by many factors such as parathyroid hormone (PTH), fibroblast growth factor-23 (FGF23) and dietary phosphate (Kempson et al., 1995; Levi et al., 1994).

Pi cotransport by NaPi-IIc is electroneutral, transporting Na^+ and Pi at a 2:1 stoichiometry (Segawa et al., 2002). Like NaPi-IIa, NaPi-IIc is expressed in the kidney but localised only to the S1 segment of the PCT BBM (Segawa et al., 2002). Its expression was found to be highest in weaning rodents which diminished with age, suggesting NaPi-IIc to be important for Pi reabsorption during growth (Segawa et al., 2002). Furthermore, NaPi-IIc protein levels

were found to be regulated by dietary Pi intake and shown to increase following NaPi-IIa gene ablation which may account for the remaining 30% of Pi transport in the PCT (Ohkido et al., 2003; Segawa et al., 2002; Tenenhouse et al., 2003). Although NaPi-IIc does not appear to be a major regulator of renal Pi reabsorption in adult mice, studies in humans have revealed otherwise. Genetic screening studies in humans have identified mutations in NaPi-IIc in patients with the Pi-wasting disorder, hereditary hypophosphatemic rickets with hypercalcuria (HHRH) (Bergwitz et al., 2006; Lorenz-Depiereux et al., 2006), leading to the proposal that NaPi-IIc may play a more significant role in Pi homeostasis in humans compared to mice.

Less is known about the type I and III Na^+/Pi cotransporter family in regulating Na^+/Pi cotransport except that their contribution is very little compared to the type II family. The type III Na^+/Pi cotransporters, PiT1 (Glvr-1 (Gibbon ape leukemia virus), *SLC20A1*) and PiT-2 (Ram-1 (amphotropic murine retrovirus), *SLC20A2*) were originally identified as ubiquitously expressed cell surface retroviral receptors (Johann et al., 1992; Miller et al., 1994; O'Hara et al., 1990). These proteins were later identified as high-affinity Na^+-dependent phosphate cotransporters (Kavanaugh et al., 1994; Olah et al., 1994), and mRNA expression and supporting immunohistochemical studies primarily localised PiT2 to the apical BBM of the PCT but with a lower abundance compared to NaPi-II cotransporters (Kavanaugh et al., 1994; Tenenhouse et al., 1998; Villa-Bellosta et al., 2009). Previous RNAse hybrid depletion analysis in *Xenopus laevis* oocyte expression models have shown no effect on Pi transport following degradation of NaPi-I and NaPi-III mRNAs whereas degradation of NaPi-IIa mRNA completely inhibited Pi uptake (Miyamoto et al., 1997). Furthermore, in NaPi-IIa-deficient mice, although expression for NaPi-I and NaPi-III cotransporters increased, this was not sufficient enough to compensate for the loss of NaPi-IIa function, confirming a minor contribution for NaPi-I and NaPi-III to overall renal Pi reabsorption and further highlighting NaPi-IIa as

the major regulator (Hoag et al., 1999). Further research is required to elucidate the functional role of the type III Na^+/Pi cotransporters.

1.4.1.2 Thick ascending limb (TAL)

The TAL reabsorbs up to 25% of filtered NaCl and plays a crucial role in the formation of concentrated or dilute urine. This is accomplished by the generation and maintenance of the countercurrent multiplication mechanism which utilises the segment's impermeability to water to reabsorb NaCl. The major NaCl transport pathway is mediated by the electroneutral Na^+-K^+-$2Cl^-$ cotransporter, NKCC2 (or BSC1 (bumetanide-sensitive cotransporter 1), *SLC12A1*) (**Fig.1.2c**) (Greger, 1981b; Greger and Schlatter, 1981a).

NKCC2 is the kidney-specific isoform of this family and is expressed at the apical membrane of the TAL where it facilitates the symport of Na^+, K^+ and Cl^- at a stoichiometry of 1:1:2 (Ecelbarger et al., 1996; Greger and Schlatter, 1981a; Greger et al., 1983; Payne and Forbush, 1994). Immunoelectron microscopy and immunocytochemistry have also shown the localisation of this transporter in the macula densa cells, which proposes a role in TGF (Nielsen et al., 1998; Obermüller et al., 1996). NKCC2 was originally cloned and sequenced from rat and mouse kidney and later in corresponding cDNAs from other species such as human and rabbit (Gamba et al., 1994; Igarashi et al., 1995; Payne and Forbush, 1994; Simon et al., 1996a). Mouse NKCC2 was found to share 93.5% and 97.6 % amino acid identity to the rabbit and rat sequence, respectively (Igarashi et al., 1995). Sequence analysis also revealed NKCC2 to share 60% homology to the secretory NKCC isoform, NKCC1 (or BSC2, *SLC12A2*) (Payne and Forbush, 1994). NKCC1 is mainly involved in the regulation of Cl^- secretion. NKCC1 was identified by screening and cDNA isolation from shark rectal gland and mouse inner medullary collecting duct (mIMCD-3) cell line libraries (Delpire et al., 1994; Xu et al., 1994). Later isolation of the human NKCC1 homologue revealed 91% and

74% homology to mouse and shark NKCC1, respectively (Payne et al., 1995). Unlike NKCC2, NKCC1 is localised to the BLM of secretory epithelial cells and is ubiquitously expressed in a wide variety of tissues, such as the brain, thymus, lung, heart, skeletal muscle, colon and testis (Delpire et al., 1994; Payne et al., 1995; Xu et al., 1994).

As NKCC2 provides the major pathway for the uptake and maintenance of NaCl content in the Loop of Henle, its regulation must be tightly controlled. Several hormones regulate NaCl reabsorption in this segment, the most widely-studied stimulatory hormone is vasopressin. Vasopressin and other stimulatory hormones act by increasing intracellular cyclic adenosine monophosphate (cAMP), which, in turn, enhances NKCC2 activity (Giménez and Forbush, 2003; Hall and Varney, 1980; Hebert et al., 1981a, 1981b, 1981c; Kim et al., 1999; Sasaki and Imai, 1980). The mechanism by which cAMP stimulates NKCC2 activity remains complex, however, most studies suggest the involvement of phosphorylation and trafficking of NKCC2 to the apical membrane. Both NKCC2 and NKCC1 amino acid sequence analyses in rat, mice, rabbit and humans have identified potential phosphorylation sites. Three phosphoacceptor sites located in the N-terminal domain of shark NKCC1, Thr184, Thr189 and Thr202, have been previously identified and further site-directed mutagenesis experiments have demonstrated the Thr189 residue, in particular, to be critical for activity (Darman and Forbush, 2002). This region of the N-terminus containing the three regulatory threonines is highly conserved between NKCC1 and NKCC2 (equivalent to Thr96, Thr101 and Thr114 in the mouse and rat NKCC2 sequence, and Thr100, Thr105 and Thr118 in the human NKCC2 sequence, respectively) suggesting that the phosphoregulatory mechanisms are conserved among the isoforms (Darman and Forbush, 2002).

The generation and use of an antibody that specifically recognises residues Thr212 and Thr217 of the human NKCC1 cotransporter (corresponding shark

NKCC1 Thr184 and Thr189 residues, respectively), in mice following vasopressin infusion showed phosphorylation at equivalent residues Thr96 and Thr101 of mouse NKCC2 and a significant increase in NKCC2 immunostaining at the apical membrane, suggesting stimulated trafficking of NKCC2 to the apical membrane from an intracellular compartment (Flemmer et al., 2002; Giménez and Forbush, 2003). Further mutagenic analysis of the three N-terminal threonines in oocytes expression models, using the rabbit NKCC2 sequence, demonstrated that the corresponding threonines Thr99, Thr104 and Thr114 (Thr96, Thr101 and Thr114 in rat/mouse NKCC2, respectively) are required for NKCC2 activation in response to hypertonic conditions, but none of these residues were found to be individually critical, unlike the Thr189 residue in NKCC1 (Giménez and Forbush, 2005). Additional threonine and serine residues have been found to be phosphorylated under other conditions. For example, intracellular chloride depletion or hypotonic low-chloride stimuli in oocyte expression models promote NKCC2 phosphorylation at human NKCC2 residues Ser91, Thr95, Thr100, Thr105, and Ser130 (Ponce-Coria et al., 2008; Richardson et al., 2011). In addition, site-directed mutagenesis in oocyte expression models at two asparagine sites, Asn442 and Asn452, also showed a significant reduction in NKCC2 activity, suggesting that NKCC2 activity is mediated by glycosylation (Paredes et al., 2006).

The driving force for NKCC2-dependent NaCl reabsorption is provided by the basolateral Na^+-K^+-ATPase pump, the apical K^+ channel and a basolateral Cl^- channel. These enable Cl^- movement across the cell, recycling of K^+ across the apical membrane and the generation of a positive lumen potential to drive paracellular Na^+ transport and complete net transcellular NaCl transport in the TAL. This segment also reabsorbs any residual HCO_3^- via the NHE3 antiporter (Capasso et al., 1991). Potassium concentrations at this segment is regulated by both NKCC2 and the renal outer medullary K^+ channel, ROMK (or Kir1.1, *KCNJ1*) (Bleich et al., 1990; Ho et al., 1993),

which drives the paracellular reabsorption of Na^+, K^+, Mg^{2+} and Ca^{2+}. Chloride is reabsorbed through the basolateral chloride voltage-gated channel Kb, ClCNKB (*CLCNKB*) (Kieferle et al., 1994). This segment is the target of loop diuretics such as bumetanide and furosemide and its importance in ion transport balance has been highlighted in genetic analyses of the renal disease, Bartter syndrome. Bartter syndrome is an autosomal recessive tubular disease characterised by hypokalemia (low serum potassium levels), metabolic alkalosis (increase in serum pH) and hypochloremia (low serum chloride levels) with normal blood pressure and is caused by mutations in either NKCC2 (Simon et al., 1996a), ROMK (Derst et al., 1997; Simon et al., 1996b) or the ClCNKB chloride channel (Simon et al., 1997).

1.4.1.3 Distal convoluted tubule (DCT)

The distal segments of the nephron are important regulators of blood pressure and play a critical role in the fine-tuning of NaCl transport. The DCT reabsorbs around 5–10% of filtered NaCl via the thiazide-sensitive sodium-chloride cotransporter, NCC (TSC, *SLC12A3*), which transports NaCl at a 1:1 stoichiometry (**Fig.1.2d**) (Ellison et al., 1987; Gamba et al., 1993; Plotkin et al., 1996). NCC was the first member of the Na^+-K^+-Cl^- cotransporter family to be identified and characterised at a molecular level. Its corresponding cDNA was originally isolated from epithelial cells in the urinary bladder of the winter founder (Gamba et al., 1993), and using a fragment of this isolated cDNA, its mammalian homologue and the NKCC2 cotransporter was later isolated from a rat renal cortex and outer medulla cDNA library, respectively (Gamba et al., 1994). Northern blot and *in situ* hybridisation analysis of NCC transcripts showed the expression of this cotransporter is restricted to the short-convoluted tubule segments in the cortex of the mammalian kidney, alongside, immunoblotting, immunoelectron microscopy and immunofluorescence experiments confirmed its precise localisation to the

apical membrane and subapical vesicular structures of the DCT cells (Gamba et al., 1994; Loffing et al., 2001; Plotkin et al., 1996). As NCC plays a major role in NaCl reabsorption at this segment, like NKCC2, its regulation must be tightly controlled. This involves a series of complex phosphorylation cascades which, in turn, result in the trafficking of the phosphorylated cotransporter from the cytosol to the apical membrane of the DCT. Mouse models of NCC inactivating mutations have demonstrated diminished expression of the cotransporter at the apical membrane and detainment in the cytosol (Yang et al., 2013). NCC is a target of thiazide diuretics such as chlorothiazide, hydrochlorothiazide and bendroflumethiazide, and is commonly administered to treat hypertension, thereby demonstrating this transporter as an important regulator of blood pressure. Loss-of-function mutations in this transporter cause Gitelman syndrome, an autosomal recessive salt wasting disorder characterised by hypotension, hypokalemia, metabolic alkalosis, hypocalciuria (low urinary calcium excretion) and hypomagnesemia (low serum magnesium level) (Simon et al., 1996c). Furthermore, gain-of-function mutations in the known regulators of NCC, that result in an increase in NCC activity, have been shown to cause Pseudohypoaldosteronism Type II (PHAII) (also known as Gordon syndrome or familial hyperkalemic hypertension (FHHt)), an autosomal dominant disease characterised by hypertension, hyperkalemia and metabolic acidosis (refer to **Section 1.4.3.4**) (Boyden et al., 2012; Louis-Dit-Picard et al., 2012; Wilson et al., 2001).

1.4.1.4 Collecting duct (CD)

This last segment of the nephron reabsorbs 3–5% of filtered NaCl and plays a major role in acid-base regulation. This segment is composed of three cell types (**Fig.1.2e)**; the principal cells (reabsorbs Na^+ and secretes K^+) and the acid-base regulatory α-intercalated (secretes H^+) and β-intercalated

(secretes HCO_3^-) cells. As in the TAL, K^+ concentration is regulated by ROMK in the principal cells. Sodium is reabsorbed through the aldosterone-sensitive epithelial Na^+ channel, ENaC. ENac is composed of three homologous α-, β- and γ-subunits (*SCNN1A*, *SCNN1B* and *SCNN1G*, respectively) and is localised to the apical membrane of the principal cells (Canessa et al., 1994; Schmitt et al., 1999b). Loss-of-function mutations in either subunits of this channel have been shown to mimic the autosomal recessive disease, Pseudohypoaldosteronism Type 1 (PHAI), characterised by salt-wasting, hyperkalemia, metabolic acidosis and unresponsiveness to mineralocorticoid hormones (Chang et al., 1996; Gründer et al., 1997; Pradervand et al., 1999a). Gain-of-function mutations in either the β- or γ-subunits cause the autosomal dominant disease, Liddle syndrome, characterised by salt-sensitive hypertension, hypokalemia and metabolic alkalosis (Firsov et al., 1996; Shimkets et al., 1994; Snyder et al., 1995). These gain-of-function mutations have been previously introduced into mice to generate models of Liddle syndrome (Pradervand et al., 1999b). The activity of this channel has been shown to be salt-sensitive and regulated by aldosterone (Loffing et al., 2000; Pacha et al., 1993). Studies in isolated tubules of rats fed Na^+-depleted (0.0003%) diets, where serum aldosterone levels were high, demonstrated a significantly higher mean number of open channels compared to Na^+-repleted diets (normal chow with saline drinking water), where serum aldosterone levels were low (Pacha et al., 1993). In addition, immunohistochemical analysis in kidneys of mice fed a high (3%) Na^+ diet was unable to detect the α-subunit at the apical membrane, while the β- and γ-subunits were detected in the cytoplasm (Loffing et al., 2000). In contrast, analysis in mice fed a low (0.05%) Na^+ diet showed all three ENaC subunits localised to the apical membrane (Loffing et al., 2000). This suggests the regulation of ENaC, in response to dietary Na^+ intake, is associated with changes in serum aldosterone levels which regulate ENaC abundance via the translocation from the cytoplasm and insertion of all three subunits into the apical membrane.

Also within this segment, lies the Cl^-/HCO_3^- exchanger, pendrin (*SLC26A4*). RT-PCR, immunoblot and immunofluorescence analysis have localised pendrin to the BBM of the β-intercalated cells of the cortical collecting duct (CCD) (Royaux et al., 2001; Soleimani et al., 2001). Expression studies have shown that pendrin plays a critical role in HCO_3^- secretion in the kidney (Royaux et al., 2001; Soleimani et al., 2001). Although pendrin does not transport Na^+ directly, its role has been implicated in controlling net NaCl reabsorption as overexpression of pendrin in mice exhibited increased Cl^- reabsorption and chloride-sensitive hypertension (Jacques et al., 2013). Pendrin has also been previously suggested to a facilitate Na^+ transport by functioning alongside NDCBE (*SLC4A8*), a Na^+-dependent Cl^-/HCO_3^- exchanger that transports Na^+ and HCO_3^- at a stoichiometry of 1:2 (**Fig.1.2e**) (Grichtchenko et al., 2001; Leviel et al., 2010). However, this interaction remains to be confirmed.

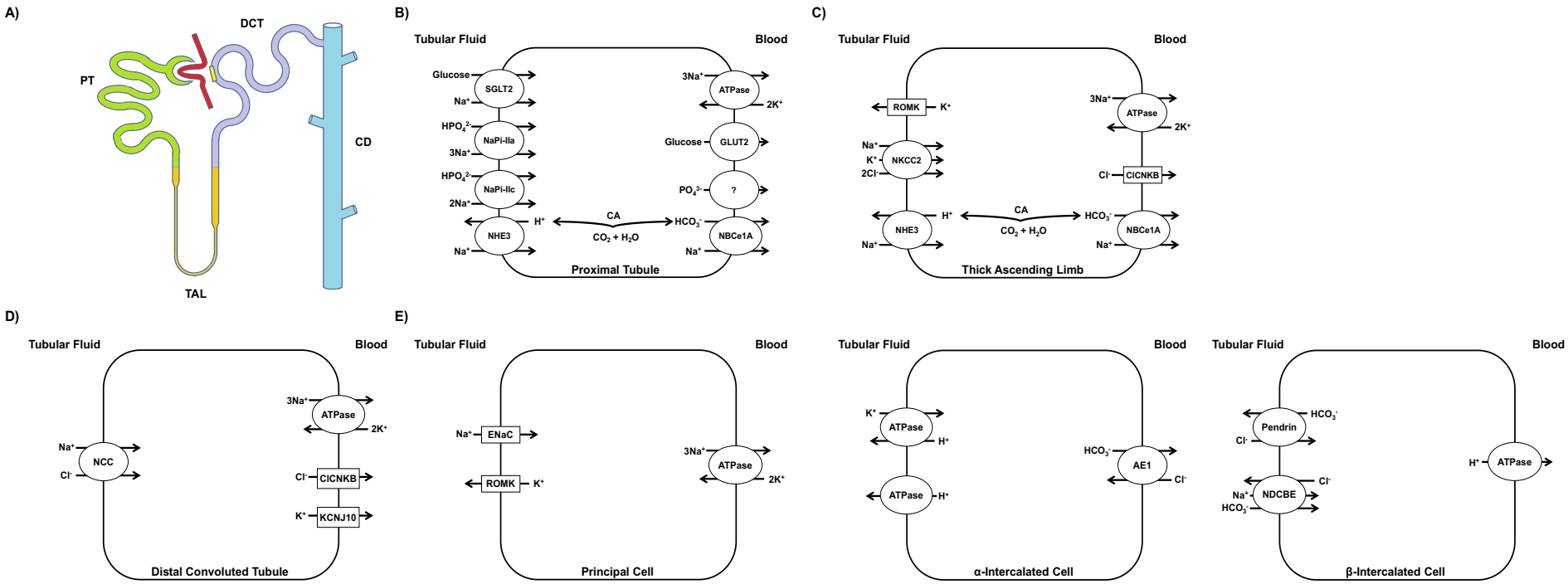

Figure 1.2. Renal sodium reabsorption. A) In the nephron, incoming plasma Na^+ content is sensed by the macula densa cells (yellow), which is in close proximity to the glomerulus and adjusts filtration and reabsorption processes throughout the nephron accordingly, from the PT (green), to the TAL (orange), DCT (purple) and the CD (blue). Sodium reabsorption in the nephron is closely regulated by a number of Na^+-coupled transporters and channels at the **B)** PT, **C)** TAL, **D)** DCT and **E)** CD. The driving force for Na^+ transport is provided by the electrochemical gradient generated by the basolateral Na^+-K^+-ATPase and movement of other electrolytes such as K^+ and Cl^-.

1.4.2 Gastrointestinal sodium transport

The gastrointestinal tract is the site of enzymatic digestion and nutrient and electrolyte absorption. The intestine is divided into three main segments; the proximal small intestine (consisting of the duodenum and jejunum), the distal small intestine (ileum), and the large intestine (colon). Sodium absorption at these segments occurs by diffusion, cotransport with amino acids, glucose, HCO_3^-, Pi and Cl^-, and H^+ exchange across the BBM, which will be described in the following sections.

1.4.2.1 Proximal small intestine (PSI)

The proximal small intestine is where a majority (~80%) of Na^+ absorption occurs, this is due to its large surface area, absorptive capacity and high expression of Na^+-dependent transport proteins, particularly in the jejunum. Like in the kidney, Na^+ absorption is driven by the ionic gradient maintained by the Na^+-K^+-ATPase pump throughout the gastrointestinal tract (**Fig.1.3**).

Sodium transport in this section is coupled to glucose transport via the apical SGLT1 transporter. As mentioned previously, SGLT1 is a high affinity/low-capacity Na^+/glucose cotransporter which transports Na^+ and glucose at a 2:1 stoichiometry. Molecular characterisation and tissue distribution analyses revealed SGLT1 to be predominantly expressed and localised to the BBM of the small intestine and expressed at low concentration in the kidney, in contrast to its kidney-specific isoform, SGLT2 (Lee et al., 1994; Yoshikawa et al., 2011). Sequence analysis showed rat SGLT1 was 86% identical to rabbit and 87% identical to pig and human SGLT1 (Lee et al., 1994), implying the molecular characteristics of SGLT1 are similar across species. Functional characteristics were also previously determined through cloning, sequencing and expression studies of SGLT1 from rabbit small intestinal BBM which

exhibited a significant increase in Na^+-dependent glucose uptake in cRNA-injected oocytes, whilst water-injected controls did not (Hediger et al., 1987; Ikeda et al., 1989). Furthermore, SGLT1-knockout mice display glucose-galactose malabsorption, indicating that SGLT1 predominantly mediates intestinal glucose absorption (Gorboulev et al., 2012). SGLT1 facilitates glucose uptake working alongside its basolateral counterpart, GLUT2, to ensure efficient Na^+/glucose absorption (**Fig.1.3a**). GLUT2 was first isolated and cloned from rat liver (Thorens et al., 1988). Northern blot and immunofluorescence experiments established its expression and localisation to the small intestine, liver, kidney and β-pancreatic islet cells (Thorens et al., 1988). Both SGLT1 and GLUT2 are expressed throughout the small intestine with higher levels at the proximal segment (Yoshikawa et al., 2011). Although GLUT2 has been identified at the BLM of enterocytes, reports have also demonstrated increased GLUT2 protein levels at the BBM in response to increased luminal glucose concentrations (Affleck et al., 2003; Kellett and Helliwell, 2000). These studies thereby proposed a new model for glucose absorption at the small intestine, which involves the rapid translocation and insertion of GLUT2 into the BBM in response to fluctuations in luminal glucose concentrations.

Sodium absorption in the small intestine is also mediated by the NHE3 exchanger (**Fig.1.3a**) (Murer et al., 1976). As mentioned previously, cloning, sequencing and expression experiments showed this exchanger was expressed in the kidney and throughout the gastrointestinal tract, except in the duodenum (Bookstein et al., 1994; Tse et al., 1992). Western blot and immunohistochemical analysis in human and rabbit tissues later supported NHE3 expression and localisation to the BBM of the villus epithelial cells in the jejunum, ileum and colon (Hoogerwerf et al., 1996).

Not much is known about intestinal Pi transport in comparison to renal Pi absorption. Early studies in rats reported that the proximal small intestine

was responsible for the bulk Pi absorption and the later identified type II Na^+/Pi cotransporter, NaPi-IIb (Npt2b, *SLC34A2*), was proposed as the main regulator of intestinal Pi transport (**Fig.1.3a**) (Hilfiker et al., 1998; Walling, 1977). Kinetic and expression studies in oocyte models have revealed NaPi-IIb as a high-affinity, electrogenic transporter, localised to the enterocyte BBM where it mediates the transport of Na^+ and Pi at a stoichiometry of 3:1 (Hilfiker et al., 1998). NaPi-IIb has shown to be upregulated by a number of factors such as 1,25-dihydroxyvitamin D3 ($1,25(OH)_2D_3$), low-dietary phosphate and estrogen (Giral et al., 2009; Hattenhauer et al., 1999; Marks et al., 2006; Radanovic et al., 2005; Walling, 1977; Xu et al., 2003). Its role in Pi absorption has been confirmed in mouse studies whereby NaPi-IIb knockout mice fed on a low Pi diet, followed by an acute Pi load, showed ~50% reduction in overall Pi absorption in comparison to wild type controls, with the remaining 50% of Pi absorption most likely occurring paracellularly (Sabbagh et al., 2009). In this study, NaPi-IIb was shown to account for >90% of total Pi absorption in isolated ileum segments, supporting this transporter as the predominant mediator of intestinal Pi absorption (Sabbagh et al., 2009). However, the exact contribution of NaPi-IIb to intestinal Pi absorption in different species remains controversial as the expression profile throughout the gastrointestinal tract appears to differ. One of the most significant findings was that NaPi-IIb protein was expressed in the ileum of mice (Radanovic et al., 2005; Stauber et al., 2005), a segment of the small intestine that was not originally considered a site of Pi reabsorption. *In vivo* studies utilising the intestinal loop technique in mouse small intestine confirmed the maximal rate of Pi absorption occurs in the ileum (Marks et al., 2006). In contrast, *in vivo* uptake and *in vitro* studies, using BBM vesicles (BBMV), showed maximal Pi absorption and NaPi-IIb mRNA and protein expression at the duodenum and jejunum of rat small intestine, a pattern that was similarly observed in humans (Giral et al., 2009; Marks et al., 2006; Walling, 1977; Walton and Gray, 1979). Therfore, it is clear that Pi absorption differs among species, highlighting the difficulty to draw any conclusions with

regards to its role and significance to overall Pi absorption along the small intestine. However, the current belief is that, in response to low dietary Pi conditions, NaPi-IIb mediates Na^+-dependent Pi transport in the rat jejunum and mouse ileum, but that an unknown Na^+-independent transporter may contribute to overall Pi absorption in the small intestine when luminal Pi concentrations are high.

A role for the type III Na^+/Pi transporters, PiT1, in intestinal Pi transport has also been an area of interest and uncertainty. PiT1 transports Na^+ and $H_2PO_4^-$ at a stoichiometry of 2:1. PiT1 mRNA has shown to be present in both rat and mouse small intestines (Giral et al., 2009; Tenenhouse et al., 1998). Analysis of PiT1 protein confirmed its presence and localisation to the BBM of enterocytes in rat duodenum and jejunum. However, interestingly, PiT1 protein could not be detected in the ileum, despite its high mRNA expression (Giral et al., 2009). Furthermore, PiT1 mRNA and protein levels do not appear to be regulated by dietary phosphate (Giral et al., 2009), thus emphasising how little is known about the precise role of PiT1 in the small intestine. Nevertheless, owing to the absence of residual Na^+-dependent Pi absorption in NaPi-IIb knockout mouse studies (Sabbagh et al., 2009), it is unlikely that PiT1 largely contributes to Pi homeostasis.

The NKCC1 transporter has also been identified in the BLM throughout the small intestine; however, its main role in this organ has shown to lie towards the regulation of Cl^- secretion rather than Na^+ absorption (Grubb et al., 2000; Payne et al., 1995; Xu et al., 1994).

1.4.2.2 Distal small intestine (DSI)

The distal small intestine has a lower absorptive capacity compared to jejunum so only a small proportion of electrolyte absorption occurs

(**Fig.1.3b**). This segment is responsible for the 'fine-tuning' of electrolyte transport and for the absorption of vitamins and bile salts.

Transcripts for the SGLT1 and GLUT2 transporters have been detected in this segment in order to facilitate Na^+/glucose uptake, but at lower levels in comparison to the proximal segment (Lee et al., 1994; Yoshikawa et al., 2011). However, chronic streptozotocin-induced rats demonstrate a significant upregulation in SGLT1 and SGLT1-mediated glucose transport, and an increase in villus length in this segment, indicating an adaptable response under conditions of high glucose load and diabetic conditions (Debnam et al., 1995). NHE3 has also been identified in this segment (Bookstein et al., 1994; Hoogerwerf et al., 1996; Tse et al., 1992).

As previously mentioned, this segment is also suggested to be the main site of Na^+-dependent Pi transport in mice and is largely mediated by the apical NaPi-IIb transporter (Hilfiker et al., 1998; Marks et al., 2006; Radanovic et al., 2005; Sabbagh et al., 2009; Stauber et al., 2005). PiT1 mRNA has also been detected in this segment at high levels, however, its protein expression negligible (Giral et al., 2009) and so is not believed to contribute to Pi absorption.

1.4.2.3 Large intestine (LI)

Most nutrients would have been absorbed before reaching the large intestine and so its role involves absorption of the remaining water and electrolytes and secretion of HCO_3^- before the complete excretion of waste products (**Fig.1.3c**).

The Na^+ channel, ENaC, and the Na^+/H^+ exchanger, NHE3, mediate Na^+ transport in this segment. ENaC has been detected at high levels in the large intestine (Canessa et al., 1994), to facilitate electrogenic Na^+ absorption

along an electrochemical gradient where it then leaves the cell via the Na^+-K^+-ATPase pump. NHE3 has also been identified at high levels in this segment (Bookstein et al., 1994; Tse et al., 1992). It should be noted that, although mice lacking the NHE3 exchanger displayed impaired HCO_3^- reabsorption in the kidney, these mice also exhibited enlarged epithelial thickness in the large intestine and decreased pH of excreted colonic contents, indicative of a severe absorptive defect in the intestine which was most likely compensated for by increasing the surface absorptive area (Schultheis et al., 1998a). In addition, serum aldosterone levels were significantly increased in these mice which, in turn, led to enhanced ENaC activity and altered Na^+ homeostasis, further demonstrating the importance of both NHE3 and ENaC in acid-base and Na^+ balance in the kidney and gastrointestinal tract.

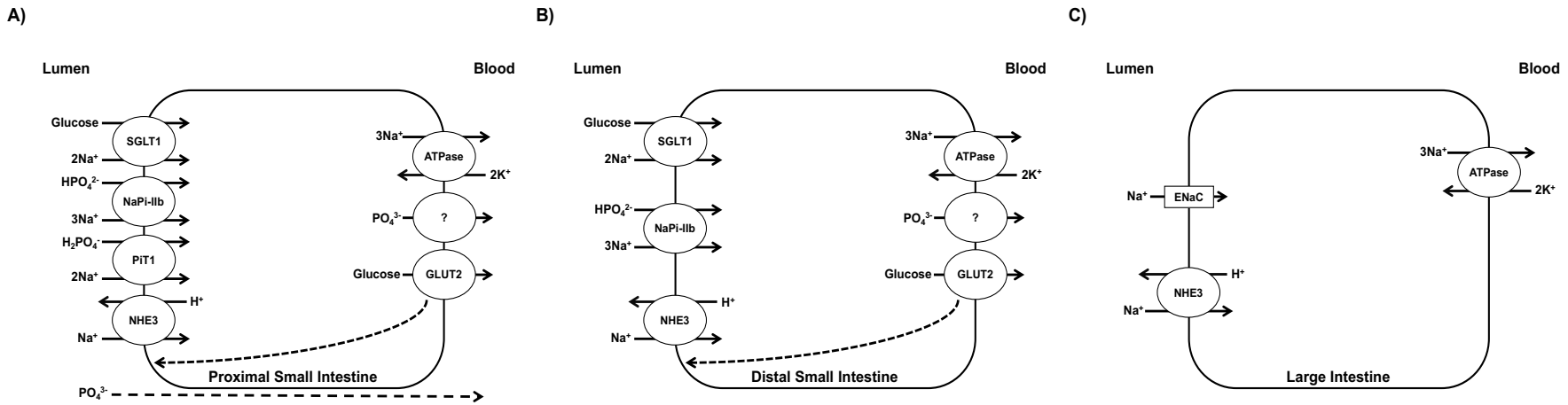

Figure 1.3. Intestinal sodium absorption. Sodium absorption across the BBM and BLM of **A)** PSI, **B)** DSI, and **C)** LI segments is mostly coupled to Pi transport via the NaPi-IIb and PiT1 transporters, glucose transport via the SGLT1 transporter, and H^+ exchange via the NHE3 exchanger. Like the kidney, sodium absorption is driven by the electrochemical gradient provided by the basolateral Na^+-K^+-ATPase pump.

1.4.3 Regulation of the renal sodium chloride cotransporter: NCC

1.4.3.1 Role of NCC in blood pressure regulation

Sodium transport in both the kidney and gastrointestinal tract is tightly regulated by numerous transporters and channels fuelled by electrochemical gradients. Defects in these transporters can have drastic consequential effects on blood pressure and plasma/urine electrolyte levels, and can lead to various renal tubular disorders.

NCC has been particularly identified as an important regulator of blood pressure. As mentioned, NCC is expressed at the apical membrane of the DCT and is the main regulator of NaCl transport in this segment. This protein is the target of thiazide diuretics, which are key agents for hypertension treatment. NCC has been shown to play a crucial role in regulating extracellular fluid and blood pressure as inactivating mutations in this transporter cause the salt-wasting renal disease, Gitelman syndrome (Simon et al., 1996c). NCC-deficient mice display significantly reduced mean arterial blood pressure and an imbalance in electrolyte handling including hypomagnesemia and hypocalciuria (Schultheis et al., 1998b), clinical phenotypes of which resemble Gitelman syndrome. In addition, homozygous NCC mutation at T58M in mice (equivalent to human T60M, a common mutation in patients with Gitelman syndrome), also exhibited the typical characteristics of Gitelman syndrome; hypotension, hyperaldosteronism, hypokalemia, hypomagnesemia and hypocalciuria, as well as a blunted response to thiazide diuretics, all as a consequence of reduced phosphorylation and apical expression of NCC (Yang et al., 2013). The clinical symptoms of Gitelman syndrome are the ‘mirror-image’ of those observed in patients with PHAII. These imply that the regulation of NCC in the kidney is important, not only for the homeostatic regulation of Na^+, Cl^- and K^+, but also in the pathogenesis of PHAII.

1.4.3.2 WNK-SPAK/OSR1-NCC phosphorylation cascade

The cellular mechanisms behind the regulation of NCC activity is of particular interest to this research project and is composed of a complex cascade of serine/threonine kinases and ubiquitin ligases. As depicted in **Fig.1.4a**, NCC function is regulated by sequential inhibitory and stimulatory interactions which in turn results in the trafficking of NCC to the apical membrane where it facilitates NaCl reabsorption. This regulatory pathway has been well established in many *in vitro* and *in vivo* murine and oocyte expression models. This cascade initiates with the activation of the With-No-Lysine [K] kinases, WNK1 and WNK4, which then phosphorylates and activates two closely related STE20-like serine/threonine kinases, SPAK (STE20/SPS1-related proline/alanine-rich kinase) and OSR1 (oxidative stress-responsive kinase-1) (Anselmo et al., 2006; Moriguchi et al., 2005; Richardson et al., 2008; Vitari et al., 2005). Following activation, SPAK and OSR1 kinases then phosphorylate the cytoplasmically inactive NCC cotransporter permitting its translocation to the apical membrane and allowing NaCl reabsorption (Richardson et al., 2008).

1.4.3.2.1 With-No-Lysine kinases

WNK kinases are a subfamily of serine/threonine kinases that act as ‘molecular switches’ and are implicated in the regulation of electrolyte and blood pressure homeostasis. WNK kinases are so-named owing to their unusually unique localisation of the catalytic lysine residue, Lys233, in subdomain I, which is crucial for ATP binding, rather than in subdomain II where it is localised in other serine/threonine kinases (Min et al., 2004; Verissimo and Jordan, 2001; Xu et al., 2000). Subsequent database searches and sequence alignment revealed the existence of 4 homologous WNK kinases (WNK1 – 4) in mammals, all of which lacked this conserved lysine residue (Verissimo and Jordan, 2001).

WNK1 was the first identified member of the WNK family cloned and characterised from a rat brain cDNA library in search for novel members of the mitogen-activated protein kinase family (Xu et al., 2000). Sequence analysis found this kinase to be 85% identical to human WNK1 thereby allowing the regulatory effects of WNK1 to be mapped to humans (Verissimo and Jordan, 2001). All four WNK kinases exhibit a similar domain structure consisting of a small N-terminal domain followed by a highly conserved kinase domain, an autoinhibitory domain (which inhibits kinase activity via 2 crucial phenylalanine residues, Phe524 and Phe526), and a long C-terminal coiled coil domain (Lenertz et al., 2005; Xu et al., 2002). The catalytic domains of WNK2, WNK3, and WNK4 were reported to be 95% homologous to WNK1 (Verissimo and Jordan, 2001). Although the four WNK4 kinases are highly similar, each differ in both chromosomal and tissue location. Expression analysis showed WNK1 as the most ubiquitous WNK kinase expressed in most tissues, the strongest being in the kidney, heart, muscle and testis (Choate et al., 2003; Verissimo and Jordan, 2001; Wilson et al., 2001; Xu et al., 2000). WNK2 is predominantly expressed in the heart, brain and colon, WNK3 expression is mostly in the brain and intracellular junctions in all nephron segments, and WNK4 is expressed in the colon, skin and in the intracellular junctions of the DCT (Rinehart et al., 2005; Verissimo and Jordan, 2001; Wilson et al., 2001). WNK1 is rapidly activated by hyperosmotic stress or low Cl^- depletion (Lenertz et al., 2005; Moriguchi et al., 2005; Richardson et al., 2008; Zagórska et al., 2007). Activation occurs through the autophosphorylation of a conserved key serine residue, Ser382, which is located within its activation loop (Xu et al., 2002; Zagórska et al., 2007). This residue was found to be required for WNK1 activity as mutation of this residue to alanine ablated WNK1 activation, while mutation to glutamic acid enhanced WNK1 activity (Xu et al., 2002; Zagórska et al., 2007). As this residue is conserved among all the WNK isoforms, it suggests that the other isoforms are activated in a similar manner.

1.4.3.2.2 SPAK/OSR1

As mentioned, SPAK and OSR1 protein kinases are substrates of WNK1 and WNK4 phosphorylation (Anselmo et al., 2006; Moriguchi et al., 2005; Vitari et al., 2005). SPAK, previously known as PASK, was first isolated from rat brain tissue and was identified as a member of the STE20/SPS1 protein kinase family with high sequence identity to the human SPAK sequence (Johnston et al., 2000; Ushiro et al., 1998). OSR1 was identified through large-scale sequencing and cloning studies, and was found to share 39% amino acid sequence identity to the human SOK1 (Ste20/oxidant stress response kinase-1) sequence (Tamari et al., 1999). Both SPAK and OSR1 are ubiquitously expressed and share a similar conserved structure with an N-terminal catalytic domain, which is similar to other members of the STE20 protein kinase subfamily, a serine motif (S-motif) and the conserved C-terminal (CCT) domain (Johnston et al., 2000; Tamari et al., 1999; Ushiro et al., 1998; Vitari et al., 2006). A major difference between the two kinases is the presence of a unique N-terminal extension that mainly comprises of alanine and proline repeats in SPAK (Johnston et al., 2000; Ushiro et al., 1998).

The specific interactions of WNK1 and WNK4 with these protein kinases emerged from co-immunoprecipitation experiments and yeast two-hybrid screenings designed to identify binding partners of WNK1 and WNK4 (Anselmo et al., 2006; Moriguchi et al., 2005; Vitari et al., 2005). Subsequent confirmation of SPAK and OSR1 as substrates for WNK1 was demonstrated through induced activation of endogenous SPAK/OSR1 in cells under WNK1 stimulating conditions (Anselmo et al., 2006; Moriguchi et al., 2005; Zagórska et al., 2007). These studies also revealed the association between SPAK and OSR1 with WNK kinases was mediated by their CCT domains and though interactions with specific RFx[V/I] motifs (x represents any amino acid) present in both WNK1 and WNK4 (Delpire and Gagnon, 2007; Moriguchi et

al., 2005; Vitari et al., 2005, 2006). SPAK and OSR1 activation by WNK isoforms was accompanied by phosphorylation at two conserved sites, a threonine residue within the T loop catalytic domain, Thr233 (SPAK) and Thr185 (OSR1), and a serine residue located within the S-motif C-terminal non-catalytic domain, Ser373 (SPAK) and Ser325 (OSR1) (Vitari et al., 2005). Phosphorylation of these threonine residues in the T-loop is important for SPAK/OSR1 activation as confirmed through inhibited activation upon mutation to alanine and enhanced activity upon mutation to glutamic acid, whereas the role for S-motif phosphorylation is still not yet known (Vitari et al., 2005). In addition, siRNA WNK1 depletion showed markedly impaired SPAK/OSR1 phosphorylation at the T-loop and S-motif by >50% and thus impaired SPAK/OSR1 kinase activity (Zagórska et al., 2007).

1.4.3.2.3 NCC

Phosphorylation of SPAK and OSR1 kinases, in turn, results in the phosphorylation and activation of NCC, linking the signalling cascade that connects the WNK kinases and the NCC cotransporter. The CCT domains of SPAK and OSR1 were previously shown to associate with NCC via a docking interaction through the RFx[V/I] motif at the N-terminal tail (Richardson et al., 2008). Following this interaction, SPAK and OSR1 phosphorylate NCC at conserved residues within the N-terminal regulatory region; Thr46, Thr55, and Thr60 (human NCC), stimulating NaCl reabsorption (Moriguchi et al., 2005; Richardson et al., 2008). This phosphorylation mechanism was initially demonstrated in oocyte expression models, whereby a phosphorylation-defective NCC mutant, which was present on the apical surface of the membrane, showed a significant decrease in transport activity, highlighting the importance of the phosphorylation reaction for NCC function (Pacheco-Alvarez et al., 2006). *In vivo* analysis of NCC phosphorylation in the kidney has also shown that

phosphorylated NCC (pNCC) is localised exclusively to the apical membranes of the DCT (Pedersen et al., 2010; Yang et al., 2013), suggesting that the phosphorylation of NCC regulates its expression and function at the plasma membrane. The phosphorylated residue, Thr60 (Thr58 in mice), was found to be essential for NCC activation and maintenance at the membrane, as mutation to alanine prevented NCC activation under activating hypotonic low-Cl^- conditions and also suppressed phosphorylation of other residues, Thr46 and Thr55 (Pacheco-Alvarez et al., 2006; Richardson et al., 2008). Numerous studies have investigated the regulatory role of WNK4 on NCC regulation. Immunoprecipitation studies have demonstrated a direct interaction between WNK4 and NCC, whilst WNK1 does not affect NCC directly (Cai et al., 2006; Wilson et al., 2003; Yang et al., 2005). However, the role of WNK4 as a positive or negative regulator on NCC activity continues to remain controversial. Initial *in vitro* experiments in oocyte expression models and mammalian cells showed significantly suppressed NCC-mediated Na^+ uptake and reduced NCC surface expression, suggesting WNK4 is a negative regulator of NCC (Cai et al., 2006; Wilson et al., 2003; Yang et al., 2003). In addition, an interaction between WNK1 and WNK4 has been reported and have shown that WNK1 suppresses the inhibitory effect of WNK4 on NCC activity (Yang et al., 2005). In contrast, various *in vivo* studies using WNK4 mutant animals have implicated WNK4 as a positive regulator of NCC activity and an important contributor in PHAII pathogenesis, which will be discussed later (see **Section 1.4.3.4**) (Castaneda-Bueno et al., 2012; Takahashi et al., 2014).

1.4.3.2.4 NKCC cotransporters

SPAK and OSR1 have also been identified as regulators of the bumetanide-sensitive Na^+-K^+-$2Cl^-$ cotransporters, NKCC1 and NKCC2 (Moriguchi et al., 2005; Piechotta et al., 2002, 2003).

NKCC1 was the first substrate for SPAK and OSR1 kinases to be identified (Dowd and Forbush, 2003; Piechotta et al., 2002, 2003). *In vitro* studies revealed SPAK and OSR1, in response to hyperosmotic stress or low intracellular Cl^-, to effectively phosphorylate 3 highly conserved sites located within the NKCC1 N-terminal domain; Thr184, Thr189 (essential for activation in NKCC1) and Thr202 (Darman and Forbush, 2002; Moriguchi et al., 2005; Vitari et al., 2006). Both kinases interact with NKCC1 via their CCT domains on the RFx[V/I] motif located within the N-terminal domain of NKCC1 (Delpire and Gagnon, 2007; Piechotta et al., 2003; Vitari et al., 2006). The importance of this interaction was demonstrated upon mutation of these binding motifs (or the SPAK/OSR1 kinases to prevent activation by WNKs), which resulted in the inhibition of SPAK/OSR1 binding and activation of NKCC1 (Gagnon et al., 2007; Thastrup et al., 2012). As well as maintaining Na^+, K^+ and Cl^- homeostasis, NKCC1 and its regulation by the WNK cascade has been confirmed in the regulation of vascular tone and contractile responses (Garg et al., 2007; Meyer et al., 2002; Susa et al., 2012).

The region of NKCC1 containing the 3 residues phosphorylated by SPAK and OSR1 have shown to be highly conserved in NKCC2 and NCC (Darman and Forbush, 2002; Moriguchi et al., 2005; Richardson et al., 2011; Vitari et al., 2006), implicating this transporter in the WNK-SPAK/OSR1 regulatory pathway. In validation of this hypothesis, yeast two-hybrid screening confirmed NKCC2 interaction with SPAK and OSR1, and further experiments showed phosphorylation of the N-terminal of NKCC2 at these 3 sites in response to hypotonic low-Cl^- conditions (Moriguchi et al., 2005; Piechotta et al., 2002; Richardson et al., 2011). In addition, an *in vitro* study using oocytes overexpressing the WNK3 kinase has also demonstrated NKCC2 activation via interaction with SPAK and OSR1 (Ponce-Coria et al., 2008; Rinehart et al., 2005), further linking NKCC2 in the WNK regulatory cascade. Like NCC,

NKCC2 is also a target for loop diuretics as a treatment for hypertension, and its regulation via the upstream WNK-SPAK/OSR1 signalling cascade has been shown to play a major role in blood pressure homeostasis.

1.4.3.3 Regulators of the WNK-SPAK/OSR1-NCC phosphorylation cascade

The WNK-SPAK/OSR1-NCC phosphorylation cascade is highly adaptable to changes in dietary electrolyte intakes (Na^+ and K^+) and hormones (vasopressin, aldosterone and angiotensin II). Phosphorylation of SPAK/OSR1 and NCC were shown to be activated when mice were fed on a low-Na^+ diet which was correlated with increased aldosterone levels, the reverse was observed when mice were placed on a high-Na^+ diet, thus enabling adjustment of Na^+ excretion to dietary salt intake (Chiga et al., 2008). This regulation is abolished in PHAII. Reponses to changes in dietary salt have been shown to arise from the subcellular redistribution of NCC in the DCT. Immunogold staining and immunoelectron microscopy in rat DCT cells show pronounced NCC localisation at the apical membrane in rats fed a low-Na^+ diet, whilst NCC under a high-Na^+ diet resides in subapical vesicles (Sandberg et al., 2006). Aldosterone-mediated NCC activation by the serum- and glucocorticoid-regulated kinase, SGK1, has also been described previously (Rozansky et al., 2009; Vallon et al., 2009; Webster et al., 1993). Up-regulation and phosphorylation of NCC in response to a low-Na^+ diet is significantly impaired in homozygous SGK1 mutant mice (Vallon et al., 2009), illustrating another component of NCC regulation. Dietary K^+ intake also regulates this signalling cascade. Low-K^+ diet causes the activation of the WNK-SPAK/OSR1-NCC signalling, whilst, high-K^+ diets decrease cascade signalling (Vallon et al., 2009). As dysfunction of this cascade results in either hyper- or hypokalemia in PHAII and Gitelman syndrome, respectively, it is

therefore reasonable to assume that this cascade also plays a role in K^+ homeostasis, however the mechanisms involved are still not yet clear.

The WNK signalling cascade is also regulated by hormonal factors. In addition to aldosterone, angiotensin II (AngII) has been reported to activate this signalling cascade (Castaneda-Bueno et al., 2012; San-Cristobal et al., 2009; Talati et al., 2010), however the mechanisms are still not well understood. *In vitro* oocyte expression models show AngII increases NCC-mediated Na^+ uptake (San-Cristobal et al., 2009). The addition and infusion of AngII to mpkDCT cells and mouse kidneys, respectively, demonstrated an increase in NCC and SPAK/OSR1 phosphorylation (Talati et al., 2010). In addition, AngII infusion in mice lacking WNK4 exhibited mild Gitelman-like phenotypes with reduced NCC phosphorylation, due to impaired SPAK/OSR1 phosphorylation (Castaneda-Bueno et al., 2012), thereby identifying AngII (or rather the renin-AngII-aldosterone (RAA) system) as a WNK4-SPAK-dependent regulator of NCC. Vasopressin is another hormone reported to stimulate NCC activity. It is well known that vasopressin regulates Na^+ reabsorption in the kidney via NKCC2, however, short-term administration of vasopressin in rats has also been shown to enhance NCC phosphorylation and abundance at the plasma membrane (Mutig et al., 2010; Pedersen et al., 2010).

1.4.3.4 Pseudohypoaldosteronism II (PHAII)

1.4.3.4.1 WNK1/WNK4

In summary, the WNK-SPAK/OSR1-NCC phosphorylation cascade has the capability to respond to changes in stimuli by stimulating the phosphorylation of NCC accordingly, underlining the importance of the WNK signalling cascade in the kidney for homeostatic regulation of electrolyte transport and blood pressure under different pathophysiological conditions. Numerous *in*

vitro and *in vivo* studies have been conducted to determine the importance of this pathway and NCC function in the pathogenesis of hereditary forms of hypertension.

Wilson *et al*., first identified mutations in the WNK1 and WNK4 kinases as being responsible for the autosomal dominant inherited form of hypertension, PHAII (**Fig.1.4b**) (Wilson et al., 2001). Mutations in WNK1 are comprised of large intronic deletions in intron 1 that result in gain-of-function mutations (Wilson et al., 2001). Transgenic mouse models of WNK1 PHAII-causing mutations exhibit increased full-length WNK1 transcription and expression in the kidney, an increase in NCC phosphorylation and display all the clinical characteristics of PHAII, including hypertension, hyperkalemia, metabolic acidosis and hypercalciuria (Vidal-Petiot et al., 2013).

PHAII-causing mutations in WNK4 are missense and cluster within a short, highly conserved acidic domain (Wilson et al., 2001). Four missense PHAII-causing mutations have been identified in PHAII kindreds; E562K, D564A, Q565E and R1185C (Wilson et al., 2001). The effects of WNK4 and its PHAII-causing mutations has been extensively studied in *in vitro* oocyte expression models and genetically-modified mouse models, however, as previously mentioned, the influence of WNK4 on NCC activity is still a topic of controversy. Oocytes expression models overexpressing WNK4 have shown to inhibit NCC-mediated Na^+ uptake by reducing NCC abundance at the apical membrane (Wilson et al., 2003; Yang et al., 2003). Some studies have shown the inhibitory effects of WNK4 on NCC are kinase-dependent (Wilson et al., 2003), while others report the effect of WNK4 to be kinase-independent (Yang et al., 2005). Functional studies have revealed a direct association between WNK1 and WNK4 and claim that WNK1 acts by suppressing WNK4 inhibitory effects on NCC activity (Yang et al., 2005). However, there is little *in vivo* evidence to support the conclusion of WNK4 acting as a negative regulator. One exception is a study by Lalioti *et al*., who

generated WNK4 transgenic mice harbouring a single copy of the wild-type WNK4 gene, which exhibited a Gitelman-like phenotype (Lalioti et al., 2006). However, a major limitation of this study is that whether WNK4 levels were increased or whether the observed negative effect on NCC was dependent on WNK4 levels was not clarified, thus, conclusions from this study must be considered with caution, particularly with the pitfalls of using transgenic mice. In contrast, numerous *in vivo* studies of WNK4 knockout and PHAII-causing WNK4 knock-in mouse models have swayed the functionality of WNK4 on NCC activity towards an activating role (Castaneda-Bueno et al., 2012; Lalioti et al., 2006; Ohta et al., 2009; Takahashi et al., 2014; Wakabayashi et al., 2013; Yang et al., 2010a, 2007). $WNK4^{D561A/+}$ knock-in mice display increased apical expression of pNCC as well as its upstream regulators, SPAK/OSR1, and exhibited the PHAII phenotype (Yang et al., 2010a, 2007). An increase in pNCC levels and PHAII phenotype was also observed in transgenic mice expressing the Q562E PHAII WNK4 mutant, which could be reversed when bred with mice lacking NCC (Lalioti et al., 2006). The opposite was observed in WNK4 hypomorphic and WNK4 knockout mice which exhibit a significant decrease in pNCC levels as well as the clinical phenotypes reminiscent of Gitelman syndrome (Castaneda-Bueno et al., 2012; Takahashi et al., 2014). Furthermore, a study by Wakabayashi *et al*., generated several lines of WNK4 transgenic mice using the same method as the study by Lalioti *et al*., (Lalioti et al., 2006), with different levels of WNK4 overexpression (Wakabayashi et al., 2013). They observed a significant increase in WNK4 levels that was associated with increased phosphorylation of SPAK/OSR1 and NCC and their mice also mimicked the PHAII phenotype (Wakabayashi et al., 2013). These mouse models thereby identify WNK4 as a positive regulator of the WNK-SPAK/OSR1-NCC phosphorylation cascade *in vivo* and that the PHAII-causing missense mutations are gain-of-function mutations which increase NCC activity at the apical membrane (**Fig.1.4c**).

1.4.3.4.2 KLHL3/CUL3

Alongside WNK1 and WNK4, using whole-exome sequencing and combined linkage analysis in PHAII kindreds, two further genes, Kelch-like 3 (KLHL3) and Cullin 3 (CUL3), were identified in the cascades (Boyden et al., 2012; Louis-Dit-Picard et al., 2012). Several studies investigating the roles of KLHL3/CUL3 and the WNK kinases have been conducted in order to, not only to provide an insight into their molecular contribution to PHAII pathogenesis, but also to identify potential targets for anti-hypertensive therapy and have confirmed their involvement in the regulation of the WNK-SPAK/OSR1-NCC phosphorylation cascade.

KLHL3 is a member of the Kelch-like protein family, it contains a bric-a-brac, tramtrack, broad complex (BTB) domain, a BTB and C-terminal Kelch (BACK) domain, and a kelch domain containing 6 kelch repeats (Lai et al., 2000; Louis-Dit-Picard et al., 2012). KLHL3 interacts with CUL3 to form an E3 ubiquitin ligase complex. PHAII-causing mutations within KLHL3 are either recessive or dominant whilst mutations in CUL3 are dominant and are the result of skipping exon 9 (Boyden et al., 2012; Louis-Dit-Picard et al., 2012). It has been previously identified that WNK1 and WNK4 are substrates of KLHL3/CUL3 (Ohta et al., 2013; Shibata et al., 2013; Wakabayashi et al., 2013; Wu and Peng, 2013). Immunoprecipitation studies have confirmed an interaction between KLHL3/CUL3 with WNK4 and have postulated a role for this ubiquitin ligase in maintaining WNK4 protein levels (and therefore its stimulatory influence on NCC) by subjecting it to ubiquitination and lysosomal degradation (**Fig.1.4a**) (Mori et al., 2013; Ohta et al., 2013; Shibata et al., 2013; Wakabayashi et al., 2013). PHAII-causing mutations abolishes this binding between KLHL3 and WNK4 therefore impairing WNK4 degradation (**Fig.1.4c**). Known PHAII-causing mutations in different KLHL3 domains have also been studied to determine the severity of mutations with regards to maintaining WNK4 protein levels. Mutations in the BTB and BACK domain

result in the impairment of protein stability and the ability of KLHL3 to binding to CUL3, whilst mutations in the kelch domain impair the ability of KLHL3 to bind and regulate WNK1 and WNK4 (Mori et al., 2013; Wu and Peng, 2013). Nevertheless, impairment of KLHL3 to bind to either CUL3 or WNK4 all result in the same consequence; loss of WNK4 protein level maintenance due to diminished KLHL3/CUL3-mediated degradation, which result in an increase in WNK4 levels within the cell, and thus, enhancement of downstream activation of the WNK-SPAK/OSR1-NCC pathway. This increase in WNK4, as well as pNCC protein levels has been confirmed in WNK4$^{D561A/+}$ and in KLHL3$^{R528H/+}$ PHAII mouse models (Susa et al., 2014; Wakabayashi et al., 2013).

1.4.3.4.3 SPAK/OSR1

As well as the PHAII consequences linked with mutations in WNK1/WNK4 and KLHL/CUL3, mutations in the SPAK/OSR1 intermediates between the WNK kinases and NCC have also shown to have significant effects on blood pressure. Mutant SPAK knock-in mice that cannot be activated by WNK kinases exhibit a salt-dependent decrease in blood pressure, NCC and NKCC2 phosphorylation and are mildly hypokalemic under Na^+-restriction (Rafiqi et al., 2010). Homozygous SPAK knockout mice also exhibit hypotension and significant electrolyte abnormalities that recapitulate Gitelman syndrome, as well as marked reductions in pNCC levels with blunted responses to dietary Na^+-restriction and thiazide diuretic administration (McCormick et al., 2011; Yang et al., 2010b). Interestingly, genetic cross studies of WNK4$^{D561A/+}$ PHAII mice with SPAK$^{-/-}$ knockout mice show normalised blood pressure, response to thiazides, plasma and urine biochemistries and similar levels of total NCC, pNCC, total NKCC2 and phosphorylated NKCC2 (pNKCC2) as the wild-type controls, thus, eliminating the PHAII phenotype and suggesting that SPAK deficiency can correct for

PHAII WNK4 mutations (Chu et al., 2013). In addition, mutation and disruption of the CCT domain of SPAK which recognises the RFx[V/I] motifs in its upstream activators and downstream substrates is associated with a significant reduction in pNCC and pNKCC2 levels and the typical features of Gitelman syndrome, including hypotension, upon dietary Na^+-restriction (Zhang et al., 2015). Therefore, this effective lowering of blood pressure upon SPAK-NCC disruption may provide a promising new target for future anti-hypertensive therapy.

1.4.3.5 WNK-SPAK/OSR1 signalling cascade: Extrarenal roles

As well as regulating Na^+, K^+ and blood pressure homeostasis in the kidneys, the WNK-SPAK/OSR1 signalling cascade has been shown to be involved in the regulation of arterial tone. In this regard, the main transporter thought to be involved is NKCC1. NKCC1 is reported to play a major role in the regulation of vascular tone through establishing an outward Cl^- gradient and membrane depolarisation which causes the opening of voltage-gated Ca^{2+} channels, leading to smooth muscle contractility (Akar et al., 2001; Garg et al., 2007; Meyer et al., 2002). NKCC1-mediated vascular smooth muscle contractions are stimulated by the vasoconstrictors, AngII and phenylephrine, and are inhibited by the nitrovasodilators, nitric oxide and nitroprusside (Akar et al., 1999). Inhibition of NKCC1 significantly reduces contraction of the aorta, therefore, NKCC1 is believed to also contribute to blood pressure maintenance. Studies with NKCC1 knockout mice exhibit significant reductions in blood pressure and showed abolished suppressive actions of bumetanide infusion on phenylephrine-stimulated vascular smooth muscle cell contractions (Garg et al., 2007; Koltsova et al., 2009; Meyer et al., 2002), thereby supporting the hypothesis of NKCC1 influencing blood pressure via the regulation of vascular smooth muscle cells. WNK1 and WNK3 have also been identified in vascular smooth muscles cells and have been shown to

phosphorylate the downstream substrate, SPAK, which in turn, phosphorylates NKCC1 (Bergaya et al., 2011; Moriguchi et al., 2005; Susa et al., 2012; Vitari et al., 2006). Animal studies using heterozygous WNK1 mutant mice show decreased NKCC1 phosphorylation and vasoconstrictive responses in the aorta, which were confirmed through decreased blood pressure responses following stimulation with phenylephrine and the loss of pressure-induced contractile responses in thoracic aortic rings and mesenteric arteries (Bergaya et al., 2011; Susa et al., 2012). Similarly, SPAK knockout mice also show decreased NKCC1 phosphorylation in aortic tissues and impaired aortic contractility in response to phenylephrine and bumetanide (Yang et al., 2010b). More recently, the regulation of the WNK-SPAK/OSR1-NKCC1 signalling cascade in the aorta was additionally found to be mediated by dietary Na^+ intake and AngII, as both phosphorylated SPAK and NKCC1 were significantly increased in mice fed a low-Na^+ diet and in mice infused with AngII (Zeniya et al., 2013). Thus, the WNK-SPAK/OSR1 signalling cascade plays a major role in regulating the influence of NKCC1 on smooth muscle contractility and further emphasises the importance of the WNK-SPAK/OSR1 signalling cascade in controlling blood pressure.

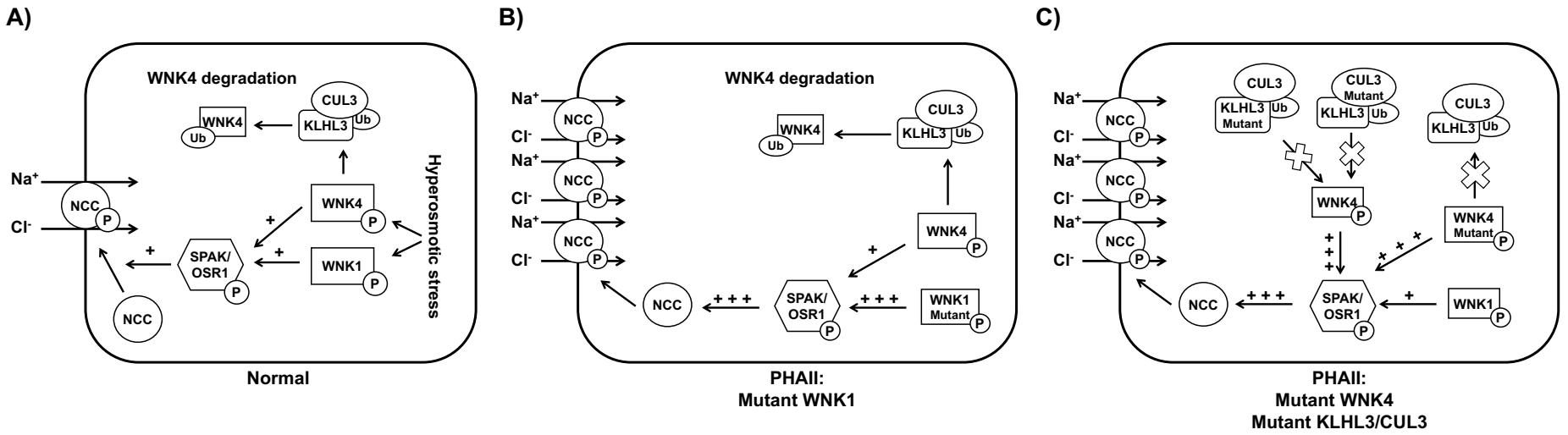

Figure 1.4. The WNK-SPAK/OSR1-NCC phosphorylation cascade and its contribution in PHAII pathogenesis. A schematic diagram of the WNK-SPAK/OSR1-NCC phosphorylation cascade showing the regulation of the sodium chloride cotransporter, NCC. **A)** Under normal conditions, upon activation via hyperosmotic stresses, WNK1 and WNK4 phosphorylate and activate the SPAK/OSR1 kinases which then go on to phosphorylate and activate NCC, mediating its trafficking towards the apical membrane where it facilitates NaCl reabsorption. WNK4 levels are maintained by ubiquitin-tagged degradation by interactions with KLHL3/CUL3 ubiquitin ligases. In PHAII, **B)** gain-of-function mutations in WNK1 result in the overactivation of the WNK-SPAK/OSR1 signalling pathway which increases pNCC expression at the apical membrane and NaCl reabsorption. **C)** Mutations in WNK4, KLHL3 or CUL3 impair WNK4 ubiquitination/degradation by loss of interactions with KLHL3/CUL3, which leads to uncontrolled rises in WNK4 levels. This increase in WNK4 levels results in the overactivation of the WNK-SPAK/OSR1 signalling pathway and ultimately, leads to augmented NaCl reabsorption in the kidney.

1.4.4 Calcineurin inhibitors

There is sufficient evidence to support the involvement of the WNK-SPAK/OSR1-NCC phosphorylation cascade in blood pressure regulation. Imbalances in this cascade result in PHAII and Gitelman syndrome renal disorders that elicit increased Na^+ reabsorption or increased Na^+ excretion, respectively. Interestingly, the clinical features associated with PHAII are also observed in renal transplant patients treated with CNIs, suggesting that the molecular mechanisms underlying PHAII pathogenesis could explain the sodium retentive and hypertensive effects of CNIs. Based on this observation, CNI-treated animal studies have been conducted to explore this link. One such study confirmed the PHAII-like phenotype in wild-type mice treated with FK506 for two weeks; with mice displaying salt-sensitive hypertension, hyperkalemia, metabolic acidosis and hypercalciuria, which could be reversed by thiazide administration (Hoorn et al., 2011). This hypertensive effect was not induced in NCC knockout mice and was exaggerated in NCC-overexpressing mice (Hoorn et al., 2011). On a molecular level, FK506 treatment increased renal pNCC protein abundance as well as WNK3, WNK4 and SPAK. These findings were also extended to CNI-treated renal transplant patients where the examination of renal biopsies using immunohistochemical analysis revealed increased apical expression of pNCC (Hoorn et al., 2011). In further support, a study using rats treated with another CNI, CsA, for two weeks demonstrated an increase in blood pressure, as well as hyperkalemia and hypercalciuria, and a significant increase in renal WNK4, NCC and pNCC protein abdunance (Melnikov et al., 2011). These findings thereby demonstrate that CNI-induced hypertension is largely mediated through increased NCC activation.

Recently, new evidence has come into light to suggest that the CNI-enhancing effects on NCC may be due to CNIs inhibiting calcineurin-mediated dephosphorylation of sodium transporters in the kidney. Mice fed

on a high-K^+ diet (to activate calcineurin activity) showed rapid de-phosphorylation of NCC, which was significantly inhibited by FK506- and W7- (calmodulin inhibitor) treatment (Shoda et al., 2017). In either treatment, there was no significant difference in WNK4, OSR1 and SPAK expression, suggesting that the rapid reduction of pNCC expression under high-K^+ intake is independent of the WNK-SPAK/OSR1 signalling cascade and is instead largely mediated by the phosphatase activity of calcineurin. In addition, disruption of the FKBP12 protein in mice, followed by treatment with FK506, results in a decline in blood pressure and renal pNCC abundance, and further analysis in FK506-treated HEK-293 cells demonstrated inhibited dephosphorylation of NCC (Lazelle et al., 2016). Intriguingly, the abundance of WNK4 and SPAK in FK506-treated FKBP12 mutant mice was similar to that of the controls, further promoting the hypothesis that CNIs induce hypertension predominantly by inhibiting calcineurin-mediated dephosphorlyation of NCC. Studies with CsA-administered animals have also observed a significant increase in pNKCC2 abundance (Borschewski et al., 2016; Esteva-Font et al., 2007). This has been further corroborated in urinary exosome analysis of hypertensive CNI-treated renal transplant patients where a high level of NKCC2 and NCC expression was observed in comparison to non-CsA and normotensive control patients (Esteva-Font et al., 2014; Rojas-Vega et al., 2015). In conclusion, it is well established that CNI-induced hypertension is largely mediated through increased NCC (and possibly NKCC2) activation and therefore implicates calcineurin as an important modulator of Na^+ homeostasis and blood pressure. However, whether these effects are dependent on the WNK-SPAK/OSR1 signalling cascade still remains to be clarified.

1.5 CNI-induced hypertension: Vascular tone

Hemodynamic changes play a major role in CNI-induced hypertension (**Fig.1.5**). This has been observed in numerous animal studies whereby CsA

infusion in rats causes a significant fall in renal blood flow and a rise in vascular resistance (Kaye et al., 1993; Murray et al., 1985). The cause of these hemodynamic alterations is speculative but implicates several pathophysiological changes that, as a result, complicates its clinical use.

There is evidence to suggest that CNIs elicit vasoconstrictive effects that are responsible for its nephrotoxic and arterial hypertensive outcomes (English et al., 1987; Golub and Berger, 1987; Kaye et al., 1993; Lamb and Webb, 1987; Lanese and Conger, 1993; Xue et al., 1987). Preclinical models of CsA-treated rats show a significant decline in GFR and a progressive decrease in the diameter of the renal afferent arteriole (English et al., 1987), consistent with the notion that the renal response to CsA is an ischemic or glomerular process rather than via direct tubular injury. Various *in vitro* experiments in isolated rat vascular ring segments, tail arteries, portal veins and thoracic aortic tissues treated with CsA have demonstrated augmented contractile responses upon transmural or sympathetic nerve stimulation (Golub and Berger, 1987; Lamb and Webb, 1987; Xue et al., 1987), confirming the direct actions of CNIs on vascular smooth muscle and/or on adrengeric neurotransmission.

Several studies have reported the CNI-induced vasoconstrictive effects to be mediated through the overproduction and release of the vasoconstrictor, endothelin (Cauduro et al., 2005; Cavarape et al., 1998; Lanese and Conger, 1993; Takeda et al., 1992, 1995, 1999). In cultured human endothelial cells, incubation with CsA induced endothelin synthesis, which could be inhibited by the protein synthesis inhibitor, cycloheximide (Bunchman and Brookshire, 1991). This suggests that CsA may directly induce endothelin activity in systemic or renal vasculature. This was also illustrated in *in vivo* rat studies in which treatment with CsA and FK506 resulted in, not only elevated blood pressure, but also increased endothelin synthesis in the mesenteric artery. This could be partially prevented following co-treatment with an endothelin

receptor antagonist (Takeda et al., 1992, 1995, 1999). Furthermore, CsA exposure in isolated rat arterioles caused a direct release of endothelin from the endothelium alongside a concentration-dependent decrease in lumen diameter of the afferent arteriole, all of which could be inhibited by an endothelin receptor antagonist (Lanese and Conger, 1993). In clinical settings, renal transplant patients receiving CsA treatment also displayed significantly higher levels of endothelin compared to control patients (Cauduro et al., 2005). These studies provide evidence to suggest an important role for endothelin in CsA-induced vascular smooth muscle contractions.

There is also evidence that suggests that CNIs may act by impairing vasodilation as opposed to stimulating vasoconstriction (Richards et al., 1989; Roullet et al., 1994; Stein et al., 1995). In human subcutaneous resistance vessels, CsA incubation decreases the rate of spontaneous relaxation and inhibits endothelium-dependent relaxation (Richards et al., 1989). However, endothelium-independent relaxation was augmented in response to the vasodilator, sodium nitroprusside, and blunted vasoconstrictive response to noradrenaline and K^+ upon CsA treatment was also observed (Richards et al., 1989), suggesting the hypertensive effects of CsA may, in part, be due to inhibited endothelium-dependent resistance vessel relaxation. Similar findings have been observed in isolated aortic rings from rats treated with CsA (Cartier et al., 1994). Chronic exposure of CsA significantly decreased maximal endothelium-dependent relaxation responses to acetylcholine. However, in this case, endothelium-independent relaxations to sodium nitroprusside was not effected in CsA- or vehicle-treated groups and both endothelium-dependent and independent vasoconstriction was observed in CsA-treated animals in response to serotonin, aggregating platelets and norepinephrine (Cartier et al., 1994). This suggested that exposure to CsA may contribute to altering vasoregulation by decreasing endothelial-relaxing factors and increasing

production of endothelial-constricting factors. Supporting studies in isolated rat mesenteric artery vessels have shown impaired CsA-induced vasodilation via the inhibited production of the vasodilator, nitric oxide (NO) (Marumo et al., 1995; Morris et al., 2000; Oriji and Keiser, 1998). Analysis of the effect of CsA on NO synthase induction confirmed significantly reduced expression of inducible nitric oxide synthase mRNA and nitrate/nitrite accumulation (metabolites of NO) in rat smooth muscle cells (Marumo et al., 1995). In addition, acetylcholine-induced endothelium-dependent relaxation was significantly inhibited by 65% in thoracic aortic rings from CsA-treated rats compared to untreated controls (Oriji and Keiser, 1998). These hypertensive and inhibitory effects of CsA were found to be reversible in both *in vivo* and *in vitro* experiments by pretreatment with L-arginine, a precursor of NO (Oriji and Keiser, 1998). Clinical studies in renal transplant patients receiving CsA also confirmed the impaired vasodilatory effect, which was attributed to a reduction in endothelial basal and stimulated NO synthesis (Morris et al., 2000). Although these inhibitory effects of CNIs on NO synthesis in vascular smooth muscle have mostly been demonstrated for CsA, a decrease in both the level and activity of endothelial NO synthase in the aorta of rats has also been observed for FK506 (Takeda et al., 1999).

Another proposed mechanism by which CNIs induce hypertension, via changes in vascular tone, involves activation of the RAA system. Supporting studies have found CsA to increase plasma renin secretion/production and cystolic Ca^{2+} concentration and efflux in cultured human vascular smooth muscle cells when stimulated with AngII (Avdonin et al., 1999; Kurtz et al., 1988). This was accompanied by a two-fold increase in the number of angiotensin II type 1 receptors suggesting that CsA upregulates the transcription of AngII receptors, and therefore AngII action, in human vascular smooth muscle cells which likely leads to vasoconstriction. This effect was also observed in CsA-treated rats; whereby CsA treatment caused a significant increase in SBP that was paralleled with enhanced aortic

contractile responses to AngII which could also be counteracted by administration of the RAA inhibitors, losartan and captopril, or inhibitors of vasoconstriction, prostanoids or endothelin receptors (Hoskova et al., 2014; Nasser et al., 2016). However, it remains unclear if and how CNIs induce AngII production and activation of the RAA system.

1.6 CNI-induced hypertension: Sympathetic nervous system

The sympathetic nervous system (SNS) plays an important role in the regulation of blood pressure. Activation of sympathetic activity mediates vasoconstrictive and renal sodium absorptive actions which may be accelerated during hypertension development. It has been suggested that CNI-induced rises in blood pressure and nephrotoxicity may be associated with, to a substantial extent, the excitation of the SNS (**Fig.1.5**) (Scherrer et al., 1990).

Studies have been conducted to record sympathetic action potentials/nerve firing using intraneural microelectrodes to confirm CNI-induced sympathetic activation. In cardiac transplant recipients who were being treated with CsA, measurements of sympathetic neural activation showed significantly increased rates of sympathetic nerve firing as well as a rise in mean arterial pressure (MAP) (Scherrer et al., 1990). However, in other human studies, sustained use of CNIs has reported either unaltered sympathetic activity or short-lived sympathetic activation (Hausberg et al., 2006; Kaye et al., 1993; Klein et al., 2010; Stein et al., 1995). Analysis of muscle sympathetic nerve activity (MSNA) and blood pressure before and after withdrawal of CsA in renal transplant patients showed that, although MAP decreased significantly after CsA withdrawal, which is in line with the CNI-induced effects on blood pressure, MSNA was unchanged at both time points, suggesting that CNI treatment may not cause sympathetic nerve activation to elicit blood pressure elevations (Hausberg et al., 2006). However, the patients in this study were

receiving low doses of CsA that was accompanied by low CsA whole-blood trough levels, so it is possible that higher doses of CsA may elicit sympathetic activation. In other experiments, acute CsA administration at both normal and high doses showed increased MSNA, however, sustained treatment with CsA resulted in MSNA suppression (Klein et al., 2010). Acute administration of FK506 did not affect MSNA or MAP, however, the subjects used in this study were healthy volunteers and so the effects observed for CsA and FK506 cannot be applied under conditions of compromised organ dysfunction (Klein et al., 2010). Whilst these studies in humans may or may not implicate augmented sympathetic activation in the pathogenesis of CNI-induced hypertension, these findings are only correlational and do not provide experimental evidence of this association.

In contrast, numerous studies have provided supporting evidence using rat models that the hypertensive responses to CsA treatment are sympathetically mediated. Animal studies have clearly demonstrated both CsA and FK506 infusion induces sympathetic nerve activity which is paralleled by an increase in blood pressure and renal vascular resistance (Lyson et al., 1993; Morgan et al., 1991; Moss et al., 1985; Zhang and Victor, 2000a; Zhang et al., 2000b). These effects are abolished upon elimination of sympathetic discharge (Morgan et al., 1991). Administration of rapamycin/sirolimus, an immunosuppressant that forms a complex with FKBP12 but does not interact with calcineurin, failed to induce sympathetic activation and increase blood pressure (Lyson et al., 1993), suggesting that the regulation of sympathetic nerve activity may be tightly linked to calcineurin-mediated inhibition of T-cell signalling. In addition, these CNI-induced elevations have also confirmed CNI-induced sodium-retention outcomes due to activation of the SNS, which was abolished upon renal denervation (Moss et al., 1985). Further animal studies have gone on to suggest that CNIs increase sympathetic nerve activity through increasing renal afferent nerve activation (Moss et al., 1985; Zhang and Victor, 2000a),

by acting on renal sensory nerve endings mediated by vesicle phosphoproteins such as synapsins (which are essential for neurotransmitter release), rather than on central synapses (Zhang et al., 2000b). Therefore, in summary (**Fig.1.5**), activation of afferent renal nerve activity and SNS may be a primary mechanism by which CNIs induce hypertension, resulting in renal vasoconstriction, decreased GFR, increased renal vascular resistance and renal tubular sodium reabsorption. However, the mechanisms by which CNIs activate sympathetic activity are still not fully elucidated.

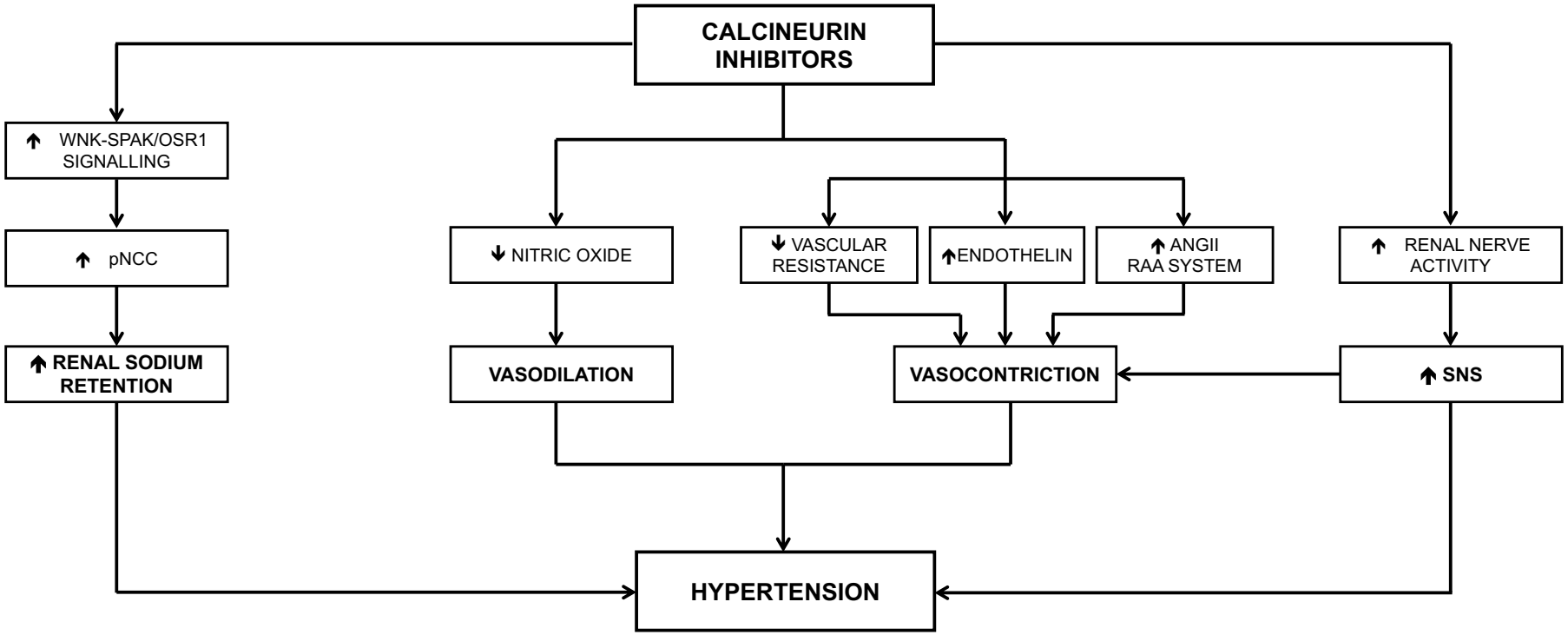

Figure 1.5. A mechanistic model for the pathogenesis of CNI-induced hypertension. CNIs influence abnormal rises in blood pressure through provoking hemodynamic alterations by vasoconstriction, impaired vasodilatory responses, activation of renal sympathetic nerve activity/SNS (which may also stimulate vasoconstriction), and increased renal sodium retention by activation of the WNK-SPAK/OSR1-NCC signalling pathway.

1.7 CNIs: Post-transplant Diabetes Mellitus (PTDM)

Post-transplant diabetes mellitus (PTDM), or new-onset diabetes after renal transplantation (NODAT), is a recognised common and severe complication after transplantation.

The incidence of PTDM among non-diabetics have reported to range between 2–25% of renal allograft recipients within the first 3 years post-transplant and is associated with decreased graft and patient survival and increased cardiovascular mortality (Cosio et al., 2001, 2005; Kasiske et al., 2003; Porrini et al., 2008a; Woodward et al., 2003). Analyses of risk factors have shown PTDM to be dependent on older age, age at time of transplant, increased weight/BMI, pre-transplant hypertriglyceridemia (elevated triglyceride), elevated total serum cholesterol and pre- and post-transplant hyperglycemia (elevated blood glucose) (Cosio et al., 2001, 2002, 2005; Porrini et al., 2008b). Pre- and post-transplant hyperglycemia were particularly identified as strong predictors of PTDM and highly associated with post-transplant cardiac events and disease (Cosio et al., 2005). Pre- and post-transplant hypomagnesemia were also suggested to be risk factors for PTDM development (Sinangil et al., 2016; Van Laecke et al., 2009).

Although there are multiple factors that contribute to the risk of PTDM, CNIs have been identified as the dominant factor (Boudreaux et al., 1987; Heisel et al., 2004; Kasiske et al., 2003; Roth et al., 1989; Woodward et al., 2003). Data recorded from randomised trials and meta-analysis have reported significantly higher incidences of PTDM in patients receiving FK506 than CsA (Araki et al., 2006; Heisel et al., 2004; Kasiske et al., 2003; Woodward et al., 2003). Follow up studies have shown the prevalence of PTDM over the first 2 years post-transplant was almost 30% and 18% in FK506- and CsA-treated renal transplant patients, respectively (Woodward et al., 2003). Interestingly, in renal transplant recipients, FK506 was shown to be more diabetogenic

than CsA but only in patients with elevated pre-transplant triglyceride levels (Porrini et al., 2008b) . Although it is clear that CNIs are major risk factors for PTDM development, the detailed pathophysiological mechanisms underlying their diabetogenic affects remains to be clarified.

A vast majority of studies evaluating these CNI-induced PTDM effects in renal transplant recipients, diabetic animals and cell line models have drawn attention to pancreatic β-cell dysfunction and impaired insulin synthesis and secretion as the main mode of action (Helmchen et al., 1984; Hirano et al., 1992; Redmon et al., 1996; Tamura et al., 1995). In rats, FK506 caused a dose-dependent, but reversible, impairment in insulin secretion and lowered insulin levels in the pancreas (Hirano et al., 1992). These studies also reported both severe morphological and functional alterations in pancreatic β-cells following CNI-treatment (Helmchen et al., 1984; Hirano et al., 1992), which may correspond to decreased pancreatic and plasma insulin content, leading to hypergylcemia. Similar observations were found in insulin-secreting β-cell lines, where FK506 exposure demonstrated a reversible, time- and dose-dependent decrease in insulin secretion which was accompanied by a dose-dependent decrease in insulin content and mRNA levels (Redmon et al., 1996; Tamura et al., 1995). These findings indicate that CNIs may directly act by reversibly inhibiting insulin gene expression, synthesis and secretion and, therefore, may portray a role for calcineurin in regulating glucose homeostasis. In validation, NFAT, FKBP12 and calcineurin protein expression have all been confirmed in pancreatic β-cells, and later analysis in the rat insulin I (INS1) gene revealed 3 putative NFAT binding sites located within the promoter and also confirmed NFAT-DNA binding activity (Lawrence et al., 2001; Tamura et al., 1995). Activation of this promoter was inhibited by FK506 but not by the immunosuppressant rapamycin indicating specificity towards calcineurin (Lawrence et al., 2001). In further support, mice with a β-cell specific deletion of the regulatory B

subunit of calcineurin developed age-dependent diabetes characterised by severe hyperglycemia, decreased β-cell proliferation, via decreased expression of β-cell transcription factors, decreased pancreatic insulin production and hypoinsulinemia, all of which could be rescued upon conditional expression of nuclear NFAT1 (Heit et al., 2006). These studies thereby suggest that calcineurin/NFAT signalling specifically regulates insulin gene expression and involves multiple factors that mediate β-cell function, and implicates that disruption of this pathway largely contributes to the diabetogenic effects of FK506.

As mentioned, previous studies have suggested that the diabetic-onset effects of FK506 is greater in comparison to CsA but only in patients with elevated pre-transplant triglyceride levels, which serves as an indicator of insulin resistance (Porrini et al., 2008b). In recent studies using insulin-resistant obese Zucker rat models, FK506 treatment inhibited β-cell proliferation and insulin gene expression, whilst none of the lean Zucker rats developed diabetes (Rodriguez-Rodriguez et al., 2013; Triñanes et al., 2017). This was partially recovered or improved upon CNI withdrawal or after conversion to CsA (Rodriguez-Rodriguez et al., 2013; Rodríguez-Rodríguez et al., 2015; Triñanes et al., 2017). The conclusions drawn from these studies suggest that the exacerbated diabetogenic effects of FK506 by β-cell dysfunction, impaired insulin transcription and secretion are dependent on a pre-existing insulin resistant background, which may underlie PTDM development. These studies also establish calcineurin as a regulator of insulin synthesis and thus, glucose homeostasis. Unfortunately, the question remains as to the underlying mechanisms by which calcineurin regulates insulin transcription and what other β-cell factors are affected upon calcineurin inhibition.

1.8 Aims of this thesis

The prevalence of post-transplant hypertension, nephrotoxicity and PTDM development is continuously growing and yet our knowledge of the regulatory pathways upon which CNIs act remains limited. The elucidation of the mechanisms underlying CNI-induced hypertension would allow a deeper understanding of its pathogenesis following transplantation and its implications for primary hypertension, another common form of hypertension, as well as aiding future prevention and therapeutic strategies.

The research described in this thesis aims to further facilitate our current understanding of CNI-induced blood pressure alterations via the sodium retention side effect as well as to determine whether calcineurin, the target of CNIs, is therefore a regulator of sodium homeostasis and blood pressure. This has been investigated through three approaches.

Previous studies have shown that CNIs induce the activation and phosphorylation of the renal NCC cotransporter to increase sodium reabsorption in the kidney, however, there are many other transporters and channels located throughout the kidney and gastrointestinal tract which also regulate sodium (re)absorption. Experiments were therefore designed to investigate the effects of CNIs on sodium transport in different regions of the nephron and gastrointestinal tract (**Chapter III**).

CNIs are also major risk factors for PTDM and are known to provoke other electrolyte abnormalities that mimic the clinical features of other conditions which, together, resemble metabolic syndrome. Experiments were therefore designed to establish a mouse model of metabolic syndrome by CNI-treatment and confirm whether CNI treatment may predispose individuals to this condition (**Chapter IV**).

Finally, this investigation also sought to optimise a urinary exosome isolation technique to determine whether NCC/pNCC excretion levels in CNI-administered transplant patietns parallel immunohistochemical analyses, in hopes of providing a new non-invasive method to assist disease diagnosis (**Chapter V**).

Chapter II
Materials and Methods

2.1 Animal Studies

2.1.1 Ethical Approval

All procedures were carried out in accordance with the UK Animals Scientific Procedures Act 1986, Amendment Regulations 2012. All protocols were approved by the University College London (Royal Free Campus) Comparative Biology Unit Animal Welfare and Ethical Review Body (AWERB) committee and performed in accordance with project licenses PPL 70/8064 and PPL 70/7647.

Mice used were male littermates (8 - 10 weeks, weighing between 20 – 25g) of a C57BL/6J background and were housed under a 12:12-hour light-dark cycle and maintained in ventilated metabolic cages with *ad libitum* access to food and water. Mice were fed a standard maintenance diet (RM1 (E) SQC, Specialised Diets Services, Witham, UK). Body weight was closely monitored and measured regularly. Loss of over 20% of their initial body weight resulted in termination of the experiment by an approved Schedule 1 method.

At the end of the treatments, mice were placed under terminal anaesthesia via intraperitoneal (I.P) injection of pentobarbitone sodium (40 – 50mg/kg, Pentoject, Animalcare Ltd, York, UK) in 0.9% (w/v) sterile saline. Deep anaesthesia was achieved through monitoring of corneal and pedal reflexes before obtaining terminal blood samples by cardiac puncture (using a 23G needle) and final urinary samples by bladder puncture (using a 25G needle). Cervical dislocation was then performed and death confirmed before removing the kidneys and intestinal segments.

2.1.2 CNI Treatment

For treatment studies, mice were administered a daily dose of either 2mg/kg Tacrolimus (FK506, LC Laboratories, Woburn, MA USA) or vehicle via I.P injections for two weeks. FK506/vehicle was dissolved in 10% (v/v) ethanol, 10% (v/v) Tween20 and 0.9% (w/v) sterile saline.

Alongside, mice were either fed a standard maintenance diet (RM1 (E) SQC, Specialised Diets Services, Witham, UK), or, as a "high-salt" alternative, maintenance diet supplemented with 1.5% (w/w) sodium chloride (NaCl).

2.1.3 Metabolic Syndrome

To induce metabolic syndrome, 3-week old male mice had *ad libitum* access to a high-fat diet (containing 60% energy-from-fat (58Y1, TestDiet, London, UK)), or standard maintenance diet for ten weeks **(Table.2.1)**. Aside from the differences in fat/energy content, both diets contained similar nutritional profiles with regards to sodium, potassium, chloride, magnesium, calcium and phosphate.

Energy from:	**Standard maintenance diet**		**High-fat diet**	
	Kcal	**%**	**Kcal**	**%**
Protein	0.575	17.49	0.924	18.1
Fat	0.244	7.42	3.140	61.6
Carbohydrates	2.470	75.09	1.035	20.3

Table 2.1. Breakdown of the energy derivation from the standard maintenance and high-fat diets. The standard maintenance diet provides 3.29 kcal/g energy and the 60% fat diet provides 5.10 kcal/g energy. For the standard maintenance diet, most of the energy is provided in the form of carbohydrates to compensate for the lower fat component.

Over the 10-week period, food and water intake and body weight were closely monitored. From week 8, mice were administered a daily dose of either 2mg/kg FK506 or vehicle by I.P injections for the remaining 2 weeks. Towards the last 5 days of treatment, mice were housed in metabolic cages to enable 24-hour urine collections.

2.1.4 Plasma and Urine Biochemistry

Blood samples were spun at 7,500 x g at 4°C for 5 minutes, the plasma was collected, and immediately snap frozen in liquid nitrogen. Urine samples were immediately snap frozen following collection. Measurements for triglycerides, high-density lipoproteins (HDLs), urate, magnesium, calcium and bicarbonate were carried out at the Department of Clinical Biochemistry (Royal Free Hospital, London, UK).

2.1.5 Plasma and Urine Biochemistry: Sodium

Sodium concentrations were measured using a sodium enzymatic assay kit (Dialab, Alpha Laboratories, Hampshire, UK) according to the manufacturer's instructions. Absorbance at 405nm was measured on a microplate reader (DTX 880 Multimode Detector, Beckman Coulter, High Wycombe, UK). The principle of this assay determines sodium through the enzymatic activity of the sodium-dependent β-galactosidase which uses o-nitrophenyl-β-D-glycoside (ONPG) as a substrate (**Fig.2.1**). The absorbance measured for the product, o-nitrophenyl, at 405nm, is proportional to the sodium concentration.

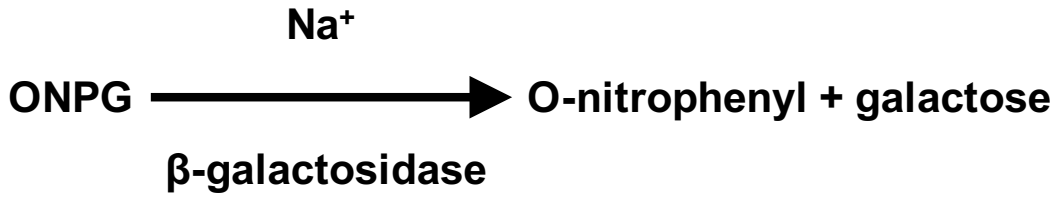

Figure 2.1. Sodium assay principle.

2.1.6 Plasma and Urine Biochemistry: Creatinine

Creatinine concentrations were measured according to Jaffe's method with the use of a colorimetric assay (Bonsnes and Taussky, 1945; Toora and Rajagopal, 2002). To obtain a calibration curve, creatinine standards at 0, 0.02, 0.04, 0.08, 0.17, 0.33, and 0.67µg/ µl were prepared. Urine samples were used at a 1:20 dilution in distilled water whilst plasma samples were used neat. Standards and samples were added to 100µl distilled water and 20µl trichloroacetic acid (TCA, from a 20% stock solution), left to precipitate at room temperature (25°C) for 10 minutes before centrifuging at 3000 rpm for 10 minutes at 25°C. The supernatant (100µl) was taken and added to 0.75M NaOH and 0.04M picric acid (50µl each) and left to react in the dark for 20 minutes at room temperature before reading the absorbance at 520nm. The principle of this assay relies on the reaction between creatinine and picric acid, under alkaline conditions, to form a chromogenic complex, resulting in a colour change to yellow/orange (**Fig.2.2**). The absorption at 520nm of this complex is proportional to the creatinine concentration.

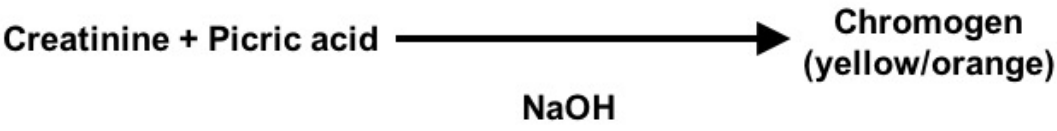

Figure 2.2. Creatinine assay principle.

2.1.7 Plasma and Urine Biochemistry: Glucose

Glucose concentrations were measured using a glucose oxidase assay (Huggett and Nixon, 1957). Glucose standards at 0, 2.5, 5, 7.5, 10, 12.5, 15 and 20 mM were prepared. Standards and samples (1µl) were added to 20µl distilled water and 160µl of glucose oxidase reagent (phosphate buffered saline (PBS, Sigma Aldrich, Dorset, UK), 0.025% (w/v) glucose oxidase, 0.00006% (w/v) peroxidise and 0.0001% (w/v) o-dianisidine) and left at room temperature for 1 hour before reading absorbance at 450nm. The principle of this assay is based upon the conversion of glucose to gluconic acid and hydrogen peroxide (H_2O_2) by glucose oxidase. This is then followed by the oxidation of o-dianisidine which leads to a colour change to orange/brown (**Fig.2.3**).

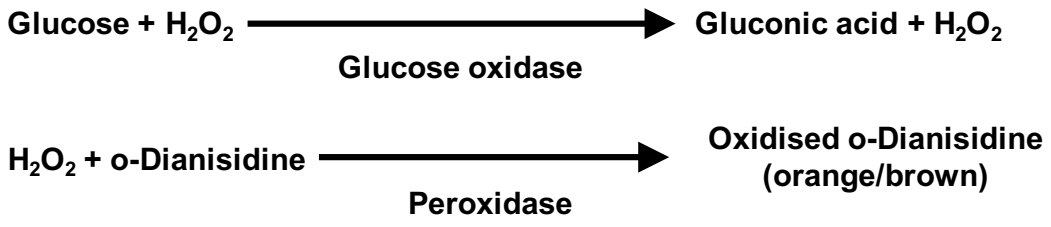

Figure 2.3. Glucose assay principle.

2.1.8 Plasma and Urine Biochemistry: Phosphate

Phosphate concentrations were measured using a phosphate colorimetric assay kit (BioVision, California, US) according to the manufacturer's instructions. This assay utilises complex formation between malachite green and ammonium molybdate with phosphate ions to form a chromogenic complex which can be measured at 650nm (**Fig.2.4**).

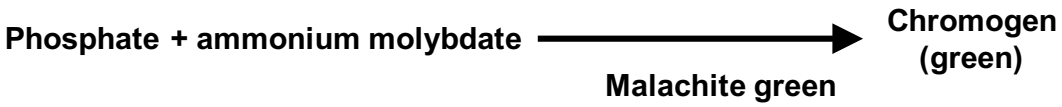

Figure 2.4. Phosphate assay principle.

2.2 Reverse Transcription Polymerase Chain Reaction (RT-PCR)

2.2.1 RNA Extraction

Whole mouse kidneys were harvested and the surrounding capsule was removed. Intestinal contents were removed and the mucosa was collected from defined regions of the intestinal tract; duodenum (beginning at the stomach and ending at the ligament of Treitz), jejunum (beginning from the ligament of Treitz and ending at half the length of the remaining small intestine), ileum (the remaining distal section of the small intestine ending at the cecum) and the colon (beginning at the cecum to the end of the intestinal tract). Each of the intestinal segments were flushed through with ice-cold saline to remove contaminants, opened up along an ice-cold glass surface and then, using glass microscope slides, the mucosa was scraped away. Both kidney and intestinal tissues were immediately snap frozen in RNAlater Stabilization Solution (ThermoFisher Scientific, Paisley, UK). Total RNA was extracted using TRIzol reagent (Ambion Life Technologies, ThermoFisher Scientific, Paisley, UK) according to the manufacturer's instructions, using 100mg of tissue following homogenisation in liquid nitrogen with a pestle and mortar. The concentration and purity of the extracted RNA was determined using the Nanodrop (Bio-Rad Laboratories Ltd, Hemel Hempstead, UK).

2.2.2 cDNA Synthesis

One microgram of isolated RNA was subjected to DNase treatment using a DNase I Amplification kit (Invitrogen Life Technologies, Paisley, UK) according to the manufacturer's instructions. This was followed by cDNA synthesis using a qPCRBIO cDNA synthesis kit (PCR Biosystems, London, UK) according to the manufacturer's instructions. A reverse transcriptase negative control was included for all samples.

2.2.3 RT-PCR

All primers used for RT-PCR were purchased from Qiagen (Qiagen, Manchester, UK) or Sigma (Sigma Aldrich, Dorset, UK) and are described in **Tables.2.2** and **2.3**. RT-PCR was performed in duplicates, alongside a non-template negative control and the housekeeping gene β-actin using the qPCRBIO SyGreen Mix Lo-ROX (PCR Biosystems, London, UK) on a LightCycler96 (Roche Diagnostics Ltd, West Sussex, UK). RT-PCR cycle conditions are described in **Table.2.4.** All data collected were normalised to β-actin.

2.2.4 Agarose Gel Electrophoresis

In order to determine successful RNA extraction and primer efficiency, RNA and final RT-PCR products were run via agarose gel electrophoresis. For RNA samples, the gel was prepared by dissolving 1% (w/v) agarose in 150ml 1x TAE (40mM TRIS-Base, 20mM acetic acid, 1mM EDTA, pH 8.3), with the addition of 5µl (0.003% (v/v)) ethidium bromide solution (Gibco BRL, ThermoFisher Scientific, Paisley, UK) for visualisation of samples upon imaging. For RT-PCR products, a 2% (w/v) agarose gel was prepared. To assist sample loading and visualise migration, RNA sample-loading buffer

(without ethidium bromide, Sigma Aldrich, Dorset, UK) was added to the extracted RNA samples, and for RT-PCR products a 5x loading dye (5x DNA loading buffer, blue, Bioline, London UK) was added. One kb or 100 bp ladders (New England Biolabs, Herts, UK) were run alongside samples as size markers. Samples were run at 75V for 1 hour and imaged with a UV transiluminator (PEQLAB Biotechnologie, Erlangen, Germany).

2.3 Antibodies

All primary and secondary antibodies used in immunofluorescence and western blot applications have been described in **Table.2.5 and 2.6**, respectively, including their source, dilution and species specificity.

Primer (Assay) Name	Gene	Target species	Catalog number	Amplicon length (bp)
Mm_Prkwnk1_1_SG	WNK1	Mouse	QT00170604	64
Mm_Prkwnk4_1_SG	WNK4	Mouse	QT00109403	77
Mm_Slc12a3_1_SG	NCC	Mouse	QT00110600	112
Mm_Klhl3_2_sg	KLHL3	Mouse	QT01056657	131
Mm_Cul3_1_SG	CUL3	Mouse	QT00108010	150
Mm_Slc9a3_2_SG	NHE3	Mouse	QT01039829	101
Mm_Slc5a1_1_SG	SGLT1	Mouse	QT00112679	120
Rn_RGD:620889_1_SG	NaPi-IIb	Rat	QT00188594	83
Rn_Slc34a3_1_SG	NaPi-IIc	Rat	QT00185633	125
Mm_Slc12a1_2_SG	NKCC2	Mouse	QT02521057	150
Mm_Scnn1g_1_SG	ENaC-γ	Mouse	QT00126168	81
Mm_Slc26a4_1_SG	Pendrin	Mouse	QT00131908	77
Mm_Slc4a8_1_SG	NDCBE	Mouse	QT00138621	115
Mm_Slc2a2_1_SG	GLUT2	Mouse	QT00103537	105
Mm_Actb_1_SG	Actin	Mouse	QT00095242	149

Table 2.2. Qiagen primers utilised for RT-PCR.

Gene	Accession number	Forward sequence	Reverse sequence	Target species	Amplicon length (bp)
NaPi-IIa	NM_013030	951 - 969	1315 - 1300	Rat	364
PiT1	NM_031148	768 - 787	1007 - 988	Rat and mouse	239
SGLT2	NM_022590	838 - 857	1088 - 1069	Rat	231

Table 2.3. Sigma primers utilised for RT-PCR.

Stage	Condition
Pre-incubation Denaturation	95°C, 600 seconds
Three-step Amplification Primer annealing and extension cDNA synthesis	95°C, 10 seconds
	60°C, 10 seconds
	72°C, 10 seconds – 35 cycles
Melting Reaction termination	95°C, 10 seconds.

Table 2.4. Conditions used for RT-PCR.

2.4 Immunofluorescence

2.4.1 Perfusion Fixation

Anesthetised mice were perfused, via transcardial perfusion, through the left ventricle with heparin sodium in 0.9% saline (1000units/ml, Workhardt, Wrexham, UK), followed by 4% (w/v) paraformaldehyde (PFA) in PBS. Kidney tissue was harvested and post-fixed in 4% PFA/PBS overnight at 4°C.

2.4.2 Paraffin-embedding

PFA-fixed tissue was washed in distilled water for 1 hour at room temperature followed by sequential incubations in increasing concentrations of isopropanol; 50%, 75%, 90%, and 100% (v/v), every 2 hours at room temperature, before an overnight incubation in equal parts 100% isopropanol and melted paraffin (Sigma Aldrich, Dorset, UK) at 62°C. Tissue was then placed in pure melted paraffin at 62°C for up to 2 days to allow the wax to perfuse through the whole tissue, before arranging and setting on a plastic grid for sectioning. Tissues were sectioned using a microtome (HM335E, Microm, Minnesota, USA) at a thickness of 8 – 10μm and mounted onto gelatin-coated slides.

2.4.3 Immunofluorescence Staining

Paraffin-embedded tissues were de-paraffinised in 2 washes of xylene (10 minutes each) and then in short washes (3 – 5 minutes each) of decreasing concentrations of ethanol; 100%, 90%, 70% and 50%, followed by washing in distilled water for 10 minutes and a brief wash in PBS.

Following de-paraffinisation, sections were placed in pre-heated (95 - 100°C) citrate buffer (10mM sodium citrate, pH 6) for 10 minutes, and washed under running water for 10 minutes. The sections were then blocked in 10% donkey serum in PBS for 30 minutes. After blocking and washing with PBS, the sections were incubated with primary antibody in PBS or block, alongside a negative control (PBS or block only), at a 1:100 dilution overnight at 4°C. As an additional control, primary antibodies were incubated alongside a marker for defined regions of the renal tubule (calbindin for the DCT or AQP2 for the CD). After subsequent washing with PBS (3x 5 – 10 minutes), sections were then incubated with their corresponding secondary antibodies at a 1:1000 dilution in PBS for 1 hour at room temperature in the dark, washed with PBS (3x 5-10 minute washes) and mounted with mounting medium (Vectashield hardest mounting medium, Vector Laboratories Ltd, Peterborough, UK).

2.4.4 Confocal Microscopy

Fluorescence signals were detected with a Leica DMI4000b fluorescence microscope (Leica Microsystems, Milton Keynes, UK). Confocal images were captured using a Nikon Eclipse Ti inverted confocal microscope (Nikon UK Ltd, Surrey, UK) and analysed using the NIS-elements (Nikon UK Ltd, Surrey, UK) and ImageJ (ImageJ, Maryland, USA) software.

Primary antibodies					
Name	**Company**	**Catalog Number**	**Species**	**Dilution**	**Species Specificity**
Calbindin (D28K)	Santa Cruz Biotechnology, Heidelberg, Germany	sc-7691	Goat polyclonal	1:100	Mouse Human
Phospho-NCC Threonine 58 (pNCC T58)	A kind gift from Omar Tutakhel and Dr Rene Bindels, Physiomics Radboud University, The Netherlands	N/A	Rabbit polyclonal	1:100	Mouse Human
Secondary antibodies					
Alexa-Fluor 488 Donkey anti-rabbit	Invitrogen, ThermoFisher Scientific, Paisley, UK	A21206		1:1000	Mouse Human
Alex-Fluor 594 Donkey anti-goat	Invitrogen, ThermoFisher Scientific, Paisley, UK	A11058		1:1000	Mouse Human

Table 2.5. Primary and secondary antibodies used for immunofluorescence.

Primary antibodies					
Name	**Company**	**Catalog Number**	**Species**	**Dilution**	**Species Specificity**
β-Actin	Santa Cruz Biotechnology, Heidelberg, Germany	sc-69879	Mouse monoclonal	1:500	Mouse Human
AIP1/ALIX	Merck Millipore, Hertfordshire, UK	ABC40	Rabbit polyclonal	1:500	Human
α-ENaC	StressMarq Biosciences, Victoria, Canada	SPC-403D	Rabbit polyclonal	1:1000	Mouse Human
GLUT2	Santa Cruz Biotechnology, Heidelberg, Germany	sc-7580	Goat polyclonal	1:1000	Mouse
Na+K+ATPase-α	Santa Cruz Biotechnology, Heidelberg, Germany	sc-28800	Rabbit polyclonal	1:1000	Mouse Human
NaPi-IIa	A kind gift from Prof. Carsten Wagner and Dr. Nilufar Moebbi, University of Zurich, Switzerland	N/A	Rabbit polyclonal	1:3000	Mouse Human
NaPi-IIb	A kind gift from Prof. Carsten Wagner and Dr. Nilufar Moebbi, University of Zurich, Switzerland	N/A	Rabbit polyclonal	1:2000	Mouse Human
NaPi-IIc	Abcam, Cambridge, UK	ab155986	Rabbit monoclonal	1:1000	Mouse
NHE3	Santa Cruz Biotechnology, Heidelberg, Germany	sc-16103-R	Rabbit polyclonal	1:1000	Mouse
NCC	MRC Protein Phosphorylation Unit, Dundee, UK	S703C	Sheep polyclonal	1:500	Mouse Human
Phospho-NCC Threonine 60 (pNCC T60)	MRC Protein Phosphorylation Unit, Dundee, UK	S995B	Sheep polyclonal	1:300	Mouse Human

NKCC2	MRC Protein Phosphorylation Unit, Dundee, UK	S838B	Sheep polyclonal	1:1000	Mouse
Phospho-NKCC2	A kind gift from Prof. Carsten Wagner, University of Zurich, Switzerland	N/A	Rabbit Polyclonal	1:1000	Mouse
PiT1	Custom-made antibody from Davids Biotechnolgie, Regensburg, Germany Targeted for the rat Pit1 sequence: SLVAKGQEGIKWSELIK	N/A	Rabbit polyclonal	1:100	Mouse
SGLT1	Santa Cruz Biotechnology, Heidelberg, Germany	sc-20584	Goat polyclonal	1:1000	Mouse
SGLT2	Santa Cruz Biotechnology, Heidelberg, Germany	sc-98975	Rabbit polyclonal	1:1000	Human
SGLT2	Santa Cruz Biotechnology, Heidelberg, Germany	sc-47402	Goat polyclonal	1:1000	Mouse
Anti-TSG101	AbCam, Cambridge, UK	ab83	Mouse monoclonal	1:500	Human
Secondary antibodies					
Donkey anti-goat	Santa Cruz Biotechnology, Heidelberg, Germany	sc-2033		1:1000	Mouse Human
Donkey anti-rabbit	GE Healthcare Life Sciences, Buckinghamshire, UK	NA9340V		1:1000	Mouse Human
Rabbit anti-sheep	Invitrogen Life Technologies, Paisley, UK	618620		1:1000	Mouse Human
Goat anti-mouse	Sigma Aldrich, Dorset, UK	A4416		1:5000	Mouse Human

Table 2.6. Primary and secondary antibodies used for Western blotting.

2.5 Western Blot Analysis

2.5.1 Tissue Lysis and Preparation

Snap frozen mouse kidney and intestinal muscosal tissues were thawed and homogenised using a turrax homogeniser (Ultra Turrax homogeniser, Janke & Kunkel, Staufen, Germany), on ice, in homogenisation buffer (300 mM sucrose, 5 mM EDTA, pH 7.5) containing phosphatase and protease inhibitors (1x cOmplete mini (Roche Life Sciences, West Sussex, UK), 1x PhosSTOP (Roche Life Sciences, West Sussex, UK) and 3 mM phenylmethanesulfonyl fluoride (PMSF)) at setting 10 for 1 minute and 30 seconds. Homogenates were centrifuged at 2000 x g for 1 minute at 4°C, followed by addition of 1% Triton X-100 and incubation for 10 minutes at 4°C. Samples were then centrifuged at 2000 x g for 5 minutes at 4°C. A sample of the resulting supernatant (taken as the whole cell/ post-nuclear supernatant (PNST) fraction) was stored at -80°C, and the remaining supernatant was subjected to ultracentrifugation using the Beckman Coulter Optima MaxX-XP ultracentrifuge (Beckman Coulter, High Wycombe, UK), at 150,000 x g for 45 minutes at 4°C. The resulting supernatant was kept as the cytosolic fraction and the final pellet was resuspended and sonicated in 200 µl distilled water using an ultrasonic processor (UP200S, Hielscher Ultrasounnd Technology, Teltow, Germany), both fractions were stored at -80°C and protein concentrations were determined using the Bradford protein assay.

2.5.2 Kidney Brush Border Membrane Vesicle (BBMV) Preparation

Renal BBM vesicles were prepared as described previously (Biber et al., 1981). All buffers used in this preparation were supplemented with Kallikrein inhibitor units (KIU) aprotinin (Nordic Pharma, Reading, UK) and 0.085% (w/v) PMSF/DMSO protease inhibitors and kept at 4°C. Snap frozen mouse kidneys were thawed, weighed and submerged in homogenising buffer containing; 300mM mannitol, 5mM ethylene glycol-bis(2-amino-ethylether)-

N,N,N',N'-tetraacetic acid (EGTA), 12mM Tris/HCl, pH 7.4, at a 20ml per g ratio. The kidneys were then homogenised, using a turrax homogensiser, at half speed for 2 minutes on ice, followed by the addition of cold distilled water (at a 28ml per 20ml of homogenising buffer used) and $MgCl_2$ (from a 1.2M stock) to a final concentration of 12mM, and stirred (at low speed) on ice for 15 minutes. Prior to the addition of $MgCl_2$, a sample of the homogenate fraction was kept. The solution was then centrifuged at 2000 x g for 15 minutes at 4°C and the supernatant re-centrifuged at 33,000 x g for 30 minutes at 4°C. The resulting pellet was resuspended in resuspension buffer 1 containing; 150mM mannitol, 2.5mM EGTA, 6Mm Tris/HCl, pH 7.4, using a hand-operated glass-Teflon homogeniser for about 10 cycles. $MgCl_2$ was added to a final concentration of 12mM and stirred on ice for 15 minutes. The low and high-speed centrifugations as described above were repeated. The resulting pellet was then resuspended in resuspension buffer 3 containing; 300mM mannitol, 2.5mM EGTA and 12mM Tris/HCl, pH 7.4, using a hand-operated homogeniser and centrifuged at 33,000 x g for 30 minutes at 4°C. The final pellet, containing the BBM vesicles was resuspended in resuspension buffer 3 to a protein concentration of 3 – 6mg/ml using 10-12 passes through a pipette tip. The protein concentration and activity of alkaline phosphatase for the initial homogenate fraction and BBM vesicles were determined to confirm enrichment of this marker enzyme. All fractions were stored at -80°C.

2.5.3 Intestinal Brush Border Membrane Vesicle Preparation

Intestinal BBM vesicles were prepared from the proximal (duodenum and jejunum fractions) and distal (ileum) segments as described previously (Kessler et al., 1978). All buffers used in this preparation were supplemented with EDTA-free protease inhibitor (Roche Life Sciences, West Sussex, UK) and kept at 4°C. Mucosal samples were added to homogenising buffer containing; 50mM mannitol, 2mM 4-(2-hydroxyethtl)-1-

piperazineethanesulfonic acid (HEPES), pH 7.1, at a 28ml per g ratio, and homogenised, using the turrax homogeniser, at half speed three times for 20 seconds followed by 5 second intervals in between. A sample of the homogenate fraction was kept. $MgCl_2$ (from a 1M stock) was added to a final concentration of 10mM and stirred (at low speed) on ice for 20 minutes. The solution was then centrifuged at 4600 x g for 10 minutes at 4°C and the supernatant re-centrifuged at 41,600 x g for 30 minutes at 4°C. The resulting pellet was resuspended, using 10-12 passes through a pipette tip, in resuspension buffer containing; 300mM mannitol, 20mM HEPES, 0.1mM $MgSO_4$, pH 7.2, at a 20ml per g ratio. The suspension was centrifuged at 9300 x g for 15 minutes at 4°C and the supernatant re-centrifuged at 41,600 x g for 30 minutes at 4°C. The final pellet, containing the BBM vesicles, was resuspended in resuspension buffer to a protein concentration of 3 – 6mg/ml using 10 – 12 passes through a pipette tip. The protein concentration and activity of alkaline phosphatase for the initial homogenate fraction and BBM vesicles were determined to confirm enrichment of this marker enzyme. All fractions were stored at -80°C.

2.5.4 Protein Quantification

Protein concentrations of the different fractions were measured using the Bradford protein assay (Bradford, 1976). Standards at; 0, 0.15, 0.30, 0.45, 0.60, 0.75 and 0.9mg/ml, were prepared from stock solutions of BSA (1mg/ml) in 0.1M NaOH. Samples were diluted either at 1:10 or 1:100 in 0.1M NaOH. Both standards and protein samples (5µl) were added to 200µl Bradford reagent (0.01 % (w/v) Coomassie brilliant blue g-250, 5% (v/v) ethanol and 10% (v/v) orthophosphoric acid) and the absorbance was read at 595nm. The principle of this assay is based on the binding of proteins to coomassie dye, under acidic conditions, resulting in a colour change from brown to blue (**Fig.2.5**). The absorption at 595nm of this complex is proportional to the protein concentration.

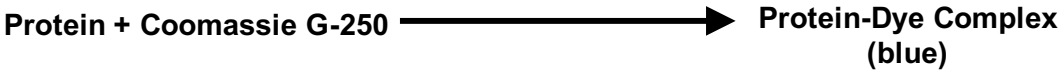

Figure 2.5. Bradford assay principle.

2.5.5 Alkaline Phosphatase Assay

In order to ensure the kidney and intestinal BBM vesicles extracted were free from contamination from basolateral membrane and subcellular components, an alkaline phosphatase assay was used to calculate an enrichment value for this enzyme in the BBM vesicles, relative to the initial homogenate, as a measure of purity. Alkaline phosphatase activity was measured as previously described (Forstner et al., 1968) in the initial homogenate, at a 1:1 dilution in distilled water (1:20 for proximal and 1:1 for distal small intestinal samples), and in the final BBM vesicles, at a 1:20 dilution (1:200 for proximal and 1:20 for distal small intestinal samples). Standards at 0, 50, 100, 150, 200, 250 and 300nM of p-Nitrophenol (p-NP) were prepared. Following sample and standard preparations, 50μl of each (in duplicates) were transferred to a fresh tube and 250μl of alkaline substrate buffer (0.652% (w/v) p-Nitrophenyl phosphate (p-NPP) dissolved in buffer containing; 50mM glycine, 5mM $MgCl_2$, 1mM zinc acetate, pH 9.4) was added. The standards and samples were incubated at 37°C for 15 minutes before terminating the reaction with the addition of 1.25ml of 0.001M NaOH. The solutions were transferred to a 96-well plate and absorbance was read at 405nm. The principle of this assay is based on the rate of hydrolysis of the p-NPP substrate by alkaline phosphatase, under alkaline conditions, to produce p-Nitrophenol, which gives a yellow colour change (**Fig.2.6**). BBM vesicle and homogenate alkaline phosphatase activity and protein concentrations were used to calculate the enrichment factor (**Fig.2.7**).

Figure 2.6. Alkaline phosphatase assay principle.

$$\text{Enrichment Factor} = \frac{\text{BBM Vesicle Alkaline Phosphatase}}{\text{BBM Vesicle Protein}} \times \frac{\text{Homogenate Protein}}{\text{Homogenate Alkaline Phosphatase}}$$

Figure 2.7. Enrichment factor calculation.

An enrichment value between 6 – 8 for kidney and 10 – 15 for intestinal BBM vesicles were regarded as pure.

2.5.6 Sodium Dodecyl Sulphate Polyacrylamide Gel Electrophoresis (SDS-PAGE)

Mouse kidney and intestinal PNST, cytosolic and membrane lysates (at 50 – 100µg), human cortex PNST (at 25µg), BBM vesicles (at 20 - 30µg) and homogenate (at 30 - 50µg) protein samples were solubilised in 2x Laemmli sample buffer (BioRad, Hemel Hempstead, UK) in a 1:1 buffer: sample ratio and run on a 10% SDS-PAGE gel (AE-6530M mPAGE electrophoresis tank, LabTech International Ltd, East Sussex, UK) in running buffer (25mM TRIS-Base, 200mM glycine, 0.1% (v/v) SDS) at 20mA per gel for about 1 hour. Protein samples were run alongside a kaleidoscope prestained SDS-PAGE standard molecular weight marker (BioRad, Hemel Hempstead, UK). Separated proteins were transferred onto a methanol-activated

polyvinylidene difluoride (PVDF) membrane (Bio-Rad, Hemel Hempstead, UK) using a BioRad trans-blot SD semi-dry transfer cell (BioRad, Hemel Hempstead, UK), in transfer buffer (25mM TRIS-BASE, 200mM glycine, 0.1% (v/v) SDS, 10% (v/v) methanol), at 15V for 1 hour 15 minutes. Membranes were blocked in 6% (w/v) milk in PBS-Tween (PBST, 0.1% (v/v) Tween20 in PBS) for 1 hour at room temperature and then rinsed in PBST, followed by an overnight incubation with primary antibody (**Table.2.6**) in PBST at 4°C. Membranes were washed with PBST (1x 15 minutes, 3x 5 minutes) followed by a 1 hour incubation with the corresponding secondary antibody (**Table.2.6**) in PBST at room temperature, the membranes were then washed again with PBST (1x 15 minutes, 3x 5 minutes). To visualise, enhanced chemiluminescence solution (ECL, 2.5mM 3-aminophthalhydrazide, 0.4mM p-coumaric acid, 100mM Tris-HCl, 200mM NaCl, 30% hydrogen peroxide, pH 8.5) was added over the membrane and detected using a BioRad Fluor-S MultiImager (BioRad, Hemel Hempstead, UK). Densitometry was measured using the BioRad Multi-Analyst software (Bio-Rad, Hemel Hempstead, UK) and analysed using the Graphpad Prism software.

Following visualisation, membranes were stripped in stripping buffer (Takara Bio Europe SAS, France) for 5 – 10 minutes at room temperature, followed by washing in PBST (3x 5 minutes), and then blocked in 6% (w/v) milk/PBST. The membrane was then re-probed for β-actin.

2.5.7 Gel Staining: Silver Nitrate

Following SDS-PAGE, gels were placed in fixing solution (40% (v/v) ethanol, 10% (v/v) acetic acid) for 35 minutes, followed by washing in distilled water for 30 minutes – overnight. Gels were sensitised in 0.02% (w/v) sodium thiosulfate for 1 minute and then washed in distilled water. Cold silver nitrate solution (0.1% (w/v) silver nitrate supplemented with 0.02% (v/v)

formaldehyde) was added and incubated for 20 minutes and then washed again in distilled water. Developing solution (3% (w/v) sodium carbonate supplemented with 0.01% (v/v) formaldehyde) was added until sufficient staining was achieved, after which, staining was terminated by transferring the gel to a 5% acetic acid (v/v) solution and stored in 1% acetic acid (v/v) solution.

2.6 Clinical Studies

2.6.1 Ethical approval

The protocols used in this study received full ethical approval from the Royal Free Hampstead NHS Trust, NHS Research Ethics Committee (Project ID: 7727) and informed consent was received from all patients and control subjects. Twelve patients who had previously undergone renal transplantation and were currently being administered tacrolimus were recruited; these patients were receiving an oral dosage between 2 – 10mg, twice a day. Alongside, four patients diagnosed with Gitelman syndrome were also recruited. All patients and controls were age- and gender-matched to avoid bias (**Table.2.7 and 2.8**).

2.6.2 Human Plasma and Urine Biochemistry

Blood and urine samples were routinely collected on the day of renal biopsies (for CNI-treated renal transplant patients) and analysed by the Department of Clinical Biochemistry (Royal Free Hospital, London, UK).

2.6.3 Urinary Exosome Isolation

Urine samples were collected from patients and age-/gender-matched healthy subjects. Protease inhibitors (cOmplete Protease Inhibitor Cocktail,

Roche Diagnostics Ltd, West Sussex, UK) were immediately added to the urine samples and stored at -80°C. Twenty millilitres or 100 ml of collected urine was centrifuged at 17,000 x g for 15 minutes at 25°C (Allegra 64R Centrifuge, Beckman Coulter, High Wycombe, UK). The supernatant was transferred to ultracentrifuge tubes, whilst the pellet was re-suspended with 200µl isolation solution (250mM sucrose, 10mM triethanolamine-HCL, pH 7.6) and 50µl 3.24M dithiothreitol (DTT), incubated at room temperature for 2 minutes, vortexed thoroughly and then centrifuged at 17,000 x g for 15 minutes at 25°C. The resulting supernatant was collected and combined with the supernatant obtained from the previous spin and centrifuged at 200,000 x g for 2 hours at 25°C. The supernatant was discarded and the final exosome pellet was dissolved in 100µl of 2x laemmli sample buffer. All samples were stored at -80°C until further use. Urinary creatinine levels were determined for normalisation between samples and, prior to gel loading, samples were heated at 65°C for 15 minutes.

ID Number	Patient		Matched Control	
	Gender	Age (Years)	Gender	Age
1	M	33	M	33
2	M	39	M	41
3	M	37	M	33
4	M	39	M	34
5	M	56	M	55
6	M	41	M	45
7	M	46	M	46
8	M	62	M	55
9	M	71	M	63
10	F	27	F	27
11	F	32	F	31
12	F	32	F	31

Table 2.7. Age- and gender-matched controls for renal transplant patients currently receiving CNI medication.

ID Number	Patient		Matched Control	
	Gender	Age (Years)	Gender	Age
1	F	35	F	31
2	F	39	F	35
3	F	43	F	44
4	M	34	M	34

Table 2.8. Age- and gender-matched controls for Gitelman syndrome patients.

2.7 Statistical analysis

The data are summarised as the mean ± standard error of the mean (SEM). An N number of 5 – 6 samples were used for each treatment group. Statistical analysis was performed using the GraphPad Prism software (GraphPad Prism, California, USA). Unpaired T-test was used for comparisons between two groups and, for multiple comparisons, a one-way ANOVA with the Bonferroni post-test was used. Significance was represented as: *P < 0.05, **P < 0.01, ***P < 0.001.

Chapter III
The effects of calcineurin inhibitors on renal and intestinal sodium transport

3.1 Introduction

3.1.1 Sodium retention via the WNK-SPAK/OSR1-NCC pathway in Pseudohypoaldosteronism II and CNI treatment

The WNK-SPAK/OSR1 signalling pathway has been extensively proven to be an important regulator of blood pressure. Its involvement in PHAII pathogenesis is the result of increased sodium reabsorption via activation of the thiazide-sensitive sodium chloride cotransporter, NCC. Mutations in WNK1 and WNK4 kinases were first identified as responsible for PHAII. These mutations result in an increase in their protein levels, and ultimately, activation of downstream signalling (Wilson et al., 2001). Two additional PHAII-causing genes, KLHL3 and CUL3, were later identified (Boyden et al., 2012; Louis-Dit-Picard et al., 2012), however, their contribution to the PHAII phenotype is due to the inability to maintain intracellular WNK4 levels via ubiquitination/degradation (Mori et al., 2013; Shibata et al., 2013; Wakabayashi et al., 2013; Wu and Peng, 2013). The consequence of these mutations is the enhanced activation of the WNK-SPAK/OSR1 signalling pathway, which leads to increased NCC expression at the apical membrane of the DCT where it facilitates sodium reabsorption and contributes to elevated blood pressure.

Numerous mouse models of PHAII have been generated and have confirmed these conclusions (Chiga et al., 2011; Susa et al., 2014; Wakabayashi et al., 2013; Yang et al., 2010a, 2007). PHAII WNK4$^{D561A/+}$ and KLHL3$^{R538H/+}$ knock-in mouse models display impaired WNK4 degradation via the loss of WNK4-KLHL3/CUL3 interactions, which is paralleled with increased WNK4 protein

as well as the phosphorylated forms of SPAK, OSR1 and NCC (Susa et al., 2014; Wakabayashi et al., 2013). Further studies also showed that these PHAII phenotypes and augmented apical expression of pNCC could be restored upon partial interruption of the signalling between WNK and SPAK/OSR1 kinases (Chiga et al., 2011; Chu et al., 2013; McCormick et al., 2011; Rafiqi et al., 2010; Yang et al., 2010b).

As already mentioned, CNIs have been demonstrated to induce hypertension by enhanced NCC activation leading to increased sodium retention and reabsorption (Hoorn et al., 2011; Melnikov et al., 2011). FK506-treated mice exhibited all the clinical features of PHAII as well as increased phosphorylation and apical expression of NCC and its upstream regulators WNK4 and SPAK (Hoorn et al., 2011). This was also explored further in clinical settings, where immunohistochemical analysis of renal biopsies from CNI-treated renal transplant recipients showed increased pNCC localisation at the apical membrane of the DCT (Hoorn et al., 2011). With these findings in mind, using this model of an acquired form of PHAII, the detailed pathogenic mechanisms of both PHAII and post-transplant hypertension onset can be studied and, in particular, the role for calcineurin in blood pressure and sodium homeostasis.

3.1.2 WNK-SPAK/OSR1 regulation of renal and intestinal sodium transporters

It is well known that the downstream targets of WNK-SPAK/OSR1 kinases include the NCC and NKCC transporters (Anselmo et al., 2006; Dowd and Forbush, 2003; Moriguchi et al., 2005; Ponce-Coria et al., 2008; Richardson et al., 2008, 2011; Vitari et al., 2006). In addition to these, SPAK and/or OSR1 are also known to regulate the function of other sodium-coupled transporters and channels in the kidney and gastrointestinal tract.

This includes the renal and intestinal Na^+/Pi cotransporters, NaPi-IIa and NaPi-IIb, respectively (Fezai et al., 2015; Pathare et al., 2012a). Voltage clamp experiments in oocyte expression models injected with cRNA encoding NaPi-IIa showed a significant up-regulation of phosphate-induced currents following co-expression with OSR1 (Pathare et al., 2012a). Additional *in vivo* analysis in WNK-resistant OSR1 mice, revealed decreased serum phosphate concentrations and increased urinary phosphate excretion, which was paralleled by a significant reduction in NaPi-IIa protein abundance at the BBM (Pathare et al., 2012a), specifying OSR1 as a stimulator of NaPi-IIa in the kidney. More recent voltage clamp oocyte experiments have also identified SPAK and OSR1 kinases as stimulators of the intestinal NaPi-IIb transporter (Fezai et al., 2015).

Studies using these WNK-resistant OSR1 mice have also shown that the sodium transport function of the NHE3 exchanger is altered in the small intestines (Pasham et al., 2012). Measurements of transport activity in these mutant mice showed higher intestinal NHE3 activity in comparison to wild-type littermates (Pasham et al., 2012), proposing OSR1 as a potential negative regulator of NHE3. Furthermore, co-expression studies with oocytes have reported that WNK4 inhibits ENaC and that this inhibition is reversed in PHAII-causing WNK4 mutations (Ring et al., 2007a). This was likewise observed in Ussing chamber experiments. In the colonic epithelium of PHAII-mutant WNK4 and WNK-insensitive OSR1 mutant mice, an increase in sodium flux and ENaC activity was observed compared to wild-type littermates (Pasham et al., 2012; Ring et al., 2007a). Recently, SPAK was also identified to play a role in the regulation of ENaC activity; oocyte co-expression of ENaC with either wild-type or constitutively active SPAK induced a significant increase in amiloride-sensitive currents but not when co-expressed with WNK-insensitive and catalytically inactive SPAK (Ahmed et al., 2015). Moreover, colonic amiloride-sensitive currents were significantly

lower in WNK-insensitive SPAK mutant mice compared to wild-type littermates (Ahmed et al., 2015), supporting a stimulatory role for ENaC.

Studies in oocytes and mice have also demonstrated SPAK as a negative regulator of the sodium-coupled glucose cotransporter, SGLT1. Co-expression of SGLT1 with wild-type SPAK or constitutively active SPAK caused a significant decrease in glucose-dependent currents, whilst co-expression with WNK-insensitive or catalytically inactive SPAK did not (Elvira et al., 2014). This was paralleled in WNK-insensitive SPAK mutant mice where intestinal electrogenic glucose transport was significantly higher compared to their wild-type littermates. Furthermore, analysis from chemiluminescence experiments indicated that the SPAK-induced inhibition of SGLT1 was attributed to a decrease in SGLT1 insertion into the cell membrane (Elvira et al., 2014).

In summary, these studies not only support the WNK-SPAK/OSR1 signalling pathway as an important regulator of NCC- and NKCC-mediated sodium transport in the kidney, but also implies these kinases participate in the regulation of other epithelial transport processes in both the kidney and gastrointestinal tract. The up- or down-regulation of these sodium-coupled transporters/channels has not been fully investigated under CNI-treated conditions. It is possible that any alterations in these transporters that may occur may contribute further to sodium retention or other clinical abnormalities associated with CNI use.

3.1.3 Aims of this study

In the work described, analyses of sodium-coupled transporters and sodium channels in renal and intestinal tissues were performed in a mouse model of CNI-induced sodium retention. This analysis was conducted at a translational level in vehicle or FK506-treated mice fed either a standard or high-salt diet.

The aims of this chapter were to confirm the previously observed effects of CNIs on sodium and acid-base transport proteins and to investigate the currently unknown effects of CNIs on other renal and intestinal sodium transporters/channels. This was done in order to gain a further understanding as to which transporters might be up- or down-regulated, or even unaffected, in the sodium retentive actions of CNI use. This chapter also aimed to determine whether the sodium-mediated transport of the accompanying electrolyte may contribute to the associated electrolyte abnormalities of CNI-treatment such as metabolic acidosis, hypophosphatemia and hyperglycemia.

3.2 Materials and Methods

3.2.1 Animals

Male C57BL/6J mice, aged 8 weeks (weighing between 20 – 25g), were used in accordance with the Animals Scientific Procedures Act 1986, Amendment Regulations 2012. All protocols were approved by the University College London (Royal Free Campus) Comparative Biology Unit Animal Welfare and Ethical Review Body (AWERB) committee and performed in accordance with project license PPL 70/8064.

3.2.2 FK506 treatment and/or high-salt diet

Full procedures have been described in **Section.2.1.2.** Mice were administered either vehicle or FK506 at a dose of 2 mg/kg/day via I.P injection for two weeks and supplemented with either standard maintenance diet or a high-salt (HS) diet (standard maintenance diet supplemented with 1.5% (w/w) NaCl).

At the end of the experiments, mice were placed under terminal anaesthesia and checked for withdrawal to corneal and pedal reflexes before sample collection. Terminal blood samples were collected by cardiac puncture and urinary samples were collected by bladder puncture. Cervical dislocation was performed and death was confirmed by cessation of heartbeat before removing renal and intestinal tissues.

3.2.3 Plasma biochemistry

Plasma samples were collected, as described in **Section.2.1.4**, and biochemical analysis for sodium, creatinine, glucose and phosphate was performed as described in **Sections 2.1.5 - 2.1.8**.

3.2.4 Immunofluorescence analysis

Anesthetised mice were perfused with 4% PFA/PBS and kidney tissue was harvested, processed, paraffin-embedded, stained and imaged as described in **Section.2.4**, using the primary and corresponding secondary antibodies listed in **Table.2.5**. A negative control was run alongside where the primary antibody was omitted.

3.2.5 Protein preparations from kidney and intestinal mucosa tissues

Protein samples from kidney tissues were prepared using the technique described in **Section.2.5.1,** or subjected to BBM vesicle preparations as described in **Section.2.5.2**. Snap-frozen small intestinal mucosa samples were thawed and subjected to BBM vesicle preparations described in **Section.2.5.3** and large intestinal mucosal samples were processed as described in **Section.2.5.1**. Total protein concentration was determined using the Bradford assay as described in **Section.2.5.4**. For BBMV and homogenate samples, purity was assessed using an alkaline phosphatase assay as described in **Section.2.5.5**.

3.2.6 Western blot analysis

Western blot protocols were carried out as described in **Section.2.5.6**. Whole kidney homogenate (100μg), kidney/small intestinal BBMV (25μg) or kidney/small intestinal homogenate (50 μg), and large intestinal homogenate (100μg) protein samples were run on an SDS-PAGE gel. Samples were then transferred onto a PDVF membrane and incubated with the primary antibody and their corresponding secondary antibodies listed in **Table.2.6**. Following visualisation, membranes were then stripped and re-probed for β-Actin.

Densitometry was measured and samples were normalised to β-actin. Unfortunately, due to the lack of access to overexpressing and/or knockdown mouse models, no further positive or negative controls were used in western blot applications.

3.2.7 Statistical analysis

Data are presented as mean ± SEM, relative to β-actin. N refers to the number of samples within each group. Significance was determined by one-way ANOVA with Bonferroni post-hoc, relative to vehicle-treated mice. *P < 0.05, **P < 0.01, ***P < 0.001.

3.3 Results

3.3.1 Physiological parameters

Mice were administered a daily intraperitoneal injection of 2 mg/kg of FK506 for 14 days and supplemented with either a standard or high-salt (HS) diet. There were no observed differences between groups in mouse survival, gross physical appearance and organ morphology. Body weight was measured daily and body weight changes were calculated to monitor fluctuations during the course of treatment.

Weight gain tended to be higher in the vehicle- and vehicle/HS-treated groups whilst mice treated with FK506 or FK506/HS tended to drop in weight (**Fig.3.1a**). Comparisons of body weight changes between groups on the final day of treatment showed a significantly lower gain in body weight in FK506/HS-treated mice compared to vehicle-treated mice on a standard diet (**Fig.3.1b**). There was also a significant difference, under high-salt conditions, between vehicle and FK506 groups. No significant difference was observed between vehicle- and FK506-treated mice, and mice fed on a high-salt diet suggesting that FK506- or high-salt alone does not affect body weight, whilst a combination likely attributes to the comparably greater reduction in body weight observed. However, this loss in body weight was overall relatively minor (~5% on day 14) and did not exceed the outlined humane endpoint (>20% of initial body weight) and so is unlikely to influence the data outcome.

On both standard and high-salt diets, plasma electrolytes were not significantly different between vehicle and FK506-treated mice (**Table.3.1**), which implies that the FK506 treatment used in this model may not have prompted the clinical phenotypes commonly associated with CNI use. Unfortunately, due to limited volumes of plasma obtained, plasma FK506 levels could not be measured to confirm FK506 delivery and presence in the

circulatory system. Furthermore, plasma potassium and bicarbonate levels could also not be measured to confirm the associated hyperkalemia and metabolic acidosis phenotypes, respectively. Mean plasma creatinine was significantly higher than previously observed in mice using the Jaffe's method (~10-44 µmol/L) (Dunn et al., 2004; Meyer et al., 1985; Palm and Lundblad, 2005). However, this reference range is relatively large and arises from the significant overestimations for plasma creatinine reported with this method due to its low specificity and sensitivity. The use of high-performance liquid chromatography (HPLC) has been recommended for plasma creatinine measurements in rodents (Dunn et al., 2004; Meyer et al., 1985; Palm and Lundblad, 2005). It should also be noted that animals were not placed in metabolic cages and due to the unreliability of urine collection, via bladder puncture, no urinary biochemical analysis could be performed and so any sodium retaining effects caused by FK506 administration cannot be confirmed in this study.

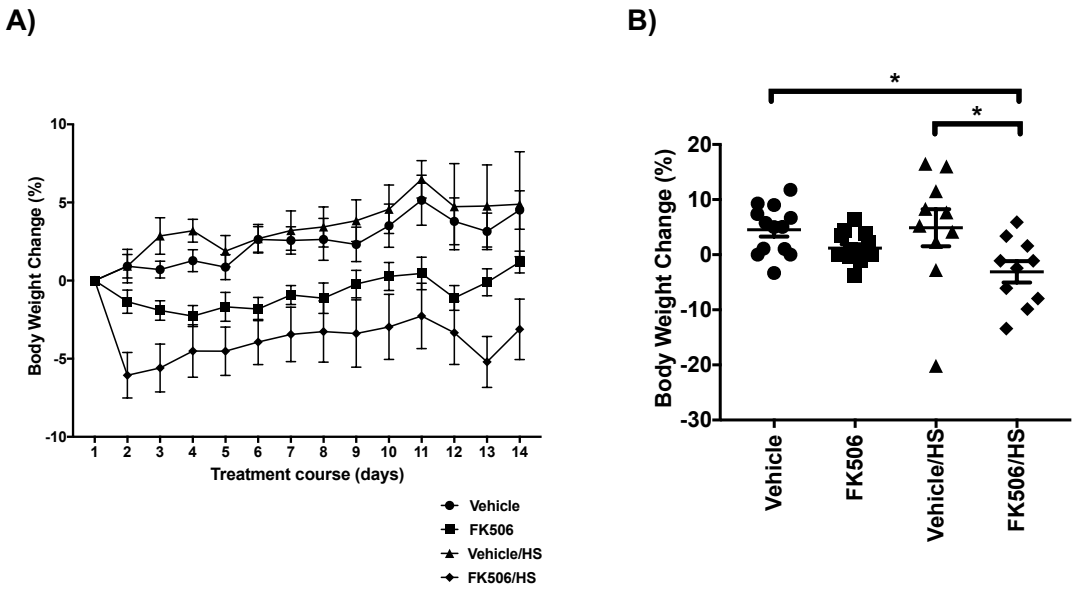

Figure 3.1. Body weight. Vehicle (n = 13), FK506 (n = 14), vehicle/HS (n = 10) and FK506/HS (n = 10) treated mice were weighed daily throughout the course of treatment to monitor changes in body weight. **A)** The change in body weight over the 14-day treatment period with vehicle or FK506 ± high-salt (HS) diet was calculated and compared. **B)** Comparisons of the change in body weight on the final day (Day 14) of treatment. All data are presented as the mean percentage (%) change in body weight, normalised to initial weight at Day 1, ± SEM. Significance was determined by one-way ANOVA with Bonferroni post-test. * $P < 0.05$.

Parameter	Vehicle (N = 13)	FK506 (N = 14)	Vehicle/HS (N = 10)	FK506/HS (N = 10)
Sodium (mmol/L)	142.97 ± 7.36	141.31 ± 10.86	124.43 ± 9.83	132.34 ± 6.25
Glucose (mmol/L)	10.59 ± 0.85	11.31 ± 1.17	10.32 ± 0.63	9.38 ± 1.31
Phosphate (mmol/L)	3.13 ± 0.26	2.73 ± 0.14	2.61 ± 0.10	2.67 ± 0.21
Creatinine (µmol/L)	248.23 ± 21.70	192.67 ± 17.63	246.28 ± 27.13	251.22 ± 41.45

Table 3.1. Plasma biochemistry. Effects of FK506 and HS diet on plasma electrolytes. Values are presented as the mean ± SEM. Significance was determined by one-way ANOVA with Bonferroni post-test, relative to vehicle-injected mice.

3.3.2 NCC/pNCC expression following FK506-treatment

In the present study, direct confirmation of FK506-induced changes in blood pressure, via telemetry devices, were not available. The use of tail cuff measurements was not considered for this study as this method can induce further stress/anxiety on the mice, which may lead to inaccurate results, and also readings obtained from this approach do not reflect central arterial pressure. Therefore, as an indirect measure, the consequential effects of FK506 on sodium reabsorption via the NCC cotransporter was determined. Protein levels for total and phosphorylated NCC (pNCC) were measured in whole kidney tissues from vehicle- and FK506-treated mice fed a standard diet or provided with a high-salt diet with the aim of producing a hypertensive response (Chiga et al., 2008). As shown, no significant changes in total NCC was observed in any of the treatment groups (**Fig.3.2a**). This was also shown for pNCC (**Fig.3.2b**). Unexpectedly, the addition of a high-salt diet with or without FK506 treatment also did not affect pNCC levels (**Fig.3.2b**).

Although the expected increase in pNCC under CNI-induced conditions was not significant in this study, there is an obvious trend for increased pNCC in the FK506-treated group compared to vehicle. To confirm that FK506 was indeed affecting pNCC levels in the kidney and to support and extend the western blot findings, immunohistochemical analysis was performed to compare the effects of FK506 on the abundance and localisation of NCC in the DCT. Low power immunofluorescence revealed a pronounced increase in pNCC staining at the apical membrane in the DCT in FK506-treated mice compared with the vehicle group (**Fig.3.3a**). High power microscopy further confirmed localised pNCC staining to the apical membrane of the DCT, as identified by D28K-positive staining (**Fig.3.3b**). These findings are in line with previous observations and confirm that FK506 is affecting sodium reabsorption in these mice through the up-regulation of pNCC expression at the apical membrane. This confirms the likely establishment of a CNI-

induced sodium retentive, and possibly hypertensive, model for this study and was therefore used for the analysis of other sodium transporters within the kidney and gastrointestinal tract.

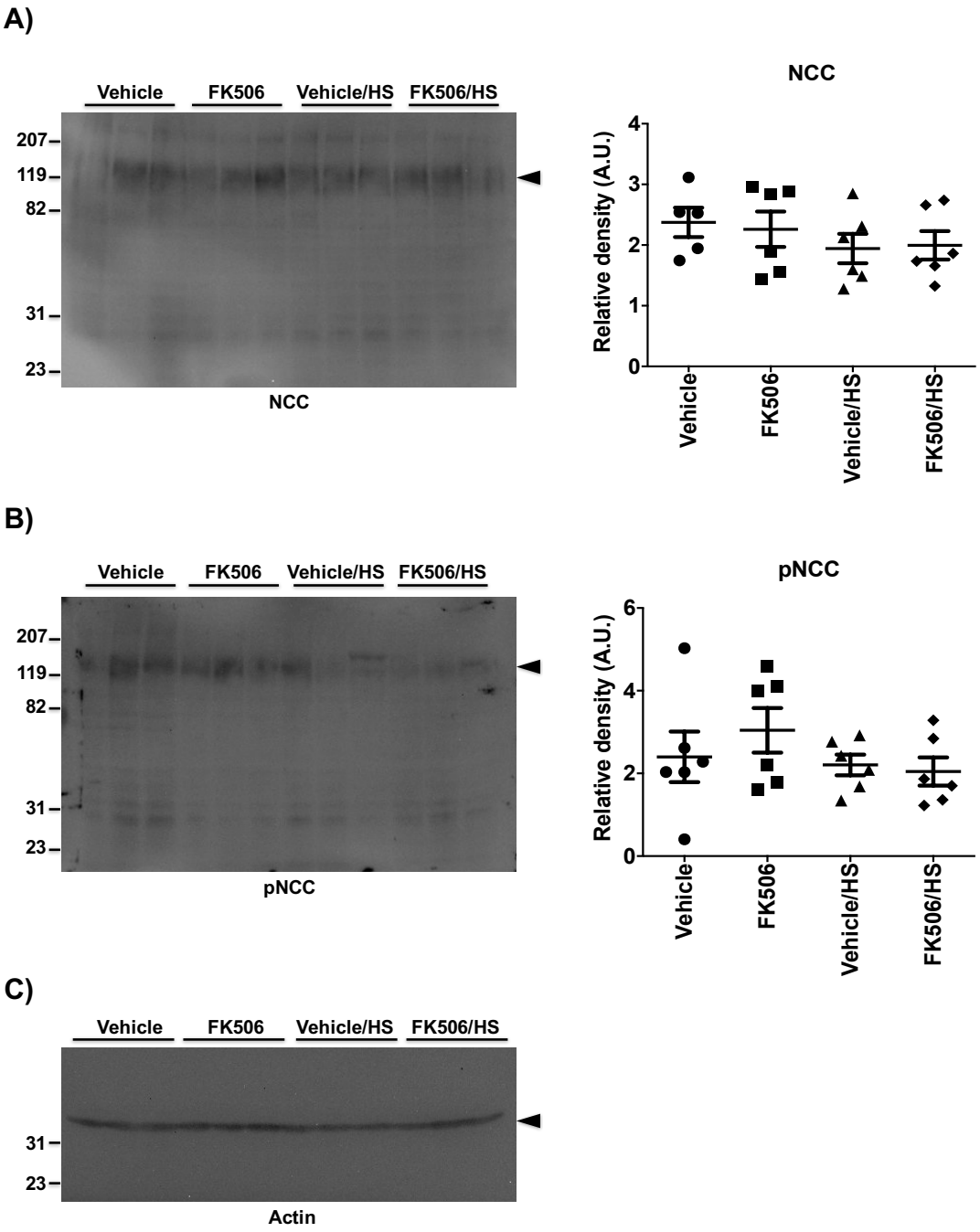

Figure 3.2. Effects of FK506 on the NCC cotransporter. Representative western blots showing the effects of vehicle- or FK506-treatment ± HS diet on **A)** NCC and **B)** phosphorylated NCC protein levels. **C)** β-Actin was run as a loading control. NCC is detected at ~130–160 kDa (*arrow*), pNCC is detected ~130 kDa (*arrow*) and β-actin is detected ~42 kDa (*arrow*). Densitometric analyses (*right*) were performed for each group and normalised to β-actin. Values are presented as the mean ± SEM (n = 5–6). Significance was determined by one-way ANOVA with Bonferroni post-test.

A)

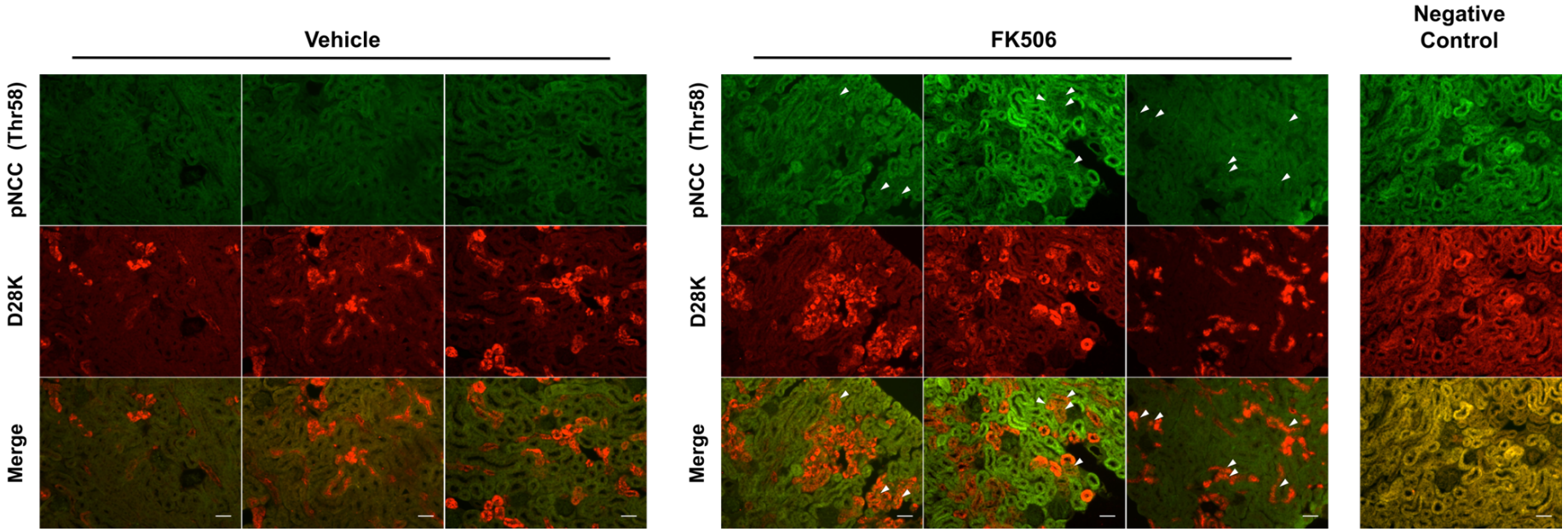
Vehicle
FK506
Negative Control
pNCC (Thr58)
D28K
Merge
pNCC (Thr58)
D28K
Merge

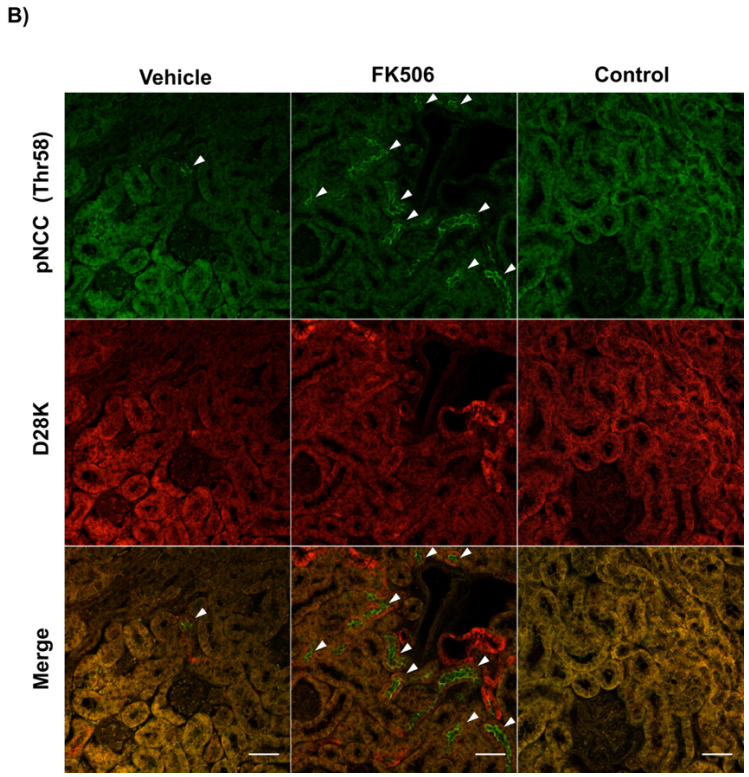

Figure 3.3. Effects of FK506 on NCC phosphorylation and distribution. A) Representative low power immunofluorescence images of renal tissue from vehicle and FK506-treated mice showing pNCC expression and localisation (*arrows*) at the apical membrane colocalised with calbindin (D28K), a marker for DCT tubules. n = 3 per group. Images were taken at a 20x magnification. Negative controls were included whereby the primary antibody was omitted. **B)** Confocal immunofluorescence images of renal tissue from vehicle and FK506-treated mice showing pNCC expression (*arrows*) colocalised with D28K. Images were taken at a 10x magnification. Scale bars measure 50 μm.

3.3.3 Alterations in protein abundance of key sodium transporters in the kidney following FK506 treatment

Alongside NCC and NKCC2, other renal and intestinal sodium-coupled transporters have been reported as downstream targets of the WNK-SPAK/OSR1 cascade and suggests these transporters may also be affected by CNIs. This includes the proximal tubular NHE3 Na^+/H^+ exchanger, the NaPi-IIa and NaPi-IIc type II Na^+/Pi cotransporters and the SGLT2 and SGLT1 Na^+/glucose cotransporters, all of which were investigated in the CNI-treated mouse model. To validate the changes observed for these renal and intestinal sodium transporters, protein analyses were performed using antibodies which have been previously shown in other studies to change under disease conditions in both western blot and immunohistochemistry applications, including SGLT1 in Zucker *fa/fa* obese rats (Aime et al., 2014) and NaPi-IIa in phosphaturia-induced rats (Marks et al., 2008).

The NHE3 exchanger is not only one of the major sodium transporters in the PT but is also a regulator of acid-base balance. Protein dysregulation of NHE3 may therefore potentially contribute to the associated metabolic acidotic side effect of CNI treatment, as well as sodium retention. Western blot and densitometric analyses showed a significant decrease in NHE3 protein abundance in BBMVs of FK506-treated and vehicle/HS-treated mice compared with vehicle-treated mice (**Fig.3.4**).

The NaPi-IIa and NaPi-IIc transporters are also recognised as regulators of acid-base balance and phosphate reabsorption in the kidney. Dysregulation of protein abundances for these transporters result in abnormal phosphate reabsorption processes and may also contribute to the sodium retentive side effect of CNI-treatment and the hypophosphatemic clinical symptoms. Thus, protein abundances of these transporters were also measured in all four treatment groups and were found not to be significantly different following

FK506-treatment or in combination with a high-salt diet (**Fig.3.5**). A slight trending decrease in NaPi-IIc protein abundance was observed in FK506-treated mice compared to the vehicle group (**Fig.3.5b**), but this did not reach statistical significance.

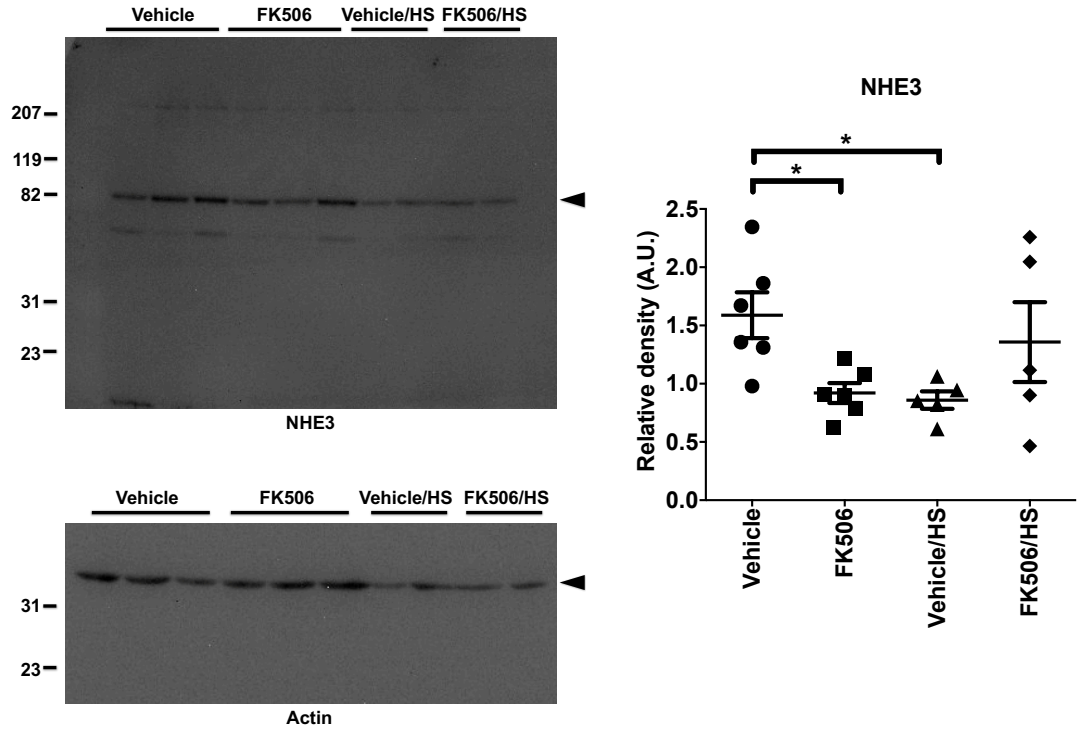

Figure 3.4. Expression of the renal Na^+/H^+ exchanger, NHE3, after FK506 treatment. Representative western blots for the NHE3 exchanger in kidney BBMVs from mice treated with vehicle or FK506 and maintained on a standard or HS diet for two weeks. β-actin (*arrow*) was run as a loading control. NHE3 is detected ~80–100 kDa (*arrow*). Densitometric analyses (*right*) were performed for each group and normalised to β-actin. Values are presented as the mean ± SEM (n = 5–6). Significance was determined by one-way ANOVA with Bonferroni post-test. *P < 0.05.

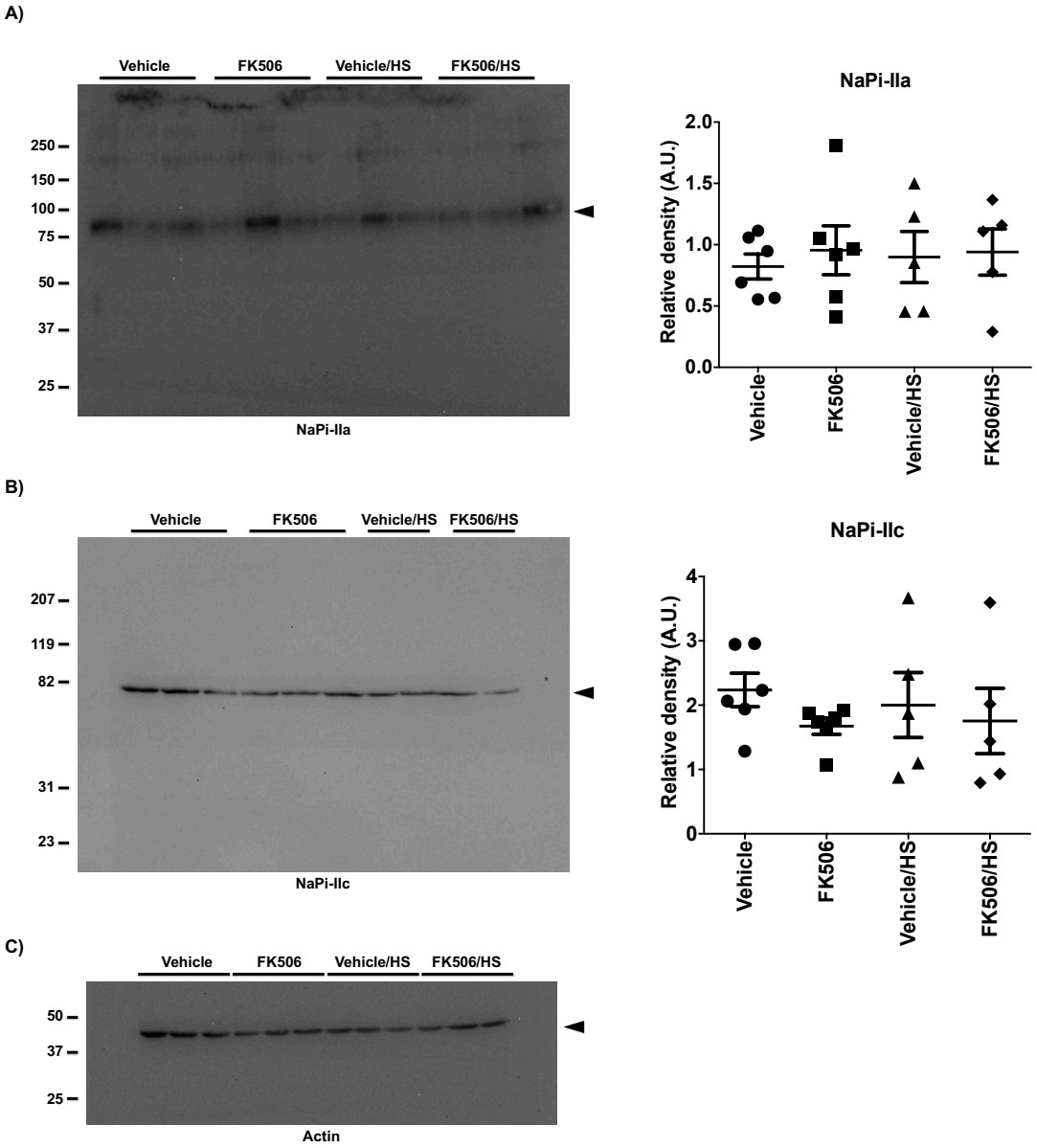

Figure 3.5. Expression of the renal type II Na^+/Pi cotransporters after FK506 treatment. Representative western blots for the **A)** NaPi-IIa and, **B)** NaPi-IIc cotransporters in kidney BBMVs from mice treated with vehicle or FK506 and maintained on a standard or HS diet for two weeks. **C)** β-actin (*arrow*) was run as a loading control. NaPi-IIa is detected ~70–75 kDa (*arrow*) and NaPi-IIc is detected ~64 kDa (*arrow*). Densitometric analyses (*right*) were performed for each group and normalised to β-actin. Values are presented as the mean ± SEM (n = 5–6). Significance was determined by one-way ANOVA with Bonferroni post-test.

The SGLT cotransporters, particularly SGLT2, are the main transporters involved in glucose reabsorption in the kidney and may be involved in the onset of CNI-induced post-transplant diabetes. Analyses of the renal protein abundance for these transporters revealed no significant changes for both SGLT2 and SGLT1 in all treatment groups (**Fig.3.6**). A trending increase was seen for SGLT1 in the high-salt groups compared with the vehicle group (**Fig.3.6b**), but this did not reach statistical significance. These observations do, however, support the biochemical data where no significant elevations in plasma glucose were observed between all four groups (**Table.3.1**). In addition, no significant differences in protein abundance was seen for the basolateral GLUT2 glucose transporter in all treatment groups (**Fig.3.7**).

In the TAL, NKCC2 is the main sodium transporter. Like NCC, it is also under the regulation of the WNK-SPAK/OSR1 signalling pathway and is activated upon phosphorylation by SPAK/OSR1 kinases. Following FK506-treatment with or without the supplement of the high-salt diet, no significant differences in protein abundance were observed for both total and phosphorylated NKCC2 (**Fig.3.8**).

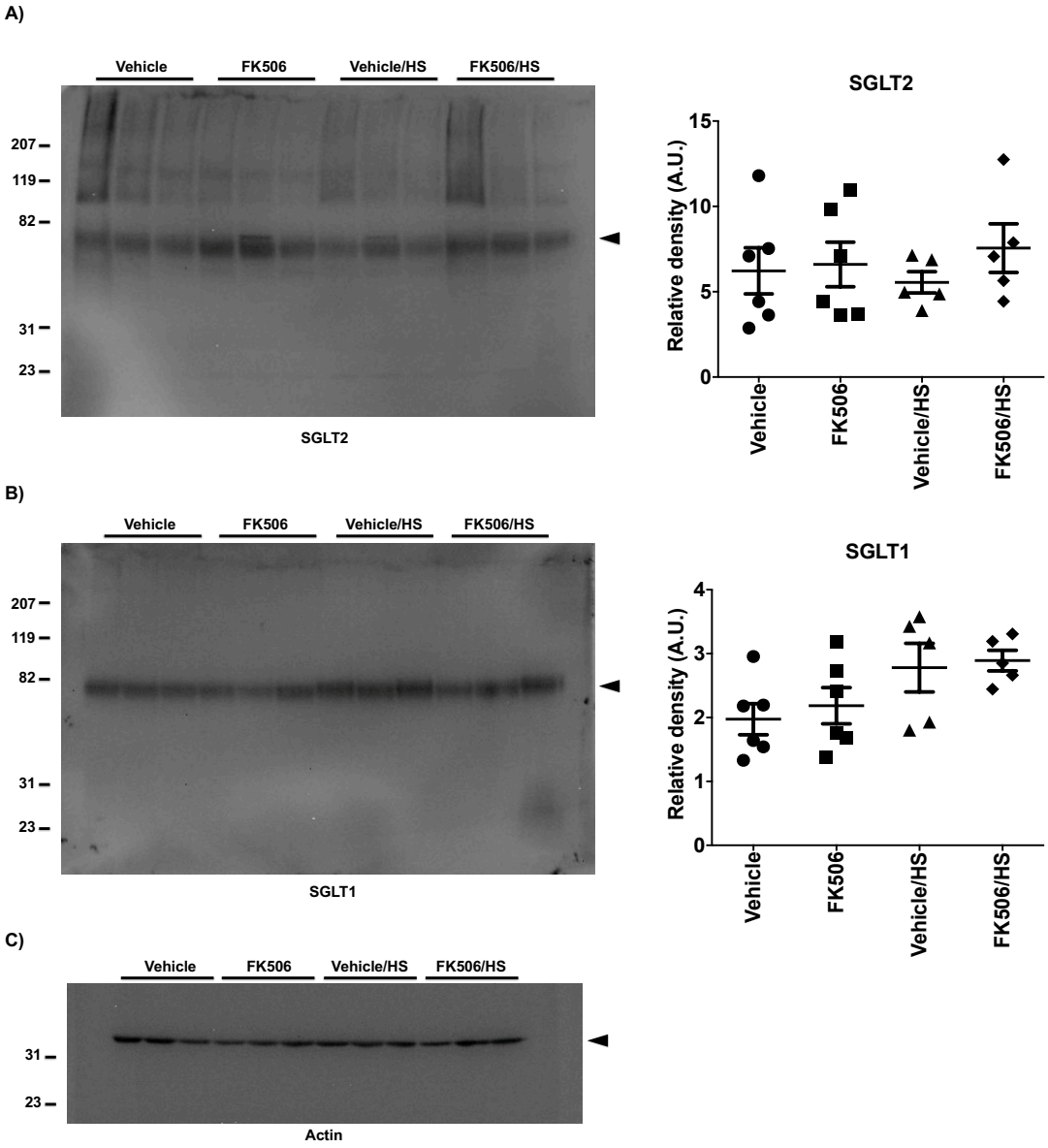

Figure 3.6. Expression of the renal Na^+-glucose cotransporters after FK506 treatment. Representative western blots for the **A)** SGLT2 and, **B)** SGLT1 Na^+/glucose cotransporters in kidney BBMVs from mice treated with vehicle or FK506 and maintained on a standard or HS diet for two weeks. **C)** β-actin (*arrow*) was run as a loading control. SGLT2 is detected ~70–77 kDa (*arrow*) and SGLT1 is detected ~75 kDa. Densitometric analyses (*right*) were performed for each group and normalised to β-actin. Values are presented as the mean ± SEM (n = 5–6). Significance was determined by one-way ANOVA with Bonferroni post-test.

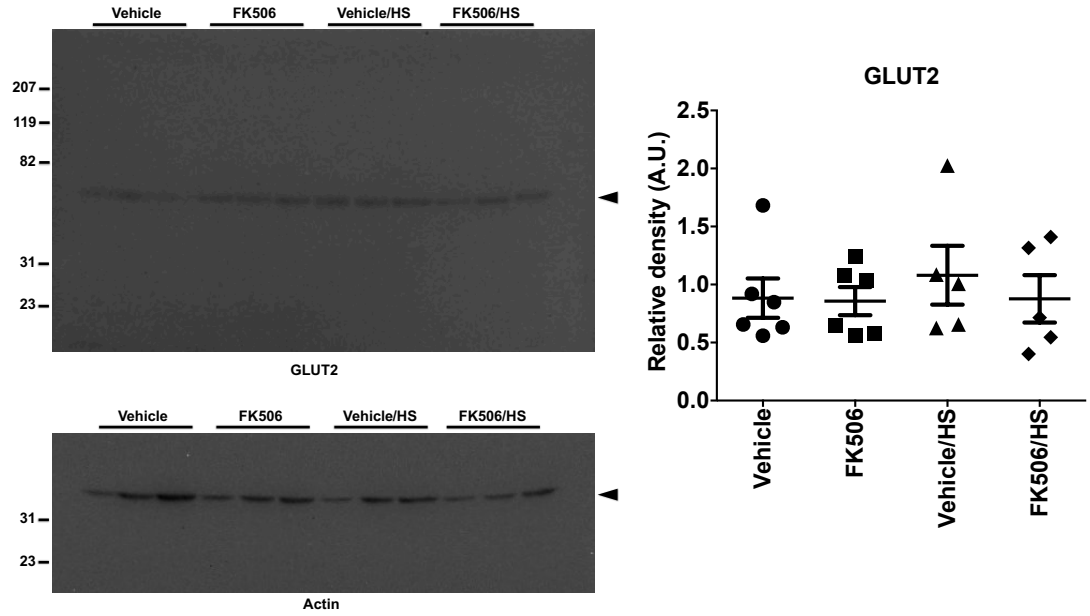

Figure 3.7. Expression of the renal glucose transporter, GLUT2, after FK506 treatment. Representative western blots for the GLUT2 transporter in whole kidney homogenate fractions from mice treated with vehicle or FK506 and maintained on a standard or HS diet for two weeks. β-actin (*arrow*) was run as a loading control. GLUT2 is detected ~60-62 kDa (*arrow*). Densitometric analyses (*right*) were performed for each group and normalised to β-actin. Values are presented as the mean ± SEM (n = 5–6). Significance was determined by one-way ANOVA with Bonferroni post-test.

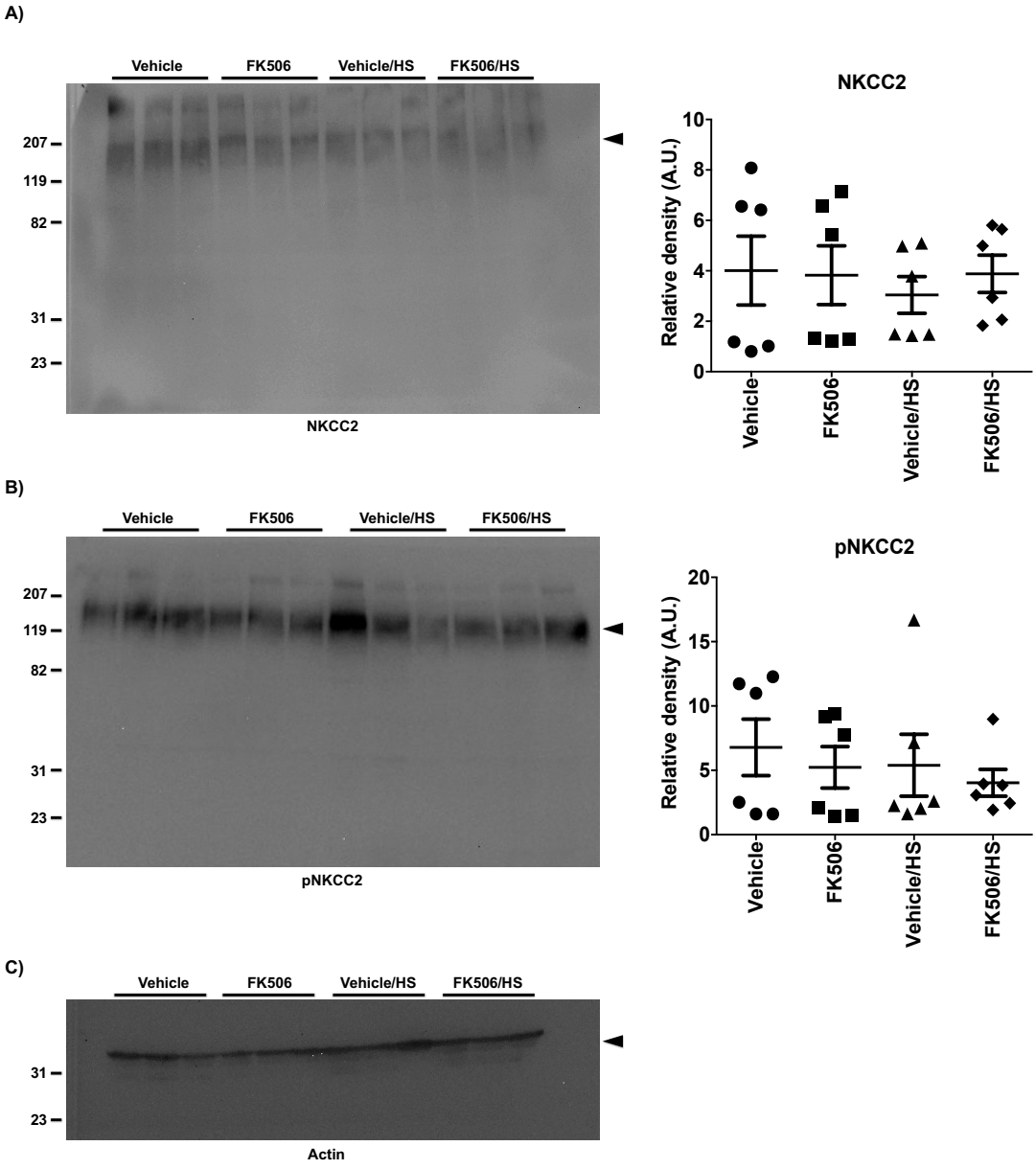

Figure 3.8. Expression of the renal Na^+-K^+-$2Cl^-$ cotransporter, NKCC2, after FK506 treatment. Representative western blots for the Na^+-K^+-$2Cl^-$ cotransporter, **A)** NKCC2 and its phosphorylated form, **B)** pNKCC2, in whole kidney homogenate fractions from mice treated with vehicle or FK506 and maintained on a standard diet or HS diet for two weeks. **C)** β-actin (*arrow*) was run as a loading control. Both forms are detected ~120–130 kDa (*arrow*). Densitometric analyses (*right*) were performed for each group and normalised to β-actin. Values are presented as the mean ± SEM (n = 6). Significance was determined by one-way ANOVA with Bonferroni post-test.

The sodium channel, ENaC, regulates sodium transport in the distal segment of the nephron. Treatment with FK506 was associated with a significant decrease in the α-subunit of ENaC (**Fig.3.9**). This significance was also observed in FK506-treated mice maintained on the high-salt diet. The β- and γ-ENaC subunits were not tested in this study.

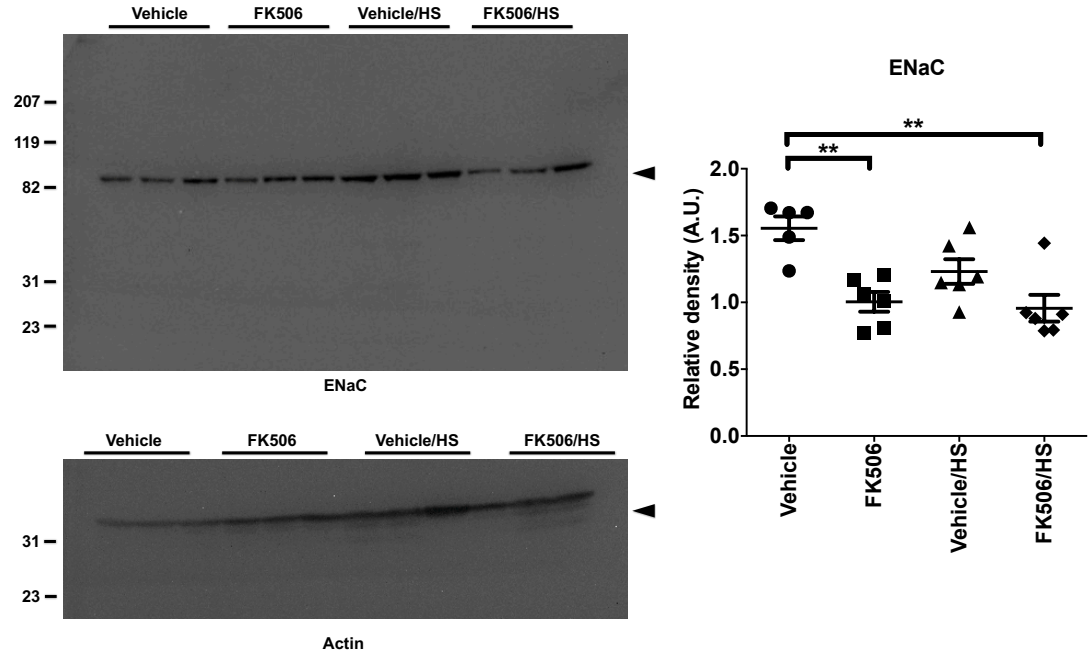

Figure 3.9. Expression of the renal Na^+ channel, ENaC, after FK506 treatment. Representative western blots for the α-subunit of the ENaC Na^+ channel in whole kidney homogenate fractions from mice treated with vehicle or FK506 and maintained on a standard or HS diet for two weeks. β-actin (*arrow*) was run as a loading control. αENaC is detected ~85 kDa. Densitometric analyses (*right*) were performed for each group and normalised to β-actin. Values are presented as the mean ± SEM (n = 5–6). Significance was determined by one-way ANOVA with Bonferroni post-test. ** $P < 0.01$.

3.3.4 Alterations in protein abundance of key sodium transporters in the gastrointestinal tract following FK506 treatment

Sodium transport proteins were also examined in small and large intestinal tissues from FK506-treated mice. As some of the sodium transporters expressed in the kidney are also differentially expressed in the intestines, alterations in these transporters following FK506 treatment were investigated in the different segments of the intestines and were compared to the renal observations to determine whether the effects of FK506 may be tissue-specific.

BBMVs were prepared from mucosa scrapes from proximal and distal small intestinal tissues, and homogenate fractions were prepared from large intestinal tissues. Both proximal and distal small intestinal sodium transporters include NHE3, SGLT1, NaPi-IIb and PiT1. The large intestine contains the NHE3 exchanger and the ENaC channel. Protein abundances for all these transporters were analysed.

In contrast to the kidney observations, western blot analysis showed no significant differences in NHE3 protein abundance in all treatment groups in the proximal small intestine (PSI) (**Fig.3.10**).

Similarly, no changes in protein levels were observed for SGLT1 and GLUT2 (**Fig.3.11**). However, GLUT2 was not expected to be expressed at the BBM under these conditions.

The NaPI-IIb and PiT1 Na^+/Pi cotransporters were also detected in BBMVs prepared from the PSI and displayed no significant changes in protein expression following FK506 treatment (**Fig.3.12**). However, it should be noted that the SEM values are relatively high for PiT1. This, along with the relatively low detection for NaPi-IIb in this segment, is most likely due to the

discrepancy surrounding NaPi-IIb and PiT1 protein localisation in the mouse small intestine, which is predominantly in the distal small intestine (DSI).

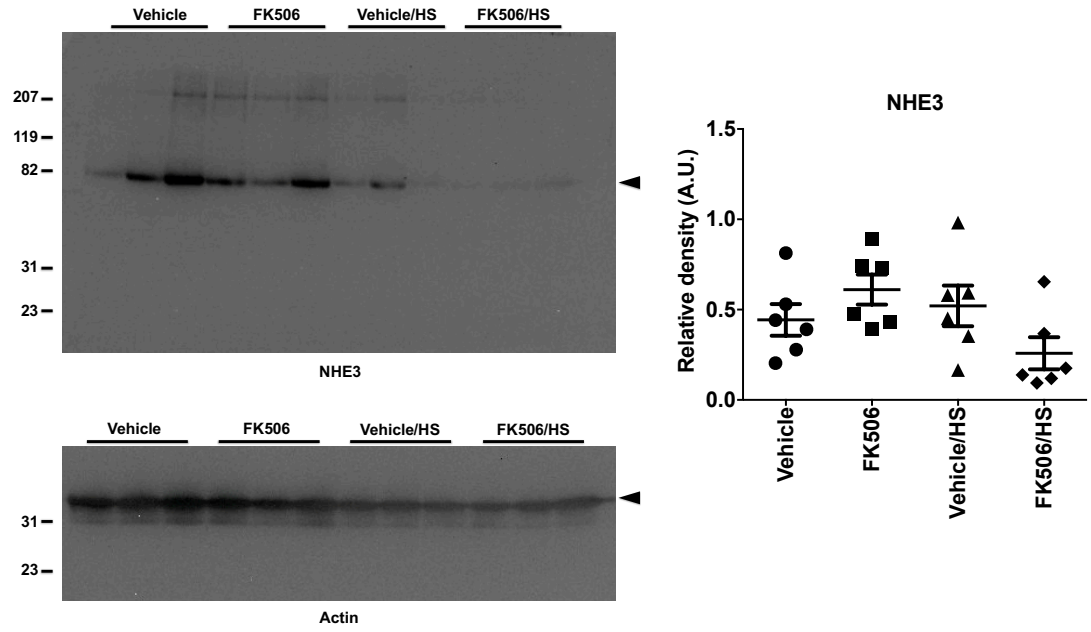

Figure 3.10. The effects of FK506 on NHE3 expression in the proximal small intestine (PSI). Representative western blots of the NHE3 exchanger (*arrow*) in PSI BBMVs from mice treated with vehicle or FK506 and maintained on a standard or HS diet for two weeks. β-actin (*arrow*) was run as a loading control. Densitometric analyses (*right*) were performed for each group and normalised to β-actin. Values are presented as the mean ± SEM (n = 6). Significance was determined by one-way ANOVA with Bonferroni post-test.

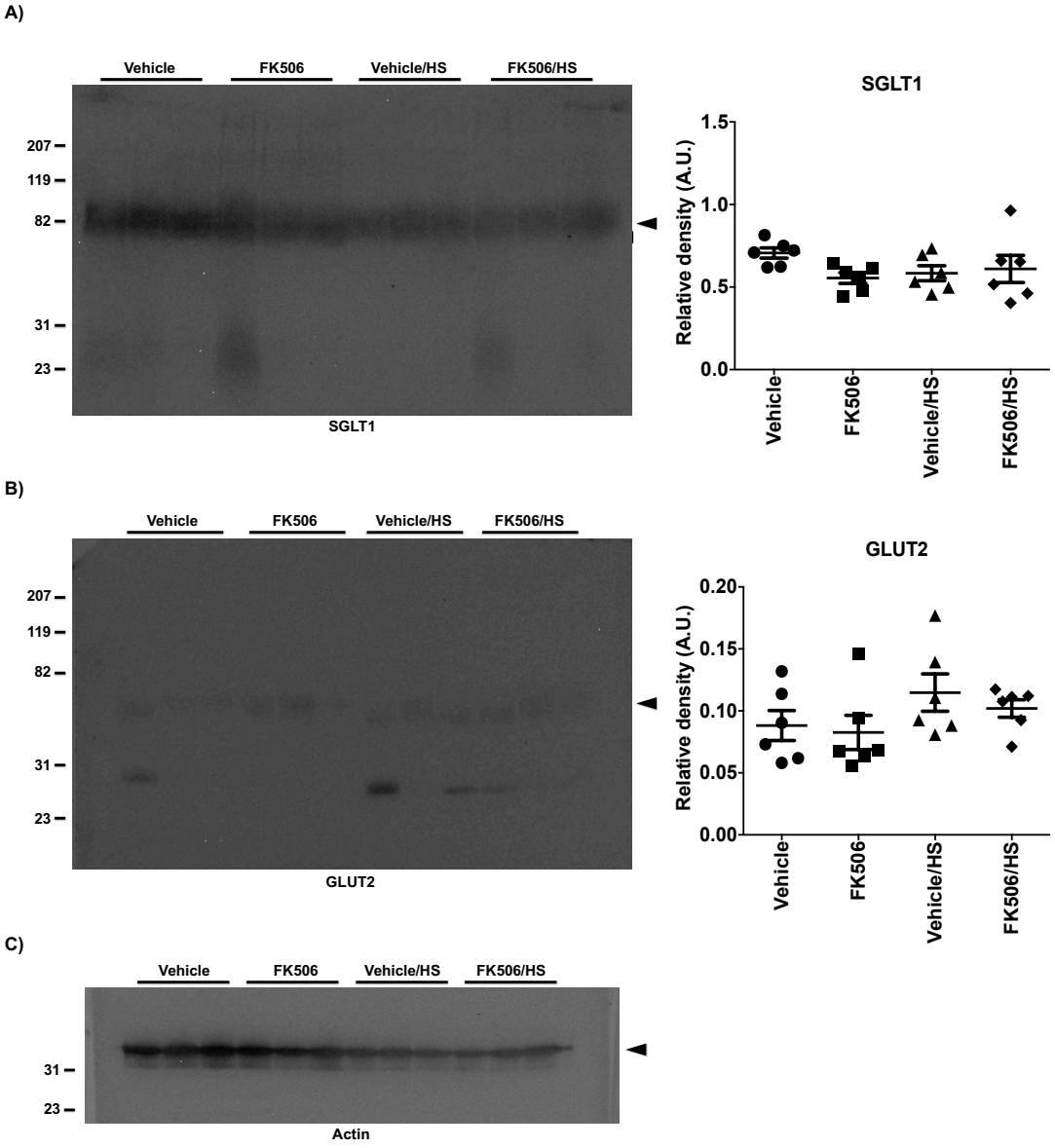

Figure 3.11. The effects of FK506 on SGLT1 and GLUT2 expression in the PSI. Representative western blots of the **A**) Na^+/glucose cotransporter, SGLT1, and **B**) glucose transporter, GLUT2, in PSI BBMVs from mice treated with vehicle or FK506 and maintained on a standard diet or HS diet for two weeks. **C)** β-actin (*arrow*) was run as a loading control. Densitometric analyses (*right*) were performed for each group and normalised to β-actin. Values are presented as the mean ± SEM (n = 6). Significance was determined by one-way ANOVA with Bonferroni post-test.

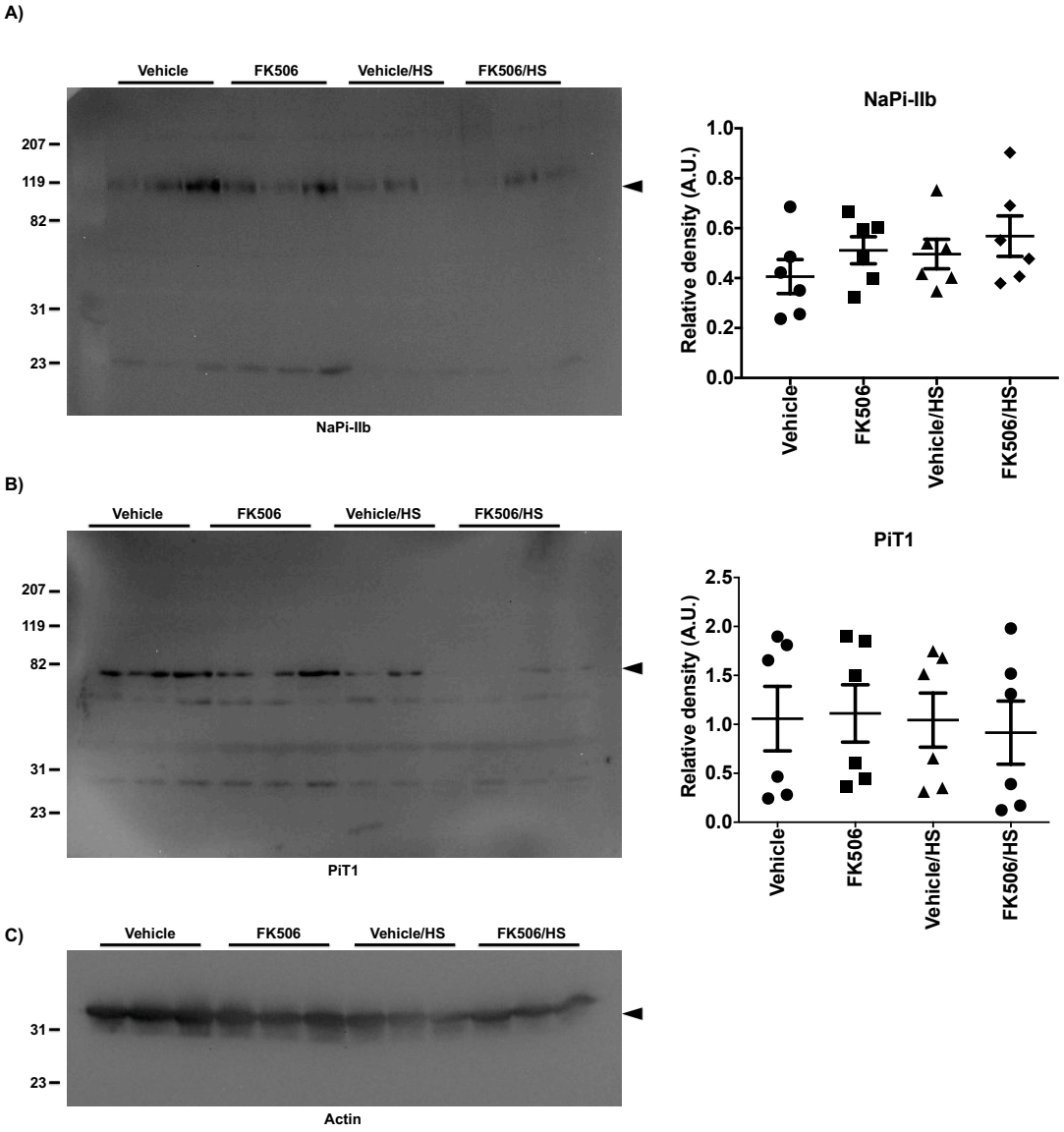

Figure 3.12. The effects of FK506 on NaPi-IIb and PiT1 expression in the PSI. Representative western blots of the Na^+/Pi cotransporters, **A)** NaPi-IIb and, **B)** PiT1 in PSI BBMVs from mice treated with vehicle or FK506 and maintained on a standard diet or HS diet for two weeks. **C)** β-actin (*arrow*) was run as a loading control. NaPi-IIb is detected ~105–110 kDa and PiT1 is detected ~75-80 kDa (*arrow*). Densitometric analyses (*right*) were performed for each group and normalised to β-actin. Values are presented as the mean ± SEM (n = 6). Significance was determined by one-way ANOVA with Bonferroni post-test.

In western blot analyses for the sodium transporters in the distal small intestine, similar observations were found. No changes were seen in protein expression of the NHE3 exchanger following all treatments (**Fig.3.13**).

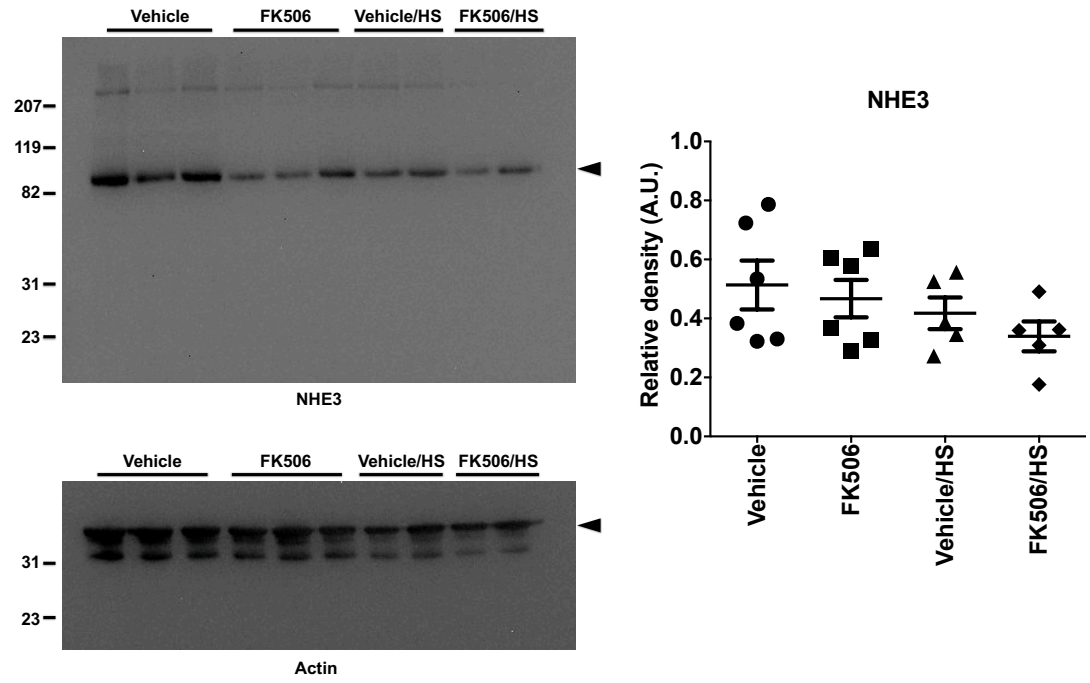

Figure 3.13. The effects of FK506 on NHE3 expression in the distal small intestine (DSI). Representative western blots of the NHE3 exchanger (*arrow*) in DSI BBMVs from mice treated with vehicle or FK506 and maintained on a standard or HS diet for two weeks. β-actin (*arrow*) was run as a loading control. Densitometric analyses (*right*) were performed for each group and normalised to β-actin. Values are presented as the mean ± SEM (n = 5-6). Significance was determined by one-way ANOVA with Bonferroni post-test.

No significant differences were found for the SGLT1 cotransporter in this segment (**Fig.3.14**) and GLUT2 could not be detected in these protein samples.

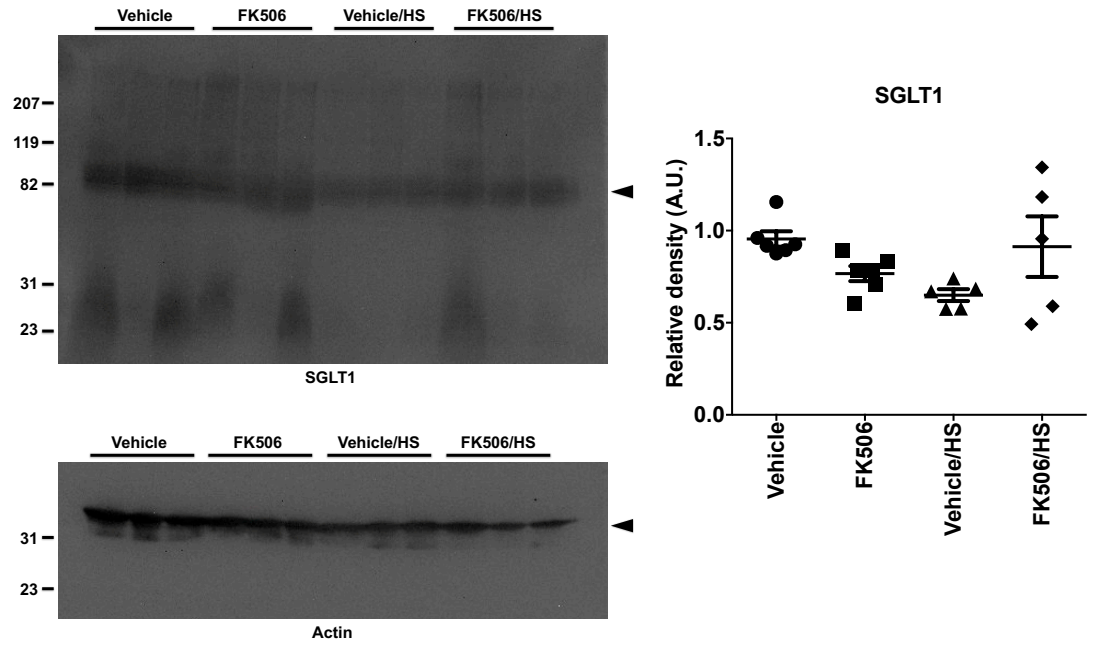

Figure 3.14. The effects of FK506 on SGLT1 expression in the DSI. Representative western blots of the SGLT1 Na^+/glucose cotransporter (*arrow*) in DSI BBMVs from mice treated with vehicle or FK506 and maintained on a standard or HS diet for two weeks. β-actin (*arrow*) was run as a loading control. Densitometric analyses (*right*) were performed for each group and normalised to β-actin. Values are presented as the mean ± SEM (n = 5-6). Significance was determined by one-way ANOVA with Bonferroni post-test.

No significant differences were also observed for the Na^{+}/Pi cotransporters, NaPi-IIb and PiT1 (**Fig.3.15**), in all treatment groups.

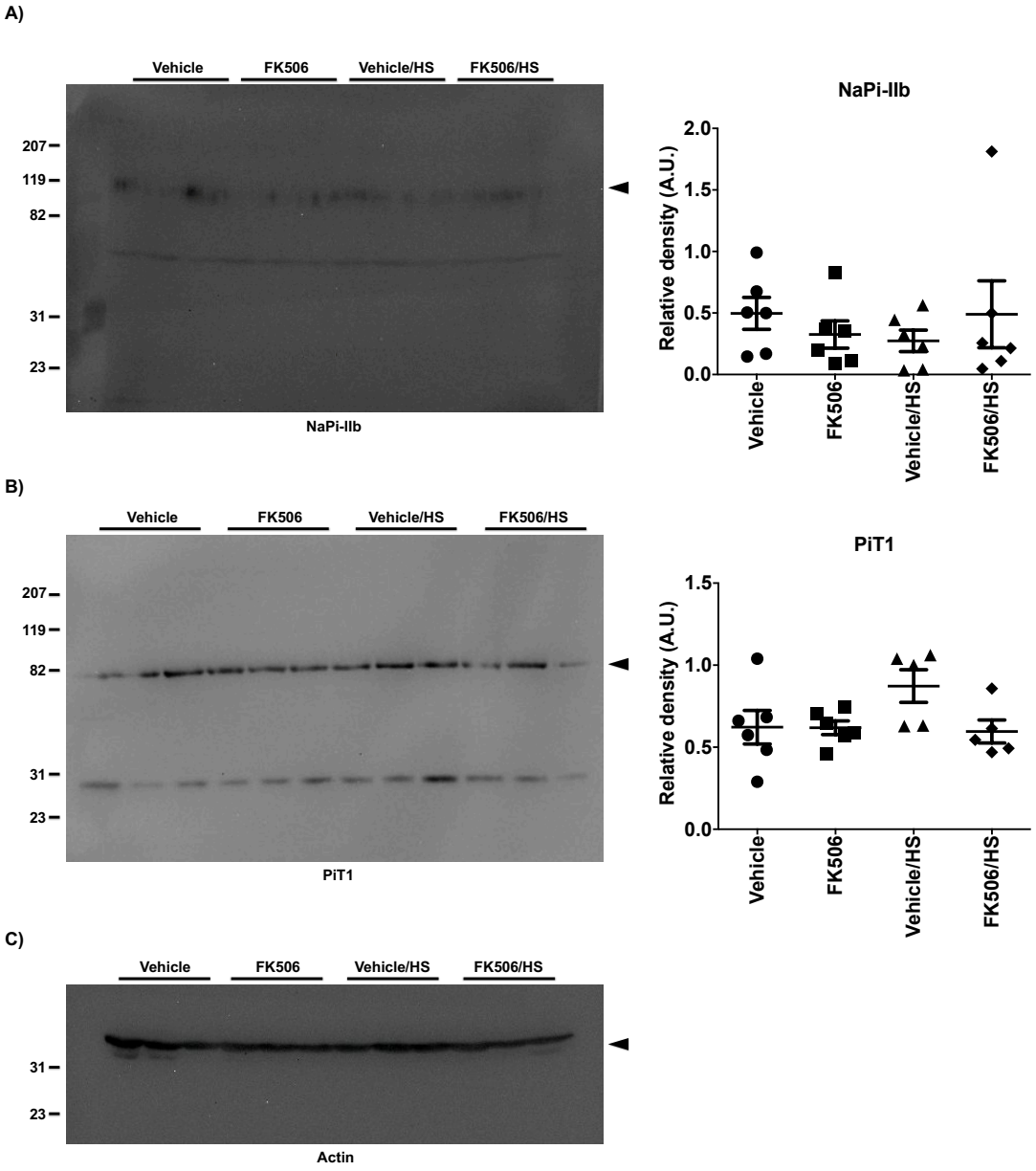

Figure 3.15. The effects of FK506 on NaPi-IIb and PiT1 expression in the DSI. Representative western blots of the Na^{+}/Pi cotransporters, **A)** NaPi-IIb and, **B)** PiT1 (*arrows*), in DSI BBMVs from mice treated with vehicle or FK506 and maintained on a standard diet or HS diet for two weeks. **C)** β-actin (*arrow*) was run as a loading control. Densitometric analyses (*right*) were performed for each group and normalised to β-actin. Values are presented as the mean ± SEM (n = 5-6). Significance was determined by one-way ANOVA with Bonferroni post-test.

As the large intestinal segment does not have villi, protein analyses were performed on homogenate samples prepared from large intestinal mucosal scrapes. The NHE3 exchanger could not be detected, whilst ENaC protein expression was unaffected in all treatment groups (**Fig.3.16**).

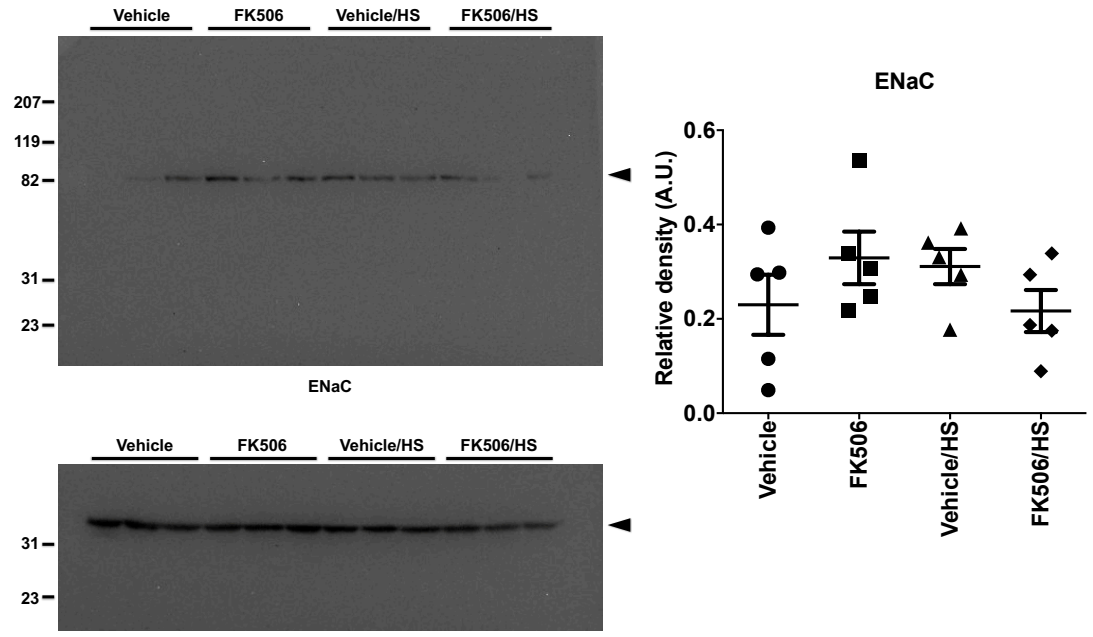

Figure 3.16. The effects of FK506 on ENaC expression in the large intestine (LI). Representative western blots for the α-subunit of the ENaC Na^+ channel in large intestinal homogenate fractions from mice treated with vehicle or FK506 and maintained on a standard or HS diet for two weeks. β-actin (*arrow*) was run as a loading control. Densitometric analyses (*right*) were performed for each group and normalised to β-actin. Values are presented as the mean $\pm$ SEM (n = 5). Significance was determined by one-way ANOVA with Bonferroni post-test.

In summary, the data obtained from these western blot analyses clearly demonstrate that the sodium transport proteins in the gastrointestinal tract are not affected by FK506 treatment. Taken together, treatment with FK506 is associated with a renal-specific response where sodium reabsorption is enhanced predominantly by increased pNCC expression at the apical membrane of the DCT.

3.4 Discussion

Hypertension following renal transplantation is a commonly encountered complication and poses a significant risk for cardiovascular and renal disease, graft failure and patient death. Extensive research has demonstrated that the administration of CNI immunosuppressants are the main risk factors for hypertension development (Campistol et al., 2004; Chapman et al., 1987; Curtis et al., 1988; Kiberd, 1989; Ponticelli et al., 1993). Further reports have indicated that the overactivation of the NCC cotransporter plays a major role in CNI-induced hypertension (Hoorn et al., 2011; Melnikov et al., 2011). The work described in this chapter focused on characterising the effects of these CNIs on renal and intestinal sodium-dependent transporters, other than NCC, using a mouse model of CNI-treatment. The aim was to investigate whether novel and additional transporters may potentially contribute to enhanced sodium retention and the secondary PHAII-like electrolyte abnormalities, via their accompanying ions, after CNI treatment.

3.4.1 Establishment of a CNI-induced model of sodium retention

Tacrolimus (FK506) is used as an alternative immunosuppressant to CsA owing to its lower rate of allograft rejection (Grimm et al., 2006; Kim et al., 2004; Krämer et al., 2005; Margreiter, 2002; Webster et al., 2005). However, the use of these drugs is still associated with elevations in blood pressure. Studies in CNI-treated rodents have shown that CNIs exerts their effects by increasing the abundance of phosphorylated (activated) NCC, pNCC, and its upstream regulators, WNK4 and SPAK, leading to increased sodium reabsorption in the kidney and hypertension (Hoorn et al., 2011; Melnikov et al., 2011). Additional clinical side effects observed in CNI administered renal transplant patients and rodents, include hyperkalemia, metabolic acidosis and hypophosphatemia, all of which are characteristic of human PHAII.

Therefore, due to these similarities, rodent models of CNI-induced hypertension may be used as a model of PHAII and provide important insights into the progression and treatment of hypertension following renal transplantation and in the pathogenesis of PHAII and other forms of blood pressure-related conditions such as essential hypertension.

Protein abundance of pNCC demonstrated an increasing trend following FK506 treatment. Although this was not statistically significant in this study, further analysis using immunohistochemistry supported previous findings of increased pNCC expression following FK506 treatment (Hoorn et al., 2011; Melnikov et al., 2011). It is possible that the absence of significance between vehicle- and FK506-treated groups may be due to a number of limitations. First, a relatively small sample size (n = 5-6) was used in this study and so may not be representative of the actual effects of FK506 treatment, although, the sample size used was comparable with those previously reported (Hoorn et al., 2011). Second, total protein was analysed from samples prepared from whole kidney tissue and not from isolated cortical segments, which may have masked any changes in protein abundance under the investigated conditions. Further studies are required for protein analyses from isolated segments to allow for precise comparisons of pNCC expression under the investigated conditions and would eliminate any masked changes in protein abundance influenced by total protein concentrations from whole kidney tissue.

The supplementation of a high-salt diet with or without FK506 treatment did not affect pNCC protein abundance. This is in contrast to previous studies who have shown the phosphorylation states of NCC and its upstream regulators, SPAK/OSR1, are regulated by dietary salt and are decreased under high-salt conditions (Chiga et al., 2008). However, this regulation is lost in PHAII WNK4 mutant knock-in mice (Chiga et al., 2008), which was initially expected to happen with CNI treatment in this study. It is possible that

the salt content of the high-salt diet may have not been be high enough, in comparison to the maintenance diet, to elicit a significant regulatory response by pNCC and is therefore able to maintain sodium homeostasis at baseline levels. Although, as no changes were seen with FK506 treatment and the addition of the high-salt diet, it is also possible that the FK506 dosage used here may not have been sufficient enough to overcome the dietary salt regulation of pNCC, or, as the FK506/HS group displayed the most loss in body weight during and at the end of the treatment course, it is possible that another pathway might be compensating for this change and therefore counteracting the actions of FK506. Overall, these findings suggest the CNI treatment regimen used in this study was suboptimal. However, data from protein localisation analyses provided sufficient evidence for the presence of CNI-induced sodium retention in this model and allowed for further investigations.

3.4.2 Analysis of FK506 treatment on renal and intestinal sodium transporters

Additional clinical symptoms of PHAII includes metabolic acidosis which is also a common side effect in renal transplant patients and is significantly correlated with CNI administration, particularly with FK506 (Keven et al., 2007; Schwarz et al., 2006). Under chronic metabolic acidosis, the kidneys adapt through coordinated responses to increase H^+ and NH_4^+ excretion, increase luminal buffer titration and reduce (or eliminate) urinary base. These actions occur by 1) increased NHE3 activity and protein, which increases H^+ excretion for the titration of a number of H^+ acceptors, and 2) decreased NaPi-IIa protein, which reduces phosphate uptake (Ambühl et al., 1998; Ambuhl et al., 1996; Amemiya et al., 1995; Laghmani et al., 1997; Soleimani et al., 1992; Wu et al., 1996). Additionally, previous mouse studies have demonstrated stimulated sodium-dependent phosphate uptake at the BBM of the small intestine, particularly at the ileum, by increased NaPi-IIb protein, in

response to metabolic acidosis-induced conditions (Stauber et al., 2005). This reduction in NaPi-IIa protein is paralleled with increased urinary phosphate excretion (phosphaturia) and subsequent hypophosphatemia which are conditions associated with metabolic acidosis and CNI use, as demonstrated in FK506-treated rats (Mohebbi et al., 2009; Moorhead et al., 1974). This marked reduction was similarly observed for NaPi-IIa mRNA expression in CsA-treated rats and in cultured proximal tubule cell lines even when supplemented with a low-phosphate diet or medium, respectively, which is a known regulator of NaPi-IIa expression (Levi et al., 1994; Moz et al., 2004). These studies implicate the involvement of calcineurin in the regulation of renal acid-base balance and phosphate absorption. Supporting studies in calcineurin $A\beta^{-/-}$ mice displayed a marked decrease in NaPi-IIa mRNA levels and also show impaired compensatory responses to a low-phosphate diet and medium in both kidney tissue and cells, respectively, further suggesting an important role for calcineurin in responses to low-phosphate stimuli (Moz et al., 2004).

In contrast to these findings, FK506 treatment caused a significant decrease in renal NHE3 and had no effect on the renal Na^+/Pi cotransporters, NaPi-IIa and NaPi-IIc, the intestinal Na^+/Pi cotransporters, NaPi-IIb and PiT1, and plasma phosphate. The absence of changes seen for these Na^+/Pi transport proteins are not known but it is clear from these observations that metabolic acidosis was not induced in this model. However, in previous studies, FK506-treated rats also failed to show signs of acid-base disturbance unless challenged with an acid load to induce metabolic acidosis and observed a lower abundance of NHE3 at baseline conditions (Mohebbi et al., 2009). This may explain the absence of acid-base imbalance in this study and suggests this reduction in NHE3 may be a regulatory response to transient metabolic acidosis, as well as a feedback mechanism for the upregulation of pNCC at the DCT. In further support, recent studies in tubule-specific NHE3 knockout mice displayed an increase in pNCC and αENaC abundance under NaCl

restriction and proposed a role for these transporters in compensatory responses in the absence of NHE3 to maintain sodium balance (Fenton et al., 2017). This coordinated feedback mechanism may also explain for the downregulation of renal αENaC following FK506 treatment.

Post-transplant diabetes mellitus (PTDM) is a serious complication after renal transplantation. Treatment with CNIs, especially FK506, have been associated as a risk factor for PTDM (Grimm et al., 2006; Heisel et al., 2004; Kasiske et al., 2003; Kim et al., 2004; Pirsch et al., 1997; Woodward et al., 2003). As previously mentioned, SGLT2 mediates the majority of glucose reabsorption in the kidney and its mutation in both patients and animal models causes glycosuria as a result of impaired glucose reabsorption (Calado et al., 2004; Heuvel et al., 2002; Magen et al., 2005; Santer et al., 2003; Vallon et al., 2011). SGLT2 inhibitors are currently used as an antidiabetic drug for type 2 diabetes mellitus to reduce renal glucose reabsorption and plasma glucose levels, and have been recently found to be effective in improving FK506-induced hyperglycemia and protect against renal injury (Jin et al., 2017). Previous investigations in rats treated with FK506 revealed a significant increase in SGLT2 expression which was alleviated by treatment with an SGLT2 inhibitor and also led to increased plasma insulin levels, pancreatic islet size and glucose-stimulated insulin secretion (Jin et al., 2017). Additionally, FK506 treatment has shown to increase intestinal permeability (transport across the BBM), glucose absorption in the jejunum and up-regulated intestinal SGLT1 expression (Li et al., 2015; Yanchar et al., 1996). In these studies, blood glucose and insulin levels were significantly higher in FK506-treated mice, which led investigators to suggest a gradual resistance to insulin induced by FK506 use (Li et al., 2015). These studies demonstrate that CNIs influence SGLT2 protein and/or function, which may contribute towards PTDM development and insulin resistance in renal transplant patients. However, in this study, FK506 treatment did not appear to affect renal glucose homeostasis. No

elevations in plasma glucose were observed following FK506 administration and no changes were seen for renal SGLT2, and for renal and intestinal SGLT1 cotransporters. This was also the same for the facilitative GLUT2 transporter. It is possible that the two-week treatment course with FK506 in this study may not have been long enough to induce changes in glucose absorption processes and, as plasma insulin levels were not measured, it was not possible to detect any early signs of insulin resistance. However, the findings for these transport proteins, along with the other proteins analysed, further confirm the unreliability of the CNI treatment model used.

There are conflicting findings on the exact impact of CNIs on NKCC2 expression and whether NKCC2 is in fact regulated by calcineurin. Prior studies have observed no changes in either total NKCC2 and pNKCC2 protein abundances following FK506 treatment in mice, which was also observed in the present study. In more recent investigations, augmented phosphorylation of NKCC2 was observed in CsA-treated rats, but only with concomitant stimulation by arginine vasopressin (AVP), suggesting that additional factors may need to be present for CNIs to exert their effects (Blankenstein et al., 2017; Borschewski et al., 2016). Moreover, the evaluation of the upstream NKCC2-phosphorylating kinases, SPAK and OSR1, did not show significant activation in microdissected TAL tubules following CsA treatment in comparison to the DCT, suggesting activation of NKCC2 in the TAL upon CNI administration may be via a SPAK/OSR1-independent pathway or by direct inhibition of calcineurin-mediated phosphatase activity (Borschewski et al., 2016). Interestingly, NKCC2 phosphorylation by the AMP-activated protein kinase, AMPK, under osmotic stresses and low intracellular chloride conditions has been demonstrated, which may be a contributing regulatory pathway in the TAL under CNI-treated conditions (Fraser et al., 2007; Richardson et al., 2011). Further studies in oocyte expression models have also shown the participation of AMPK in the regulation of electrogenic sodium-dependent glucose transport,

via SGLT1 (Sopjani et al., 2010), and renal tubular phosphate transport, via NaPi-IIa (Dërmaku-Sopjani et al., 2013), suggesting a potentially universal role for AMPK in sodium transport processes. In addition, previous work has insinuated an antagonistic link between calcineurin and AMPK, and speculates that calcineurin suppresses AMPK-dependent signalling (He et al., 2014; Park et al., 2011). If this is the case, then the relieved suppression of AMPK by CNIs may lead to increased activation of the NKCC2 transporter, however, current understandings as to how calcineurin regulates AMPK remains rudimentary. With regards to the present study, no significant changes were observed for NKCC2 and pNKCC2 following FK506 treatment. Although, it should be noted that, in prior studies, NKCC2 protein analyses were performed in microdissected mouse TAL tubules (Borschewski et al., 2016), and so the data observed in the present study may be the result of total protein samples from whole kidney preparations masking the proportion composed of NKCC2 and thereby concealing any significant changes in protein expression. These observations may also be the result of the model used in this study. Further confirmation of these interpretations by examining NKCC2/pNKCC2 protein expression in isolated cortical and medullary segments and/or microdissected tubules are therefore required.

A significant decrease in protein abundance was observed for the amiloride-sensitive epithelial sodium channel, ENaC, in mouse kidneys following FK506 treatment with and without the supplement of the high-salt diet. Research regarding the effects of CNIs, and thus calcineurin-mediated regulation, on ENaC expression is very complex but limited. Previous *in vitro* analysis using patch clamp techniques showed a significant increase in ENaC activity by CsA, however, this stimulatory effect was not confirmed to be calcineurin-mediated as, in another study, FK506 did not affect basal ENaC activity (Wang et al., 2009; Yue et al., 2000). ENaC expression is regulated by a number of kinases including the serum/glucocorticoid-regulated kinase 1, SGK1 (Chen et al., 1999). Following stimulation of

aldosterone-induced mineralocorticoid receptor (MR)-mediated expression of SGK1, WNK1 phosphorylates this kinase, which in turn, leads to phosphorylation and suppression of the inhibitory actions of the ubiquitin ligase, Nedd4-2, and WNK4 on ENaC expression (Chen et al., 1999; Debonneville et al., 2001; Heise et al., 2010; Ring et al., 2007b; Snyder et al., 2004; Xu et al., 2005). This pathway has also been demonstrated to regulate NHE3 (Fuster et al., 2007; Grahammer et al., 2006), SGLT1 (Dieter et al., 2004; Grahammer et al., 2006; Shojaiefard et al., 2007), NaPi-IIb (Palmada, 2004), and NCC (Arroyo et al., 2011; Ronzaud et al., 2013; Rozansky et al., 2009; Vallon et al., 2009), suggesting that SGK1 may be an important universal mediator for aldosterone-dependent sodium transport processes. PHAII is typically associated with low or normal plasma aldosterone which may explain for the downregulation of both ENaC and NHE3 transport proteins following FK506 treatment. Treatment with CNIs has also shown to induce aldosterone resistance in renal transplant patients, which is also associated with the clinical diagnosis for PHAII, via the down-regulation of MR (Heering et al., 2004). The likely explanation for the observed decrease in ENaC is due to a compensatory mechanism to account for increased sodium reabsorption at the upstream DCT segment via pNCC, rather than direct interactions with FK506. The decrease observed following a combination of FK506 and the high-salt diet is also most likely a compensatory mechanism owing to decreased aldosterone levels under high dietary salt conditions. Nevertheless, without confirmation of a downregulation in MR expression and levels of plasma aldosterone or attenuated ENaC transport activity, a reduction in channel expression in response to aldosterone cannot be ruled out.

3.4.3 Gastrointestinal-renal signalling

The experiments performed in this study aimed to identify further renal and intestinal sodium transport proteins involved in CNI-induced sodium

retention, which were also known to be regulated by the WNK-SPAK/OSR1 pathway. In addition, these experiments were also used to determine any interplay between the kidneys and gastrointestinal tract, which has been previously reported for a number of electrolytes such as phosphate, potassium and sodium (Berndt et al., 2007; Carey, 1978; Lee et al., 2007; Lennane et al., 1975; Rabinowitz et al., 1988). In a study by Berndt *et al*, a significant increase in urinary phosphate excretion was shown within 20 minutes of duodenal infusion of 1.3M phosphate in rats (Berndt et al., 2007). This effect was found to be phosphate specific and unaffected by stomach infusion (Berndt et al., 2007), suggesting the presence of a gastrointestinal-renal signalling axis for phosphate, whereby the intestines act as a 'phosphate sensor' which then signals the kidney to adjust phosphate reabsorption and excretion accordingly. However, recent reports have challenged this phosphate gastrointestinal-renal signalling mechanism (Lee et al., 2017; Thomas et al., 2017). A study by Lee *et al*, showed that duodenal infusion of phosphate at physiological concentrations (10 mM) had no effect on plasma phosphate concentrations, PTH and urinary phosphate excretion (Lee et al., 2017), opposing the previously proposed signalling between the gastrointestinal tract and kidneys (Berndt et al., 2007). However, there is stronger evidence for this gastrointestinal-renal signalling axis for potassium and sodium. Intragastric potassium infusion in rats, combined with a potassium-deficient diet, showed a significant increase in renal potassium excretion and suppressed elevations in plasma potassium concentrations (Lee et al., 2007). A similar effect was seen in humans and rats who display profound natriuresis following sodium loading (Carey, 1978; Lennane et al., 1975; Mu et al., 1995). These findings are consistent with the existence of a sodium sensing mechanism in the gastrointestinal tract which was suggested to be mediated by the intestinal natriuretic peptides, guanylin and uroguanylin (Carrithers et al., 2002; Fukae et al., 2002; Lorenz et al., 2003).

Taken together, the sodium retaining effects of CNI-treatment was expected to either activate this gastrointestinal-renal signalling axis and mediate compensatory responses for increased sodium reabsorption by pNCC, or potentially disrupt this signalling interplay and prevent this adaptation. In the present study, a significant downregulation was only observed for renal NHE3 and ENaC transport proteins with FK506 treatment and/or the high-salt diet, which were most likely compensatory responses for increased pNCC-mediated sodium retention at the DCT. However, no significant differences were seen for any of the intestinal transport proteins studied, even though the components of the WNK-SPAK/OSR1 cascade are expressed in this organ and have been shown to regulate the intestinal sodium transporters (Ahmed et al., 2015; Elvira et al., 2014; Fezai et al., 2015; Pasham et al., 2012; Pathare et al., 2012a; Verissimo and Jordan, 2001; Wilson et al., 2001). It is clear from these findings that the downregulation for renal NHE3 and ENaC transport proteins are mediated by intra-renal signalling and are not consistent with gastrointestinal-renal signalling, which supports earlier discussions that the CNI treatment conditions used was not sufficient enough to induce an intestinal response. At the same time, it should also be noted that sodium transport across the intestinal BBM was not measured so an increase in the transport activity of these proteins cannot be ruled out and requires further investigations.

3.4.4 Conclusions

To date, this is currently the first report to simultaneously investigate the protein abundances of renal and intestinal sodium transporters/channels in the kidney and intestine of FK506-treated mice. It is apparent that the overactivation of NCC, by CNIs, is the sole contributor to enhanced sodium reabsorption/retention in the kidney, and therefore, elevations in blood pressure. Although a hypertensive response was not determined, the detection of enhanced pNCC expression at the apical membrane of the DCT

was used to assume increased sodium reabsorption/retention in these mice and provided sufficient evidence to support using the model for further analyses of other sodium transporters that may contribute to this side effect.

Taken together, FK506 treatment, under normal or high dietary salt conditions, was associated with significant downregulation of NHE3 and ENaC protein expression in the kidney, most likely as a feedback mechanism to compensate for enhanced sodium reabsorption by pNCC. No significant changes were observed for other sodium-coupled transporters in the kidney, though this may be attributed to the protein preparation protocols used. In addition, no change in protein abundance was observed for the intestinal sodium-coupled transporters, which may be suggestive of a renal-specific effect of FK506. However, as the clinical symptoms associated with CNIs and PHAII were not observed in this study, it is likely that the FK506-treatment regimen used was not an optimally established model of CNI-induced sodium retention and requires re-analysis. Additionally, as AMPK and SGK1 signalling pathways are also involved in WNK-SPAK/OSR1-independent regulation of these sodium transporters, their influence on these transporters cannot be ruled out and so requires further investigations under CNI treatment.

In conclusion, the present study used a mouse model of CNI treatment, in an attempt to investigate the influences of CNIs on renal and intestinal sodium transport proteins. Although the model proved not to be optimal for drawing conclusions from the observations seen, it is clear that CNI treatment alone did not have a significant impact on renal and intestinal sodium transport proteins, and the changes observed in this study were most likely compensatory to pNCC activation. Therefore, these findings along with previous CNI-treated rodent models points to the conclusion that CNIs exert their effects only in the presence of other stimuli.

Chapter IV
Investigation of calcineurin inhibitors as a risk factor for Metabolic Syndrome

4.1 Introduction

4.1.1 Metabolic syndrome

Metabolic syndrome is characterised by a cluster of clinical dysfunctions and biochemical abnormalities, which include obesity, hypertension, hyperglycemia, impaired glucose metabolism, insulin resistance and hyperlipidemia. The current clinical diagnosis for metabolic syndrome is defined by the presence of any three of the following traits; abdominal obesity (waist circumference >102 cm for men and >88 cm for women), hypertriglyceridemia (≥150 mg/dl (1.69 mmol/l)), low serum high-density lipoproteins (HDL, <40 mg/dl (1 mmol/l) for men and <50 mg/dl (1.3 mmol/l) for women), high blood pressure (≥140/90 mmHg) and high fasting glucose levels (≥110 mg/dl (≥5.6 mmol/l)) (National Cholesterol Education Program (NCEP), 2012; National Institute for Health and Care Excellence (NICE), 2011).

Metabolic syndrome is common after renal transplantation and is an associated risk factor for cardiovascular disease (CVD), chronic graft dysfunction, graft loss, and patient death (Espinola-Klein et al., 2007; Pedrollo et al., 2016; Porrini et al., 2006; de Vries et al., 2004). Its prevalence among renal transplant patients has been reported to vary widely in numerous retrospective cross-sectional studies, ranging from between 14.9% to as high as 63% (Courivaud et al., 2007; Ford et al., 2002; Israni et al., 2012; Kishikawa et al., 2009; Luan et al., 2010; Porrini et al., 2006; de Vries et al., 2004). The development of these metabolic syndrome-affiliated conditions results from a complex association of different environmental,

genetic and metabolic factors. Multivariate analysis of clinical predictors associated with its development has shown to vary between studies and have included; older age, male gender, high pre-transplant body mass index (BMI), post-transplant weight gain and increased post-transplant BMI (Courivaud et al., 2007; Luan et al., 2010). Immunosuppression regimens, via CNIs, are associated with these individual parameters and may therefore play an important role in the increased risk and prevalence of metabolic syndrome after transplantation and contribute to long-term morbidity. This high prevalence and consequential outcome strongly underscores the urgent need for efforts directed towards early detection of metabolic syndrome development in this patient group and targeted therapeutic interventions.

In the following sections, these individual components will be further discussed in terms of their association with metabolic syndrome development after renal transplantation and as a consequence of the immunosuppression therapy recieved.

4.1.2 Obesity

Obesity is considered one of the main phenotypic hallmarks of metabolic syndrome and greatly contributes to insulin resistance, hyperinsulinemia and hyperlipidemia. The development or worsening of obesity has demonstrated to play a major role in metabolic syndrome pathogenesis after kidney transplantation. An increase in BMI following transplantation has revealed a strong correlation with glucose intolerance, dyslipidemia and hypertension which can result in a further escalated risk for CVD, as well as an increased risk of delayed graft function, acute rejection, allograft failure and mortality (Ducloux et al., 2005; El-Agroudy et al., 2004; Gore et al., 2006; Kovesdy et al., 2010; Luan et al., 2010; Meier-Kriesche et al., 2002). Though the prevalence of obesity before and after renal transplantation varies regionally, a significant universal increase in post-transplant weight is commonly

observed. In a retrospective review of transplant patients at 1 year after renal transplantation, 43% of patients were found to be obese and 57% of patients experienced an average weight gain of 10% (Johnston et al., 1993). Additionally, multivariate analysis revealed that patients with an increase in BMI of more than 5% at 1 year post-transplantation have a ~3-fold increased risk of graft loss (Ducloux et al., 2005). It is clear that BMI can have a long-term impact on graft function and thus, early evaluation of BMI should allow for individual interventions, such as the incorporation of dietary restrictions to prevent excessive post-transplant weight gain and minimise these associated risks. However, further prospective clinical trials are required to assess the impact of dietary and pharmacological interventions on graft survival in renal transplant patients. Immunosuppression has not been found to be directly associated with elevations in BMI (Ducloux et al., 2005), and so it is likely that their main contribution in this regard may be to provoke the associated insulin resistance, hyperlipidemia and hypertensive conditions.

4.1.3 Hyperlipidemia/Hypercholesterolemia

Hyperlipidemia is also common in renal transplant patients and often co-exists with obesity and hyperinsulinemia. More than 60% of renal transplant patients develop hyperlipidemia, characterised by elevated total- and low-density lipoprotein (LDL)-cholesterol, either alone or in combination with hypertriglyceridemia (Del Castillo et al., 2004; Ong et al., 1994; Tse et al., 2004). Post-transplant hyperlipidemia has shown to persist even at 5 years post-transplantation, and has also been linked to increased risks for CVD as well as mortality, allograft rejection and graft failure (Ong et al., 1994; Wissing et al., 2000). Both CsA and FK506 have been demonstrated to induce hyperlipidemia in numerous clinical studies. CsA-treated renal transplant patients display significant elevations in triglycerides, total cholesterol and LDL levels with variable effects on HDL levels (Ligtenberg et al., 2001; McCune et al., 1998; Pirsch et al., 1997; Vincenti et al., 2007).

Treatment with FK506, however, appears to have a less pronounced effect on lipid profiles compared to CsA. In a US multicentre randomised trial, FK506-treated renal transplant patients had significantly lower levels of total cholesterol, LDLs and triglycerides compared to CsA-treated patients (Pirsch et al., 1997), and these parameters remained low even at 5 years post-transplantation (Vincenti et al., 2002). Similar findings have also been found in European multicentre studies (Grimm et al., 2006; Krämer et al., 2005; Margreiter, 2002). Interestingly, conversion from CsA to FK506 has been associated with significant improvements in lipid and cardiovascular profiles (Artz et al., 2003; Baid-Agrawal et al., 2004; McCune et al., 1998). In a multicentre study, renal transplant patients receiving CsA treatment who were then randomised to FK506 displayed significant reductions in total cholesterol and LDLs by around 16-17% and 22-25%, respectively, but showed no changes in triglyceride and HDL levels, and no effects on renal allograft function and glycemic control (Artz et al., 2003; Baid-Agrawal et al., 2004; Ligtenberg et al., 2001; McCune et al., 1998). Others have observed a significant decrease, by 18%, in triglycerides following conversion to FK506 (Artz et al., 2003). Therefore, both CNIs are associated with hyperlipidemia development in renal transplant patients but with FK506 having greater improvements in lipid profiles, less hypertension and reduced rates of acute rejection.

4.1.4 Hypertension

As discussed in detail in **Sections.1.2** and **1.3**, hypertension is very common following transplantation and is highly correlated with long-term graft survival, CVD and patient mortality (Campistol et al., 2004; Kasiske et al., 2004; Opelz et al., 1998). Post-transplant hypertension, as well as its associated detrimental effects, has been widely demonstrated to be aggravated by the administration of CNIs**.** The CsA-induced hypertensive effects are multifactorial, inducing stimulated vasoconstriction, increased sympathetic

nerve activity and activation of the renin-angiotensin system (Avdonin et al., 1999; English et al., 1987; Kurtz et al., 1988; Scherrer et al., 1990; Xue et al., 1987). Although FK506 causes similar actions to CsA, FK506 has shown to be associated with a lower incidence of allograft rejection and post-transplant hypertension, as well as a higher rate of patient/graft survival, compared to CsA (Grimm et al., 2006; Kim et al., 2004; Krämer et al., 2005; Margreiter, 2002; Webster et al., 2005).

4.1.5 Post-transplant diabetes mellitus

As discussed in detail in **Section.1.7**, PTDM is another common complication by CNI use, affecting between 2 – 25% of initially non-diabetic renal transplant patients and rendering them vulnerable to risks of decreased graft / patient survival and increased CVD (Boudreaux et al., 1987; Cosio et al., 2001, 2005; Heisel et al., 2004; Kasiske et al., 2003; Porrini et al., 2008a, 2008b; Roth et al., 1989; Vincenti et al., 2007; Woodward et al., 2003). Increased prevalence of PTDM has been associated with the type of immunosuppressant used, African American ethnicity, BMI, age, family history of diabetes, pre-transplant hypertriglyceridemia, elevated total serum cholesterol and prior abnormalities in glucose metabolism and insulin resistance (Cosio et al., 2001, 2002, 2005; Kasiske et al., 2003; Porrini et al., 2008b). Both CsA and FK506 predispose renal transplant patients to PTDM through mechanisms such as B-cell toxicity, inhibited insulin synthesis and release, and increased insulin resistance (Boots et al., 2002; Helmchen et al., 1984; Hirano et al., 1992; Redmon et al., 1996; Tamura et al., 1995). However, the diabetogenic effects of CNIs are not fully defined. Multiple registry analyses, clinical studies and single centre cohorts have shown that the risks for PTDM differs between the two immunosuppressants; FK506 is associated with a much higher incidence of PTDM than CsA (Boots et al., 2002; Heisel et al., 2004; Kamar et al., 2007; Kasiske et al., 2003; Pirsch et al., 1997; Roland et al., 2008; Sato et al., 2003; Vincenti et al., 2007;

Woodward et al., 2003). Further studies have shown that conversion from FK506 to CsA is associated with an improvement in glucose metabolism, with a remission rate of 42% at 1 year after conversion (Ghisdal et al., 2008). However, though these studies imply the conversion from FK506 to CsA may result in improved glucose control, CsA is also associated with a higher incidence of hypertension and hyperlipidemia in comparison to FK506, suggesting the need for individualisation of the immunosuppressive regimen in order to balance its efficacy and toxicity.

4.1.6 Other clinical features

Additional clinical features observed with metabolic syndrome and are also associated with CNI immunosuppression include hypomagnesemia, hypophosphatemia and hyperuricemia.

Hypomagnesemia is a frequent complication in transplant patients and is a known side effect of CNIs (Andoh et al., 1996; McDiarmid et al., 1993; Nozue et al., 1992). Hypomagnesemia is also common in patients with diabetes, occurring in 25–47% of these patients (Lima et al., 2009a, 2009b; Mather et al., 1979). Previous cross-sectional studies have shown both dyslipidemia and hypertension were related to lower serum Mg^{2+} levels (Guerrero-Romero and Rodríguez-Morán, 2002). Furthermore, low serum Mg^{2+} was also found in 65.6% of individuals with metabolic syndrome suggesting, as confirmed through multivariate analysis, a strong independent relationship between lower serum Mg^{2+} levels and metabolic syndrome (Guerrero-Romero and Rodríguez-Morán, 2002, 2006). In a retrospective single-centre study, renal transplant patients on CNIs showed significantly lower Mg^{2+} levels during the first month post-transplantation and these patients were found to develop PTDM much faster (Van Laecke et al., 2009), suggesting hypomagnesemia as an independent predictor of PTDM. Numerous multicentre studies have also observed that hypomagenesmia was more frequent in patients treated

with FK506 than CsA (Margreiter, 2002; Van Laecke et al., 2009; Webster et al., 2005), although the mechanisms for the effects of CNIs on Mg^{2+} is not fully clear. Prior studies in FK506-treated rats displaying hypomagnesemia was associated with excessively high fractional excretion of Mg^{2+}, suggesting impaired Mg^{2+} reabsorption (Andoh et al., 1996; Lote et al., 2000). Additionally, mRNA expression of the renal Mg^{2+} channel, TRPM6, was significantly reduced in FK506-treated rats, indicating that FK506-induced downregulation of Mg^{2+} transport proteins may be responsible for excessive Mg^{2+} wasting and in the pathogenesis of hypomagnesemia (Nijenhuis et al., 2004).

Hypophosphatemia is another common condition encountered following renal transplantation, affecting >90% of patients (Ambühl et al., 1999; Bhan et al., 2006; Moorhead et al., 1974). It is believed that the mechanisms contributing to post-transplant hypophosphatemia are related to the dysregulation of tubular phosphate reabsorption, as a consequence of increased PTH and FGF23 levels (Bhan et al., 2006; Falkiewicz et al., 2003; Farrington et al., 1979; Mohebbi et al., 2009; Moz et al., 2004). In animal models, FK506 treatment has been previously associated with a significant decrease in the expression of the renal NaPi-IIa cotransporter (Mohebbi et al., 2009; Moz et al., 2004), which likely contributes to phosphate wasting in CNI-treated patients. However, the degree of contribution of these immunosuppressive drugs to hypophosphatemia development has not been found to be greatly significant. In a study of 72 renal transplant patients, those receiving CsA monotherapy did not experience significant hypophosphatemia in comparison to patients receiving a combination of azathioprine and prednisolone (Higgins et al., 1990), suggesting CsA may not affect phosphate handling. Furthermore, in a study of 40 renal transplant patients receiving CsA (studied at 1, 6, 12, 24, 30 and 36 months after transplantation) and 20 patients receiving FK506 (studied 3 months after transplantation), treatment with FK506 was associated with a significantly

higher tubular phosphate reabsorption rate at all time points studied compared to CsA, indicative of a faster recovery from impaired tubular phosphate reabsorption (Falkiewicz et al., 2003). It is possible that immunosuppressive drug treatment may affect plasma phosphate or urinary phosphate excretion via an indirect mechanism. However, further analyses are required to fully define the role of CNI immunosuppression in the development of hypophosphatemia following renal transplantation.

Hyperuricemia is also common after renal transplantation, occurring in 25 - 80% of patients (Armstrong et al., 2005; Gores et al., 1988; Kahan et al., 1987; Kalantar et al., 2011; Lin et al., 1989; Malheiro et al., 2012; Zurcher et al., 1996). Its high prevalence has shown to be correlated with prolonged use of CNIs, especially with CsA, and is significantly linked to reduced renal graft survival, chronic allograft nephropathy development and cardiovascular events (Akalin et al., 2008; Gerhardt et al., 1999; Lin et al., 1989; Marcen et al., 1992). The adverse effects of CsA on uric acid excretion were observed shortly after its introduction into clinical use, however, the mechanism by which this occurs remains to be fully elucidated. A number of studies have arrived at a variety of conclusions and have mostly implicated CsA in impaired renal tubular handling of uric acid. Clearance studies in CsA-treated adult and paediatric transplant patients have shown CsA-induced hyperuricemia to be related to decreased GFR, lower urinary clearance and fractional excretion of uric acid as a consequence of increased net proximal tubular uric acid absorption (Hoyer et al., 1988; Laine and Holmberg, 1996; Lin et al., 1989; Zurcher et al., 1996). Some investigations have examined the effects of FK506 on hyperuricemia development in comparison to CsA and have found no differences between both immunosuppressants in increasing serum uric acid levels (Kanbay et al., 2005; Spartà et al., 2006). However, the specific mechanisms underlying these CNI-induced alterations in uric acid handling and the relationship between hyperuricemia and other manifestations of CNI-induced nephrotoxicity are still not well defined.

Overall, despite their intention-to-treat, CNI administration continues to induce hypertension along with the conditions associated with metabolic syndrome, thereby limiting their efficacies and obstructing graft and patient survival.

4.1.7 Mouse models of diet-induced metabolic syndrome

Metabolic syndrome is a multifactorial condition and because its presentation differs among patients as a function of the components of this syndrome, different treatments must be tailored for different patients. For this to be accomplished, rodent models of metabolic syndrome are required to study the underlying mechanisms for metabolic syndrome development. Currently, a number of animal models have been established which mimic, as faithfully as possible, all the multiple components underlying human metabolic syndrome coexisting in these patients. However, currently no studies have investigated the potential use of CNI treatment as a model of metabolic syndrome, despite its evident associations with the individual components that comprise the syndrome.

Currently, the use of diets which are high in fat are generally accepted to generate rodent models of metabolic syndrome to induce the insulin resistance and obesity components under conditions which are most comparable to actual worldwide diets. Comparisons of the effects of high-fat and high-sucrose diets have shown significantly increased feeding efficiency, weight gain, plasma glucose and insulin levels in mice fed a high-fat diet whilst a high-sucrose diet did not (Black et al., 1998; Surwit et al., 1995). This indicates that dietary fat, not sucrose, is the critical stimulus for the development of hyperglycemia and hypersinsulinemia (Black et al., 1998; Surwit et al., 1995). Studies in rats and various mouse strains have also shown that an increase in dietary fat content and central adiposity displays

several correlations to human metabolic syndrome (Surwit et al., 1988; West et al., 1992; Woods et al., 2003). In particular, the C57BL/6J mouse strain has proven to be the best model for studying metabolic syndrome. Numerous studies comparing the effects of high-fat diets on C57BL/6J mice with other mouse strains have demonstrated its high susceptibility to developing obesity (hyperlipidemia and hypercholesterolemia), hyperinsulinemia, hyperglycemia and hypertension when allowed *ad libitum* access to high-fat diets, whilst other strains are relatively resistant to these effects (Gallou-Kabani et al., 2007; Surwit et al., 1988, 1995; Winzell and Ahren, 2004). In addition, the development of glucose intolerance and diabetes induced by high-fat diets in this strain has shown to closely parallel the progression of diabetes and obesity in humans, whereby the prevalence of diabetes and impaired glucose tolerance was more common in obese subjects, making this mouse strain well suited for studying metabolic syndrome (West and Kalbfleisch, 1971).

4.1.8 Aims of this study

It is evident that the detrimental impacts of CNIs on hyperglycemia, hyperlipidemia and hypertension may play a role in the development and increasing prevalence of metabolic syndrome. However, the pathophysiology of metabolic syndrome with CNI treatment has not yet been investigated.

The aims of this chapter were to establish a CNI-induced model of metabolic syndrome in attempts to understand the underlying mechanisms in both CNI-treated and metabolic syndrome states. In the work described, high-fat diet-fed mice were used as a model of metabolic syndrome and compared with FK506-treated mice. Biochemical analysis on both plasma and urine samples were performed to confirm the clinical features of metabolic syndrome and changes in renal and intestinal transport proteins were assessed at both transcriptional and translational levels. Further aims of this study were to also identify potential transport proteins that may contribute to the phenotypic

features of metabolic syndrome. Additionally, the conclusions drawn from Chapter 3 suggest that CNIs require the presence of another stimulus to exert its effects. Therefore, this study was also carried out to determine whether CNI treatment alone mirrors metabolic syndrome or whether CNIs may predispose renal transplant patients to metabolic syndrome development in combination with increased dietary fat intake / an obese background.

This study was conducted with an aim of aiding future studies by understanding the mechanisms involved in metabolic syndrome development in CNI-treated renal transplant patients as well as determining which renal and intestinal transporters may also contribute to its pathogenesis. This study hopes to facilitate future studies that may allow the design of an effective immunosuppressive regimen with minimal metabolic complications.

4.2 Materials and methods

4.2.1 Animals

Male C57BL/6J mice, aged 3 weeks (weighing between 13 – 17g), were used in accordance with the Animals Scientific Procedures Act 1986, Amendment Regulations 2012. All protocols were approved by the University College London (Royal Free Campus) Comparative Biology Unit Animal Welfare and Ethical Review Body (AWERB) committee and performed in accordance with project license PPL 70/7647.

4.2.2 Metabolic syndrome mouse model

Full procedures have been described in **Section.2.1.3**. Mice were provided with *ad libitum* access to a high-fat diet, containing 60% energy-from-fat, or a standard maintenance diet, containing 7.4% energy-from-fat, for ten weeks. At week 8, mice were administered either vehicle or FK506 at a dose of 2 mg/kg/day, via I.P injections, for the remaining two weeks. For the final five days of the experimental period, mice were housed and acclimatised in metabolic cages to obtain 24-hour urine collections prior to the final day.

At the end of the experiment, mice were placed under terminal anaesthesia and checked for withdrawal to corneal and pedal reflexes before sample collections. Terminal blood samples were collected by cardiac puncture and urinary samples were collected by bladder puncture. Cervical dislocation was performed and death was confirmed by cessation of heartbeat before removing renal and intestinal tissues.

4.2.3 Plasma and urine biochemistry

Plasma and urine samples were collected, as described in **Section.2.1.4**, and biochemical analyses for sodium, creatinine, glucose and phosphate were performed as described in **Sections.2.1.5 - 2.1.8**. Measurements for triglycerides, HDLs, urate, magnesium, calcium and bicarbonate levels were carried out by Dr. Anjly Jain in the Department of Clinical Biochemistry (Royal Free Hospital, London, UK).

4.2.4 RT-PCR

RT-PCR protocols were carried out as described in **Section.2.2.** Whole kidney and intestinal mucosa samples from proximal and distal intestinal tissues were collected and snap-frozen in an RNA stabilising solution and subjected to RNA extraction as described in **Section.2.2.1**, using 100 mg of tissue. RNA concentration and purity was confirmed using the Nanodrop and run on an agarose gel, as described in **Section.2.2.4**. Isolated RNA was then subjected to cDNA synthesis protocols as described in **Section.2.2.2**, using 1–1.5 μg RNA and included a reverse transcriptase negative control. Samples and controls, in duplicates, were then subjected to RT-PCR analysis as described in **Section.2.2.3**, using primers listed in **Tables.2.2** and **2.3**, under the conditions described in **Table.2.4**.

4.2.5 BBMV preparations from kidney and intestinal mucosal tissues

BBMVs were prepared from previously snap-frozen whole kidney and intestinal mucosa tissues using the techniques described in **Section.2.5.2** and **2.5.3,** respectively. Large intestinal mucosal samples were processed as described in **Section.2.5.1**. Total protein concentration was determined using the Bradford assay as described in **Section.2.5.4**. For BBMVs and

homogenate fractions, purity was assessed using an alkaline phosphatase assay as described in **Section.2.5.5**.

4.2.6 Western blot analysis

Western blot protocols were carried out as described in **Section.2.5.6**. Kidney and intestinal BBMVs (25 μg) or homogenate samples (50 – 100 μg) were run on an SDS-PAGE gel. Large intestinal homogenate samples were loaded at 100 μg. Samples were then transferred onto a PDVF membrane and incubated with the primary antibodies and their corresponding secondary antibodies listed in **Table.2.6**. Following visualisation, membranes were then stripped and re-probed for β-Actin. Densitometry was measured and samples were normalised to β-actin. As mentioned, due to the lack of access to overexpressing and/or knockdown mouse models, no further positive or negative controls were used in western blot applications.

4.2.7 Statistical analysis

Data are presented as mean ± SEM, relative to β-actin. N refers to the number of samples within each group. Significance was determined by one-way ANOVA with Bonferroni post-test, relative to vehicle-treated mice on the standard or high-fat diet or as stated. *$P < 0.05$, ** $P < 0.01$, *** $P < 0.001$.

4.3 Results

4.3.1 Physiological parameters

Mouse models of metabolic syndrome and CNI treatment were established in order to investigate whether immunosuppression with CNIs may influence the development of the conditions associated with metabolic syndrome. To establish a mouse model of metabolic syndrome, mice were placed on a high-fat (HF) diet for 10 weeks with the aim of inducing obesity and known metabolic syndrome-affiliated conditions, such as insulin resistance. This was followed by treatment with vehicle or FK506 for 14 days, commencing on the 8th week, and housing in metabolic cages for the remaining 5 days for 24-hour urine collections.

Body weight was measured regularly and body weight changes were calculated to monitor fluctuations during the course of treatment. Supplementation with the high-fat diet over the course of 10 weeks was associated with a continuous rise in body weight (**Fig.4.1a**). At the end of the treatment, these mice had gained an overall ~2.1-fold increase in body weight (30.32 $\pm$ 0.76g and 31.17 $\pm$ 0.78g for vehicle- and FK506-treated HF groups, respectively) compared to their initial weight (15.5 $\pm$ 0.4g and 14.6 $\pm$ 0.43g for vehicle- and FK506-treated HF groups, respectively). The daily food and water intake was lower than expected for this mouse strain, which was reported to be typically between 3-5 g/day/mouse and 3-7 ml/day/mouse, respectively (Bachmanov et al., 2002). However, despite this, the food and water intake remained stable throughout the 10-week period with some minor fluctuations and significant differences between groups (**Fig.4.1b,c**). A slight decline in body weight and food intake was observed following the commencement of vehicle and FK506 administration (**Fig.4.1a,b**), with a sharp decrease in body weight in all treatment groups over the last 4-5 days of the experiment (**Fig.4.1d**). This was most likely a

stress response to the daily injections and later housing in metabolic cages at the final stages of the experiment rather than the vehicle/FK506 treatment itself. Despite this, the final body weights were significantly higher in the high-fat diet-fed groups compared to the groups maintained on the standard diet (**Fig.4.1e**).

Plasma and 24-hour urine biochemical analyses are shown in **Table.4.1**. Mean plasma creatinine values were higher than the expected range for mice using the Jaffe's method (~10-44 µmol/L). This was most likely due to the reported complications in measuring plasma creatinine using this method, however, urinary creatinine concentrations have been found to be similar in mice when measured by the Jaffe's method and the recommended HPLC (Dunn et al., 2004; Meyer et al., 1985; Palm and Lundblad, 2005), and so supports the urinary creatinine concentrations and the calculated electrolyte excretion ratios measured in this study. Regardless, plasma creatinine was significantly increased in the FK506-treated mice placed on the high-fat diet compared to its FK506-treated standard diet counterpart, while urinary creatinine levels were significantly decreased in all treatment groups relative to vehicle-treated mice (**Table.4.1**). These observations may be indicative of kidney dysfunction possibly as a result of the high-fat diet, particularly in combination with FK506 treatment, which may contribute to the detrimental consequences on graft function/survival in obese individuals. Therefore, it should be noted that any changes in urinary electrolyte levels observed in the FK506/HF group might be a reflection of altered GFR due to possible kidney dysfunction.

No changes were found for plasma urate, magnesium and urinary calcium levels in all treatment groups. While there were no significant differences in plasma sodium between groups, mice fed on the high-fat diet treated with either vehicle or FK506 drastically excreted more sodium in their urine (**Table.4.1**). Plasma glucose was significantly increased in FK506-treated,

and both vehicle- and FK506-treated mice on the high-fat diet relative to vehicle-treated mice, with no changes in urinary glucose excretion (**Table.4.1**), indicative of altered glucose homeostasis in this model. In addition, plasma phosphate levels were significantly increased in both vehicle- and FK506-treated mice fed on the high-fat diet compared to treated mice on the standard diet (**Table.4.1**). This was similarly observed for urinary phosphate. Plasma bicarbonate was also lower in the high-fat group under both treatments. These observations may suggest impaired acid-base balance in the obese model. Interestingly, although no changes were observed for total plasma triglycerides, a significant increase in HDL-cholesterol was found in mice fed on the high-fat diet, especially when followed with FK506 treatment (**Table.4.1**), which may be a compensatory response to possible increases in circulating total- and LDL- cholesterol levels. However, as these parameters were not measured in this study, this compensatory response cannot be confirmed.

Overall, mice fed on a high-fat diet had greater weight gain and were heavier than those fed on a standard diet. Treatment with FK506 alone or the supplement of a high-fat diet with either vehicle or in combination with FK506 treatment was associated with altered glucose, phosphate and acid-base balance. The plasma and urine biochemical analyses indicate partial features of metabolic syndrome in the group fed on the high-fat diet. However, because these results reflect the dietary intake of the preceding couple of days and does not consider day-to-day variability in intake, which may have also been influenced by adjustments to the metabolic cage, the absence of alterations in urate, magnesium and triglyceride levels cannot be ruled out. In addition, the changes observed with the combined high-fat diet with FK506 treatment, as indicated by plasma and urinary creatinine levels, might be a consequence of altered GFR.

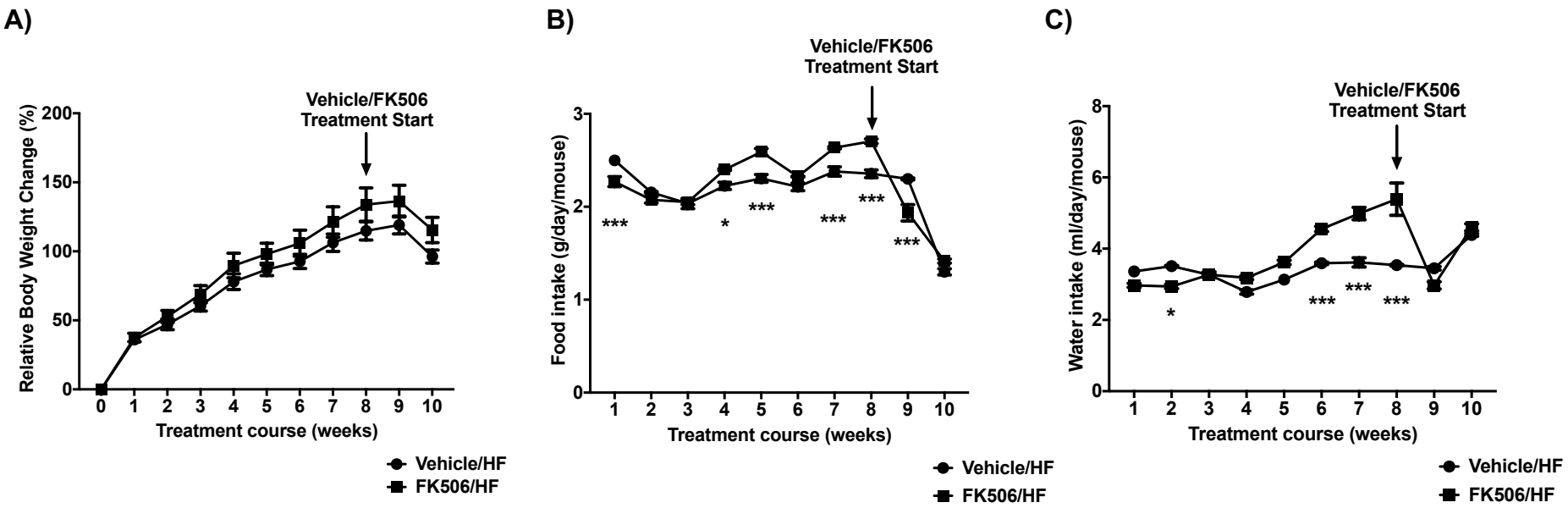
A)
Relative Body Weight Change (%)
200
150
100
50
0
Vehicle/FK506
Treatment Start
0 1 2 3 4 5 6 7 8 9 10
Treatment course (weeks)
Vehicle/HF
FK506/HF
B)
Food intake (g/day/mouse)
3
2
1
0
Vehicle/FK506
Treatment Start
***
*
***
***
***
***
1 2 3 4 5 6 7 8 9 10
Treatment course (weeks)
Vehicle/HF
FK506/HF
C)
Water intake (ml/day/mouse)
8
6
4
2
0
Vehicle/FK506
Treatment Start
*
***
***
***
1 2 3 4 5 6 7 8 9 10
Treatment course (weeks)
Vehicle/HF
FK506/HF

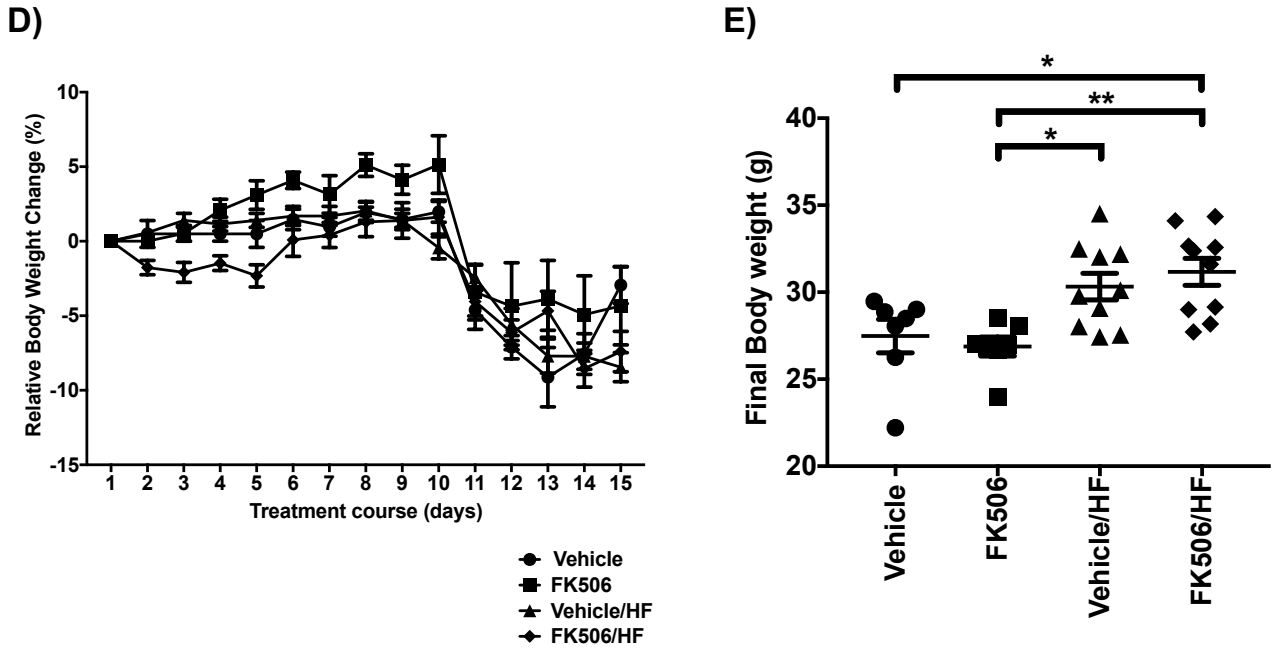

Figure 4.1. Body weight, food and water consumption during FK506 and/or high-fat diet treatment. A) Body weight change, **B)** food and, **C)** water intake of two groups of mice (n = 10 per group) fed on the high-fat (HF) diet. Mice were weighed twice weekly over the 10 weeks of the study. Vehicle and FK506 treatment commenced at week 8 (*arrow*) and was administered daily for the remaining 14 days of the study. **D)** Body weight change over the 14-day vehicle/FK506 treatment period in mice fed either the HF diet or the standard maintenance diet (n = 7 per group). From day 10, mice were housed in metabolic cages to allow for 24-hour urine collections. **E)** Comparisons of the final body weights on the final day of the treatment. All data are presented as the mean ± SEM. Body weight change is presented as the mean percentage (%) change in body weight normalised to the initial weight at day 1. Significance was determined by two or one-way ANOVA with Bonferroni post-test. *P < 0.05, **P < 0.01, ***P < 0.001.

Parameter	Vehicle (N = 7)	FK506 (N = 7)	Vehicle/HF (N = 10)	FK506/HF (N = 10)
Plasma				
Creatinine (µmol/L)	248.16 ± 42.17	168.44 ± 8.57 §§	258.48 ± 33.15	375.66 ± 50.54 ††
Na^+ (mmol/L)	133.61 ± 3.80	123.96 ± 5.64	119.19 ± 3.60	123.41 ± 3.28
Glucose (mmol/L)	5.70 ± 0.90 †† ‡‡ §	10.89 ± 1.00 **	10.30 ± 0.64 **	9.48 ± 0.84 *
Pi (mmol/L)	2.19 ± 0.09 ‡‡ §§	2.27 ± 0.10 ‡ §	2.75 ± 0.13 ** †	2.75 ± 0.08 ** †
Triglycerides (mmol/L)	0.71 ± 0.12	0.87 ± 0.12	0.53 ± 0.06	0.72 ± 0.07
HDLs (mmol/L)	1.22 ± 0.16 ‡‡ §§§	1.71 ± 0.19 §§§	1.88 ± 0.11 ** §§§	3.00 ± 0.10 *** ††† ‡‡‡
Urate (µmol/L)	29.04 ± 17.13	11.66 ± 2.38	43.20 ± 13.49	25.84 ± 7.74
Mg^{2+} (mmol/L)	0.25 ± 0.02	0.21 ± 0.01	0.21 ± 0.01	0.22 ± 0.01
HCO_3^- (mmol/L)	15.95 ± 1.62 ‡ §§	16.82 ± 0.57 ‡‡ §§§	12.02 ± 0.60 * ††	11.53 ± 0.50 ** †††
Urine				
Creatinine (µmol/L)	1041.35 ± 85.54 † ‡ §§§	659.83 ± 80.79 *	711.55 ± 89.60 *	524.58 ± 39.39 ***
U_{Na}/U_{Cr} (mmol/mmol)	48.79 ± 6.77 §§§	6.49 ± 4.34 ‡‡ §§§	116.18 ± 26.54 ††	181.32 ± 16.26 *** †††
$U_{Glucose}/U_{Cr}$ (mmol/mmol)	2.28 ± 0.26	30.59 ± 20.98	0.87 ± 0.39	1.42 ± 0.47
U_{Pi}/U_{Cr} (mmol/mmol)	51.29 ± 9.44 ‡ §	104.65 ± 21.38	239.75 ± 65.26 *	259.98 ± 25.55 *
U_{Urate}/U_{Cr} (mmol/mmol)	1.23 ± 0.14	1.62 ± 0.26	2.08 ± 0.55	2.78 ± 0.36
U_{Mg}/U_{Cr} (mmol/mmol)	43.85 ± 9.33	65.16 ± 14.27 ‡	27.51 ± 7.09 †	34.65 ± 3.03
U_{Ca}/U_{Cr} (mmol/mmol)	3.01 ± 0.37	7.09 ± 2.54	4.21 ± 1.55	6.71 ± 0.89

Table 4.1. Plasma and urine biochemistry. Effects of FK506 and/or a high-fat (HF) diet on plasma and urinary electrolytes. Values are presented as the mean ± SEM. Urine electrolytes are presented as the mean normalised to urinary creatinine. Significance was determined by one-way ANOVA with Bonferroni post-test.
* $P < 0.05$, ** $P < 0.01$, *** $P < 0.001$; vs. Vehicle
† $P < 0.05$, †† $P < 0.01$, ††† $P < 0.001$; vs. FK506
‡ $P < 0.05$, ‡‡ $P < 0.01$, ‡‡‡ $P < 0.001$; vs. Vehicle/HF
§ $P < 0.05$, §§ $P < 0.01$, §§§ $P < 0.001$; vs. FK506/HF

4.3.2 Influences of FK506 and/or diet-induced obesity on renal transport proteins

As previously mentioned, metabolic syndrome is commonly observed following renal transplantation and is comprised of a cluster of conditions including hypertension, obesity, insulin resistance, hyperlipidemia, hypophosphatemia, hypomagnesemia and hyperuricemia. Most of these individual conditions have been previously associated with CNI immunosuppression and have been linked to changes in a number of renal and intestinal transport proteins and function, suggesting that these transport proteins may also be altered in patients with metabolic syndrome in a similar manner. In the present study, these associated renal and intestinal transport proteins were analysed at both the transcriptional and translational levels to investigate whether these transport proteins are similarly altered in both CNI-treated mice and a model of diet-induced obesity/metabolic syndrome. Analyses of mice under a combination of high-fat feeding and FK506 administration were also performed to assess for an exaggerated response. The observations obtained from this study may enable the identification of transport proteins contributing to the pathogenesis of metabolic syndrome, and may also confirm the potential establishment of another mouse model of metabolic syndrome via treatment with CNIs.

As implicated from the biochemistry data with regards to the marked reduction in plasma bicarbonate and increased plasma and urinary phosphate, mice fed on a high-fat diet treated with either vehicle or FK506 appear to display altered acid-base balance. To evaluate these observations, analyses of mRNA and protein expression of the proximal tubular acid-base proteins, NHE3, NaPi-IIa and NaPi-IIc, were measured. Relative to vehicle-treated mice, NHE3 mRNA expression was significantly increased in FK506-treated mice fed either the standard or high-fat diet (**Fig.4.2a**). Western blotting showed a significant increase in NHE3 protein abundance in renal

BBMVs from vehicle- and FK506-treated mice on the high-fat diet, compared with the corresponding standard diet-fed mice (**Fig.4.2b**). However, mRNA expression of both NaPi-IIa and NaPi-IIc were only significantly increased in the FK506/HF group, with no changes following FK506 treatment or with high-fat feeding alone (**Fig.4.3a,c**), and no overall change in protein abundance (**Fig.4.3b,d**).

An increase in plasma glucose was also found in the FK506-treated group and the high-fat diet-fed group with either treatment, suggestive of altered glucose homeostasis and the possible onset of insulin resistance/diabetes. To further explore this possibility, mRNA expression and protein abundances of the Na^+/glucose cotransporters, SGLT2 and SGLT1, and the facilitative glucose transporter, GLUT2, were also measured. No significant changes in SGLT2 mRNA expression were found in FK506-treated and high-fat diet-fed control mice, whilst a combination resulted in a significant increase (**Fig.4.4a**). Only a slight but significant upregulation in SGLT1 mRNA expression was observed with control mice fed on the high-fat diet, while no overall change in SGLT1 protein was found (**Fig.4.4c,d**). Interestingly, SGLT2 protein expression was significantly decreased in the high-fat groups under both drug treatments (**Fig.4.4b**), which do not correlate with the marked elevations in plasma glucose. In addition, while GLUT2 mRNA expression was significantly upregulated in mice fed on the high-fat diet with FK506 treatment, protein levels remained unaffected in both BBMVs and homogenate samples from all treatment groups (**Fig.4.5**).

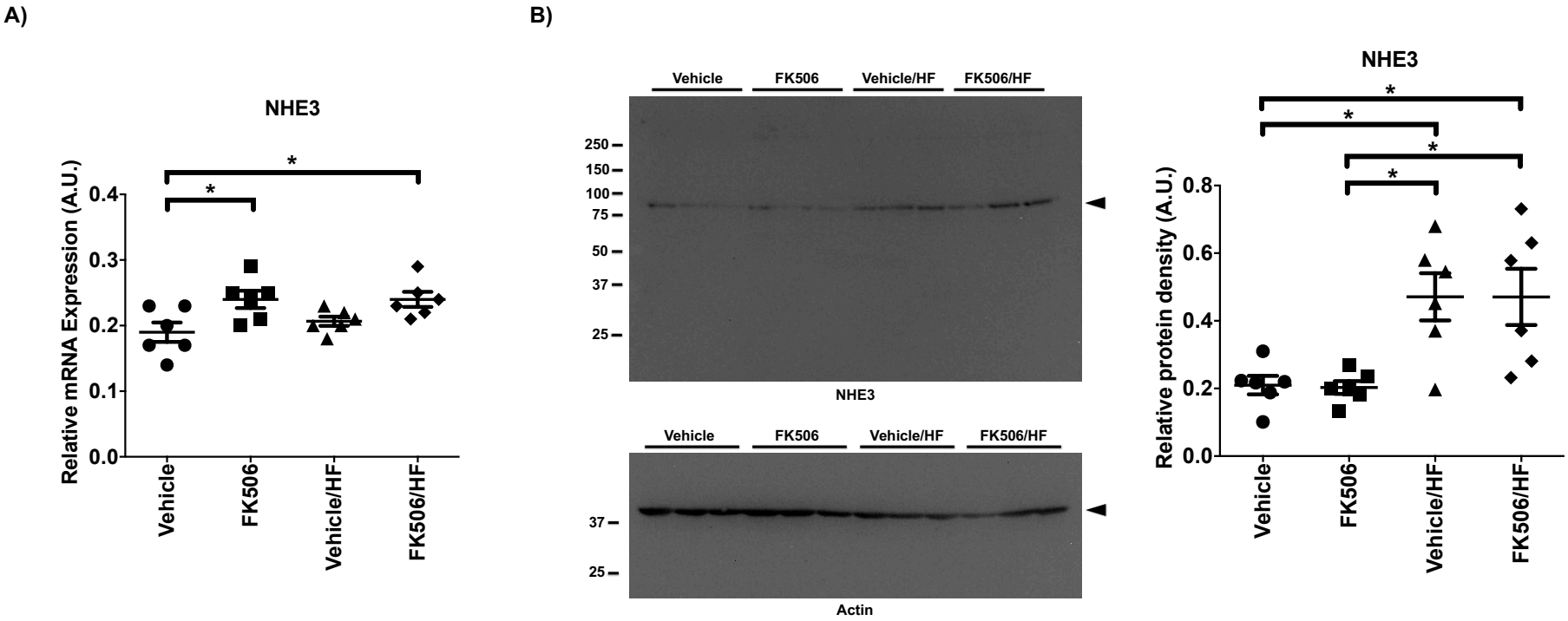

Figure 4.2. Analysis of the renal Na^+/H^+ exchanger, NHE3, after FK506 treatment and/or high-fat diet feeding. A) Relative mRNA expression of the Na^+/H^+ exchanger, NHE3, in whole kidney tissue from mice maintained on a standard or high-fat (HF) diet for 10 weeks and subjected to vehicle or FK506 treatment for 14 days. **B)** Representative western blots for NHE3 (*arrow*) in BBMVs prepared from whole kidney tissue. β-actin (*arrow*) was run as a loading control. Densitometric analyses (*right*) were performed for each group and normalised to β-actin. Values are presented as the mean ± SEM, relative to β-actin (n = 6). Significance was determined by one-way ANOVA with Bonferroni post-test. *P < 0.05.

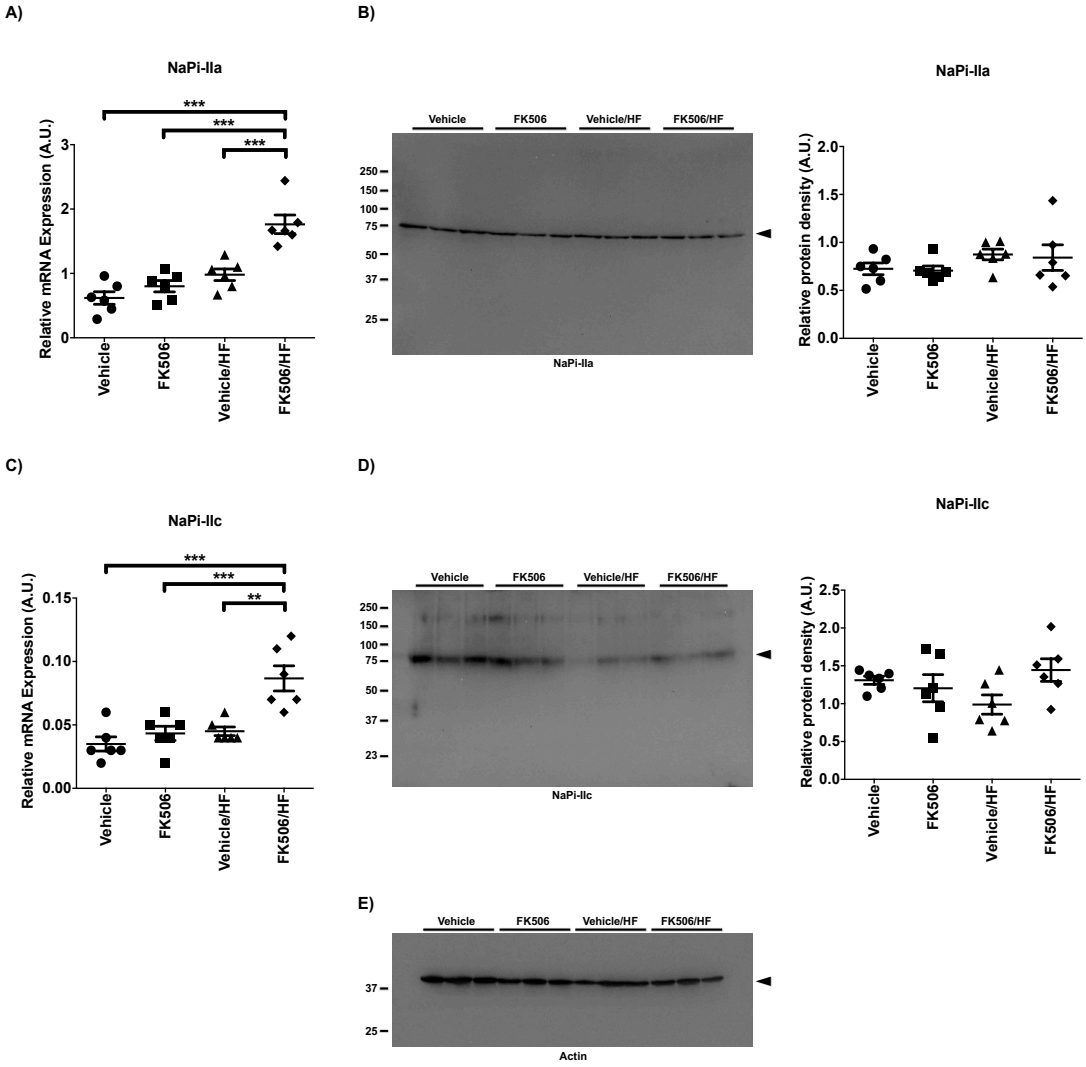

Figure 4.3. Analysis of the renal Na^+/Pi cotransporters, NaPi-IIa and NaPi-IIc, after FK506 treatment and/or high-fat feeding. Relative mRNA expression and protein quantification of the Na^+/Pi cotransporters, **A, B)** NaPi-IIa and, **C, D)** NaPi-IIc, in whole kidney tissue and BBMVs prepared from mice maintained on a standard or HF diet for 10 weeks and subjected to vehicle or FK506 treatment for 14 days. Representative western blots are shown for both proteins (*arrow*). **E)** β-actin (*arrow*) was run as a loading control. Densitometric analyses (*right*) were performed for each group and normalised to β-actin. Values are presented as the mean ± SEM, relative to β-actin (n = 6). Significance was determined by one-way ANOVA with Bonferroni post-test. **P < 0.01, ***P < 0.001.

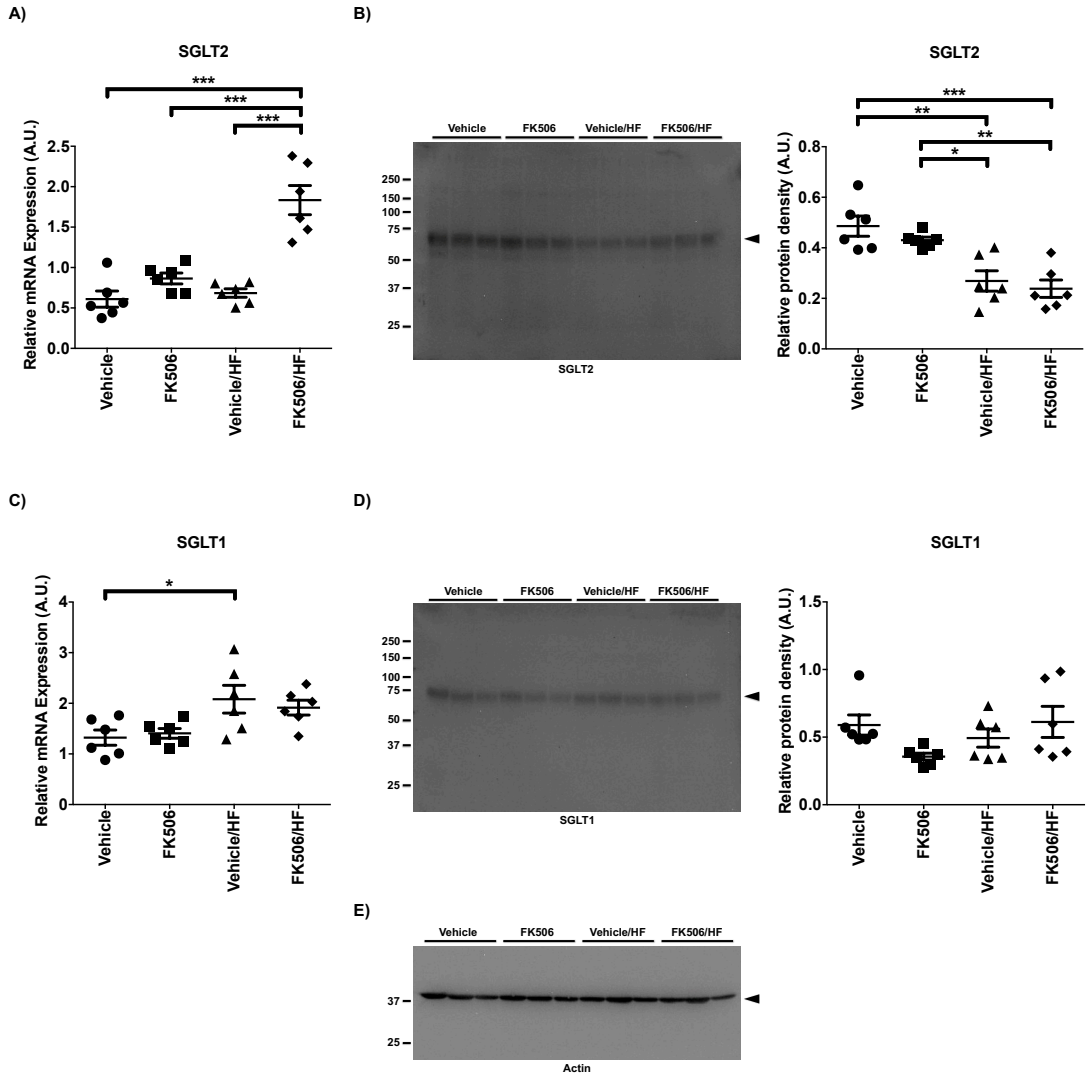

Figure 4.4. Analysis of the renal Na^+/glucose cotransporters, SGLT2 and SGLT1, after FK506 treatment and/or high-fat feeding. Relative mRNA expression and protein quantification of the Na^+/glucose cotransporters, **A, B)** SGLT2 and, **C, D)** SGLT1, in whole kidney tissue and BBMVs prepared from mice maintained on a standard or HF diet for 10 weeks and subjected to vehicle or FK506 treatment for 14 days. Representative western blots are shown for both proteins (*arrow*). **E)** β-actin (*arrow*) was run as a loading control. Densitometric analyses (*right*) were performed for each group and normalised to β-actin. Values are presented as the mean ± SEM, relative to β-actin (n = 6). Significance was determined by one-way ANOVA with Bonferroni post-test. * $P < 0.05$, ** $P < 0.01$, *** $P < 0.001$.

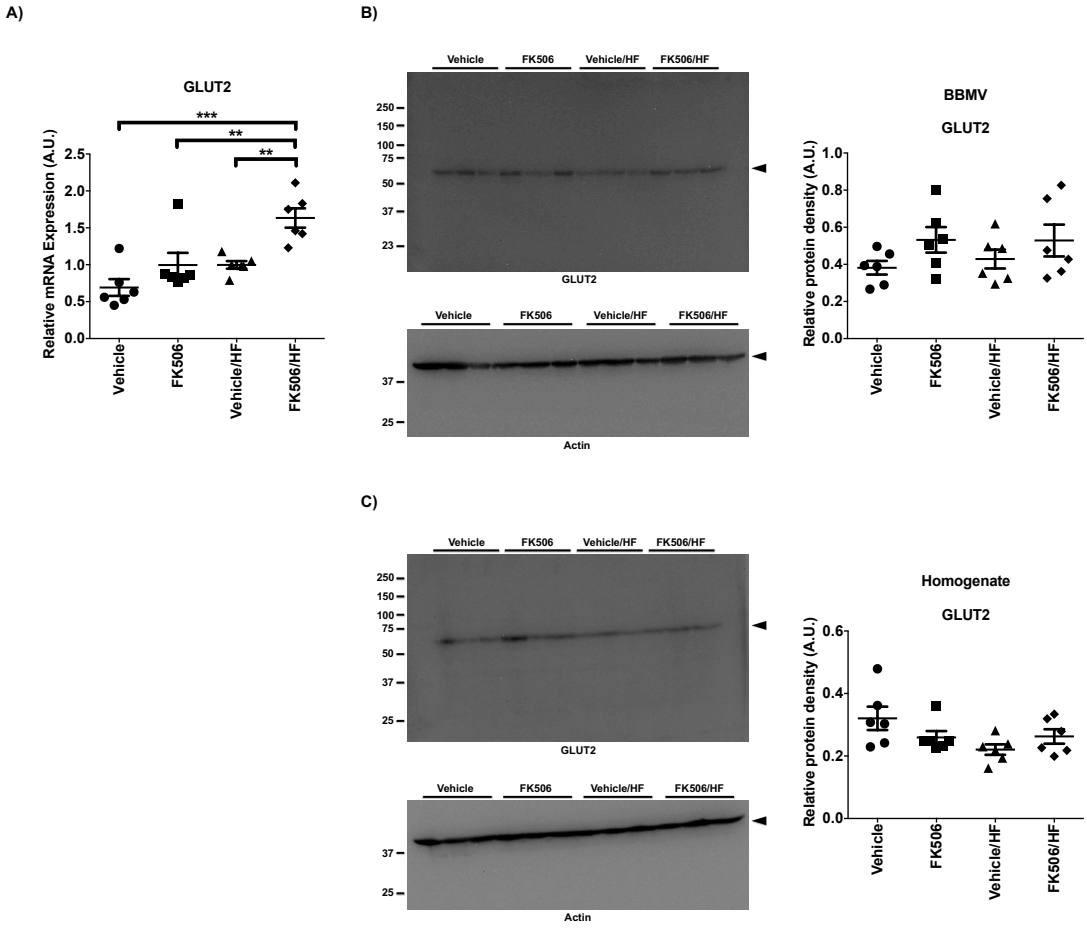

Figure 4.5. Analysis of the renal glucose transporter, GLUT2, after FK506 treatment and/or high-fat feeding. A) Relative mRNA expression of the glucose transporter, GLUT2, in whole kidney tissue from mice maintained on a standard or HF diet for 10 weeks and subjected to vehicle or FK506 treatment for 14 days. Representative western blots and protein quantification for GLUT2 (*arrow*) are shown for both **B)** BBMVs and, **C)** homogenate fractions, prepared from whole kidney tissue. β-actin (*arrow*) was run as a loading control. Densitometric analyses (*right*) were performed for each group and normalised to β-actin. Values are presented as the mean ± SEM, relative to β-actin (n = 6). Significance was determined by one-way ANOVA with Bonferroni post-test. **P < 0.01, ***P < 0.001.

Under all treatment conditions, no significant differences were observed for the TAL Na^+-K^+-$2Cl^-$ cotransporter, NKCC2, at both transcriptional and translational levels (**Fig.4.6**). Unfortunately, due to a limited stock of a gifted antibody and commercially unavailable phospho-antibodies for NKCC2, changes in pNKCC2 abundance could not be measured.

As previously explained, blood pressure could not be directly measured at the present time to confirm the hypertensive states in FK506-treated and diet-induced obese mice. Therefore, the establishment of increased sodium reabsorption, via the up-regulation and phosphorylation of the NCC cotransporter, was used as an indicator of increased sodium retention and an indirect measure for elevations in blood pressure. A significant increase in NCC mRNA expression was found in the FK506-treated group fed on the high-fat diet, while no significant differences in NCC expression were found in mice treated with FK506 or fed on the high-fat diet alone (**Fig.4.7a**). NCC protein levels were unaffected in all four groups (**Fig.4.7b**). However, pNCC was significantly increased in the FK506-treated and high-fat diet-fed control groups, relative to vehicle-treated mice, but was interestingly decreased in the FK506/HF group compared to the FK506 and vehicle/HF groups (**Fig.4.7c**). Overall, these findings confirm the establishment of a significant CNI- and diet-induced sodium retentive, and mostly likely, hypertensive state in these treatment groups.

Expression of the distal epithelial Na^+ channel, ENaC was found to be significantly higher in FK506-treated mice fed on either the standard or high-fat diets compared to control mice on either diet (**Fig.4.8a**). However, the protein abundance for the α-ENaC subunit was significantly lower in the FK506-treated and vehicle/HF groups, and showed a slight, but not statistically significant, decrease in the FK506/HF group (**Fig.4.8b**).

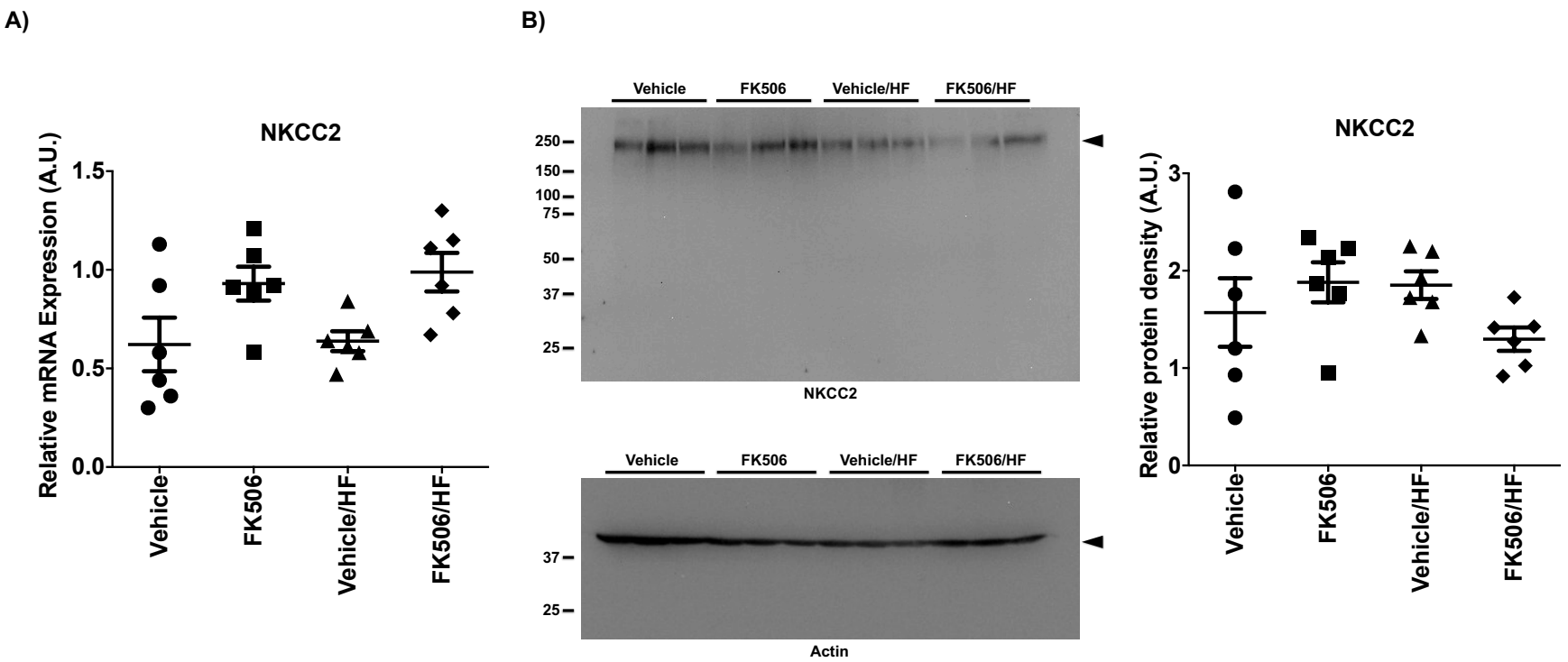

Figure 4.6. Analysis of the renal Na^+-K^+-$2Cl^-$ cotransporter, NKCC2, after FK506 treatment and/or high-fat feeding. A) Relative mRNA expression of the Na^+-K^+-$2Cl^-$ cotransporter NKCC2 in whole kidney tissue from mice maintained on a standard or HF diet for 10 weeks and subjected to vehicle or FK506 treatment for 14 days. **B)** Representative western blots for NKCC2 (*arrow*) in homogenate fractions prepared from whole kidney tissue. β-actin (*arrow*) was run as a loading control. Densitometric analyses (*right*) were performed for each group and normalised to β-actin. Values are presented as the mean ± SEM, relative to β-actin (n = 6). Significance was determined by one-way ANOVA with Bonferroni post-test.

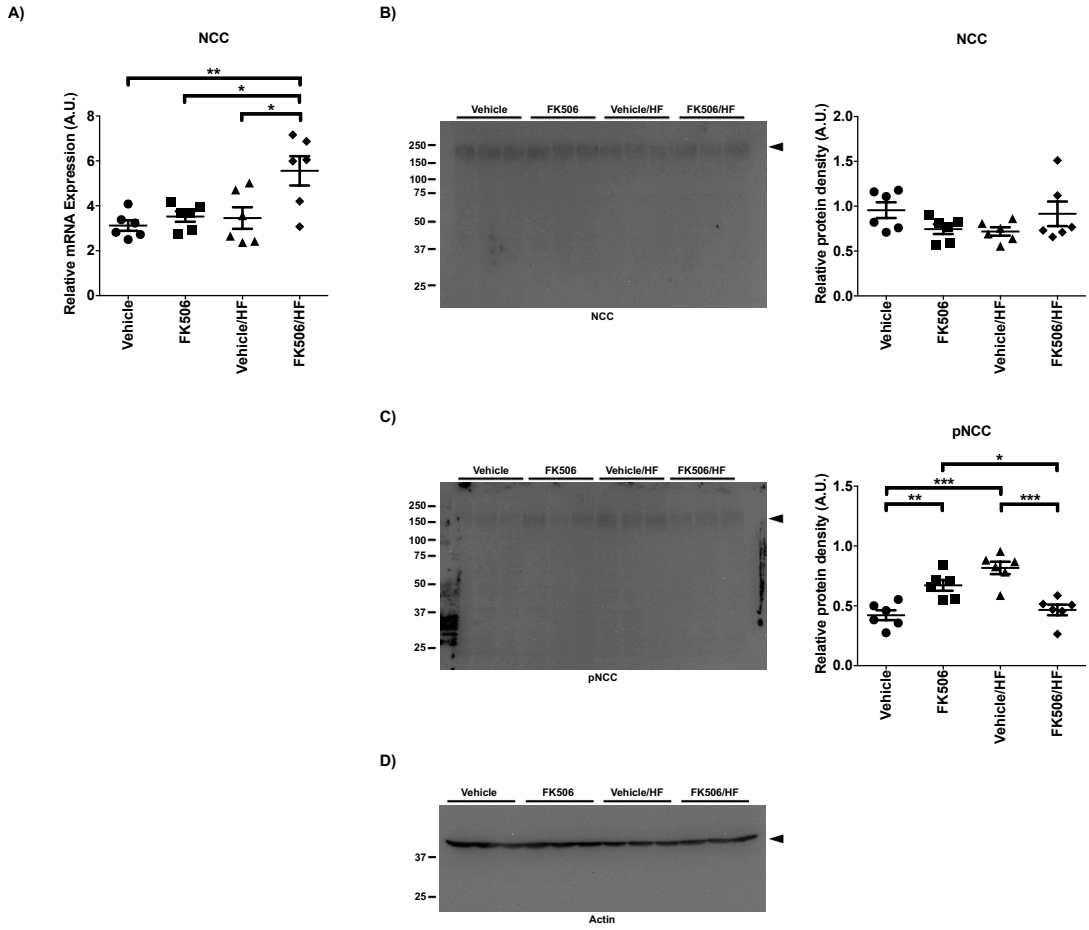

Figure 4.7 Analysis of the renal Na^+/Cl^- cotransporter, NCC, after FK506 treatment and/or high-fat feeding. A) Relative mRNA expression of the Na^+/Cl^- cotransporter, NCC, in whole kidney tissue from mice maintained on a standard or HF diet for 10 weeks and subjected to vehicle or FK506 treatment for 14 days. Representative western blots and protein quantification are shown for **B)** NCC (*arrow*) and, **C)** phosphorylated NCC (*arrow*), in homogenate fractions prepared from whole kidney tissue. **D)** β-actin (*arrow*) was run as a loading control. Densitometric analyses (*right*) were performed for each group and normalised to β-actin. Values are presented as the mean ± SEM, relative to β-actin (n = 6). Significance was determined by one-way ANOVA with Bonferroni post-test. *P < 0.05, **P < 0.01, ***P < 0.001.

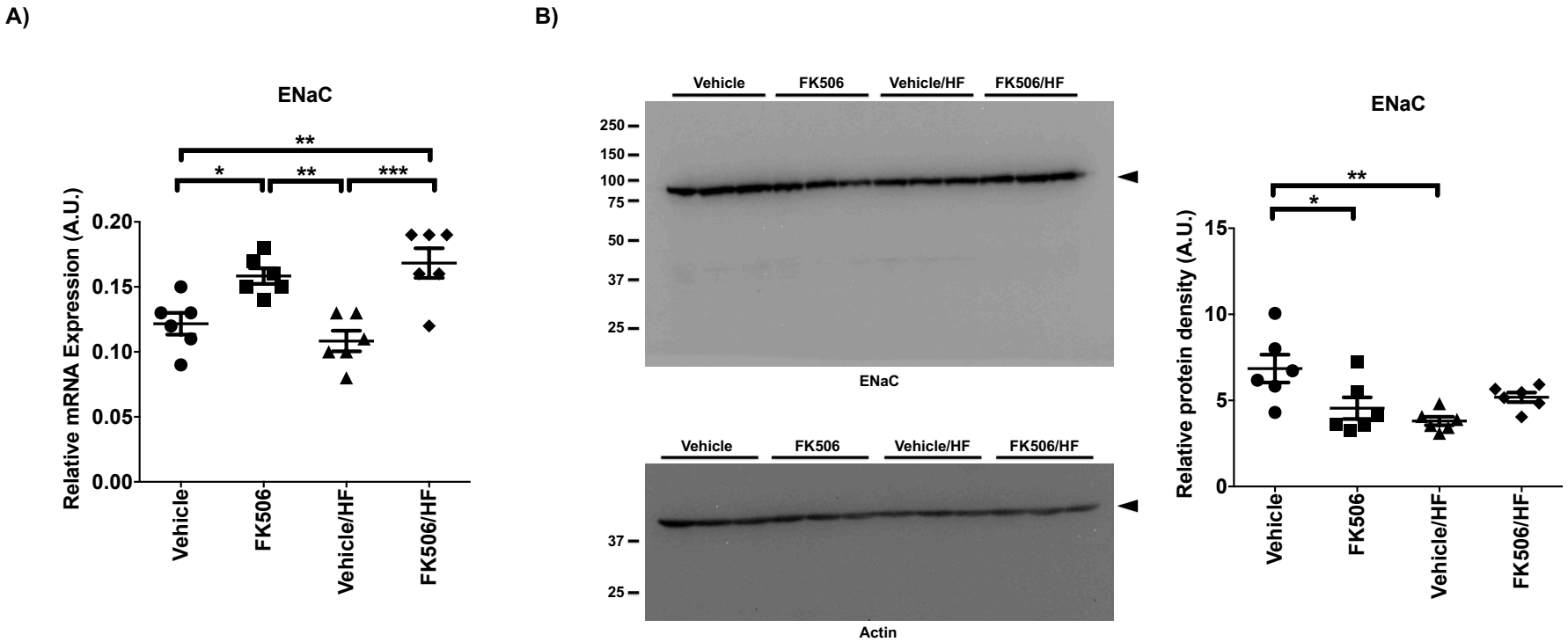

Figure 4.8. Analysis of the renal epithelial Na^+ channel, ENaC, after FK506 treatment and/or high-fat feeding. A) Relative mRNA expression of the epithelial Na^+ channel ENaC in whole kidney tissue from mice maintained on a standard or HF diet for 10 weeks and subjected to vehicle or FK506 treatment for 14 days. **B)** Representative western blots for ENaC (*arrow*) in homogenate fractions prepared from whole kidney tissue. β-actin (*arrow*) was run as a loading control. Densitometric analyses (*right*) were performed for each group and normalised to β-actin. Values are presented as the mean ± SEM, relative to β-actin (n = 6). Significance was determined by one-way ANOVA with Bonferroni post-test. *P < 0.05, **P < 0.01, ***P < 0.001.

4.3.3 Influences of FK506 and/or diet-induced obesity on proximal small intestinal transport proteins

To further investigate the mechanisms behind the alterations in sodium retention, and glucose, phosphate and acid-base homeostasis in these models, intestinal-specific transport proteins were also assessed. For this, mRNA and BBMVs/homogenate samples were prepared from mucosa scrapes from the proximal (duodenum and jejunum) and distal (ileum) small intestine and large intestinal (colon) segments and analysed for changes in NHE3, NaPi-IIb, PiT1, SGLT1 and GLUT2 transporters.

Under baseline and treated conditions, the NHE3 exchanger has relatively low expression levels in the proximal intestinal segment in comparison to the kidney and remained unchanged under all treatments (**Fig.4.9a**). Western blotting showed a significant decrease in protein abundance in the FK506/HF group relative to FK506-treated mice on the standard diet (**Fig.4.9b**). A slight, but not significant, decrease in NHE3 was also observed in the vehicle/HF group compared to the standard diet-fed control group.

In keeping with previous reports, mRNA analysis of the NaPi-IIb cotransporter in small intestinal tissues from mice demonstrated lower expression levels in the proximal segment compared with the distal segment of the small intestines (**Fig.4.10a,b and Fig.4.13a,b**) (Marks et al., 2006; Radanovic et al., 2005; Sabbagh et al., 2009; Stauber et al., 2005). Treatment with FK506 resulted in a significant increase in NaPi-IIb mRNA expression while the supplement of the high-fat diet with either treatments led to a significant decrease (**Fig.4.10a**). In contrast, mice fed on the high-fat diet with either treatments displayed a significant increase in PiT1 mRNA expression which was inversely correlated with a decrease in protein expression, compared with standard diet-fed mice (**Fig.4.10b,c**). NaPi-IIb protein could not be detected by western blot in the proximal segment, which

is mostly likely attributed to its low mRNA expression. It should be noted however, that despite these observations, due to their relatively low mRNA expression and the uncertainties in both NaPi-IIb and PiT1 protein localisation in mice, as well as the functional role for PiT1, the changes seen for these transport proteins in this segment are unlikely to have a significant impact on phosphate balance. Attention was therefore focused towards the distal segment of the small intestine, which was reported as the main site of Na^+-dependent phosphate absorption in mice (Marks et al., 2006; Radanovic et al., 2005; Sabbagh et al., 2009; Stauber et al., 2005).

As expected, compared to its expression in the kidney, SGLT1 expression was higher in the small intestines, predominantly in the proximal intestinal segment, whilst GLUT2 expression was relatively low. In contrast to the renal-related findings, intestinal SGLT1 and GLUT2 mRNA expression remained unchanged under all treatment groups (**Fig.4.11a,c**). However, SGLT1 protein was significantly lower in the high-fat diet groups under both treatments compared with the standard diet-fed control group (**Fig.4.11b**). Similar to the renal observations, GLUT2 protein levels remained unchanged in all treatment conditions in BBMV samples (**Fig.4.11d**), but as previously mentioned, under the conditions used in this study, GLUT2 was not expected to be present at the BBM and unfortunately GLUT2 could not be detected in the homogenate fractions.

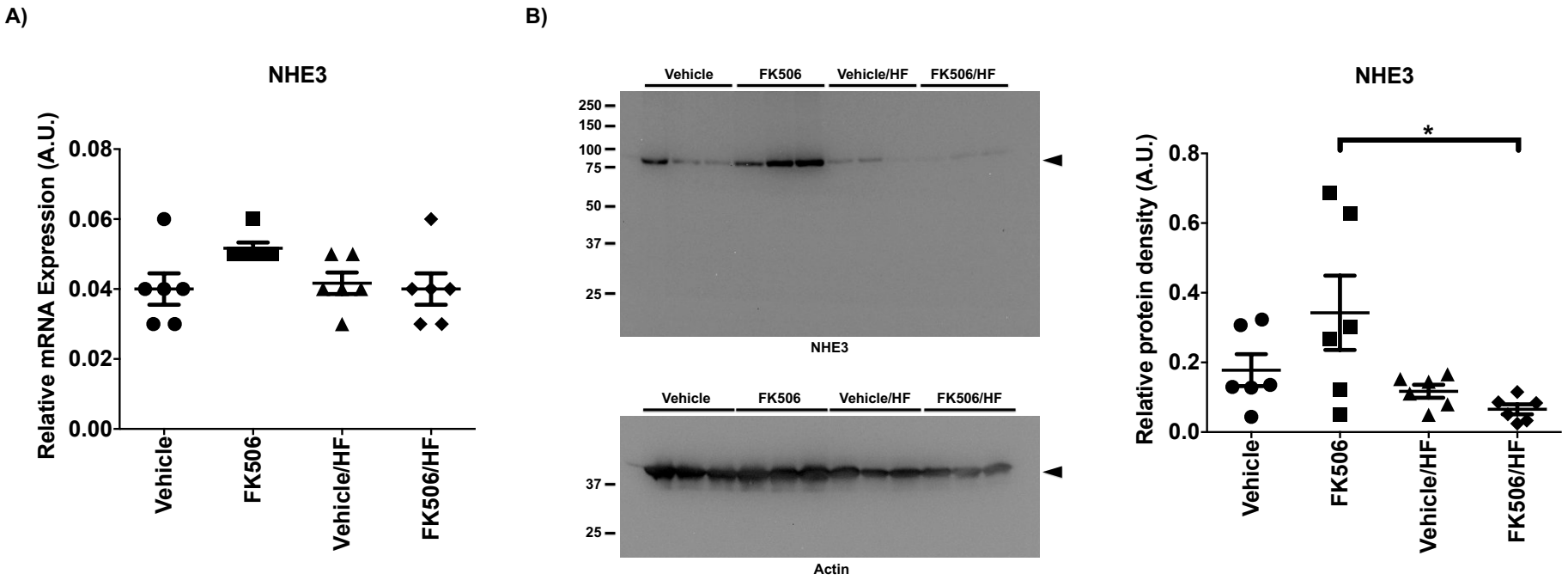

Figure 4.9. Analysis of the Na^{+}/H^{+} exchanger, NHE3, in the proximal small intestine (PSI) after FK506 treatment and/or high-fat feeding. **A)** Relative mRNA expression of the Na^{+}/H^{+} exchanger, NHE3, in PSI mucosa scrapes collected from mice maintained on a standard or HF diet for 10 weeks and subjected to vehicle or FK506 treatment for 14 days. **B)** Representative western blots for NHE3 (*arrow*) in BBMVs prepared from PSI mucosa scrapes. β-actin (*arrow*) was run as a loading control. Densitometric analyses (*right*) were performed for each group and normalised to β-actin. Values are presented as the mean ± SEM, relative to β-actin (n = 6). Significance was determined by one-way ANOVA with Bonferroni post-test. *P < 0.05.

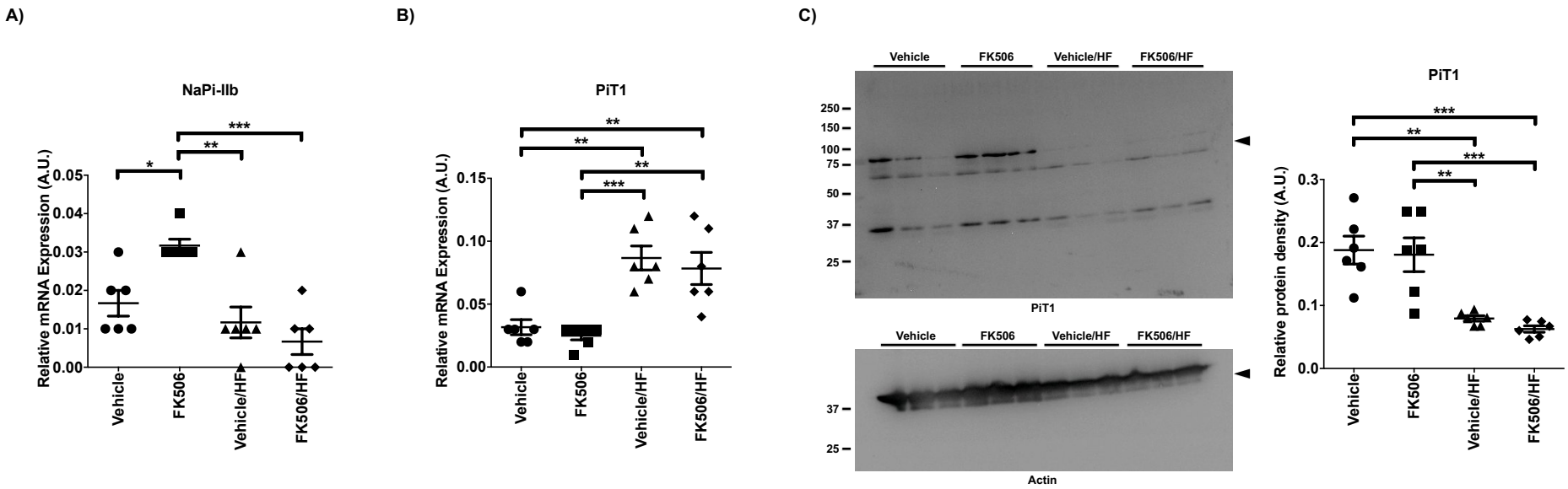

Figure 4.10. Analysis of the Na^+/Pi cotransporters, NaPi-IIb and PiT1, in the PSI after FK506 treatment and/or high-fat feeding. Relative mRNA expression of the Na^+/Pi cotransporters, **A)** NaPi-IIb and, **B)** PiT1, in PSI mucosa scrapes from mice maintained on a standard or HF diet for 10 weeks and subjected to vehicle or FK506 treatment for 14 days. **C)** Representative western blots for PiT1 (*arrow*) in BBMVs prepared from PSI mucosa scrapes. β-actin (*arrow*) was run as a loading control. Densitometric analyses (*right*) were performed for each group and normalised to β-actin. Values are presented as the mean ± SEM, relative to β-actin (n = 6). Significance was determined by one-way ANOVA with Bonferroni post-test. *P < 0.05, **P < 0.01, ***P < 0.001.

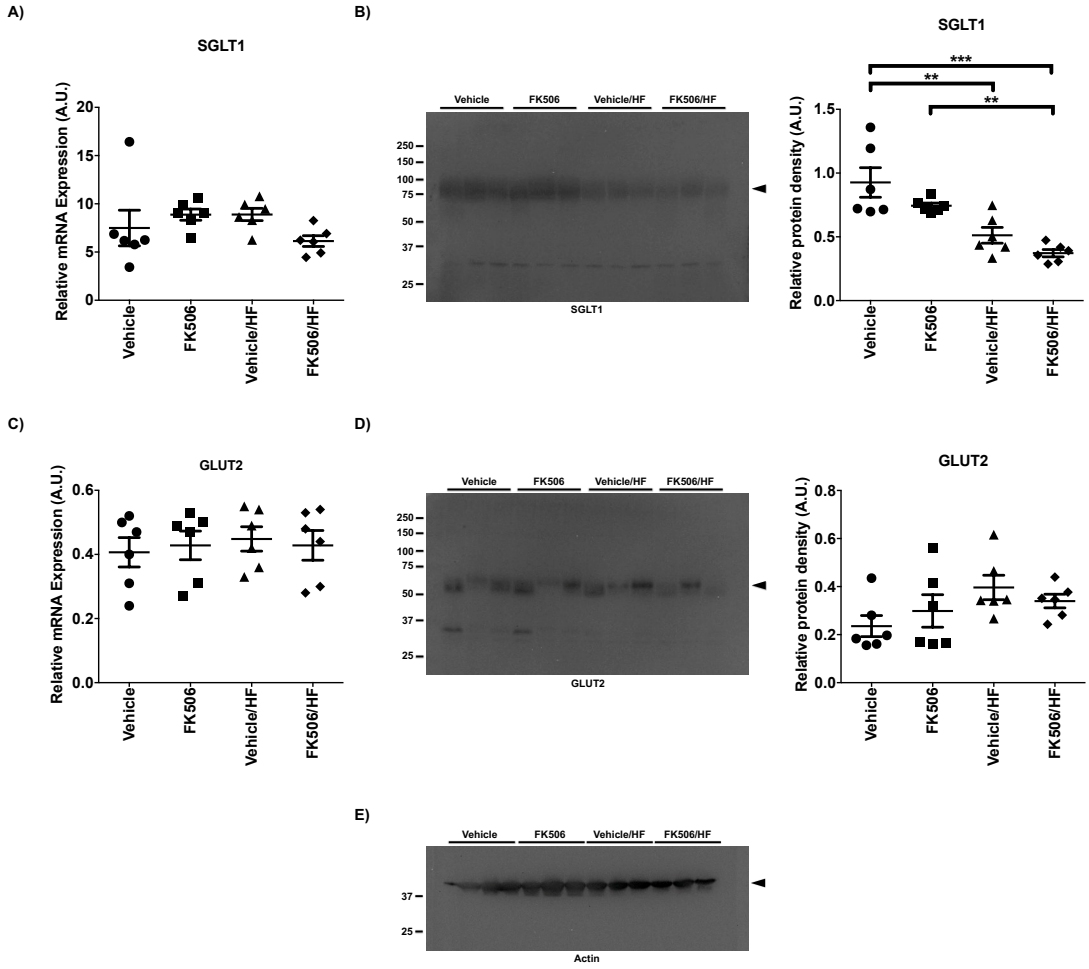

Figure 4.11. Analysis of the Na^+/glucose cotransporter, SGLT1, and the glucose transporter, GLUT2, in the PSI after FK506 treatment and/or high-fat diet feeding. Relative mRNA expression and protein quantification of the Na^+/glucose cotransporter, **A, B)** SGLT1, and the glucose transporter, **C, D)** GLUT2, in PSI mucosa scrapes and prepared BBMVs from mice maintained on a standard or HF diet for 10 weeks and subjected to vehicle or FK506 treatment for 14 days. Representative western blots are shown for both proteins (*arrow*). **E)** β-actin (*arrow*) was run as a loading control. Densitometric analyses (*right*) were performed for each group and normalised to β-actin. Values are presented as the mean ± SEM, relative to β-actin (n = 6). Significance was determined by one-way ANOVA with Bonferroni post-test. **P < 0.01, ***P < 0.001.

4.3.4 Influences of FK506 and/or diet-induced obesity on distal small intestinal transport proteins

Due to the lower presence of villi, and therefore, the isolation of BBMVs in the distal segment of the small intestines, protein levels were measured in the homogenate fractions.

In analyses for changes in acid-base proteins in the distal small intestines, NHE3 protein could not be detected with western blot applications, which was supported by the low relative mRNA expression in this segment and also showed no significant changes in all treatment groups (**Fig.4.12**). No changes were also found for NaPi-IIb mRNA expression (**Fig.4.13a**). Unfortunately, due to the poor protein quality of the homogenate fractions isolated from this segment, NaPi-IIb protein detection was not optimal and although protein quantifications showed a significant decrease in FK506-treated mice and the high-fat diet-fed groups (**Fig.4.13b**), without further clarification no conclusions in terms of intestinal phosphate absorption can be drawn from these observations. A slight but statistically significant increase in PiT1 mRNA expression was found in the FK506/HF group (**Fig.4.13c**), with no changes in protein abundance in all treatment conditions (**Fig.4.13d**). However, again, due to the uncertainties with regards to the functional role for PiT1, the impact of these changes to this transporter is unlikely to be large.

Similar to prior observations in the proximal small intestines, SGLT1 mRNA expression was unchanged in all treatment groups and was paralleled with no significant changes in protein abundance with very low-to-negligible protein detection (**Fig.4.14a,b**). GLUT2 mRNA also remained unchanged in all four groups and GLUT2 protein could not be detected in homogenate samples (**Fig.4.14c**).

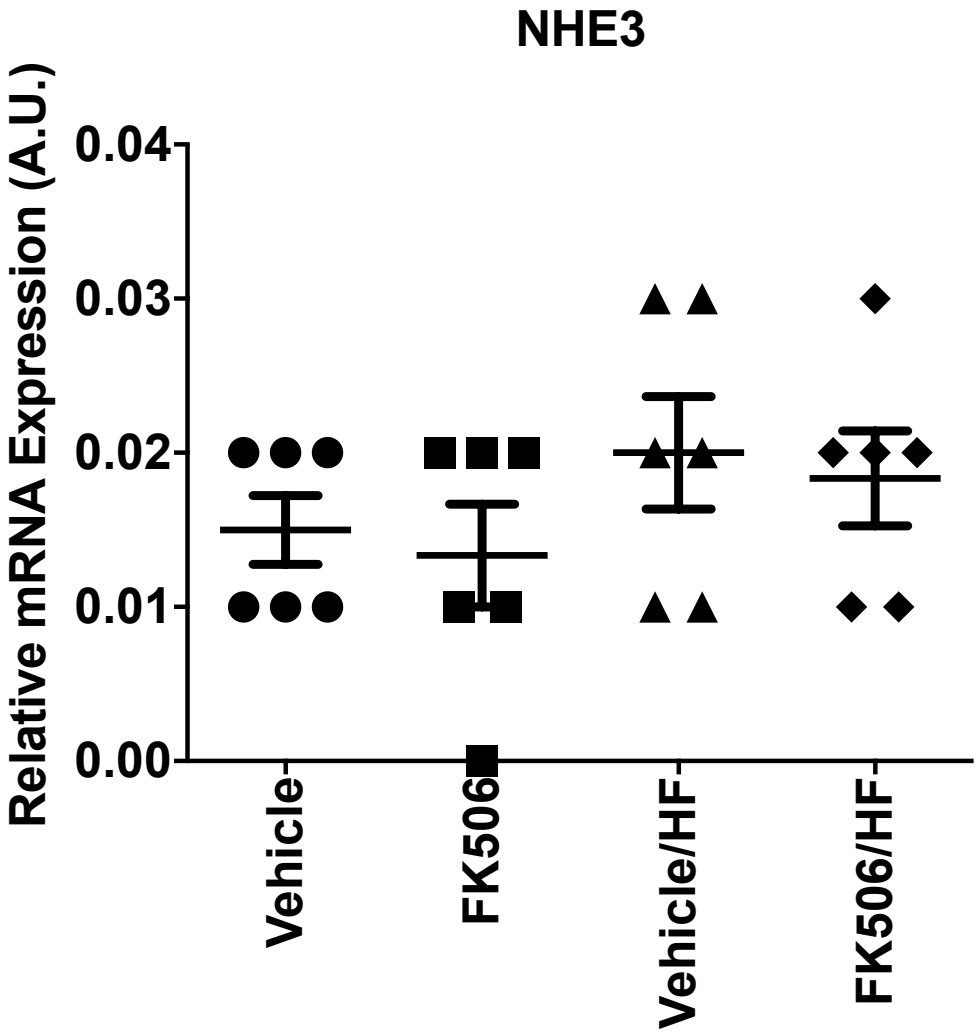

Figure 4.12. Analysis of the Na^+/H^+ exchanger, NHE3, in the distal small intestine (DSI) after FK506 treatment and/or high-fat feeding. Relative mRNA expression of the Na^+/H^+ exchanger, NHE3, in DSI mucosa scrapes collected from mice maintained on a standard or HF diet for 10 weeks and subjected to vehicle or FK506 treatment for 14 days. Values are presented as the mean ± SEM, relative to β-actin (n = 6). Significance was determined by one-way ANOVA with Bonferroni post-test.

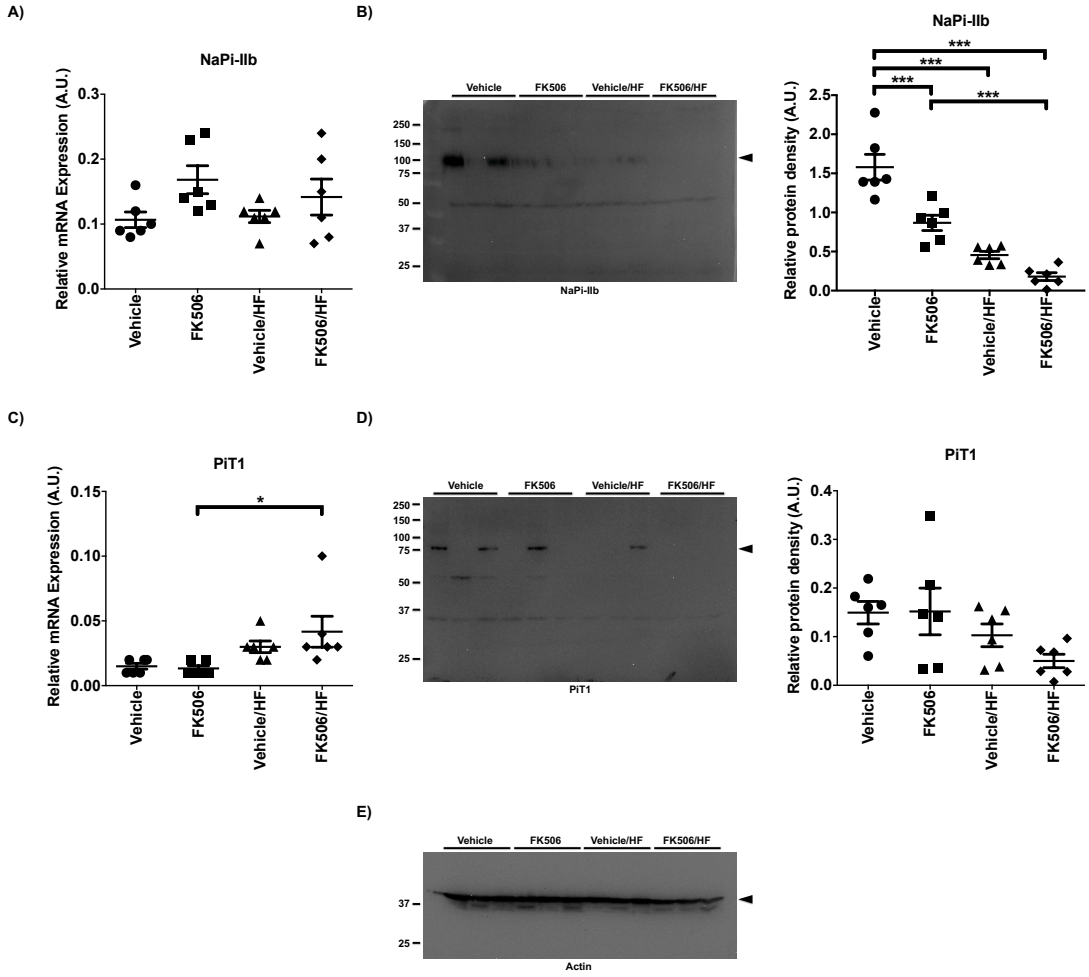

Figure 4.13. Analysis of the Na^+/Pi cotransporters, NaPi-IIb and PiT1, in the DSI after FK506 treatment and/or high-fat feeding. Relative mRNA expression and protein quantification of the Na^+/Pi cotransporters, **A, B)** NaPi-IIb and, **C, D)** PiT1, in DSI mucosa scrapes and homogenate fractions prepared from mice maintained on a standard or HF diet for 10 weeks and subjected to vehicle or FK506 treatment for 14 days. Representative western blots are shown for both proteins (*arrow*). **E)** β-actin (*arrow*) was run as a loading control. Densitometric analyses (*right*) were performed for each group and normalised to β-actin. Values are presented as the mean ± SEM, relative to β-actin (n = 6). Significance was determined by one-way ANOVA with Bonferroni post-test. *P < 0.05, ***P < 0.001.

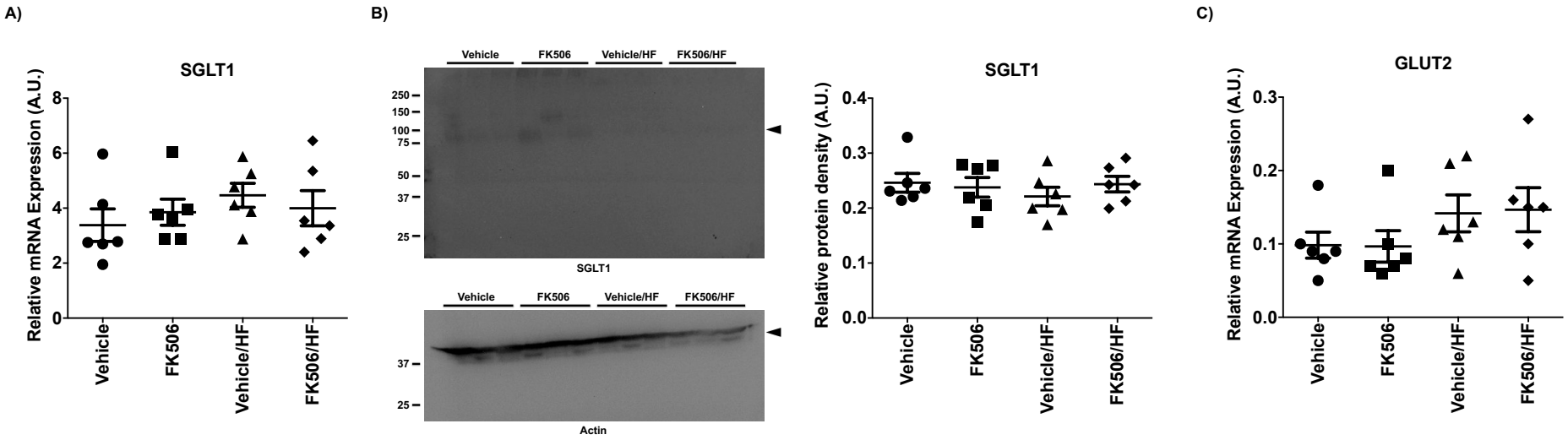

Figure 4.14. Analysis of the Na^+/glucose cotransporter, SGLT1, and the glucose transporter, GLUT2, in the DSI after FK506 treatment and/or high-fat feeding. Relative mRNA expression and protein quantification of the Na^+/glucose cotransporter, **A, B)** SGLT1 and relative mRNA expression of the glucose transporter, **C)** GLUT2, in DSI mucosa scrapes and homogenate fractions prepared from mice maintained on a standard or HF diet for 10 weeks and subjected to vehicle or FK506 treatment for 14 days. Representative western blots are shown for SGLT1 protein (*arrow*). β-actin (*arrow*) was run as a loading control. Densitometric analyses (*right*) were performed for each group and normalised to β-actin. Values are presented as the mean ± SEM, relative to β-actin (n = 6). Significance was determined by one-way ANOVA with Bonferroni post-test.

4.3.5 Influences of FK506 and/or diet-induced obesity on large intestinal transport proteins

As the large intestines are much smaller than the small intestinal segments, the collected mucosal scrapes were not sufficient for both mRNA and protein analyses, and so only protein analysis was performed on this segment. Additionally, because the large intestine does not have villi, protein abundances were measured in the homogenate fractions.

As shown, NHE3 protein levels were significantly decreased in the high-fat groups with either vehicle or FK506-treatment, compared with FK506-treatment alone (**Fig.4.15**). However, α-ENaC remained unchanged in all treatment groups (**Fig.4.16**).

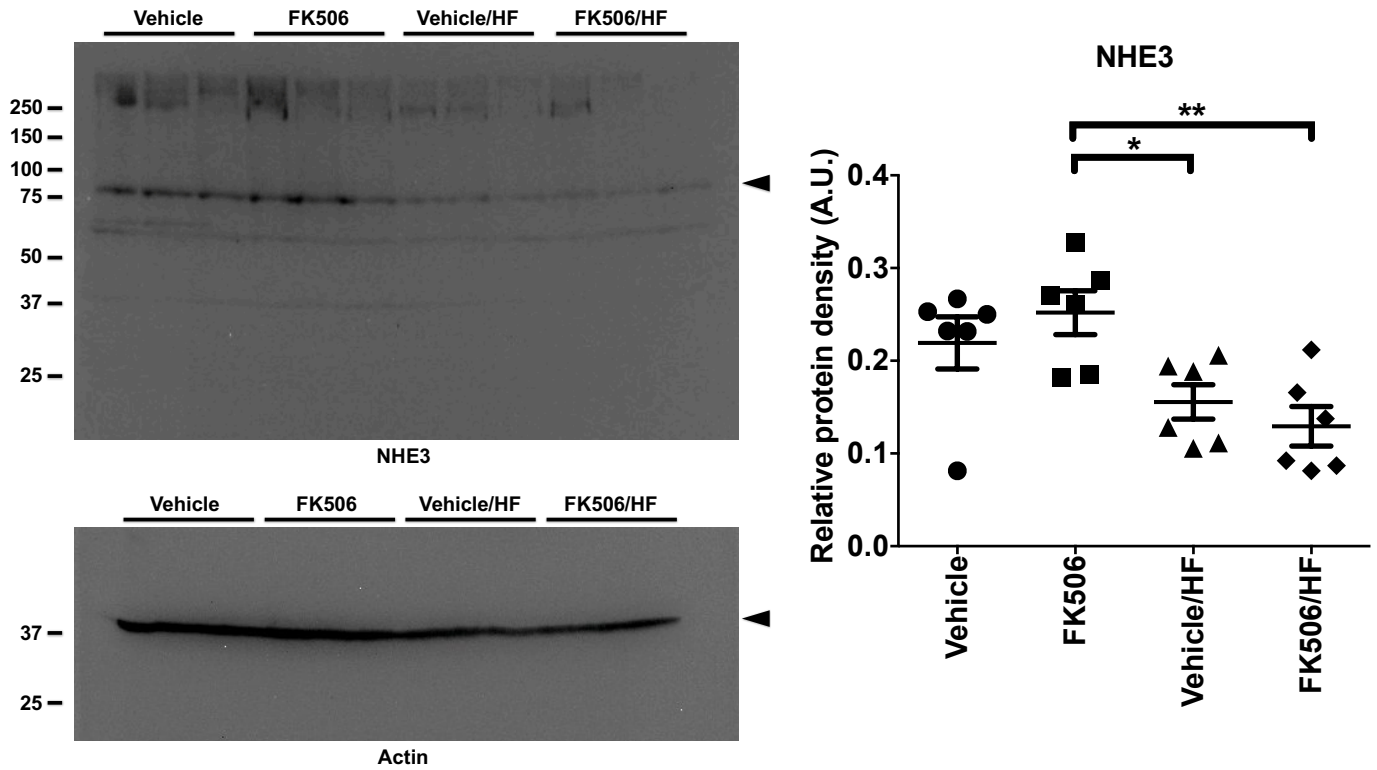

Figure 4.15. Analysis of the Na^+/H^+ exchanger, NHE3, in the large intestines (LI) after FK506 treatment and/or high-fat feeding. Representative western blots of the Na^+/H^+ exchanger, NHE3 (*arrow*), in large intestinal homogenate fractions prepared from mice maintained on a standard or HF diet for 10 weeks and subjected to vehicle or FK506 treatment for 14 days. β-actin (*arrow*) was run as a loading control. Densitometric analyses (*right*) were performed for each group and normalised to β-actin. Values are presented as the mean ± SEM, relative to β-actin (n = 6). Significance was determined by one-way ANOVA with Bonferroni post-test. *P < 0.05, **P < 0.01.

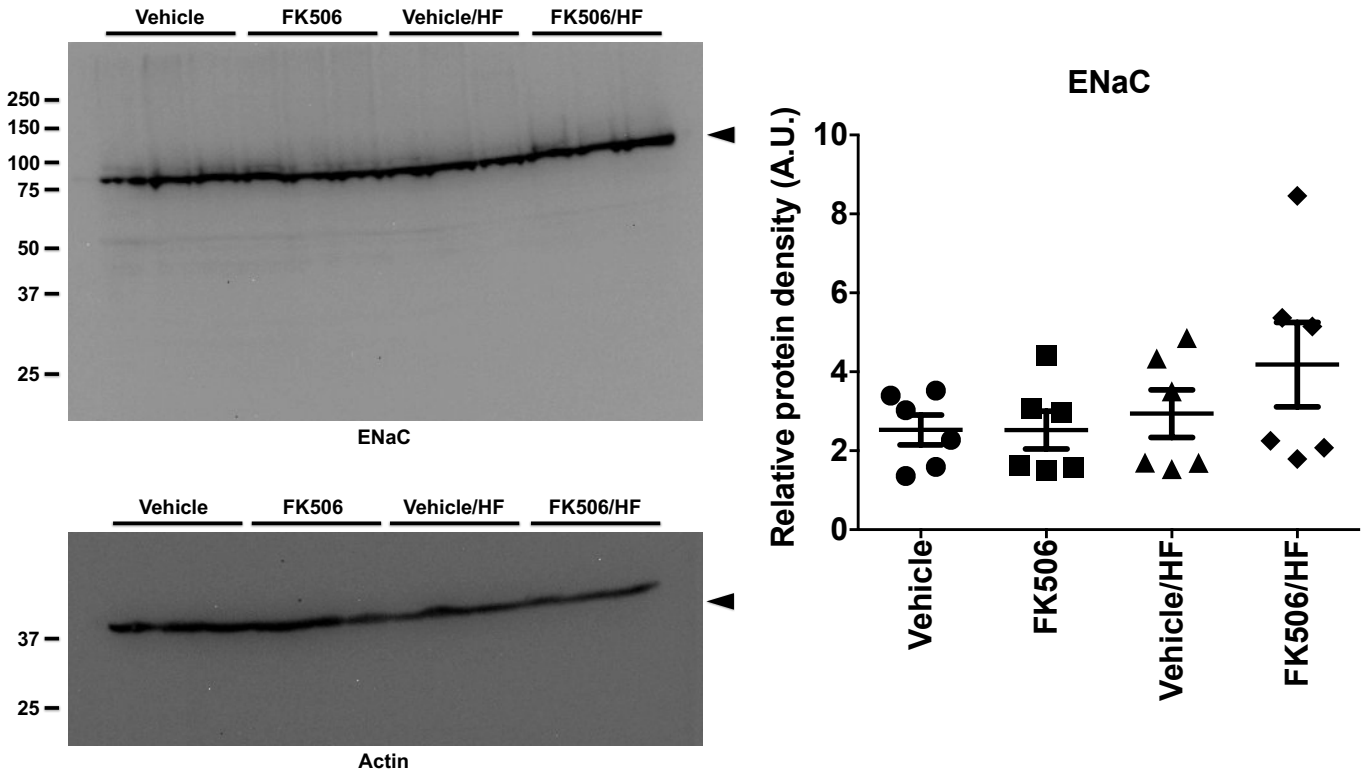

Figure 4.16. Analysis of the epithelial Na^+ channel, ENaC, in the LI after FK506 treatment and/or high-fat feeding. Representative western blots of the α-subunit of the epithelial Na^+ channel, ENaC (arrow), in large intestinal homogenate fractions prepared from mice maintained on a standard or HF diet for 10 weeks and subjected to vehicle or FK506 treatment for 14 days. β-actin (*arrow*) was run as a loading control. Densitometric analyses (*right*) were performed for each group and normalised to β-actin. Values are presented as the mean ± SEM, relative to β-actin (n = 6). Significance was determined by one-way ANOVA with Bonferroni post-test.

4.4 Discussion

Both cyclosporine (CsA) and tacrolimus (FK506) have been reported to influence the development of the individual conditions associated with metabolic syndrome in renal transplant patients (Boudreaux et al., 1987; Chapman et al., 1987; Grimm et al., 2006; Jevnikar et al., 1988; Kasiske et al., 2003; Ligtenberg et al., 2001; Margreiter, 2002; McCune et al., 1998; Pirsch et al., 1997; Roth et al., 1989; Schorn et al., 1991; Vincenti et al., 2002; Woodward et al., 2003). CsA has shown to have a greater impact on lipid profiles and blood pressure, while FK506 has been associated with a higher incidence of PTDM, which is central to the development of metabolic syndrome (Grimm et al., 2006; Kamar et al., 2007; Kasiske et al., 2003; Ligtenberg et al., 2001; Margreiter, 2002; McCune et al., 1998; Pirsch et al., 1997; Vincenti et al., 2002, 2007; Woodward et al., 2003). Due to these similarities, it was theorised that CNIs may influence the development of metabolic syndrome in renal transplant patients, however, this has not yet been investigated. Therefore, the present study sought to compare a model of CNI treatment with a model of diet-induced metabolic syndrome, which was followed by the examination of changes in transport proteins (at mRNA and protein levels) in the kidney and gastrointestinal tract to determine if specific cellular transport pathways may contribute to the development of the individual conditions associated with metabolic syndrome.

4.4.1 Establishment of a diet-induced model of metabolic syndrome

Metabolic syndrome is a commonly encountered complication following renal transplantation and is associated with CVD, graft loss and patient death (Pedrollo et al., 2016; Porrini et al., 2006; de Vries et al., 2004). Many animal studies using a high-fat feeding model investigated the pathogenic mechanisms that underlie its development. As previously mentioned, the C57BL/6J mouse strain is a particularly suitable model for studying metabolic

syndrome owing to its susceptibility to developing obesity, hyperinsulimeia, hyperglycemia and hypertension when placed on a high-fat diet (Black et al., 1998; Deji et al., 2008; Gallou-Kabani et al., 2007; Surwit et al., 1988, 1995; West et al., 1992; Winzell and Ahren, 2004). Other studies using high-fat feeding in this strain have also reported compromised immune function and atherosclerosis development (Crevel et al., 1992; Paigen et al., 1985). The results presented in this chapter demonstrate that high-fat feeding in mice for a 10-week period induced systemic changes which were similar to human metabolic syndrome including obesity, altered glucose homeostasis and possible hypertension.

The clinical diagnosis for metabolic syndrome includes hypertriglyceridemia and low plasma HDLs (National Cholesterol Education Program (NCEP), 2012), however, this was not observed in the present study. Instead, hypertriglyceridemia was not observed in either treatment groups and a significant increase in plasma HDLs were detected in the high-fat diet-fed groups, which conflicts with expected lipid profiles. The reasons for this are not yet clear. However, studies in humans and mice fed on diets rich in fat and cholesterol also displayed elevated HDL levels and did not develop hypertriglyceridemia, which was suggested to be the result of increased HDL transport rates and reduced fractional catabolic rates (Brinton et al., 1990; Hayek et al., 1993; Schreyer et al., 1998). These investigators proposed that dietary fat-induced elevations in HDL levels may be an adaptive response to the metabolic load of the high-fat diet, which may support the observations seen in the present study.

CNIs have also been associated with elevations in plasma LDLs, and have reported the involvement of a number of mechanisms including increased LDL oxidation, reduced LDL catabolism via reduced LDL receptor activity or a reduction in lipoprotein lipase activity and production, leading to impaired LDL clearance (Apanay et al., 1994; Bakar et al., 2009; Rayyes et al., 1996;

Tory et al., 2009). In the present study, CNI-treated mice did not exhibit any alterations in plasma triglyceride and HDL levels. It is possible that the absence of hypertriglyceridemia and hyperlipidemia in these CNI-treated mice may be a reflection of the lower incidence of lipid changes associated with FK506 over CsA, as confirmed in numerous clinical and animal studies (Artz et al., 2003; Baid-Agrawal et al., 2004; Ligtenberg et al., 2001; McCune et al., 1998; Pirsch et al., 1997). However, as total- and LDL-cholesterol levels were not measured in either models, diet- and CNI-induced hyperlipidemia cannot be ruled out. Further analyses are required to measure total- and LDL-cholesterol levels as well as LDL oxidation and lipoprotein lipase activity to explain for the hypertriglyceridemia observed in renal transplant patients treated with CNIs.

Overall, biochemical analyses in mice fed on a high-fat diet displayed indications of altered glucose, acid-base and sodium homeostasis which are features associated with metabolic syndrome. FK506 treatment did not mimic these changes suggesting that CNI treatment alone might not be enough to induce the development of metabolic syndrome and that other factors may need to be present. In this regard, attention was drawn towards comparisons between FK506 treatment alone and in combination with high-fat feeding. The model of metabolic syndrome established was enough to permit investigations into the renal and intestinal transport proteins that may be involved in metabolic syndrome development and, therefore, became another main focus of this study.

4.4.2 FK506 treatment and high-fat feeding on renal and intestinal acid-base and phosphate transport proteins

Patients with metabolic syndrome and type II diabetes mellitus commonly display decreased urinary pH and impaired NH_4^+ excretion, which are clinical and metabolic abnormalities associated with hyperuricemia and uric acid

nephrolithiasis, and can lead to kidney stone formation (Abate et al., 2004; Cameron et al., 2006; Daudon et al., 2006; Maalouf et al., 2007; Sakhaee et al., 2002). Studies using Zucker obese and high-fat diet-fed rats have suggested that renal lipotoxicity plays a part in the pathophysiology of these conditions through impaired NH_4^+ secretion and Na^+/H^+ exchange via a reduction in renal NHE3 protein and function (Bobulescu et al., 2008). This decrease in renal NHE3 protein was further supported in studies with Zucker obese rat models (Bickel et al., 2002; Riazi et al., 2006). However, the opposite was observed in the present study for the high-fat group and a number of possible reasons may explain this.

The more likely reason could be an adaptation to the metabolic load from the high-fat diet. From the biochemical analyses, a significant reduction in plasma HCO_3^- , and increased plasma and urinary phosphate in the high-fat groups indicate signs of altered acid-base balance and potentially an acidotic effect. It is known that under acidotic conditions, the kidneys act to increase H^+ and NH_4^+ excretion, reclaim HCO_3^- and reduce phosphate uptake via an upregulation of NHE3 and downregulation of NaPi-IIa transport proteins, respectively (Ambühl et al., 1998; Ambuhl et al., 1996; Amemiya et al., 1995; Laghmani et al., 1997; Soleimani et al., 1992; Wu et al., 1996). It is possible that the kidneys may be trying to adapt by increasing renal NHE3 protein expression, to compensate for potential NH_4^+ build up and the reduction of plasma HCO_3^-, and to provide H^+ for luminal titrations. In addition, the reduction in NHE3 in the proximal small intestine and large intestine in the high-fat diet-fed groups, may be compensating for increased renal NHE3, mostly likely to prevent excessive H^+ loss. Interestingly, previous proteomic studies in mice fed on a high-fat diet showed a downregulation of the intestinal basolateral Na^+/HCO_3^- cotransporter, NBCe1 (Wiśniewski et al., 2015), which could also explain for the reduction in plasma HCO_3^-. It should be noted that as urinary pH, NH_4^+ and plasma H^+ were not examined in the

present study, confirmed impairment of NH_4^+ excretion and a possible acidotic (or hyperuricemic) effect of NH_4^+ build up cannot be assumed.

Another possible reason for this increase in renal NHE3 in the high-fat diet-fed groups could be due to the activation of the insulin-PI3K-SGK1 pathway, which is known to regulate NHE3 (Fuster et al., 2007; Klisic et al., 2002). Previous studies have revealed significant elevations in SGK1 protein abundance in $SGK1^{+/+}$ mice after high-fat feeding as well as a marked increase in blood pressure, highlighting a potential contributing role for SGK1 in hypertension development (Huang et al., 2006). This may suggest that the high-fat diet-induced stimulation of the insulin-PI3K-SGK1 pathway could account for the over-stimulation of renal NHE3 in this study. However, this may also not be the case in the present study, as contrasting studies in fatty acid-incubated opossum kidney cell culture models have shown abolished and unaffected effects of insulin and SGK1 on NHE3 activity, respectively (Bobulescu et al., 2008). Further assessment of the involvement and impact of this signalling pathway in this model and in the pathogenesis of post-transplant hypertension and metabolic syndrome are needed.

Hypophosphatemia is commonly observed with metabolic syndrome and CNI use, and has been shown in rodent studies to be related to the dysfunction of tubular phosphate reabsorption via a reduction in NaPi-IIa expression (Mohebbi et al., 2009; Moz et al., 2004). This downregulation of NaPi-IIa has been previously supported in diabetic Zucker obese rats (Bickel et al., 2002). In contrast, in the present study, the high-fat diet-fed group had significantly elevated plasma and urinary phosphate levels, indicative of hyperphosphatemia and phosphaturia, with no changes in the major Na^+/Pi transport proteins. The consequences of hyperphosphatemia have been linked to disorders in bone remodelling with excessive bone resorption rates compared with bone formation rates. This results in calcium and phosphate release and an increased risk for vascular calcification and cardiovascular

disease, as demonstrated in previous studies of high-fat diet-fed LDL-receptor-deficient mice, another obese mouse model for human metabolic syndrome and chronic kidney disease (Davies et al., 2003, 2005). Further studies of energy-rich, high-fat feeding in rats with normal renal function and uninephrectomised rats showed increased phosphate retention due to impaired renal phosphate excretion and promoted vascular calcification (Raya et al., 2016). Despite no accompanied increases in renal phosphate excretion, significant elevations of the plasma fibroblast growth factor-23 (FGF23, a negative regulator of phosphate homeostasis) were also observed (Raya et al., 2016). These findings implicate resistance to the phosphaturic actions of FGF23 in these high-fat diet-fed animals, and was also proposed to be the result of reduced renal klotho expression, a regulatory hormone also known to affect phosphate metabolism (Raya et al., 2016). Others have also reported increased serum phosphate with no change in serum FGF23 and parathyroid hormone (PTH) levels and attenuated responses of both these regulators following oral phosphate administration in patients with type II diabetes, leading to the progression of vascular calcification and atherosclerosis (Yoda et al., 2012). The mechanisms underlying the impaired phosphaturic responses to FGF23 and PTH under high-fat feeding and metabolic syndrome-affiliated conditions are not yet clear. The impact of these regulators on phosphate retention and excretion in the present study also remains to be clarified.

The hyperphosphatemia and phosphaturia features observed in the high-fat groups may be attributed to a number of factors including the potential induction of renal dysfunction, as indicated by the creatinine values. This may have led to increased phosphate retention and deposition into the plasma from bone tissue. It is not clear why renal NaPi-IIa protein expression was unchanged with high-fat feeding considering the biochemical data obtained for plasma and urinary phosphate. However, a time-course study by Bielesz *et al*, showed that diurnal rises in renal phosphate excretion was not

accompanied by a change in NaPi-IIa protein (Bielesz et al., 2006). These authors also observed an increase in GFR, filtered load and tubular threshold, which were suggested as the main factors that determine overall renal phosphate excretion when faced with little or no changes in NaPi-IIa protein abundance and activity (Bielesz et al., 2006). However, in the present study, plasma and urinary creatinine levels indicate decreased GFR in the high-fat diet-fed mouse model and so contrasts with this conclusion. Another alterative explanation was that, in addition to regulation by BBM protein abundance, NaPi-IIa transporter activity may also be regulated.

Interestingly, recent proteomic analyses in small intestinal mucosa samples from high-fat diet-fed mice have shown a downregulation of the intestinal NaPi-IIb cotransporter (Wiśniewski et al., 2015), which could explain for the relative decrease in NaPi-IIb protein expression in the high-fat group in the distal intestinal segment. However, this requires re-analysis as it is most likely that the decrease in NaPi-IIb in the distal small intestinal segment was related to the poor protein preparations used. Overall, further studies are required for the assessment of the influences of high-fat feeding on NaPi-IIa and NaPi-IIb cotransporter activity to confirm any impact of these transport proteins on phosphate retention and excretion, and the examination of phosphate loading from bone mass to account for the hyperphosphatmic effects observed.

4.4.3 FK506 treatment and high-fat feeding on renal and intestinal sodium-glucose transport proteins

Hyperinsulinemia and insulin resistance has been observed in rodents fed on a high-fat diet and is one of the main components of metabolic syndrome (Deji et al., 2008; Gallou-Kabani et al., 2007; Surwit et al., 1988, 1995; Winzell and Ahren, 2004; Woods et al., 2003). In this study, plasma glucose

levels were significantly elevated in the FK506-treated and the high-fat diet-fed groups. This increase in plasma glucose in the FK506-treated group is in line with the known diabetogenic effects of FK506. Although these levels were not high enough to be considered clinically diabetic and plasma insulin levels were not measured to confirm hyperinsulinemia and insulin resistance in these mice, these observations are evidently indicative of altered glucose homeostasis and possible onset of insulin resistance.

Studies in established SGLT2 and SGLT1 knockout mouse models have reported increased renal SGLT2 expression and SGLT activity as the determinant for hyperglycemia and a possible contributor for diabetes (Vallon et al., 2013). In the present study, renal SGLT2 protein expression was significantly decreased in the high-fat diet-fed groups. Intestinal SGLT1 protein was also decreased in these groups and no changes were found for renal and intestinal GLUT2. The findings are in contrast to these studies in knockout mice, however, there are numerous reports that have shown variable impacts of diabetes on SGLT-mediated transport between different models. Studies in a number of streptozotocin-induced diabetic animal models have demonstrated both increased (Blank et al., 1985) and decreased (Harris et al., 1986; Yasuda et al., 1990) SGLT-mediated glucose transport. This variability was also found in mRNA and protein analyses of SGLT transporters which have also shown increased (Vestri et al., 2001), decreased (Harris et al., 1986; Yasuda et al., 1990) and unchanged (Dominguez et al., 1994) levels in these animal models. These inconsistencies were thought to be due to differences in the dose of streptozotocin used and the severity of induced diabetes between studies.

Furthermore, a study comparing rat models of type I and type II diabetes, and rats with metabolic disruptions, via junk food (high in fat and sugar) or high-fat feeding, demonstrated differential responses of the renal glucose transporters (Chichger et al., 2016), suggesting that other factors may be

involved in transport protein regulation. While the type II diabetic rats and junk food-fed rats were accompanied by increased SGLT2, SGLT1 and GLUT2 expression, the type I rat model and rats fed on the high-fat diet demonstrated increased GLUT2 expression only (Chichger et al., 2016). This implies that differential changes in renal Na^+/glucose cotransporters, and thus, the development of insulin resistance and type II diabetes appears to be influenced by the composition of the diet. Additional studies have been performed to investigate the effects of different compositions of diets on glucose transport in the small intestine and have shown variable effects. In one study, rats fed on a high-starch/low-fat diet displayed increased SGLT1 and GLUT2 mRNA expression in the jejunum, compared to rats fed on a low-starch/high-fat diet (Inoue et al., 2015). Another study reported significantly increased SGLT1 expression in the jejunum of rats fed a high-fat diet consisting of medium-chain fatty acids compared with a high-fat diet consisting of long-chain fatty acids (Yasutake et al., 1995). In addition, recent proteomic analyses in homogenised small intestinal mucosa samples from mice fed either a normal or high-fat diet (the same diet which was used in the present study), revealed a significant difference in 11% of intestinal proteins between these diets (Wiśniewski et al., 2015). This included a downregulation of the SGLT1 and GLUT2 transporters in the high-fat diet-fed group (Wiśniewski et al., 2015), which is in line with the SGLT1 data presented in this study.

Taken together, these studies show that renal and intestinal glucose transporters are not regulated by the same factors in different diets and that the ratios of fat content and carbohydrate-to-fat can differentially influence glucose transporter expression and account for the variable results between studies. Therefore, the relative decrease seen for renal SGLT2 and intestinal SGLT1 transport proteins may be explained by the composition of the high-fat diet. However, it is also likely that these reductions are compensatory responses to elevations in plasma glucose levels (induced by the

gastrointestinal-renal signalling axis), and/or possibly increased glucose transporter activity, which requires further clarification. Also, although GLUT2 remained unchanged in this study, as transport activity was not measured its diabetogenic influence in the high-fat groups cannot be fully excluded.

Another possible regulator and contributor in the pathogenesis of insulin resistance in patients with metabolic syndrome or diabetes is the AMP-activated protein kinase, AMPK. This kinase has been previously shown as a positive regulator of SGLT1 and NKCC2 (Fraser et al., 2007; Richardson et al., 2011; Sopjani et al., 2010), and a negative regulator of NaPi-IIa (Dërmaku-Sopjani et al., 2013). In rodent studies with high-fat feeding and in models of insulin resistance, both AMPK mRNA, protein and activity has shown to be reduced, along with impaired insulin-stimulated glucose uptake and disrupted glucose homeostasis, all of which was improved following treatment with AMPK activators (Buhl et al., 2002; Cool et al., 2006; Halseth et al., 2002; Liu et al., 2006; Song et al., 2002). These findings were further supported in AMPK-deficient rodent studies with high-fat feeding (Fujii et al., 2008). These studies demonstrate a possible link between AMPK and high-fat diet-induced insulin resistance and, in the case of this study, suggests that the downregulation of AMPK with high-fat feeding may contribute towards the downregulation of SGLT1. However, this does not explain the unchanged levels of NaPi-IIa and NKCC2 transport proteins and requires further investigation.

4.4.4 FK506 treatment and high-fat feeding on renal and intestinal sodium transporters and channels

Hypertension is another condition associated with metabolic syndrome and, as already mentioned, is a significant risk factor for renal dysfunction following transplantation. As previously discussed in Chapters 1 and 3, the dysregulation of renal sodium transport proteins and sodium reabsorption is

fundamental to the development of elevated blood pressure. These renal sodium transport proteins include NKCC2, NCC and ENaC.

There are a number of studies in Zucker obese rat models which have shown conflicting results regarding changes in NKCC2 transporter levels. In one study, no significant changes in NKCC2 protein abundance was observed (Bickel et al., 2001), which supports the findings from the present study. However, contrasting studies have found a decrease in whole kidney NKCC2 and an increase in outer medullary fractions (Bickel et al., 2002; Riazi et al., 2006). It is possible that the absence of changes in NKCC2 in the present study is related to decreased levels of known regulators of NKCC2. This includes vasopressin, which was found to be lower in Zucker obese rats (Bickel et al., 2001). However, it should be noted that these studies did not measure the phosphorylated active form of NKCC2 and, due to commercially unavailable antibodies and limited antibody stocks, this was also not assessed in the present study and so any sodium-retaining effects by this transporter cannot be ruled out.

As already discussed in Chapter 3, the NCC cotransporter was identified as a regulator of blood pressure and plays an important role in hereditary forms of hypertension and following renal transplantation. NCC protein levels were unchanged in this study. This was similarly reported in previous analyses of renal sodium transporters in Zucker obese rats (Bickel et al., 2002). However, pNCC was significantly increased following FK506 treatment and in mice fed on the high-fat diet, indicative of sodium retention and, indirectly, possible elevations in blood pressure. Elevated blood pressure and increased phosphorylation/activation of NCC and the WNK-SPAK/OSR1 pathway have been previously shown in diabetic db/db mice and Zucker obese rat models (Komers et al., 2012; Nishida et al., 2012; Sohara et al., 2011). The conclusions drawn from these reports were suggested to be the result of elevations in plasma insulin levels and increased PI3K/Akt pathway

signalling, which are downstream substrates of insulin signalling (Komers et al., 2012; Nishida et al., 2012; Sohara et al., 2011). These elevations in blood pressure and NCC phosphorylation were found to be corrected in kinase-dead SPAK$^{T243A/+}$ and OSR1$^{T185A/+}$ knock-in db/db mice (Nishida et al., 2012), further clarifying the involvement of WNK and SPAK/OSR1 kinases on NCC phosphorylation in models of metabolic syndrome. These studies suggest an important regulatory role for insulin signalling, via the PI3K/Akt pathway, as the driving force for the activation of WNK-SPAK/OSR1 signalling and NCC phosphorylation and function in patients with metabolic syndrome, and in the pathogenesis of salt-sensitive hypertension. Therefore, increased circulating insulin levels most likely explains for the increase in pNCC protein in the high-fat diet-fed group, but this requires confirmation. NCC phosphorylation is also known to be regulated by the SGK1 kinase and is also a known regulator of the WNK signalling cascade (Vallon et al., 2009). However, SGK1 phosphorylation was not seen in db/db mice fed low- or high-salt diets (Nishida et al., 2012), suggesting that SGK1 may not be involved in activating the WNK-SPAK/OSR1 cascade in some diabetic mouse models.

The ENaC sodium channel is another major protein involved in regulating blood pressure. ENaC is regulated by a number of mediators, including aldosterone and SGK1. Increased plasma aldosterone levels have been observed in patients with metabolic syndrome and in obese animals (Bochud et al., 2006; Engeli et al., 2005; Kidambi et al., 2007; Nagase et al., 2006). In fact, weight loss studies demonstrate significant reductions in aldosterone, components of the renin-angiotensin II-aldosterone (RAA) system, and blood pressure (Engeli et al., 2005; Tuck et al., 1981), implicating the RAA system in the development of obesity-induced hypertension. The contribution of ENaC to the sodium-retaining effects in obesity-related conditions have differed between studies. In one study, Zucker obese rats aged 2 and 4 months showed a significant increase in the β-ENaC subunit while the α- and γ-ENaC subunits were unchanged (Bickel et al., 2001; Riazi et al., 2006).

Similarly, another study by the same group in 6-month Zucker obese rats also showed a significant increase in β-ENaC, but found a marked reduction in α-ENaC (Bickel et al., 2002). The conclusions drawn from these studies demonstrated differential regulation of the ENaC subunits. However, the physiological relevance of this differential regulation is not clear and the overall effect of increased β-ENaC abundance on sodium transport without the accompanying change in the other subunits could not be deduced. Furthermore, a study by May *et al*, showed that the synthesis and abundance of the α-ENaC subunit is the rate limiting factor for the assembly of the ENaC complex (May et al., 1997). Electrophysiological experiments in oocyte expression models have also established that the assembly of the subunits and functionality of the channel was dependent on α-ENaC abundance (Canessa et al., 1994). Therefore, the marked reduction in α-ENaC abundance may result in an overall downregulation of the ENaC sodium channel at the apical membrane. The reduction in α-ENaC in the FK506-treated group observed in the present study support the previous findings and conclusions drawn in Chapter 3, and the findings from the high-fat diet-fed group are in line with previous studies in 6-month Zucker obese rat models (Bickel et al., 2002). However, the reasons for this reduction are not known. As the α-ENaC subunit is known to be upregulated by aldosterone (Loffing et al., 2000; Masilamani et al., 1999; Pacha et al., 1993), an increase in protein abundance was expected in the high-fat diet fed group. It is possible that this reduction is related to compensatory/adaptive responses to increased sodium retention induced by renal NHE3 and pNCC transport proteins, to reduce renal sodium reabsorption and blood pressure. Another possibility is that this reduction may act as a counteracting response to increased ENaC activity. Functional studies are required to measure channel activity in these mice.

4.4.5 Limitations and conclusions

To date, this is the first study to compare a model of CNI-administration with a diet-induced model of metabolic syndrome to determine whether CNIs may predispose renal transplant patients to metabolic syndrome and to analyse how the abundances of major electrolyte transport proteins may be affected during metabolic syndrome development.

In this study, mice fed on a diet rich in fat had significant weight gain compared with lean normal diet-fed mice, despite no indications of hyperlipidemia and hypertriglyceridemia. Selective increases in renal NHE3 and pNCC protein abundance were observed in the high-fat diet-fed group, which would most likely contribute towards the sodium-retaining effects, leading to hypertension. As previously described, blood pressure measurements were not available and so elevations in blood pressure could not be confirmed in this model. Therefore, for future clarification, measurements of blood pressure with the use of telemetry analysis would allow for confirmation of a hypertensive response to the high-fat diet and FK506 treatment. Alterations in plasma glucose are indicative of altered glucose homeostasis, however, further investigations are required to confirm potential insulin resistance and impaired insulin-stimulated glucose uptake. Although the plasma biochemistry results indicate hyperphosphatemia in the high-fat diet-fed groups, studies suggest that this could be linked to phosphate deposits from the bone into the plasma and for future studies, bone mass and phosphate content would be examined.

The establishment of a model for metabolic syndrome is difficult, as it requires the exhibition of the exact pathological changes associated with metabolic syndrome, which is different for each patient. Currently used rodent models vary in terms of eitiologies and it remains unclear which of these models is the most appropriate to study human metabolic syndrome.

Some characteristics, such as hyperglycemia and hyperinsulinemia, are not consistently observed in some mouse models, and obesity is not as dependent on dietary factors, as the degree of metabolic dysfunction during high-fat feeding may also depend on the genetic background. The C57BL/6J mouse strain was used in this study due its high susceptibility to obesity development and insulin resistance/glucose intolerance when placed on a high-fat diet (Gallou-Kabani et al., 2007; Surwit et al., 1988, 1995; Winzell and Ahren, 2004), however, it is unclear whether these characteristics are related to a genetic factor and may also contribute to renal, lipid and metabolic abnormalities. Genetically engineered diabetic rodent models which are used to study hyperinsulinemia are also limited as the targeted gene for knockdown may be related to other important signalling pathways and so the inactivation or activation of investigated pathways may in fact be linked to these genetic modifications. Furthermore, significant compensatory mechanisms can occur in knockout and knock-in animal models which can also affect the outcome of the investigations.

Overall, the diet-induced obese mouse model used in this study did not exhibit all the clinical features of metabolic syndrome and did not completely show comparable changes in renal and intestinal transport proteins to FK506 treatment alone. The results from this study, extends the conclusions drawn from Chapter 3 that the presence of other stimuli, rather than CNI treatment, are the main contributing factors to alterations in glucose, sodium, and acid-balance and in the development of hypertension and metabolic syndrome. Despite the limitations of establishing a model of metabolic syndrome, this model of high-fat feeding permitted the analyses and identification of the renal and intestinal transport proteins that may be involved in the development of the individual components that comprise metabolic syndrome.

Chapter V

Urinary exosome isolation and analysis of (p)NCC levels in calcineurin inhibitor-administered and Gitelman syndrome patients

5.1 Introduction

5.1.1 Urinary exosomes

The use of rodent models for CNI-induced hypertension has provided significant insights into the transport proteins involved in sodium retention and the main contributors to elevations in blood pressure, namely via enhanced phosphorylation of the NCC cotransporter within the DCT. This has been further supported through immunohistochemical analyses in renal biopsy samples collected from renal transplant patients (Hoorn et al., 2011). However, protein abundance is difficult to measure in these patients due to the inability to obtain substantial amounts of renal tissue from live patients for protein analysis. Immunohistochemical analyses are also often limited owing to the common loss of structural integrity following collection and the under-representative size of the sample obtained with regards to the whole kidney. Furthermore, renal biopsy procedures are uncomfortable and are often followed with complications such as bleeding and risks of internal damage to the targeted organ or neighbouring areas.

Currently, efforts are being directed towards the development of a non-invasive technique to identify novel biomarkers for the early detection and accurate diagnosis of renal disease, which would effectively improve the response to treatment and prevent increasing severities. In particular, the isolation and use of urinary exosomes has received substantial attention as a source of intracellular renal biomarkers for the diagnosis of renal diseases. Urine is an ideal biological sample alternative due to the ease and non-

invasive nature of collection. In addition, unlike renal biopsy procedures, urinary exosomes provide a complete molecular representation of the entire urinary tract.

Urinary exosomes are characterised as small membrane vesicles, ranging in diameter between 40 – 100 nm, with a 'cytoplasmic-side inward' orientation (Pisitkun et al., 2004). The formation and excretion of these vesicles has been described as a three-step process; 1) membrane protein ubiquitination and endocytosis, 2) fusion with the outer membrane of late endosomes called multivesicular bodies (MVBs) and then 3) fusion with the apical membrane of the renal epithelial cells which then releases exosomes into the urine. Urinary exosomes contain numerous proteins and nucleic acids, which may potentially reflect the physiological and pathological state of their cells of origin (Lv et al., 2013; Miranda et al., 2010; Pisitkun et al., 2004), and may therefore provide a non-invasive approach for determining the functional state of the kidney following renal transplantation and/or in renal- and systemic-related diseases.

5.1.2 Urinary exosome biomarkers of renal disease

In initial studies, membrane-bound proteins such as AQP2, NHE3, NKCC2 and NCC were detected in low-density membrane vesicles isolated from human urine by ultracentrifugation and were suggested as markers for renal-related disorders (du Cheyron et al., 2003; Kanno et al., 1995; McKee et al., 2000). NHE3 was proposed as a novel candidate marker of renal tubule damage, whereby patients with acute tubular necrosis or prerenal azotemia presented significantly increased levels of urinary NHE3 compared with controls (du Cheyron et al., 2003). In addition, AQP2 was also exploited as a marker in clinical studies of patients with water-balance disorders, which was confirmed with immunoblotting, radioimmunoassay and immunoelectron microscopy applications in both urine samples and isolated urinary low-

density membrane vesicles (Funayama et al., 2004; Kanno et al., 1995). These studies demonstrating the presence of membrane proteins in these small, low-density membrane vesicles led to its later characterisation as exosomes and facilitated closer analyses of the excretion processes of AQP2 and other membrane proteins.

Exosomes were first classified in urine by Pisitkun *et al*, in 2004, who demonstrated their potential use for biomarker discovery (Pisitkun et al., 2004). In their study, proteomic analysis using liquid chromatography-tandem mass spectrometry (LC-MS/MS) identified numerous proteins directly involved in the endosomal pathway, exosome synthesis and the components responsible for MVB formation (Pisitkun et al., 2004). In addition, 295 proteins originating from the renal tubule were identified, 21 of which were already known to be associated with specific renal diseases and blood pressure regulation (Pisitkun et al., 2004). The use of the highly sensitive LC-MS/MS-based techniques allowed for the identification and qualitative and quantitative analysis of proteins from single samples and has been used in further large-scale proteomic profiling studies in urinary exosomes from normal human urinary samples (Gonzales et al., 2009). In their study, Gonzales *et al* identified 1,132 proteins, including 14 phosphoproteins (including pNCC and pNKCC2) and 117 proteins associated with diseases, 34 of which were renal disease- and/or hypertension-related proteins (Gonzales et al., 2009). From both these investigations, the authors created an online urinary exosome protein database (https://hpcwebapps.cit.nih.gov/ESBL/Database/Exosome/), which provides a list of the identified 1160 proteins in urinary exosomes as well as potential disease-related biomarkers.

Since these early proteomic analyses, many more studies have attempted to identify and evaluate biomarkers for renal, urogenital and systemic diseases using urinary exosomes as the starting material (Cheruvanky et al., 2007;

van der Lubbe et al., 2012; Pisitkun et al., 2012; Zhou et al., 2006a, 2006b, 2008). To date, a variety of promising biomarkers have been identified. For example, investigations in urinary exosomes isolated from patients with acute kidney injury (AKI) have identified changes in proteins such as Fetuin-A (Sonoda et al., 2009; Zhou et al., 2006b), activating transcription factor-3 (ATF3) (Zhou et al., 2008), and aquaporin-1 (AQP1) (Sonoda et al., 2009), as possible markers for the early detection of AKI. Wilms tumor-1 (WT-1) was also identified as a marker for glomerular disease and diabetic nephropathy (Jiang et al., 2009; Zhou et al., 2008), and several biomarkers have been suggested for genetic renal diseases, such as Gitelman syndrome, Bartter syndrome and Pseudohypoaldosteronism II (PHAII) (Gonzales et al., 2009; Isobe et al., 2013; Joo et al., 2007; van der Lubbe et al., 2012). In patients with Gitelman syndrome and Bartter syndrome type I, little to no-detection for NCC and NKCC2 proteins was observed in urinary exosomes, respectively (Corbetta et al., 2015; Gonzales et al., 2009; Isobe et al., 2013; Joo et al., 2007), while patients with PHAII display increased urinary excretion of NCC and pNCC (Adachi et al., 2010; Isobe et al., 2013; Mayan et al., 2008), which was also observed in rodent models of aldosteronism and patients with primary hyperaldosteronism (van der Lubbe et al., 2012).

Urinary exosome-based approaches continue to emerge as important tools for the detection of biomarkers of renal- and systemic-related conditions. However, despite this promising outlook for utilising urinary exosome analysis in clinical settings, their use is hampered by the current lack of efficient and optimised methods for urine collection/storage, exosome isolation and protein normalisation/quantification, all of which will be discussed in the following sections.

5.1.3 Collection and storage of urine samples

The first challenge encountered with the urinary exosome isolation process is the timing of urine collection, 24-hour vs spot urine. Ideally, exosome isolation from 24-hour urine samples would allow for the calculation of biomarker excretion rates over the 24-hour period, which would be highly representative of overall kidney function and would allow quantitative normalisation and comparisons of protein levels between patients. Unfortunately, this timed collection approach is often complicated by low patient compliance and would ultimately lead to unreliable results. Therefore, investigators have used and compared total protein levels from spot urine collections of first (overnight) and second (fresh) morning urine. Initial drawbacks for the use of first morning urine were related to concerns of bacterial contamination and possible protein degradation due to long residence in the bladder and, in this regard, second morning urine was suggested to be best suited for exosome isolation. However, comparisons of exosome proteins from first and second urine collections revealed similar amounts of total protein and exosome recovery with both collections (Zhou et al., 2006a), suggesting minimal protein degradation within the bladder/urinary tract and demonstrating that both first and second morning urine can be used for exosome isolation.

Following urine collection, three important steps have been highlighted for consideration to ensure efficient preservation/storage of urine and exosome extraction; 1) the addition of protease inhibitors following collection, 2) short- and long-term storage and 3) extensive vortexing after thawing (Oosthuyzen et al., 2013; Zhou et al., 2006a).

Once urine has been collected, optimal storage conditions are essential to prevent another common problem, proteolysis. It has been shown that urinary exosome degradation can occur within 2 hours of urine collection at

room temperature (Oosthuyzen et al., 2013). For the stability and preservation of urinary exosomes, it was recommended that protease inhibitors be immediately added to urine samples to prevent protein and exosome degradation (Oosthuyzen et al., 2013; Zhou et al., 2006a). The typical cocktail of protease inhibitors includes the serine and cysteine protease inhibitors PMSF and leupeptin, and a preservative such as sodium azide. Suitable storage conditions and extensive vortexing are also required for further preservation of exosomal proteins and high exosome recovery after thawing. Different storage temperatures (-80°C, -20°C and 4°C) and short- and long-term periods (1 week and 7 months, respectively), have been previously compared and have found, with confirmation by nanoparticle tracking analysis (NTA), that long-term storage at -80°C provides the most optimal and stable conditions compared with urine stored at -20°C and 4°C (Oosthuyzen et al., 2013; Zhou et al., 2006a). Storage at -20°C was particularly found to be the least favourable condition and was associated with a major loss in urinary exosome-related proteins (Oosthuyzen et al., 2013; Zhou et al., 2006a). Extensive vortexing after thawing of samples stored at -80°C was also found to have the highest recovery of exosomes by up to 100% compared with urine stored at -20°C which recovered only 87% of exosomes after extensive vortexing (Zhou et al., 2006a). Overall, it is recommended that following collection, urine samples are supplemented with protease inhibitors, immediately stored at -80°C (for long-term) and, upon thawing/processing, are extensively vortexed for maximised exosome recovery.

5.1.4 Urinary exosome isolation

Several studies have been conducted to develop optimal methods for faster and more efficient isolation of urinary exosomes. Ultracentrifugation was the initial isolation method used which, following urine collection and protease

inhibitor addition, involves a two-step differential centrifugation protocol; a low-speed spin (17,000 x g) to remove cellular debris, followed with a high-speed spin (200,000 x g) for 1-hour to pellet the exosomes. This protocol has shown to be the most effective and reproducible method for yielding intact exosomes, but is also problematic as it requires access to expensive instrumentation and is a very time-consuming process. Furthermore, the isolated exosome pellet is commonly contaminated by highly abundant proteins such as albumin and, in particular, uromodulin (also known as Tamm-Horsfall protein (THP)), which entraps a large proportion of exosomes in double-helical fibrils, preventing efficient exosome isolation and interfering with mass spectrometry and western blotting analyses (Fernández-Llama et al., 2010; Pisitkun et al., 2004). This polymeric THP network is often reduced by the addition of dithiothreitol (DTT) before the high-speed spin but this does not completely removal all THP and interfering abundant proteins (Fernández-Llama et al., 2010; Pisitkun et al., 2004). Alternatively, additional steps in the ultracentrifugation stage can be used to separate exosomes and the contaminating proteins based on 1) density, by a sucrose gradient or double-cushion ultracentrifugation (Raj et al., 2012), or by 2) molecular weight, by ultracentrifugation followed with size exclusion chromatography (UC-SEC) (Rood et al., 2010), but this makes it even more time-consuming and expensive. Current studies are attempting to refine faster and efficient exosome isolation methods that are more accessible to standard hospital laboratories through use of membrane filtration and precipitation protocols. However, these methods have yielded variable results. Ultrafiltration methods have included using commercially available nanomembrane concentrators to filter exosomes, followed by a low-speed centrifugation at 3,000 x g for around 10 – 30 minutes (Cheruvanky et al., 2007). Although this technique was able to reduce the exosome isolation time to 0.5 – 2 hours, it also led to a low yield of urinary exosomes compared with the standard ultracentrifugation method and was complicated with protein accumulation on the filters, which could block further flow and complete protein collections.

Precipitation methods using a commercially available kit called ExoQuick-TC has also recently received significant attention, although this method is tailored more towards the isolation and analyses of exosomal nucleic acids. This kit omits the ultracentrifugation step and, in comparative studies, has shown significantly high qualitative and quantitative yields of exosomal miRNA and mRNA compared with the ultracentrifugation and nanomembrane filtration approaches, but only with using a modified version of the original protocol, which involved pellet resuspension in isolation solution/DTT and an additional low-speed spin step (similar to the standard ultracentrifugation method), prior to the addition of the ExoQuick-TC precipitation agent (Alvarez et al., 2012). Other studies have used a combination of exosome isolation methods such as ultrafiltration followed with exosomal RNA extraction kits (Channavajjhala et al., 2014). Overall, an optimal isolation method has still not yet been defined and from current investigations, different methods may be required depending on the research question.

5.1.5 Normalisation

Another challenge researchers face in the urinary exosome isolation process is defining a method of normalisation and quantification to accurately compare changes in biomarkers between patients and control exosome samples. Urine concentration is widely variable and without normalising methods, analyses of candidate urinary exosome biomarkers and comparisons between patients can lead to incorrect conclusions. Several methods have been investigated, including time-, urinary creatinine-, THP- and total protein-normalisation.

Ideally, as already mentioned, isolation and normalisation of exosomes from timed 24-hour urine collections (timed-normalisation) would be the most accurate method based on measurements and comparisons of the excretion

rate of exosomal biomarkers. However, this approach is limited by low patient compliance and so creatinine and protein normalisations are alternatively used. Previous studies have reported equal exosome-associated proteins within samples when normalised to urinary creatinine, suggesting this as the best option for clinical settings (Zhou et al., 2006a). Normalisation to urinary creatinine in spot urine essentially overcomes the complications of obtaining timed urine collections because urinary creatinine is assumed to be excreted at a constant rate. Unfortunately, this method is also limited, as it does not take into account conditions of renal diseases, such as acute kidney injury, where creatinine excretion rates are unstable. Protein normalisation methods to a particular protein in the urine have also been proposed. These proteins have included using THP or exosomal markers such as apoptosis-linked gene-2-interacting protein X (ALIX) and tumour susceptibility gene (TSG)-101 (Fernández-Llama et al., 2010; Zhou et al., 2006a). However, further studies are required to validate these as normalising proteins and to determine whether these proteins are constant under different pathophysiological conditions, which is currently unknown. More recent methods using the nanoparticle tracking analysis systems have also been utilised for exosome counting and analyses in whole urine based on their size (Oosthuyzen et al., 2013), which would be less time-consuming and would provide a more optimal normalising procedure but again requires access to expensive equipment.

5.1.6 Aims of this study

Urine is an ideal biological sample due its easy, immediate and non-invasive collection. The discovery of urinary exosomal biomarkers of disease has greatly inspired many investigations in attempts to exploit their use in diagnostic and therapeutic settings. However, this technique is yet to be fully established and some challenges remain at the urinary exosome isolation and normalisation stages. Despite this, many candidate biomarkers have

been identified including NCC and pNCC for which excretion of these proteins is significantly increased in patients with PHAII and decreased in patients with Gitelman syndrome (Adachi et al., 2010; Corbetta et al., 2015; Isobe et al., 2013; Joo et al., 2007; Mayan et al., 2008). In recent studies, western blot analyses of urinary exosomes of hypertensive CNI-treated renal transplant patients also revealed significantly increased urinary excretion of total NCC and phosphorylated NCC proteins compared with non-CNI treated controls, and was correlated with blood pressure responses to thiazides (Esteva-Font et al., 2014; Rojas-Vega et al., 2015; Tutakhel et al., 2017). This is consistent with previous observations and conclusions that NCC is the main contributor to CNI-induced hypertension (Hoorn et al., 2011; Melnikov et al., 2011).

In the work described in this chapter, the standard ultracentrifugation protocol for urinary exosome isolation was used in urine samples from CNI-administered renal transplant patients and Gitelman syndrome patients. These samples were normalised to both urinary creatinine and ALIX protein, and analysed with western blot applications. This study was conducted with the aim of aiding future developments for this non-invasive method to allow early detection/diagnosis and effective treatment for renal dysfunction following renal transplantation and in renal-related diseases. Further aims of this chapter were to also use this technique in mice to facilitate the analyses of other renal proteins in mouse models of hypertension and/or renal-related conditions.

5.2 Materials and methods

5.2.1 Patients

The protocols used received full ethical approval from the Royal Free Hampstead NHS Trust, NHS Research Ethics Committee and informed consent was received from all patients and controls. Further information on these patients are described in **Section.2.6**.

5.2.2 Human plasma and urine biochemistry

Routine plasma and urine samples were collected on the day of renal biopsies and clinical appointments. Biochemical analyses were performed as described in **Section.2.6.2**, by the Department of Clinical Biochemistry (Royal Free Hospital, London, UK). Urinary creatinine was measured as described in **Section.2.1.6**.

5.2.3 Urinary exosome isolation

Urinary exosomes were prepared as described in **Section.2.6.3** or by Gonzales *et al* (Gonzales et al., 2010). The final exosome pellet was dissolved in 100µl of 2x laemmli sample buffer and stored in -80°C until further use.

5.2.4 Silver nitrate staining

Following SDS-PAGE, gels were subjected to staining with silver nitrate, as described in **Section.2.5.7**.

5.2.5 Western blot analysis

Prior to loading on SDS-PAGE gels, samples were heated at 65°C for 15 minutes. Sample loading amounts were normalised to the patient with the lowest urinary creatinine. Western blot protocols were carried out as described in **Section.2.5.6**. Following visualisation, membranes were striped and re-probed for either TSG101 or ALIX exosomal markers. Densitometry was measured and samples were normalised to either exosomal markers.

5.2.6 Statistical analysis

Data are presented as mean ± SEM, relative to ALIX or TSG101. N refers to the number of samples within each group. Significance was determined by unpaired T-test or one-way ANOVA. Significance was represented as: * $P < 0.05$, ** $P < 0.01$, *** $P < 0.001$.

5.3 Results

5.3.1 Urinary exosome isolation

In order to optimise a method for urinary exosome isolation and to validate its efficiency by analyses of urinary NCC and pNCC protein excretion in CNI-administered transplant and Gitelman syndrome patients, a protocol for urinary exosome isolation was first determined. Two modified versions of the standard ultracentrifugation protocol were initially examined (as outlined in **Fig.5.1**). Both these methods differ at the ultracentrifugation step. The first method was composed of the standard low-speed and high-speed spins, while the second appeared to be designed for increasing exosomal yield with larger starting urine volumes and multiple ultracentrifugation spins.

Urinary exosomes were isolated from ~100 ml control urine using both these methods and analysed for detection of known renal transporter proteins. SGLT2, Na^+/K^+-ATPase α, and β-actin, were detected in isolated urinary exosomes using the protocol described by Tutakhel *et al*, (Tutakhel et al., 2016), while no protein detection was observed for the second isolation protocol (**Fig.5.2**). In comparison to the mouse control sample, SGLT2 was detected as two bands (**Fig.5.2a**), with the strongest band present at the expected molecular weight and a faint lower-density band, which may be a cleaved product of the protein. Na^+/K^+-ATPase α was detected at a lower molecular weight compared with control sample (**Fig.5.2b**), but this may due to differences among species or a product of post-translational modifications such as glycosylation or cleaving. The signal detected for β-actin was weaker in urinary exosomes compared with control tissue and suggests that this protein is not suitable for normalisation in exosome protein analyses (**Fig.5.3c**). These findings suggest that the first isolation technique was best suited for this study and so further urinary exosome isolation experiments were performed using this method. Confirmation of protein extraction in

urinary samples was further determined with silver nitrate gel staining, which showed a significantly greater amount of proteins present in the final urinary exosome pellet (**Fig.5.3a**). However, this was also accompanied with the presence of the contaminating protein, THP. The urinary exosomal markers, TSG101 and ALIX were also present in these samples (**Fig.5.3b,c**), indicating successful urinary exosome isolation.

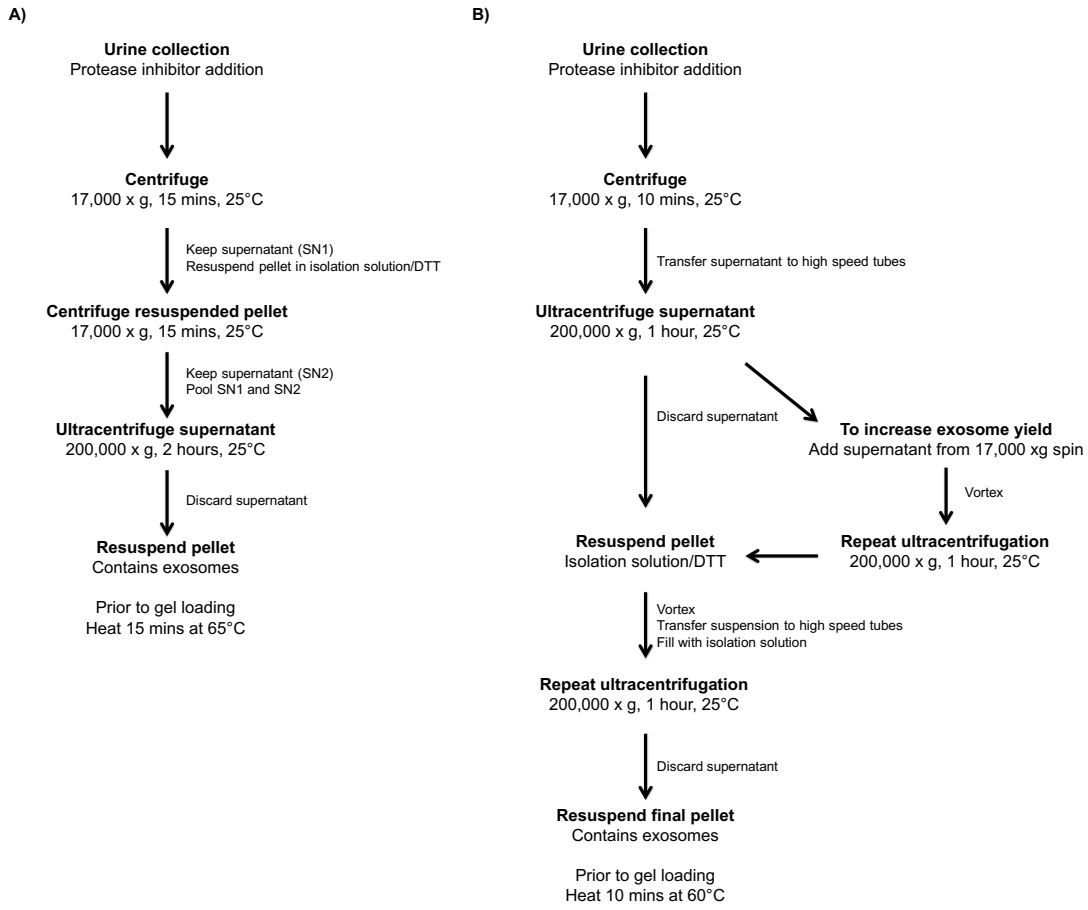

Figure 5.1. Urinary exosome isolation protocols. A schematic outline of two modified urinary exosome isolation protocols used in this study. Each of the protocols are modified versions of the original ultracentrifugation isolation method described by **A)** Tutakhel *et al*., (Tutakhel et al., 2016) and **B)** Gonzales *et al*., (Gonzales et al., 2010).

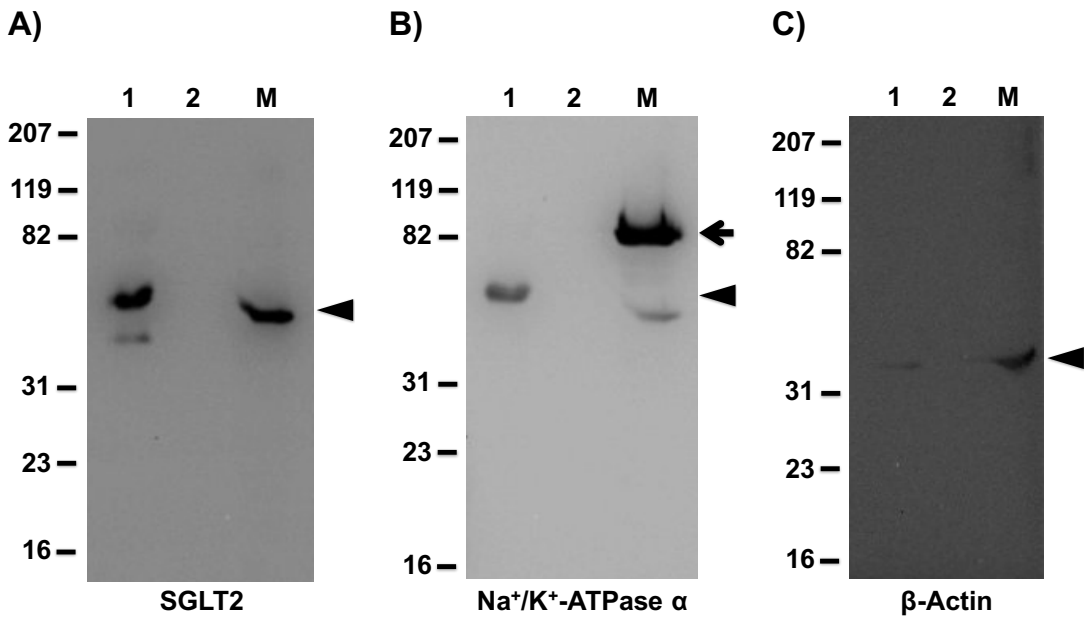

Figure 5.2. A comparison between two modified urinary exosome isolation protocols. Representative western blots for **A)** SGLT2 (*arrow*), **B)** Na^+/K^+-ATPase α (*arrow*) and **C)** β-actin (*arrow*) detection from urinary exosomes isolated from 100 mL urine using two modified protocols. The first (1) protocol was adapted from Tutakhel *et al*., (Tutakhel et al., 2016) and the second (2) from Gonzales *et al*., (Gonzales et al., 2010). Samples were run alongside a control sample from mouse (M) renal tissue. In mouse, renal SGLT2 is detected ~75 kDa, Na^+/K^+-ATPase α is detected ~100 - 113 kDa (*open arrow*) and β-actin is detected ~42 kDa.

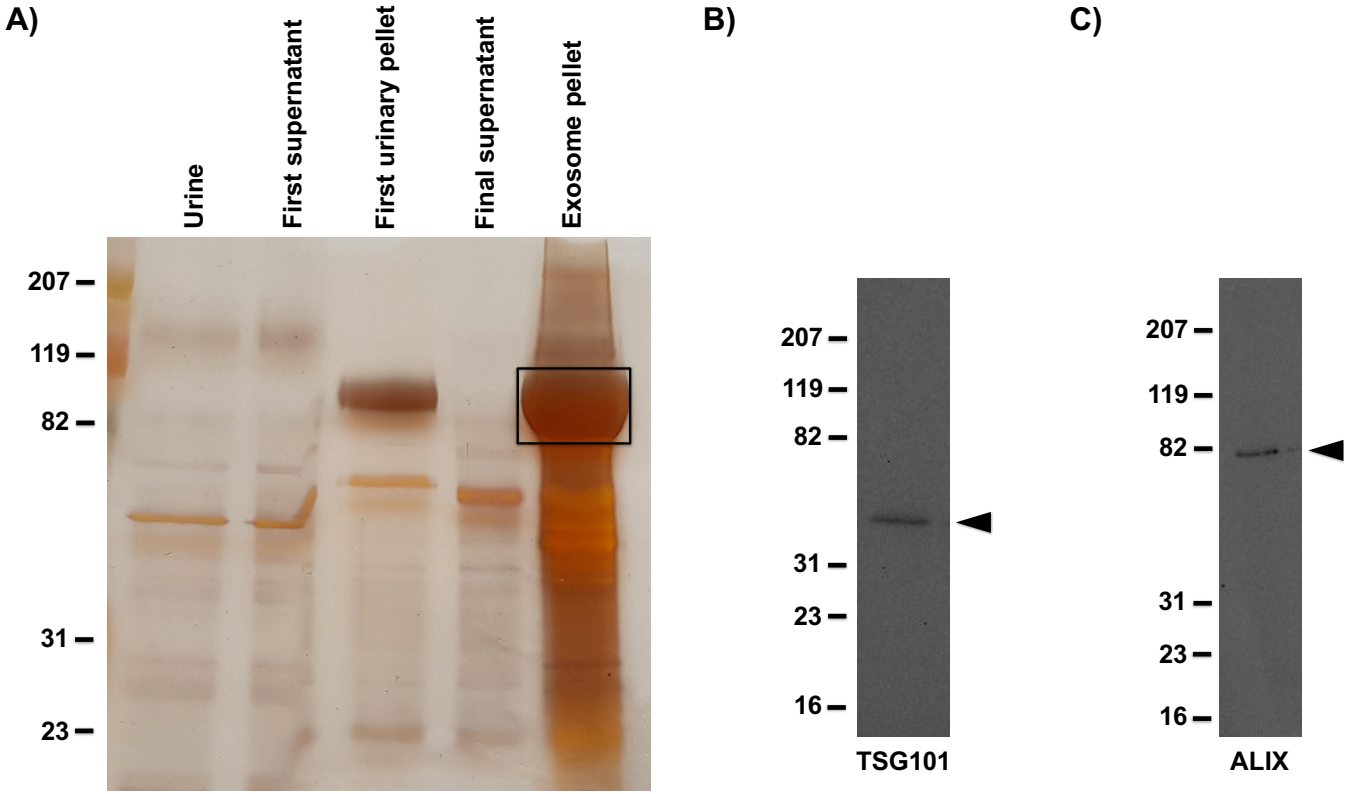

Figure 5.3. Confirmation of urinary exosome isolation. A) Silver nitrate stained gel of samples collected from each step of the urinary exosome isolation process from 100 mL urine. THP (*box,* detected ~95 kDa) was a common contamination observed following the isolation process. Representative western blots for exosomal markers **B)** TSG101 (*arrow*) and **C)** ALIX (*arrow*) as confirmation of successful urinary exosome isolation. TSG101 is detected ~43 - 47 kDa and ALIX is detected ~80 - 95 kDa.

The next experiments aimed to investigate whether these renal transport proteins could be detected in urinary exosomes isolated from lower volumes of starting urine, to allow for analyses in smaller urine volumes obtained from patients and mice. Urinary exosomes were prepared from 20 ml and 100 ml of control urine from two control subjects. At both volumes, all proteins could be detected, particularly in the first control sample (**Fig.5.4**). Again, a weaker signal was observed for β-actin (**Fig.5.4e,f**). Comparisons between the two control samples revealed lower protein detectability in the second exosomal sample which was consistent for all proteins measured (**Fig.5.4**). This was similarly observed for ALIX (**Fig.5.5a,b**) and TSG101 (**Fig.5.5c,d**) exosomal markers.

These findings suggest that urinary exosome isolation using this method is highly variable, regardless of the starting urine volume. Therefore, for the remainder of the study, urinary exosomes were isolated from ~20 ml of urine.

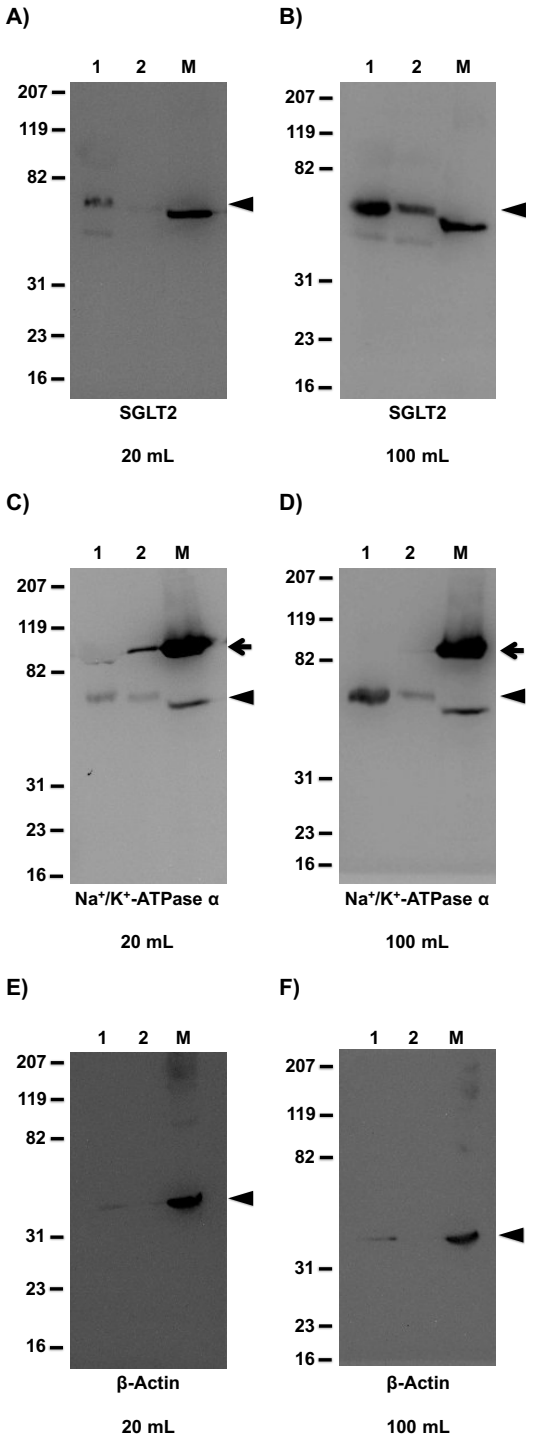

Figure 5.4. Protein detection in urinary exosomes isolated from varying volumes of starting urine. Representative western blots for **A,B)** SGLT2 (*arrow*), **C,D)** Na^+/K^+-ATPase α (*arrow;* urinary exosome, *open arrow;* M control) and **E,F)** β-actin (*arrow*) detection from urinary exosomes isolated from 20 and 100 mL of urine from two control samples. Samples were run alongside a control sample from mouse (M) renal tissue.

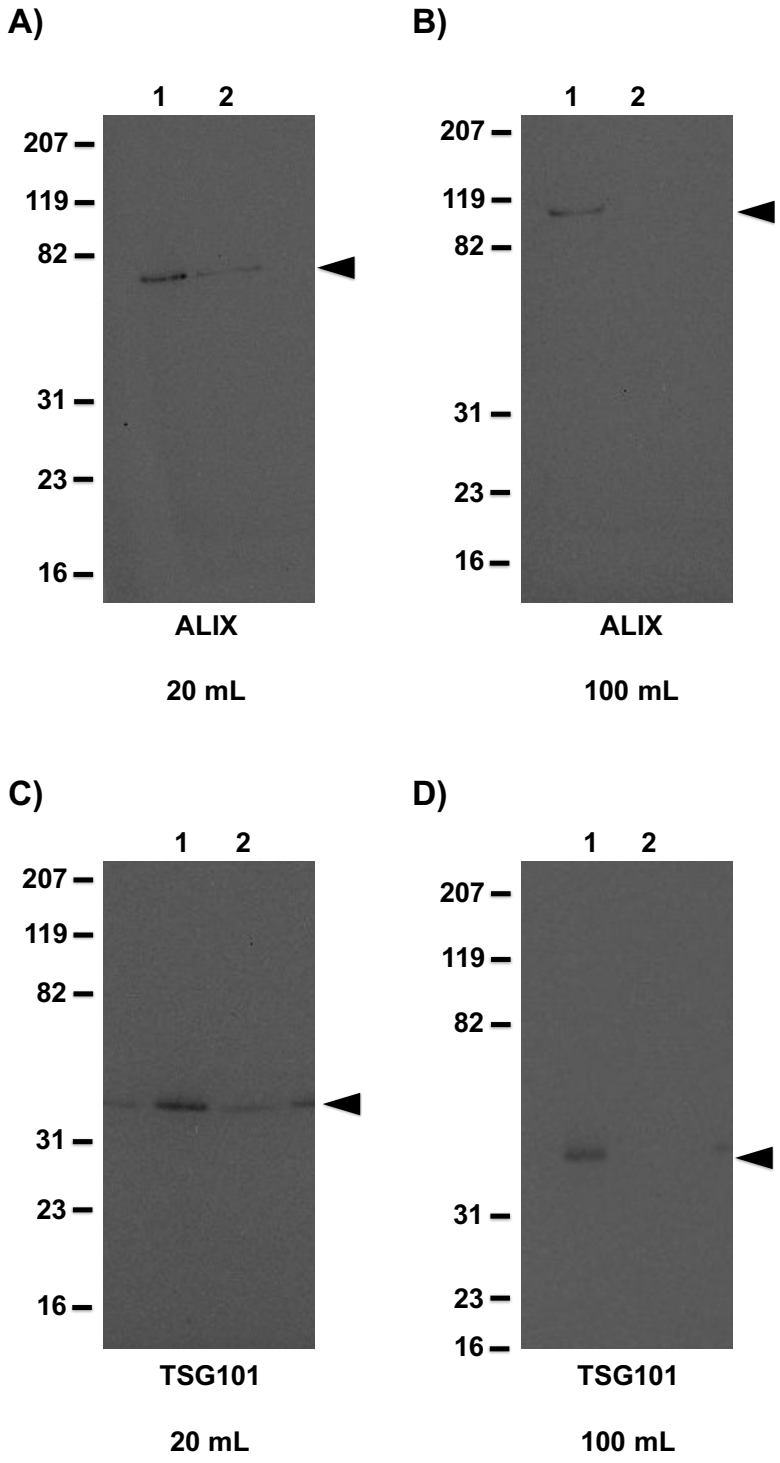

Figure 5.5. Detection of exosomal markers from varying volumes of starting urine. Representative western blots for exosomal markers **A,B)** ALIX (*arrow*) and **C,D)** TSG101 (*arrow*) from urinary exosomes isolated from 20 mL and 100 mL of urine from two control samples.

5.3.2 NCC/pNCC protein detection

In order to compare changes in NCC/pNCC excretion in patients, the ability to detect NCC/pNCC in isolated urinary exosomes from control samples was first established. NCC was observed in urinary exosomes from four control subjects and at the expected molecular weight, as confirmed from using human and mouse control renal tissues (**Fig.5.6a**). This was similarly observed for pNCC but at a lower intensity, which is most likely a reflection of its baseline levels (**Fig.5.6b**).

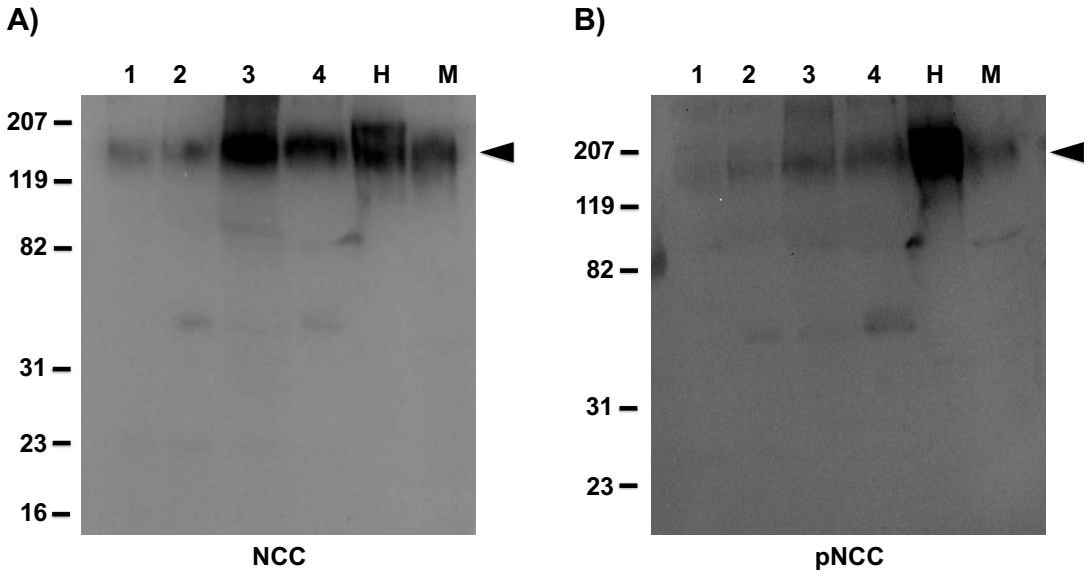

Figure 5.6. Detection of NCC and pNCC cotransporters in isolated urinary exosomes. Representative western blots for **A)** NCC (*arrow*) and **B)** pNCC (*arrow*) in isolated urinary exosomes from four control samples. Samples were run alongside control samples from human (H) and mouse (M) renal tissues. NCC is detected at ~130 – 160 kDa and pNCC is detected ~130 kDa.

5.3.3 Patient biochemistry

The present findings show that our proteins of interest, NCC and its phosphorylated form, pNCC, can be detected using the current isolation method and at lower volumes of urine, and thereby allowed for protein analyses in CNI-administered renal transplant patients and Gitelman syndrome patients.

Plasma samples were routinely collected on the day of urine collection from a total of 18 CNI-administered renal transplant patients (13 male and 5 female patients) and 4 Gitelman syndrome patients (1 male and 3 female patients). The Gitelman syndrome patients recruited for this study had been previously diagnosed on the basis of their genotype and were currently receiving treatment to manage the hypokalemia and hypomagnesemia phenotypes. Electrolyte analyses are shown in **Table.5.1**. It should be noted that no biochemical data was available for the age- and gender-matched control groups as only urine samples were collected. In both patient groups, normal plasma levels of sodium and calcium were observed, which were not significantly different between groups. Mean plasma creatinine was significantly higher in the CNI-treated transplant group, which is most likely a reflection of altered GFR from renal transplantation and CNI administration. CNI-administered renal transplant patients also displayed significantly higher levels of potassium which, although were not high enough for clinical diagnosis, were borderline hyperkalemic (potassium levels >5.5 mmol/L), which was expected for CNI-administered patients. In contrast, Gitelman syndrome patients showed lower potassium levels, which were slightly lower than the average range for potassium (3.6 – 5.2 mmol/L), and therefore, indicative of hypokalemia (<2.7 mmol/L). Bicarbonate plasma levels were also slightly but significantly lower (acidic) in CNI-administered transplant patients and higher (alkaline) in Gitelman syndrome patients compared with the average range for plasma bicarbonate (23 – 30 mmol/L). In both patient

groups, plasma phosphate was lower than the average range (0.8 – 1.5 mmol/L). Although no significant differences were found between both patient groups, plasma phosphate levels were lower in CNI-administered renal transplant patients compared to the Gitelman syndrome group, which again, was expected for these patients. The Gitelman syndrome patients also displayed lower plasma magnesium levels (0.55 $\pm$ 0.06 mmol/L), indicative of hypomagnesemia (<0.7 mmol/L), which was expected for these patients. Unfortunately, urinary calcium measurements were not available for these patients to confirm the hypocalciuria phenotype.

Overall, as expected, CNI-administered renal transplant patients displayed clinical symptoms indicative of hyperkalemia, metabolic acidosis and hypophosphatemia, while Gitelman syndrome patients showed opposing/mirroring symptoms.

Parameter	CNI-administered Kidney Transplant Patients (N = 18)	Gitelman Syndrome Patients (N = 4)
Creatinine (µmol/L)	210.50 ± 13.99	68.75 ± 8.34 ***
Na^+ (mmol/L)	138.61 ± 1.02	139.50 ± 1.04
K^+ (mmol/L)	4.92 ± 0.13	3.05 ± 0.29 ***
HCO_3^- (mmol/L)	22.83 ± 0.52	29.25 ± 0.25 ***
Corrected Ca^{2+} (mmol/L)	2.37 ± 0.03	2.43 ± 0.02
PO_4^- (mmol/L)	0.32 ± 0.02	0.41 ± 0.01

Table 5.1. Plasma Biochemistry. A summary of plasma electrolytes from CNI-administered renal transplant and Gitelman syndrome patients measured on the day of urine collection. Values are presented as mean ± SEM. Significance was determined by unpaired T-test. ***P < 0.001; vs. CNI-administered kidney transplant patients.

5.3.4 Analysis of urinary NCC/pNCC excretion in renal transplant patients

Urinary exosomes were isolated from 12 renal transplant patients who were receiving CNIs and 12 age- and gender-matched controls. Prior to gel loading, samples were normalised to the individual with the lowest urinary creatinine, to account for differences in exosome concentrations between individual samples, and densitometric analyses were initially normalised to the exosomal markers, TSG101 and ALIX. However, TSG101 detection was relatively weak compared with ALIX, which was clearly detected among isolated exosome samples, and so protein analyses were therefore normalised to ALIX only (**Fig.5.7a,b**).

Relative densities were only measured for ALIX-positive control/patient pairs, which was shown for five out of twelve pairs. Compared to matched controls, a decreased trend was observed for urinary NCC excretion in CNI-administered renal transplant patients (**Fig.5.7c,d**). However, no significant differences were observed for pNCC between controls and patients (**Fig.5.7e,f**). A band corresponding to THP was strongly detected ~95 – 100 kDa as well as multiple low-molecular weight bands, which may represent entrapped proteins as well as cleaved products of the cotransporter.

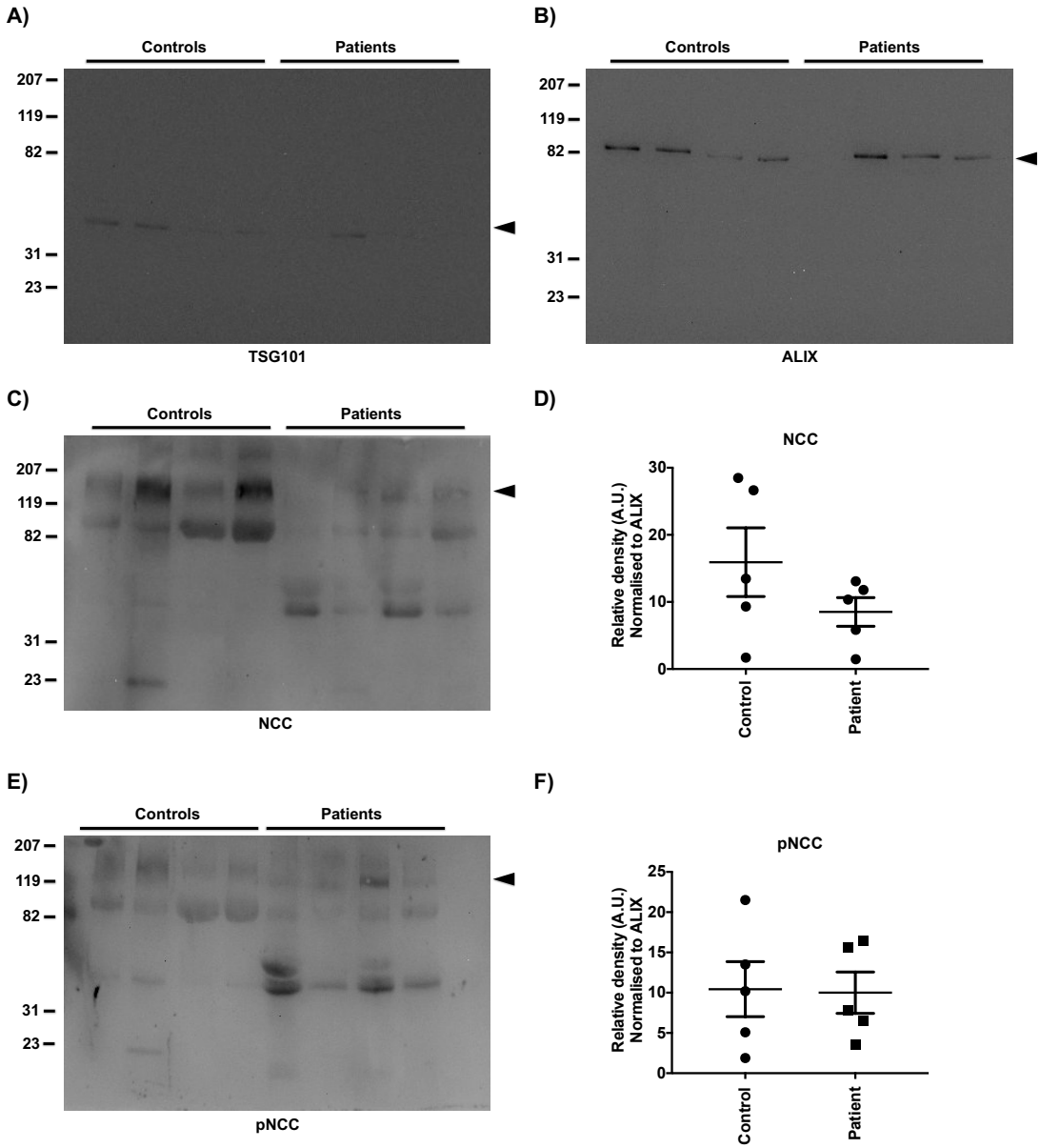

Figure 5.7. Analysis of NCC and pNCC protein excretion in CNI-administered renal transplant patients. Representative western blots and densitometric analyses for exosomal markers **A)** TSG101 (*arrow*) and, **B)** ALIX (*arrow*), and **C,D)** NCC (*arrow*) and **E,F)** pNCC (*arrow*) in urinary exosomes isolated from CNI-administered renal transplant patients. Samples were normalised to creatinine prior to gel loading. Patient samples were run alongside age- and gender-matched controls. Densitometric analyses were performed for each group and normalised to ALIX. Values are presented as the mean ± SEM, relative to ALIX (n = 5). Significance was determined using an unpaired T-test.

5.3.5 Analysis of urinary NCC/pNCC excretion in Gitelman syndrome patients

In the next experiments, urinary exosomes were isolated from 4 patients with Gitelman syndrome and 4 age- and gender-matched controls. These exosomes were isolated from freshly collected and immediately processed and stored urine in attempts to reduce THP-mediated entrapment of NCC/pNCC proteins. Loading samples were normalised to urinary creatinine and densitometric analyses were normalised to a standard exosome sample, which was loaded alongside control and patient samples as an additional method for protein normalisation. ALIX normalised to this standard showed similar relative densities between control and patient groups (**Fig.5.8a,b**).

Both NCC and pNCC proteins were detected in control and patient samples (**Fig.5.8c,f**). Densitometric analyses were normalised to either the standard sample or to standard-normalised ALIX. No significant differences were observed between the control and patient groups, however, a decreasing trend was observed in the patient group for both NCC (**Fig.5.8d,e**) and pNCC (**Fig.5.8g,h**) with either normalising methods.

Additionally, THP, as well as multiple low molecular weight bands, were still strongly detected in these samples (**Fig.5.8c,f**), suggesting that protein degradation and THP-mediated protein entrapment may still take place potentially within the kidney and bladder preceding excretion.

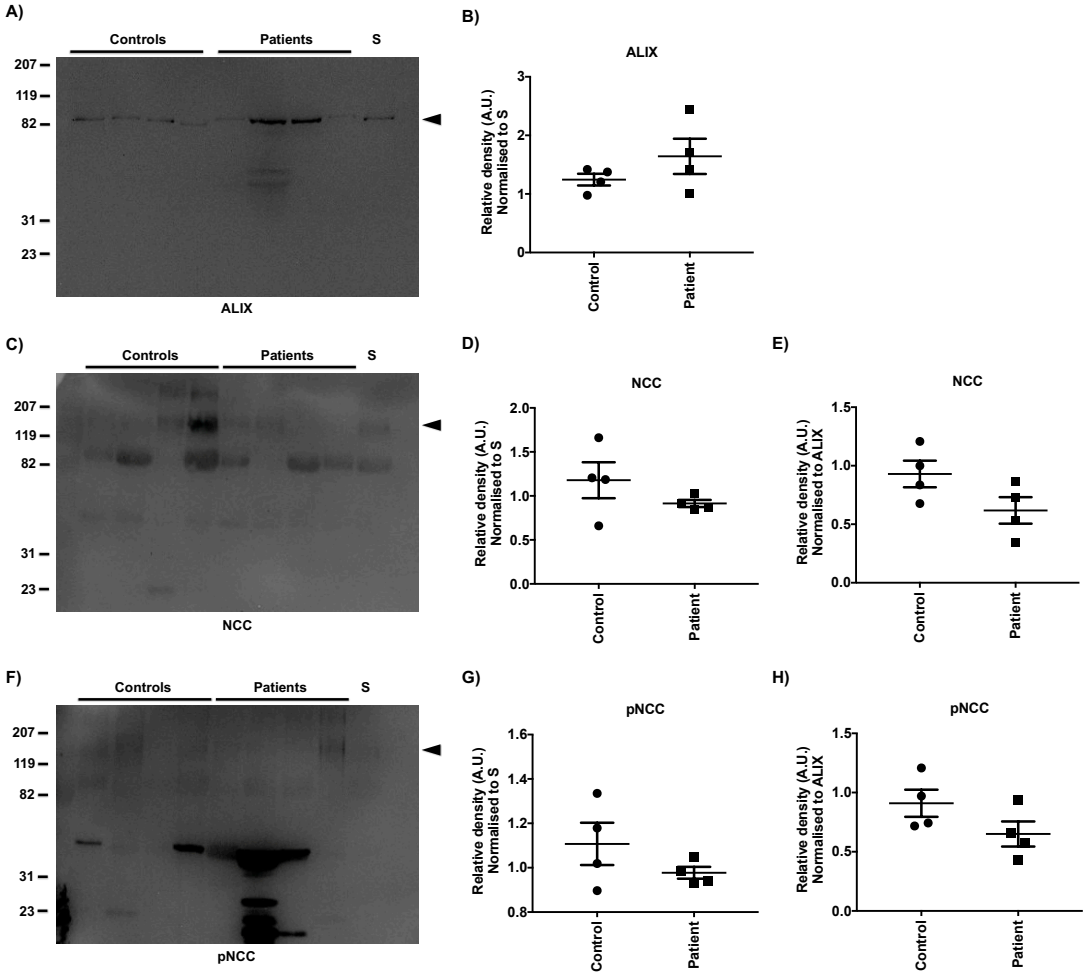

Figure 5.8. Analysis of NCC and pNCC protein excretion in Gitelman syndrome patients. Representative western blots and densitometric analyses for **A,B)** ALIX (*arrow*), **C-E)** NCC (*arrow*) and, **F-H)** pNCC (*arrow*) in urinary exosomes isolated from Gitelman syndrome patients. Samples were normalised to creatinine prior to gel loading. Patient samples were run alongside age- and gender-matched controls. Densitometric analyses were performed for each group and normalised to either **D,G)** a standard sample (S) or, **E,H)** ALIX. Values are presented as the mean ± SEM (n = 4). Significance was determined by an unpaired T-test.

Overall, there were no significant differences among CNI-administered renal transplant patients and those with Gitelman syndrome, compared with their corresponding matched controls. In addition, high levels of THP and low molecular weight products were observed which might have obscured precise protein quantification.

Despite these findings, comparisons between CNI-treated patients and those with Gitelman syndrome revealed significantly decreased NCC protein excretion in Gitelman syndrome patients (**Fig.5.9a**). This was also observed for pNCC (**Fig.5.9b**). However, it should be noted that the relative densities for the control group matched to the Gitelman syndrome patients was lower compared with the control group matched to the CNI-treated patients. This was most likely related to differences in creatinine-normalised gel loading. Urinary creatinine was not statistically significant between matched control and patient groups, but was lower with Gitelman syndrome patients vs. their matched controls (5.44 ± 1.70 vs. 16.31 ± 5.19 mmol/L, respectively), compared to CNI-administered patients vs. their matched controls (14.31 ± 2.15 vs. 14.01 ± 1.96 mmol/L, respectively). This reduction in urinary creatinine in the Gitelman syndrome group is a reflection of the inability of these patients to concentrate creatinine and so smaller volumes of control exosome samples were loaded compared to the patients, which may explain the relatively lower densities for the control group.

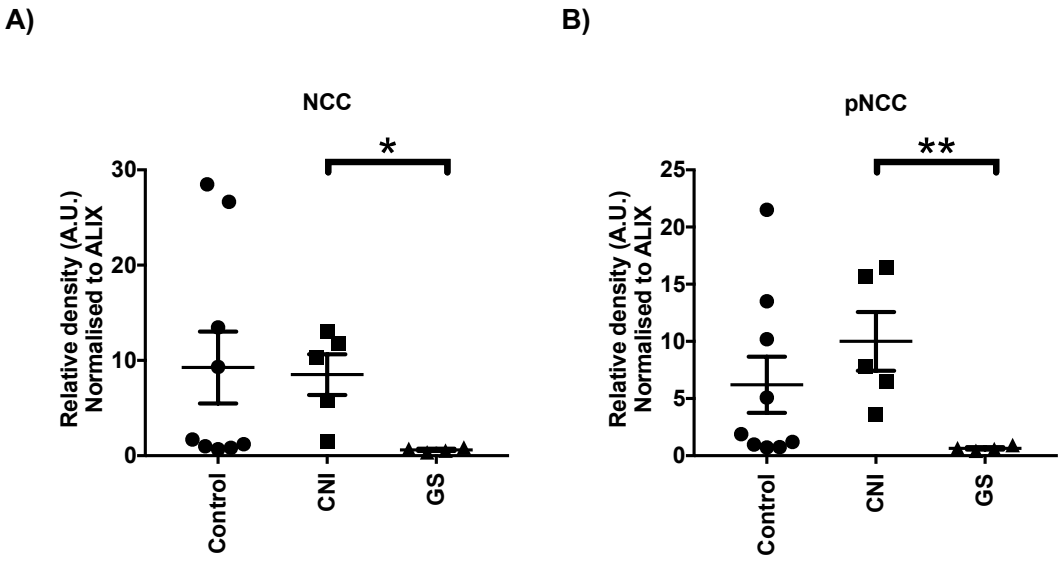

Figure 5.9. Comparisons of NCC and pNCC excretion in CNI-administered renal transplant patients and Gitelman syndrome patients. Densitometric analyses of **A)** NCC and **B)** pNCC cotransporters in age- and gender-matched controls (n = 9), CNI-administered renal transplant patients (CNI, n = 5) and Gitelman syndrome patients (GS, n = 4). Values are presented as the mean ± SEM, relative to ALIX. Significance was determined by one-way ANOVA with Dunn's post-test. *P < 0.05, **P < 0.01.

5.3.6 Further protein detection

The following experiments were performed to validate whether the isolated urinary exosomes from this protocol could be used to analyse renal sodium-dependent transporters from other segments of the nephron. These were analysed for the proximal tubule transporters, SGLT2 and NaPi-IIc, whose dysregulation/mutations result in diabetes and hereditary hypophosphatemic rickets with hypercalcuria (HHRH), respectively (Bergwitz et al., 2006; Lorenz-Depiereux et al., 2006; Rahmoune et al., 2005), and the distal tubule sodium channel, ENaC, which is known to cause Liddle's syndrome (Shimkets et al., 1994), along with ALIX, which was detected in three out of the four control samples (**Fig.5.10a**).

As already observed, SGLT2 was detected in all four samples, at the correct molecular weight, as confirmed from the human control sample (**Fig.5.10b**). However, NaPi-IIc and ENaC could not be detected in all samples (**Fig.5.10c,d**), implying the urinary exosome isolation protocol used in this study might not be suitable for protein excretion analyses of other renal transport proteins.

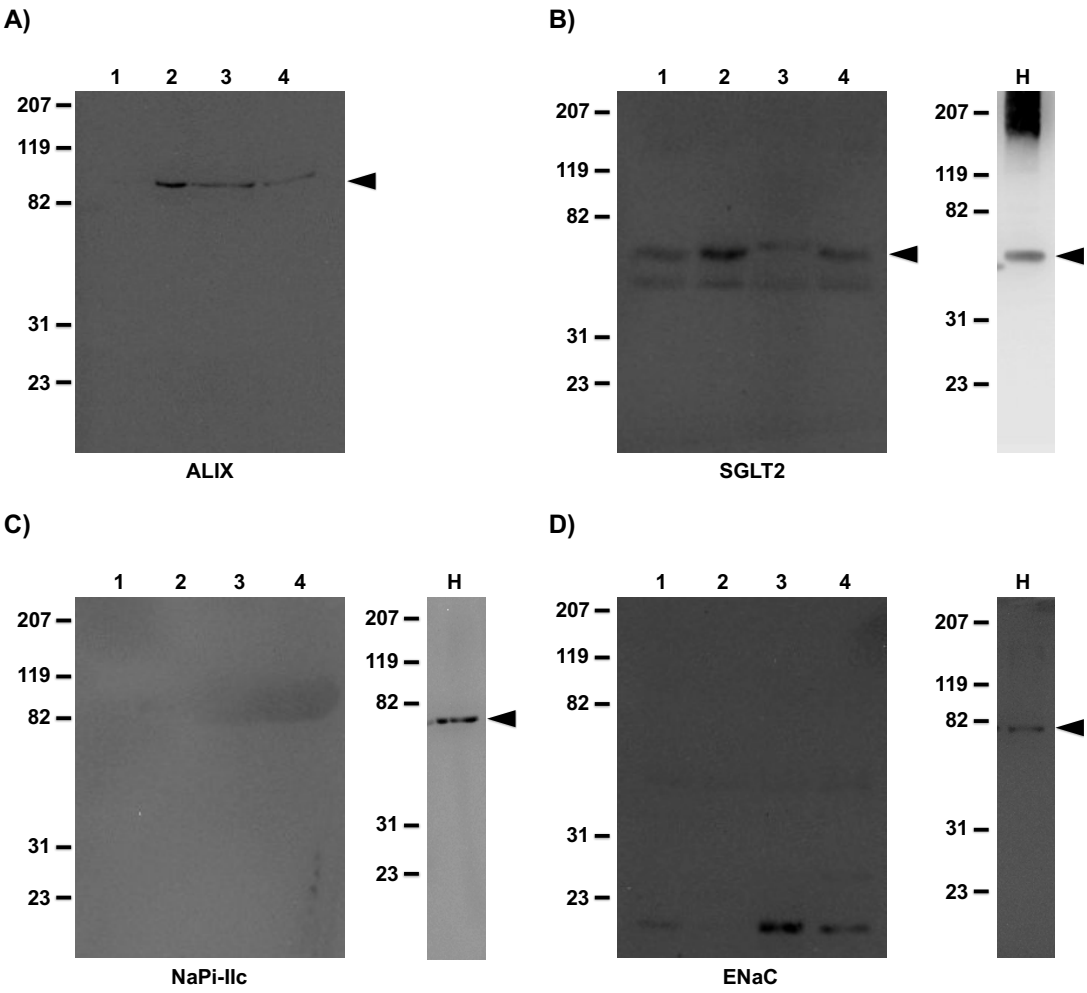

Figure 5.10. Protein detection of other renal transporters in isolated urinary exosomes. Representative western blots for **A)** ALIX (*arrow*), **B)** SGLT2 (*arrow*), **C)** NaPi-IIc and **D)** ENaC renal transport proteins from urinary exosomes isolated from four control samples. Samples were run alongside a control sample from human (H) renal tissues. ALIX is detected ~80 - 95 kDa (*arrow*), SGLT2 is detected ~75 kDa (*arrow*), NaPi-IIc is detected ~64 kDa (*arrow*) and ENaC is detected ~85 kDa (*arrow*).

5.4 Discussion

Analyses of renal protein abundance in patients is hindered by the complications in obtaining renal tissues from live patients. The practical use of renal biopsies carries a great risk of internal damage and the collected sample can often lose structural integrity, making immunohistochemical analyses difficult. Extensive research is currently ongoing to exploit urinary exosomes as a source of biomarkers for renal disease and dysfunction. The results presented in this chapter focused on optimising a method for urinary exosome isolation to compare changes in urinary NCC and pNCC excretion in CNI-administered renal transplant patients and Gitelman syndrome patients to support previous findings and to determine whether this protocol could be used to analyse other excreted renal transport proteins.

5.4.1 Urinary exosome isolation

Urinary exosomes have been found to contain proteins, mRNAs and miRNAs secreted by epithelial cells from each segment of the nephron, which may provide an accurate representation of the physiological and pathophysiological state of the kidney and, as such, may be suitable for the identification of biomarkers for renal-related conditions (Lv et al., 2013; Miranda et al., 2010; Pisitkun et al., 2004; Valadi et al., 2007). Proteomic profiling in these urinary exosomes have already identified several disease-related proteins, which may serve as potential biomarker candidates (Gonzales et al., 2009; Pisitkun et al., 2004). However, the use of the standard ultracentrifugation method for urinary exosome isolation in clinical settings is hampered by the low throughput, lengthy preparation and use of expensive instruments. Numerous investigations have been conducted to develop an alternative, faster and more efficient approach, but these have yielded variable results in exosomal yield and purity (Alvarez et al., 2012;

Channavajjhala et al., 2014; Cheruvanky et al., 2007; Merchant et al., 2010; Miranda et al., 2010; Raj et al., 2012; Rood et al., 2010).

In this study, a number of adaptations to the standard ultracentrifugation method were tested to try to improve its reproducibility in yielding intact exosomes. Comparisons of two commonly used protocols revealed that the protocol described by Tutakhel *et al* was the best suited (Tutakhel et al., 2016). This was confirmed by exosomal marker (ALIX and TSG101) and NCC/pNCC protein detection, which allowed for further investigations in patient urine. However, this exosomal isolation protocol was found be variable between samples and starting urine volume appeared to have no effect on protein detection.

5.4.2 Urinary exosome analyses in patient urine

Previous reports have observed very low or undetectable levels of urinary NCC protein excretion in patients with Gitelman syndrome and significantly increased urinary excretion of NCC in PHAII and CNI-administered renal transplant patients, which correlates with their relative abundances in the kidney under these conditions (Corbetta et al., 2015; Esteva-Font et al., 2014; Isobe et al., 2013; Joo et al., 2007; Mayan et al., 2008; Rojas-Vega et al., 2015; Tutakhel et al., 2017). This is in line with the described role for NCC in sodium retention and blood pressure regulation. Gitelman syndrome is a hypotensive autosomal salt-wasting disorder and is the result of loss-of-function mutations in NCC (Simon et al., 1996c), which accounts for the significant reduction in NCC excretion observed in these patients. As previously mentioned, clinical and rodent studies have demonstrated that CNI administration is associated with hypertension, via enhanced activation and phosphorylation of NCC, and exhibits clinical features that resemble PHAII, an autosomal dominant disease caused by gain-of-function mutations in regulators of NCC, resulting in upregulated renal sodium reabsorption and

elevated blood pressure (Boyden et al., 2012; Hoorn et al., 2011; Louis-Dit-Picard et al., 2012; Melnikov et al., 2011; Wilson et al., 2001). These clinical phenotypes are 'mirror-images' of Gitelman syndrome, which was reflected in the plasma biochemical analyses in the patients used. In the present study, although no significant differences were observed for NCC and pNCC protein excretion between CNI-administered renal transplant patients and Gitelman syndrome patients with their matched controls, comparisons in Gitelman syndrome patients compared with CNI-administered renal transplant patients was significantly lower, as expected.

5.4.3 Limitations

Despite the attempts to optimise protein detection for urinary NCC/pNCC excretion in these patients for comparative studies, and confirmed urinary exosome isolation by the detection of the ALIX exosomal marker, some limitations of this study have been recognised.

First, although the detection of exosomal markers, ALIX and TSG101, and a substantial amount of protein present in the final exosome pellet suggested successful isolation of exosomes from urine, no further methods were used for characterising the isolated exosomes such as electron microscopy or nanoparticle tracking analyses, to distinguish between exosomes and other larger microvesicles. However, as a modified version of the standard urinary exosome isolation technique was used in this study and revealed consistent ALIX detection, successful isolation of exosomes can be assumed.

Another challenge faced with this method was protein normalisation and quantification. As mentioned, previous investigations have been performed to evaluate alternative methods of normalisation including urinary creatinine, THP and exosomal markers (Fernández-Llama et al., 2010; Zhou et al., 2006a). In the present study, samples were normalised to urinary creatinine

prior to gel loading to account for differences in exosome concentrations between individual samples, and densitometric analyses were normalised to ALIX or a standard sample. The relative density of ALIX was found to be consistent among the samples, supporting that a similar number of exosomes were loaded on the gel. Normalising to THP has been previously proposed, however, this protein is also known to cause problems in exosome isolation.

Contamination by THP was a major complication in the present study and currently remains a recurring problem in exosome isolation methods. THP is a glycoprotein that is synthesized in the TAL (Bachmann et al., 1985, 1990). This protein resides along the basolateral membrane, apical cytoplasmic vesicle compartments and in/near the luminal plasma membrane (Bachmann et al., 1985). Urinary exosomes are typically concealed by THP in a polymeric fibril network, which can hinder protein identification in applications such as mass spectrometry. The addition of DTT during the low-speed spins is used to dissolve this polymeric network, but this does not completely remove all THP (Fernández-Llama et al., 2010). In the present study, the addition of DTT had no effect on THP, even in freshly collected and processed urine. Additional steps have been investigated to separate exosomes and THP using sucrose gradients, double-cushion ultracentrifugation, size exclusion chromatography and NaCl-based precipitation (Kosanović and Janković, 2014; Raj et al., 2012; Rood et al., 2010). Unfortunately, these methods still require the ultracentrifugation step, remaining both time-consuming and expensive, and although the removal of THP is required for exosome analysis, it is not clear whether the removal of THP in the urine samples with these methods may also result in the loss of potential biomarkers already entrapped by THP prior to processing, which may lead to inaccurate protein quantification.

Interestingly, it has also been suggested that THP itself may have a pathophysiological significance. THP is known to play a major role in the defence against urinary tract infections (Bates et al., 2004), however, previous studies have demonstrated that THP is involved in the pathogenesis of hyperuricemic nephropathy and chronic kidney disease (Dahan et al., 2003; Hart et al., 2002; Rampoldi et al., 2003; Wolf et al., 2003). Patients with familial juvenile hyperuricemic nephropathy and autosomal-dominant medullary cystic kidney disease were found to possess mutations in the THP gene, which suggested a role for THP in renal urate handling (Dahan et al., 2003; Hart et al., 2002; Rampoldi et al., 2003; Wolf et al., 2003). In these patients, THP was found to accumulate in the TAL as a result of the retention of mutated THP in the endoplasmic reticulum and delayed export to the plasma membrane (Rampoldi et al., 2003). In addition, alterations in THP synthesis or urinary excretion has been observed in patients with diabetic nephropathy, polycystic kidney disease, lupus nephritis and in a variant of Barttter's syndrome (Rasch et al., 1995; Schroter et al., 1993; Tsai et al., 2000), proposing THP itself as a renal disease biomarker (Zimmerhackl, 1993). Furthermore, studies in THP knockout mice revealed a significant upregulation in mRNA and protein expression of major renal transport proteins including NHE3, NKCC2, ClC-K channels, barttin, ROMK, α-ENaC and NCC, suggesting that THP may also be important in regulating renal transporter functions (Bachmann et al., 2005). It is therefore unclear whether THP or other exosomal markers such as ALIX are affected under renal disease or dysfunction, which would also limit precise biomarker normalising and protein quantification. Further investigations are required to understand the shredding processes of these transport proteins, the impact of CNIs and THP on these processes, and the effects of CNIs on THP and ALIX.

Another limitation of this study is that although the protein abundance for NCC and pNCC in the urinary exosomes analysed showed significant differences between CNI-administered and Gitelman syndrome patients,

other factors that may also regulate NCC expression and function were not considered. This includes salt loading or the use of alternative medications such as thiazides in CNI-administered renal transplant patients to treat elevated blood pressure. Previous studies in CNI-administered renal transplant patients taking thiazides and mineralocorticoids revealed a significant increase in urinary NCC excretion, indicating these thiazides might enhance NCC/pNCC shredding into the urine to account for increased phosphorylation and activation of NCC as a result of the CNI effects (Pathare et al., 2017; Tutakhel et al., 2017; Wolley et al., 2017). In addition, the data presented in this chapter are observational and do not directly establish the connection between CNIs, NCC upregulation and hypertension.

No significant differences in NCC and pNCC abundance were observed between patients and their matched controls, but the overall relative densities of these proteins were much lower in Gitelman syndrome patients compared with the CNI-treated renal transplant group. The reasons for this absence in significance with the control groups are not yet clear. One reason may be that the control samples were collected from healthy subjects which contain lower levels of urinary proteins. Previous studies have reported significant increases in total and phosphorylated NCC abundance in CNI-treated renal transplant patients compared with CNI-free renal transplant patients but not in healthy controls, when normalised to CD9, another exosomal marker (Tutakhel et al., 2017). CNI-free renal transplant patients were not analysed in this study and future comparisons between these patients, CNI-treated patients and patients with Gitelman syndrome would potentially corroborate these findings. In addition, a small sample number of ALIX-positive pairs were analysed in the CNI-treated group and so may have masked any significant differences between the patients and their corresponding controls. This was mostly likely the same for the Gitelman syndrome group, although, the lower sample number in this case was due to the rarity of the disease. However, it should also be noted that the relative densities of the control

group for the Gitelman syndrome patients were also lower compared with the matched controls for the CNI-treated group which, as already mentioned, is mostly likely the result of differences in creatinine-normalised loading.

Furthermore, as shown in further experiments, protein detection of other transport proteins was variable, suggesting that the protocol used in this study may not be suitable for analysis of renal transporters. In addition, it is not clear whether the abundance of protein per exosome vesicle varies and may be underrepresented in protein normalising and quantifying steps.

5.4.4 Conclusions

Overall, it is not yet established which method of exosome isolation and normalisation is the most suitable and whether exosomal markers such as ALIX, TSG101 and THP are affected under the pathogenic conditions investigated in this study. Though the modifications made to the current protocol improved exosome isolation, this was still not ideal for protein analyses and therefore requires further optimising.

Although no differences in urinary NCC and pNCC excretion were observed between patients and their matched controls, the finding that urinary NCC and pNCC excretion was significantly higher in renal transplant patients and lower in Gitelman syndrome patients is consistent with observations from previous studies and the role for NCC in blood pressure regulation.

However, as only a selection of renal transport proteins were identified in these isolated exosomes, it is likely the protocol used in this study was not fully optimal for the detection and analysis of transport proteins which are associated with renal-related conditions. It is clear that despite the substantial advances that have occurred in the aspects of urine storage and processing for urinary exosome isolation, a faster, efficient and reliable

method for routine exosome isolation has yet to be established. These improvements to the existing non-invasive methodology for urinary exosome isolation would drastically aid in the rapid and accurate diagnosis of a number of pathological conditions and the implementation of effective therapeutic treatments.

Chapter VI
General Discussion

6.1 Aims of thesis

Over the years, substantial advances have been made into understanding the cellular mechanisms involved in the development of hypertension, including following renal transplantation and in patients with Pseudohypoaldosteronism II (PHAII). A strong association between post-transplant hypertension and an increased risk for cardiovascular events, and long-term graft and patient survival has been demonstrated in a number of follow-up studies (Kasiske et al., 2004; Opelz et al., 1998, 2005). These studies strongly highlight the need for the characterisation of the underlying pathogenic mechanisms involved in order to facilitate the development of more targeted treatments for managing blood pressure following renal transplantation and in patients with hypertensive diseases. Attention has been particularly directed towards the cellular effects of the calcineurin inhibitor (CNI) immunosuppressant therapy received following renal transplantation. Studies from clinical and experimental models of PHAII and CNI-induced hypertension have provided convincing evidence for the overactivation of the NCC cotransporter as the key factor, which acts through increased renal sodium retention and leads to elevated blood pressure (Boyden et al., 2012; Chiga et al., 2011; Hoorn et al., 2011; Lalioti et al., 2006; Louis-Dit-Picard et al., 2012; Melnikov et al., 2011; Wilson et al., 2001; Yang et al., 2007, 2013). However, the sodium retaining effect on other sodium-dependent transporters present in the kidney and gastrointestinal tract, and their potential role in sodium retention and hypertension development under CNI or hypertensive conditions have not been studied.

It is well known that the kidneys play a major role in regulating sodium homeostasis. Sodium-coupled transport is the main mode of renal sodium reabsorption across the brush border membrane (BBM) and basolateral membrane (BLM) and includes; the Na^+/H^+ exchanger (NHE3), the Na^+/glucose cotransporters (SGLT2 and SGLT1), the facilitative glucose transporter (GLUT2), the Na^+/Pi cotransporters (NaPi-IIa and NaPi-IIc), the Na^+/HCO_3^- cotransporter (NBCe1A), the $Na^+/K^+/2Cl^-$ cotransporter (NKCC2), the Na^+/Cl^- cotransporter (NCC), the Na^+-dependent Cl^-/HCO_3^- exchanger (NDCBE) and the epithelial Na^+ channel (ENaC) (**Fig.1.2**). The expression of these transport proteins is tightly controlled by a number of factors including dietary salt and hormones such as vasopressin and aldosterone (Chiga et al., 2008; Hall and Varney, 1980; Hebert et al., 1981a, 1981b, 1981c; Loffing et al., 2000; Pacha et al., 1993). It is also known that dysregulation or mutations in some of these sodium transport proteins has a significant impact on blood pressure regulation and results in blood pressure-related diseases such as PHAII (gain-of-function NCC mutation), Gitelman syndrome (loss-of function NCC mutation) and Liddle syndrome (gain-of-function ENaC mutation) (Boyden et al., 2012; Firsov et al., 1996; Louis-Dit-Picard et al., 2012; Shimkets et al., 1994; Simon et al., 1996c; Snyder et al., 1995; Wilson et al., 2001). A number of these transport proteins are also expressed in the gastrointestinal tract, including; NHE3, SGLT1, GLUT2, the Na^+/Pi cotransporters (NaPi-IIb and PiT1), and ENaC (**Fig.1.3**).

Earlier studies have provided evidence for a complex interplay between the kidneys and intestines, which was demonstrated for phosphate, potassium and sodium ions (Berndt et al., 2007; Carey, 1978; Lee et al., 2007; Lennane et al., 1975; Rabinowitz et al., 1988). During investigations in subjects following oral and intravenous sodium loading, a greater natriuretic response was observed after orally administered NaCl feeding compared with responses seen following intravenous NaCl infusion (Carey, 1978; Lennane et al., 1975). These authors concluded that the gastrointestinal tract is

involved in sensing and effector signalling responses to changes in sodium intake, which may signal the kidneys to either excrete or conserve sodium, accordingly. However, the 'sensor' for sodium in the gastrointestinal tract and the renal-signalling mechanisms are still not known. Furthermore, this interplay between both the kidneys and gastrointestinal tract under hypertensive physiological conditions has not been previously studied.

The main aims of the experiments reported in this thesis were to investigate the effects of CNI-induced sodium retention on renal and intestinal sodium transporters and to test for the hypothesised cross-talk between the kidneys and intestines in adaptation to changes in sodium balance. In addition to these objectives, it has been demonstrated that a number of conditions, including post-transplant diabetes mellitus (PTDM) or metabolic syndrome, are also commonly encountered following renal transplantation with extensive evidence linking their development to CNI use (Boudreaux et al., 1987; Chapman et al., 1987; Jevnikar et al., 1988; Ligtenberg et al., 2001; McCune et al., 1998; Pirsch et al., 1997; Roth et al., 1989; Schorn et al., 1991; Vincenti et al., 2002; Woodward et al., 2003). However, this has not yet been investigated in detail. Therefore, in another set of experiments, animals were also maintained on a high-fat diet (as a model of metabolic syndrome) and assessed for changes in sodium transport proteins which were compared with those seen in FK506-treated animals. The initial aims of these experiments were to determine whether CNIs are the main influencers for the development of metabolic syndrome in treated transplant patients and to also identify which transporters (besides pNCC) contribute towards the development of hypertension and other post-transplant-affiliated conditions, such as PTDM and post-transplant metabolic syndrome.

6.2 Sodium and blood pressure

One of the main functions of the kidneys is to maintain sodium and water balance, and thus blood pressure. Numerous volume expansion and renal transplant studies, as well as hereditary diseases of renal sodium transport, have all revealed that sodium retention and plasma volume expansion by the kidneys plays a critical role in chronic elevations of blood pressure (Boyden et al., 2012; Greene et al., 1990; Guidi et al., 1996; Guyton et al., 1972; Louis-Dit-Picard et al., 2012; Norman et al., 1975; Rettig et al., 1990b, 1990a, 1989; Simon et al., 1996c; Wilson et al., 2001). Likewise, epidemiological studies have shown a positive correlation between dietary sodium intake and blood pressure across and within populations (Elliot et al., 1996; Rose et al., 1988). This was further supported in controlled clinical trials showing that a reduction in salt intake lowers arterial pressure in both hypertensive and normotensive people (Sacks et al., 2001). However, the precise mechanisms of how excessive salt intake increases blood pressure are still not well understood. Several studies have postulated that dietary sodium-induced hypertension is the result of extracellular fluid volume expansion and cell swelling (Coleman and Guyton, 1969; Douglas et al., 1964; Friedman, 1990a; Friedman et al., 1990b; Manning et al., 1979a, 1979b; Villamil et al., 1982). Previous experiments in saline infused nephrectomised dogs demonstrated that volume expansion raises blood pressure by an 'autoregulatory effect' on the resistance vessels as a result of increased blood flow and cardiac output, causing vessel constriction and increased total peripheral resistance, which is then subsequently decreased to return to control levels (Coleman and Guyton, 1969; Manning et al., 1979b). An increase in salt intake has also been associated with small rises in plasma sodium which increases extracellular fluid volume (Manning et al., 1979a). Studies in clinical essential and experimental hypertension models have also shown that excessive salt intake correlates strongly with increased left ventricular mass and wall thickness (du Cailar et al., 1989; Fields et al.,

1991; Frohlich et al., 1993; Leenen and Yuan, 1998; Yu et al., 1998). Spontaneously hypertensive rats (SHR) given a high-salt (4-8%) diet exhibited left ventricular hypertrophy and increased cardiac mass, while Wistar-Kyoto (WKY) rats fed on a high-salt diet showed increased cardiac mass without changes in arterial pressure (Frohlich et al., 1993; Leenen and Yuan, 1998), suggesting that dietary sodium may exacerbate a cardiac hypertrophic response to increased blood pressure. Furthermore, increased plasma sodium concentrations have been found to increase cell diameter, volume and protein content in rat myocardial myoblasts and vascular smooth muscle cells, as well as increased angiotensin type I receptor expression, angiotensin II activity and plasma renin (Gu et al., 1998; Nickenig et al., 1998; Ruan et al., 1997; Simon and Illyes, 2001), implicating the activation and contribution of the renin-angiotensin-aldosterone system in vasoconstrictive and hypertensive responses to excessive salt intake. However, whether CNI-induced sodium retention affected cardiac output, extracellular fluid volume and activation of the renin-angiotensin-aldosterone system in the present study remains to be confirmed.

In this thesis, the experiments performed in Chapter 3 aimed to assess for changes on sodium transport proteins in the kidney and gastrointestinal tract in a CNI-treated mouse model, to confirm their potential involvement in increased CNI-induced sodium retention. These sodium transport proteins were examined owing to their involvement in blood pressure regulation and as downstream targets of the WNK-SPAK/OSR1 signalling cascade. The experiments described for Chapter 4 aimed to compare these changes with a model of diet-induced metabolic syndrome, to determine whether CNIs may influence metabolic syndrome development following renal transplantation. In these studies, a clinically comparable dose of FK506 was administered, which was also twice the dose given in mice from a previous report (Hoorn et al., 2011). These studies utilised RT-PCR, western blotting and immunohistochemistry techniques in the kidneys and the three segments of

the gastrointestinal tract (proximal and distal small intestines, and the colon), alongside plasma and urine electrolyte analyses.

Although blood pressure and sodium transport across the renal BBM was not measured, western blotting and immunohistochemistry demonstrated a significant upregulation of apical pNCC expression in the DCT which suggests increased sodium transport in this model and potentially elevated blood pressure. The most striking conclusion drawn from the experiments described in Chapters 3 and 4 was that the presence of other factors, particularly high dietary fat intake or an obese background, were the main mediators of alterations in renal and intestinal transporters, and thus, the development of metabolic complications encountered following transplantation (summarised in **Fig.6.1**). Interestingly, the findings from CNI treatment showed there may be homeostatic downregulation of sodium transporter expression in nephron segments outside of the DCT; renal NHE3 and ENaC were downregulated by CNI treatment, which may be a compensatory mechanism to adapt to increases in sodium reabsorption at the DCT. Supporting this interpretion of the data, in the experiments described in Chapter 3, the supplement of a high-salt det led to a significant downregulation of renal NHE3. However, it is not fully clear what impact the downregulation of renal NHE3 and ENaC transport proteins has on blood pressure in this study, whether this downregulation is a compensatory response to upregulated transporter activity or to increased sodium transport via pNCC, or whether these are effects caused by CNIs or the WNK-SPAK/OSR1 signalling pathway.

The data obtained from Chapter 4 showed a significant increase for renal NHE3 and pNCC in mice fed on the high-fat diet, supporting an increase in sodium retention and blood pressure, which is line with conditions associated with high-fat feeding and metabolic syndrome. A significant decrease for the renal ENaC sodium channel was also observed in these mice, which was

suggested to be either a compensatory response to increased sodium reabsorption through NHE3 and pNCC or to increased ENaC activity, though this remains to be confirmed. This downregulation in renal ENaC contrasts with its expected effects in contribution to increased sodium retention and stimulation by known regulators in this model.

Alongside NCC, both NHE3 and ENaC are known to play a role in blood pressure regulation. Genetic and acquired hypertensive diseases have been associated with increased NHE3 and ENaC protein and transporter activity (Kobayashi et al., 2004; Leong et al., 2006; Pinto et al., 2008; Pradervand et al., 1999b; Shimkets et al., 1994; Snyder et al., 1995). Previous studies in NHE3-deficient mice display lower blood pressure compared with wild type (Lorenz et al., 1999; Noonan et al., 2005; Schultheis et al., 1998a), while studies in hypertensive human and spontaneously hypertensive rat models showed increased NHE3 activity and proximal tubular sodium reabsorption (Burnier et al., 1993; LaPointe et al., 2002; Pinto et al., 2008; Weder, 1986). The conclusions drawn from these studies implicate that the dysregulation of proximal tubular reabsorption can have a significant impact on blood pressure and can contribute to the pathogenesis of hypertension. Both NHE3 and ENaC are also implicated as downstream targets of the WNK-SPAK/OSR1 signalling cascade (Ahmed et al., 2015; Pasham et al., 2012; Ring et al., 2007a; Yang et al., 2007). However, unlike ENaC, investigations on the regulation of NHE3 by the WNK-SPAK/OSR1 signalling cascade in relation to hypertensive conditions are lacking. It has been shown that ENaC activity is inhibited by WNK4 under basal conditions and is activated in PHAII-causing WNK4 mutations (Ring et al., 2007a; Yang et al., 2007). Studies in mutated WNK4 transgenic mice and in patients carrying the WNK4 Q565E PHAII-causing mutation exhibit alleviated WNK4-mediated inhibition, higher responses to amiloride treatment and increased ENaC expression in the collecting duct and colon (Farfel et al., 2005; Ring et al., 2007a; Yang et al., 2007), which contributes to increased sodium reabsorption and blood

pressure. Taken together, these transport proteins are crucial in blood pressure regulation and contribute to the pathogenesis of hypertension through both genetic mutations and over-stimulation by known regulators.

It is known that these major sodium transport proteins are regulated by a number of hormones. This includes angiotensin II (AngII). Activation of the renin-angiotensin system is associated with increased sodium transport in the renal proximal tubule and stimulated NHE3 protein expression and activity (Geibel et al., 1990; Gurley et al., 2011; Li and Zhuo, 2007; Riquier-Brison et al., 2010; Xu et al., 2006), which contributes to increased blood pressure. This was demonstrated in mice where gene silencing of the angiotensin type IA receptor exhibited significantly reduced blood pressure and reabsorption at the proximal tubule compared with controls (Gurley et al., 2011; Li and Zhuo, 2007). In addition, acute inhibition of the AngII type II receptor or the angiotensin-converting enzyme also showed decreased proximal tubular sodium transport and AngII-stimulated NHE3 activity, and protein and cell surface expression in animal and cell culture models (Leong et al., 2006b; Li and Zhuo, 2007). Another stimulatory hormone is insulin, which regulates both NHE3 and ENaC (Blazer-Yost et al., 1998; Fuster et al., 2007; Gesek and Schoolwerth, 1991; Klisic et al., 2002). Previous studies have shown stimulated Na^+/H^+ exchange in the proximal tubular segments and in NHE3-expressing cultured cells by chronic treatment with insulin and have suggested this effect to be mediated by the PI3K-SGK1 pathway (Fuster et al., 2007; Klisic et al., 2002). Aldosterone is another important regulator. It is known to enhance sodium reabsorption at the distal segments of the nephron, but has also been demonstrated to stimulate NHE3 activity and increase cell surface expression at the renal proximal BBM (Drumm et al., 2006; Krug et al., 2003; Pinto et al., 2008). Aldosterone-induced sodium transport at the collecting duct occurs through ENaC activation (Blazer-Yost et al., 1998; Masilamani et al., 1999; Pacha et al., 1993). This is mediated through SGK1 signalling which reduces ENaC ubiquitination and degradation

through phosphorylating the ubiquitin ligase, Nedd4-2 (Chen et al., 1999; Debonneville et al., 2001; Snyder et al., 2002; Xu et al., 2005). This ubiquitin ligase has been shown to be important in regulating ENaC and blood pressure as Nedd4-2 knockout mice exhibit salt-sensitive hypertension and increased ENaC expression (Shi et al., 2008). Studies have also revealed that WNK1 activates SGK1 to regulate ENaC (Heise et al., 2010; Xu et al., 2005). Numerous animal, oocyte and cell culture models have also demonstrated WNK-SPAK/OSR1-mediated phosphorylation of NCC by increased AngII, insulin, aldosterone and SGK1 signalling (Castaneda-Bueno et al., 2012; Chávez-Canales et al., 2013; Chiga et al., 2008; Rozansky et al., 2009; San-Cristobal et al., 2009; Sohara et al., 2011; Talati et al., 2010; Vallon et al., 2009).

Overall, mutations in these major renal sodium transporters or the upregulation of regulatory hormones and kinases can significantly alter sodium homeostasis can lead to rises in blood pressure. In the context of the present study, as the opposite was observed following CNI treatment, the downregulation of the major transport proteins points more towards a feedback response in order to adapt to increased sodium transport by pNCC. In addition, as previously mentioned, this may also be a reflection on the CNI model used in this study. Although regulators of sodium transport, such as AngII and aldosterone, were not assessed in the present studies, the upregulation observed for renal pNCC and NHE3 transport proteins with high-fat feeding provide evidence for increased blood pressure in this model and stimulation by these regulators, which are also known to be increased in obese patients and those with metabolic syndrome. In future studies, functional and kinetic analyses for the individual transport proteins with CNI treatment would confirm their contribution to sodium retention and the efficiency of the model used in this study. Furthermore, comparative analyses of these transport proteins and sodium transport across the renal and intestinal BBM in other models, such as PHAII or NCC-mediated

hypertension, to the data obtained from the model of metabolic syndrome may also warrant further investigations into the role of the WNK-SPAK/OSR1 signalling cascade in the development of metabolic syndrome. Additionally, although substantial evidence from clinical and rodent models of hypertension implicates calcineurin, the target of CNIs, in the WNK-SPAK/OSR1-NCC signalling cascade, its role in regulating renal sodium homeostasis and blood pressure, particularly in essential and hereditary hypertensive diseases, has yet to be established. Comparisons of blood pressure and changes in these sodium transport proteins and function across the renal and intestinal BBM in calcineurin knockout mice or oocyte expression models would also allow for further investigations to determine the role of calcineurin in sodium homeostasis.

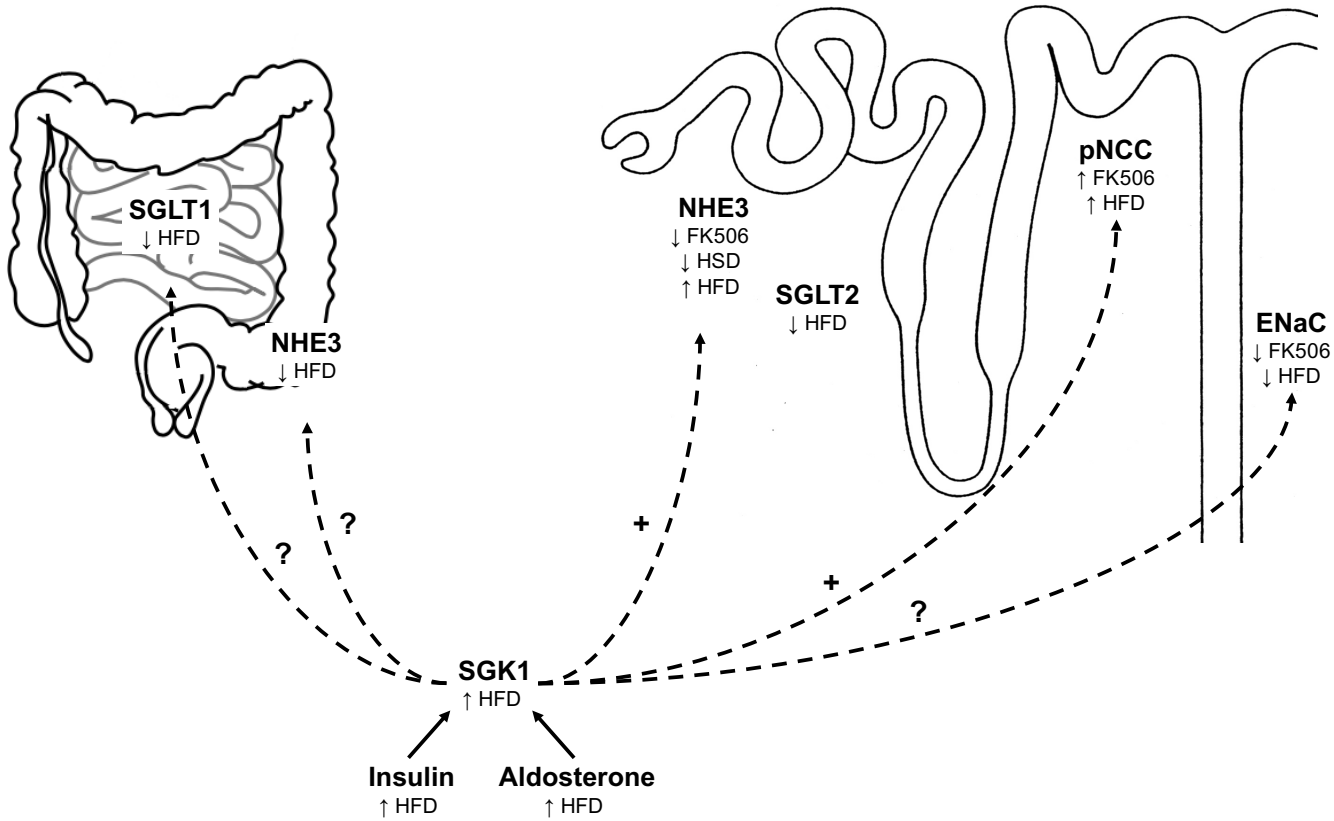

Figure 6.1. Proposed model of the effects of CNI treatment, high-salt and high-fat feeding on renal and intestinal transporters. High-fat (HFD) or high-salt (HSD) feeding and CNI treatment (FK506) influences the down- and up-regulation of a number of renal and intestinal sodium transporters (*arrows*), some of which may be compensatory to increased sodium reabsorption via pNCC at the DCT. The data also suggests the adaptations to dietary fat intake may be regulated by activation of the SGK1 kinase in response to high-fat feeding, insulin and aldosterone. This kinase may also regulate NHE3 and pNCC. The relative effects of SGK1 on renal ENaC and intestinal SGLT1 and NHE3 are unknown.

6.3 Sodium and the immune system

It is well established that the CNI-induced sodium retaining effects and increased dietary salt intake have a significant impact on blood pressure. However, alongside these hypertensive effects, it has also been revealed that dietary sodium intake can play a role in regulating the immune system. Previous mouse studies have shown that a high-salt diet can promote tissue inflammation and autoimmune disease development (Kleinewietfeld et al., 2013; Wu et al., 2013), raising the possibility that sodium homeostasis is important in driving the increased incidence of autoimmune disease, as well as hypertension. Clinical and experimental studies have proposed the mechanisms involved in dietary salt-induced inflammation and autoimmune disease development are linked to an increase in the number of monocytes, production of proinflammatory cytokines and enhanced Th17 differentiation (**Fig.6.2**) (Binger et al., 2015; Kleinewietfeld et al., 2013; Wu et al., 2013; Yi et al., 2015).

A clinical study by Yi *et al*, in healthy humans showed that subjects on a high-salt diet displayed a significantly higher number of monocytic cells compared with those on the low-salt diet and revealed a positive association between monocytes and dietary salt (Yi et al., 2015). Subjects maintained on a low-salt diet were accompanied by not only a lower number of monocytic cells, but also reduced production of proinflammatory cytokines and an enhanced production of anti-inflammatory cytokines (Yi et al., 2015), suggesting that high dietary salt intake is able to provoke an excessive immune response which can lead to the dysfunction of the immune system and thereby increase the risk of autoimmune disease. Furthermore, studies using flow cytometry, qRT-PCR and ELISA methods to investigate the effects of increasing NaCl concentrations on human Th17 cells showed dramatically increased induction of naïve $CD4^+$ T cell expression of the proinflammatory cytokine, IL-17A (Kleinewietfeld et al., 2013). A strong Th17 phenotype under

high-salt conditions was also further confirmed in comparative microarray analyses of naïve $CD4^+$ T cells differentiated with and without high-salt treatment (Kleinewietfeld et al., 2013). Additionally, high salt was shown to blunt the activation of non-inflammatory macrophages involved in suppressing effector T cell proliferation (Binger et al., 2015). These studies strongly implicate dietary sodium intake as a risk factor for autoimmune disease and chronic inflammation development, as well as hypertension.

In the context of the present study, although the primary use of CNIs in transplant patients is to suppress the adaptive immune system, the sodium retaining effects in the kidneys may also provoke further imbalances in the immune system. This may predispose these patients to further risks of inflammatory-mediated conditions, alongside hypertension, and increased risks for cardiovascular events. However, further studies measuring anti- and pro-inflammatory cytokine expression with CNI-treatment and/or high fat- and salt conditions are required.

6.4 Blood pressure regulation by the gastrointestinal tract

Despite previous investigations with human and rodent models implicating an interplay between the gastrointestinal tract and kidneys in regulating sodium, no significant changes were observed for intestinal sodium transport proteins following CNI treatment and so any cross-talk between the kidneys and intestines was not evident in the present study. However, the data obtained from Chapter 4 may suggest otherwise.

The experiments described in Chapter 4 showed that alterations in protein expression of renal and intestinal transporters following CNI treatment do not mimic those observed in mice fed on a high-fat diet, and revealed that CNI use alone does not lead to the development of metabolic syndrome. Mice became obese with high-fat feeding, and western blotting demonstrated a

significant increase in renal NHE3 and a decrease in renal SGLT2 and ENaC, while small intestinal SGLT1 and colonic NHE3 protein expression were also decreased (**Fig.6.1**). The downregulation of intestinal SGLT1 and renal SGLT2, along with elevated plasma glucose levels, are consistent with the proposed gastrointestinal-renal signalling axis and may implicate the activation of this interplay in the regulation of glucose, as well as sodium, under high dietary fat intake. This potential signalling axis between the two organs could also explain the significant increase and decrease observed for renal and colonic NHE3 expression, respectively. However, these findings suggest a feedback signalling mechanism between the kidneys and gastrointestinal tract, as opposed to the proposed feedforward signalling.

As previously mentioned in Chapter 3, a study by Berndt *et al*, was one of the first to demonstrate and propose this feedforward mechanism between the gastrointestinal tract and kidney for the regulation of phosphate balance (Berndt et al., 2007). Infusion of phosphate into the duodenum of rats was shown to induce rapid urinary phosphate excretion, suggesting the presence of an intestinal phosphaturic factor that senses phosphate load and mediates renal excretion (Berndt et al., 2007). Likewise, rats chronically fed on a low phosphate diet and then acutely switched to a high phosphate diet caused a rapid increase in plasma phosphate, due to increased NaPi-IIb protein expression at the duodenum, which was accompanied by a decrease in renal BBM Na^+/Pi transport activity and NaPi-IIa protein expression to compensate for the increased phosphate load (Giral et al., 2009). Furthermore, numerous studies in NaPi-IIb$^{+/-}$ and NaPi-IIb$^{-/-}$ knockout mice have also supported a role for this cotransporter in this feedforward signalling concept. Mice with a targeted deletion of the intestinal NaPi-IIb cotransporter display significantly reduced FGF23 levels and urinary phosphate excretion, which was correlated with increased renal NaPi-IIa and NaPi-IIc expression, in order to maintain normal phosphate balance (Ohi et al., 2011; Sabbagh et al., 2009; Schiavi et al., 2012). More recent investigations have observed similar

findings, whereby the loss of intestinal Na^+/Pi cotransport was associated with reduced phosphaturia, as a result of increased renal NaPi-IIa expression and renal BBM Na^+/Pi cotransport (Hernando et al., 2015). These findings demonstrate that the absence of the intestinal NaPi-IIb cotransporter is fully compensated for by the kidney to maintain phosphate levels. Taken together, these studies provide considerable evidence supporting this gastrointestinal-renal sensing/signalling mechanism for phosphate regulation. In addition, although limited, there is also strong evidence of this feedforward mechanism for sodium regulation. Studies in humans and rats subjected to oral sodium loading exhibit profound natriuresis, compared to intravenous sodium loading, and have proposed that the intestinal sensing mechanism is mediated by the guanylin and uroguanylin intestinal peptides (Carey, 1978; Carrithers et al., 2002; Fukae et al., 2002; Lennane et al., 1975; Lorenz et al., 2003; Mu et al., 1995).

However, to date, there are no further published investigations on the mechanisms underlying this gastrointestinal-renal sensing/signalling axis for phosphate and sodium regulation, and the identity of the putative intestinal sensing factor for phosphate remains unknown. Additionally, the findings from these NaPi-IIb knockout studies for phosphate regulation may also suggest the presence of a sensing and signalling factor in the kidney, whereby the absence of intestinal NaPi-IIb and Na^+/Pi transport, and the resulting hypophosphatemia is sensed by the kidneys and adapts by upregulating the renal Na^+/Pi cotransporters and BBM transport. Although, this remains to be clarified.

Contrastingly, previous studies have challenged the existence of this signalling axis and have observed opposing results. A recent study by Lee *et al* showed no changes in plasma phosphate, PTH concentration and urinary phosphate excretion in rats infused in the duodenum with phosphate at a physiological concentration (10mM), compared to the 1.3M phosphate

concentration used in the study by Berndt *et al* (Berndt et al., 2007; Lee et al., 2017). The expression of the renal NaPi-IIa and NaPi-IIc transport proteins were also unaffected following duodenal infusion at both 1.3M and 10mM phosphate concentrations (Lee et al., 2017). In other studies, 5/6-nephrectomised rat models of chronic renal failure exhibit increased plasma phosphate and decreased NaPi-IIa expression, whereas no change in phosphate absorption in the duodenum or jejunum, or in the expression of the intestinal NaPi-IIb transporter was observed, regardless of dietary phosphate intake (Marks et al., 2007). These findings may oppose any proposed sensing and signalling in the gastrointestinal tract as the conclusions drawn from this study demonstrate that the adaptive response to dietary phosphate in chronic renal failure was mediated by the kidney, while intestinal phosphate handling was not affected. However, as dietary phosphate intake did not affect intestinal phosphate absorption and NaPi-IIb protein abundance, these findings might also imply that chronic renal failure may have disrupted any signalling from the kidneys to the gastrointestinal tract and so is unable to adapt accordingly.

In the present study, the upregulation observed for renal NHE3 and the associated downregulation for colonic NHE3 with high-fat feeding is consistent with the concept of a feedback mechanism. In addition, the downregulation of renal SGLT2 and ENaC transport proteins in this group are also indicative of intra-renal signalling within the nephron to adapt to increased sodium retention via renal NHE3 and pNCC. This inter- and intra-organ signalling may be mediated by a number of regulators such as insulin, aldosterone and SGK1, which are known to be upregulated in this model and may partially explain for the changes seen for these transport proteins (**Fig.6.1**). Future studies analysing electrolyte transport and transporter expression/activity in conditional knockout models for specific epithelial transporters or FKBP12/calcineurin in either renal or intestinal tissues would clarify any possible signalling between the two organs in response to high-fat

feeding and CNI treatment, and would also allow for further investigations into the potential role of calcineurin in post-transplant metabolic complications.

Alongside increased renal sodium retention and associated changes in intestinal transporter protein expression, high-fat feeding may also exert an effect through alterations in gut microbiota composition, which are known to have a significant impact on blood pressure and inflammation. Previous studies have demonstrated a symbiotic relationship between gut dysbiosis (microbial imbalance) and hypertension (Mell et al., 2015; Yang et al., 2015). Rat models of hypertension typically exhibit significant decreases in microbial richness and were associated with an increased *Firmicutes/Bacteroidetes* ratio, which are the dominant microorganisms in the intestines involved in maintaining intestinal immunity and homeostasis, and are widely considered as the signature of gut dysbiosis (Yang et al., 2015). These findings of gut dysbiosis were also observed in a small cohort of hypertensive patients (Yang et al., 2015), clearly implicating the impact of gut microbiota in the pathophysiology of animal and human hypertension. More recent studies in spontaneously hypertensive rat models have also demonstrated alterations in gut pathology, including increased intestinal permeability, inflammation and microbial dysbiosis, and have proposed this to be associated with dysfunctional central nervous system-intestinal communication, leading to hypertension development (Santisteban et al., 2017).

Several lines of evidence have also shown that gut microbiota composition is altered in obese subjects and responds to changes in body weight and dietary fat, which may contribute to the dysregulation of the host's metabolic functions (Hildebrandt et al., 2009; Turnbaugh et al., 2008). Studies in mice fed on a high-fat diet exhibited gut dysbiosis, characterised by reduced numbers of *Bacteriodetes* and increased numbers of *Firmicutes* (Hildebrandt et al., 2009; Turnbaugh et al., 2008). Additionally, the obesity trait was found

to be transmissible as transplantation of cecal microbiota from obese mice into germ-free recipients significantly increased adiposity compared to transplants of microbiota from lean donors (Turnbaugh et al., 2006, 2008). These alterations were thought to be the result of either the obese status altering gut microbiota or the direct effects of dietary fat. In supporting experiments, mice deficient for RELMβ, a protein involved in intestinal immune function and whose expression is induced by a high-fat diet, remained lean on the high-fat diet and showed similar changes in the microbial communities as wild-type mice, demonstrating that the composition of the gut microbiome was dependent on dietary factors and independent of the obese state (Hildebrandt et al., 2009). Although this strongly implicates a role for altered gut microbiota in promoting diet-induced obesity, the underlying mechanisms are still not well understood.

Gut microbiota homeostasis has also been shown to be regulated by the innate immune system and plays a significant role in the pathogenesis of metabolic syndrome in both clinical and animal models. Mice deficient in toll-like receptor 5 (TLR5), an activator of innate immunity, and fed on a high-fat diet were found to develop metabolic syndrome-related conditions such as obesity, insulin resistance and hyperlipidemia (Vijay-Kumar et al., 2010). Furthermore, colonisation of gut microbiota from TLR5-deficient mice into germ-free recipients conferred features of metabolic syndrome (Vijay-Kumar et al., 2010), showing that these phenotypes are transmissible and that the gut microbiota itself can mediate metabolic syndrome development.

NHE3 has been particularly shown to be crucial for maintaining gut microbiota composition. NHE3 deficiency in mice was associated with alterations in ileum and colonic luminal and mucosal-associated microbiota composition, characterised by an increase in *Bacteroidetes* and a reduction in *Firmicutes* phyla (Engevik et al., 2013). Alongside, loss or inhibition of NHE3 was accompanied with increased sodium and pH in the stools, which

was shown to provide optimal conditions for bacterial growth and expansion in patients with *Clostridium difficile* infection (Engevik et al., 2013, 2015). Additionally, NHE3$^{-/-}$ mice develop colitis (colonic inflammation) which was correlated with increased mucosal T cell and neutrophil influx, as well as increased mucosal cytokine expression and permeability, all of which could be alleviated with broad-spectrum antibiotics (Larmonier et al., 2013; Laubitz et al., 2016). These findings show that NHE3 plays an important role in the regulation of the gut microbiota and that the absence of NHE3 may result in profound changes in colonic microbial ecology contributing to gut dysbiosis and intestinal inflammation.

From the present study, although it is not known whether the downregulation observed for colonic NHE3 in the high-fat diet-fed group had a significant impact on gut microbiota composition, the conclusions drawn from previous studies in NHE3$^{-/-}$ mice highlight potential shifts in the relative abundance of bacterial phyla in the gut microbiota and intestinal permeability in this model. Furthermore, the lack of correlation between plasma electrolytes and the corresponding intestinal transporter expression could in fact be explained by the illustrated effects of high-fat feeding on intestinal permeability and gut microbiota composition. However, this remains to be established, as well as confirmation of intestinal inflammation. Comparisons to CNI-treated mouse intestinal segments would also be required to determine whether CNI use by transplant patients alters gut pathology and microbiome, and contributes to hypertension and metabolic syndrome development following transplantation.

6.5 The impact of SGLT-mediated sodium transport on cell swelling and blood pressure

As previously mentioned, PTDM and insulin resistance are a common occurrence following transplantation. These conditions are associated with CNI use and are hallmarks of metabolic syndrome. In diabetes, renal SGLT2

is upregulated, contributing to increased glucose reabsorption and hyperglycemia (Rahmoune et al., 2005). As described in earlier chapters, the SGLT2 and SGLT1 cotransporters are expressed in the proximal tubule, where SGLT2 reabsorbs approximately 97% of filtered glucose and SGLT1 reabsorbs the remaining 3% (Turner and Moran, 1982; Vallon et al., 2011). Studies in knockout mouse models and mutation analyses in humans have reported SGLT2 as the main mediator of renal glucose reabsorption and contributor for hyperglycemia and diabetes (Santer et al., 2003; Vallon et al., 2011, 2013). In a study by Rahmoune *et al*, analyses in patients with type II diabetes revealed a three-fold increase in renal glucose uptake compared with controls (Rahmoune et al., 2005). This study also reported a significant increase in SGLT2 and GLUT2 mRNA and protein expression in these diabetic patients (Rahmoune et al., 2005), consistent with the important role for SGLT2 in renal glucose reabsorption.

SGLT2 inhibitors, such as dapagliflozin, canagliflozin and empagliflozin, are administered as treatment for type II diabetes, which act by aiding urinary glucose excretion. Numerous clinical trials in diabetic patients treated with SGLT2 inhibitors have demonstrated its benefits in increasing glycosuria and improvements in fasting plasma glucose levels (Bolinder et al., 2012; Chilton et al., 2015; Kawasoe et al., 2017; Stenlof et al., 2013; Vasilakou et al., 2013). Clinical studies have also reported a blood pressure lowering effect with SGLT2 inhibitor treatment, along with a reduction in body weight. Meta-analysis of a number of controlled studies in type II diabetic patients receiving SGLT2 inhibitors, compared with those receiving placebo or other anti-hyperglycemic agents, reported a mean reduction in SBP by 3.77-4.45 mmHg and in body weight by around 1.74-1.80 kg (Vasilakou et al., 2013). In addition, a number of studies in patients with type II diabetes randomised to either a placebo or an SGLT2 inhibitor for a period of 12-76 weeks, showed that the groups treated with the SGLT2 inhibitor were associated with significant reductions in SBP, DBP, mean body weight, waist circumference

and fat mass compared to the placebo groups (Baker et al., 2014; Blonde et al., 2016; Bolinder et al., 2012; Chilton et al., 2015; Kohan et al., 2014; Roden et al., 2013; Stenlof et al., 2013).

Taken together, these studies suggest that SGLT2 inhibitors may confer advantageous effects on blood pressure and body weight in patients with type II diabetes. However, the precise mechanisms underlying the blood pressure lowering effects remains under investigation. Studies have proposed that these effects are based on an osmotic or natriuretic effect (Baker et al., 2014; Kawasoe et al., 2017). In a study by Kawaksoe *et al*, treatment with SGLT2 inhibitors in obese patients with type II diabetes showed a significant decrease in SBP after two weeks, which was correlated with increased urinary glucose excretion but not urinary sodium excretion (Kawasoe et al., 2017). However, at 6 months after administration with SGLT2 inhibitors, the reverse was observed, the decrease in SBP was significantly correlated with urinary sodium excretion, suggesting that the long-term blood pressure-lowering effects of SGLT2 inhibitors may be explained by plasma volume reduction due to natriuresis (Kawasoe et al., 2017).

Overall, evidence from a number of studies in diabetic patients highlight the beneficial reductions in body weight and blood pressure with SGLT2 inhibitor treatment. Although these inhibitors would prove to be advantageous in plasma glucose control and lower the risk for hypertension particularly in PTDM patients, studies examining the effects of SGLT2 inhibition following transplantation are lacking. The data from these studies also imply that an increase in the accompanied sodium reabsorbed by the SGLT2 transporter can also contribute to increases in blood pressure in these diabetic patients. However, in the context of the present study, despite indications of hyperglycemia, significant reductions in renal SGLT2 and intestinal SGLT1 proteins in mice fed on the high-fat diet was observed, regardless of CNI

treatment. Although the reasons for this are not clear, without confirmation of the effects of high-fat feeding on SGLT transporter activity, conclusions on the relative contribution of these transport proteins to rises in blood pressure in these mice cannot be drawn.

6.6 Conclusions and future perspectives

In conclusion, the experiments described in this thesis provides evidence that the CNI-mediated effects on blood pressure are likely to occur solely through the overactivation of NCC in the DCT and that, in the presence of increased sodium transport, the kidneys respond by downregulating major sodium transporters in the other nephron segments. In addition, data obtained from protein and biochemical analyses in a model of diet-induced metabolic syndrome demonstrates that, following renal transplantation, high dietary fat intake is the main risk factor for the development of metabolic syndrome-associated conditions, not CNI administration alone. A significant reduction in renal SGLT2 and intestinal SGLT1 transport proteins in this model, most likely in response to elevated plasma glucose levels, are also consistent with previous proposals of a gastrointestinal-renal signalling axis for sodium. This feedback mechanism may also be the case for NHE3, however, this requires further investigations.

As described, increased sodium uptake affects a number of systems as well as blood pressure homeostasis, including the composition of gut microbiota and the regulation of the immune system (summarised in **Fig.6.2**). The interplay of these systems was not investigated in the present studies, however, future investigations particularly into alterations in intestinal permeability and pathology may provide explanations for the plasma biochemistry data obtained in the model of metabolic syndrome used, especially for phosphate. Analyses for electrolyte transport and transporter activity following CNI-treatment and in diet-induced metabolic syndrome may

warrant additional kinetic and functional studies in renal and intestinal BBMVs to clarify the changes, or absence of changes, for the individual transporters observed at a translational level. Furthermore, confirmation for the involvement and impact of the insulin-PI3K-SGK1 and renin-angiotensin-aldosterone signalling pathways in these models may also explain the data obtained. However, this would also require further investigations into the feedback/feedforward signalling pathways between the gastrointestinal tract and kidneys involved in the downregulation of renal ENaC, SGLT2, and intestinal SGLT1 proteins, which are in contrast to the regulatory effects by SGK1 and aldosterone.

The conclusion drawn from these findings, along with supporting evidence from previous studies, suggests that the implementation of a treatment regimen which includes strict management of dietary fat intake following transplantation and in hypertensive individuals would be advantageous for blood pressure, glucose and lipid control, and would greatly reduce the risk of cardiovascular and renal disease.

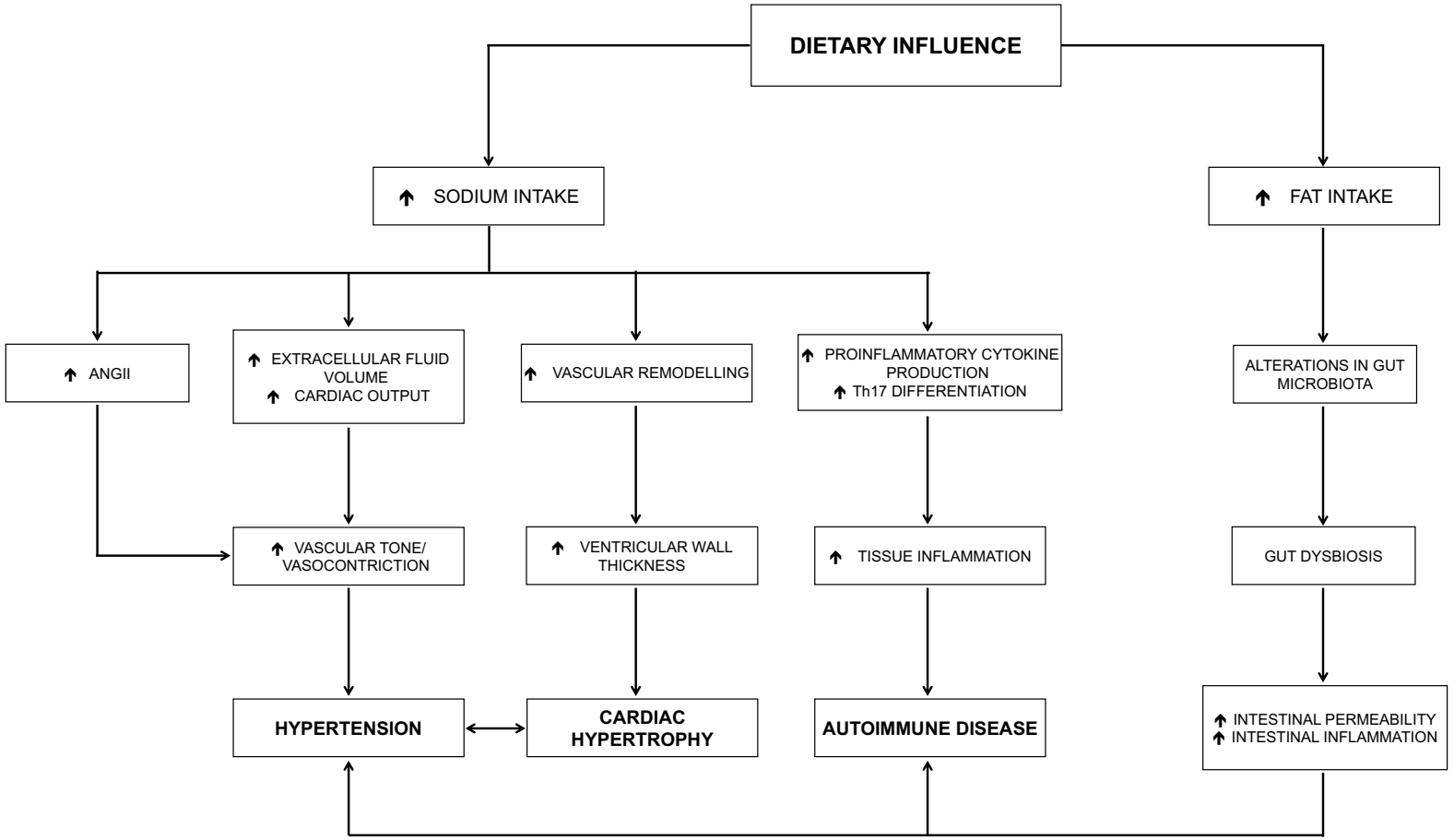

Figure 6.2. Summary of the pathways regulated by dietary sodium and fat intake. Pathways influenced by increased dietary sodium and fat intake including the regulation of blood pressure, gut microbiota composition and the immune system.

Appendix I

Country	Year of Data Collection	Age Range	Gender	Sample Size	Prevalence (%)	Awareness (%)	Treatment (%)	Control (%)	Reference
United States	1989 - 1990	35 - 64	Male	450	30	56	17	44	(Antikainen et al., 2006)
			Female	567	21	61	34	52	
	2004 - 2005	40 - 75>	Male	220	57	85	80	38	(Dickson et al., 2006)
			Female	472	59	77	75	39	
	2007 - 2010	20 - 79	Male	5033	29.4	77.7	69.1	48.7	(Joffres et al., 2013)
			Female	4970	28.8	84.6	79.1	57	
Canada	1986 - 1992	18 - 74	Male	11,376	26	53	32	40.6	(Joffres et al., 1997)
			Female	11,753	18	65	49	40.8	
	1995	35 - 64	Male	259	31	57	34	33	(Antikainen et al., 2006)
			Female	268	26	69	34	40	

	2007 - 2009	20 - 79	Male	1649	19.7	80.4	76.5	66.8	(Joffres et al., 2013)
			Female	1836	19.3	86.5	83.3	64.9	
Germany	1991 - 1992	35 - 64	Male	394	40	49	28	16	(Antikainen et al., 2006)
			Female	432	32	62	48	43	
	1994 - 1995	35 - 64	Male	819	46	52	21	12	(Antikainen et al., 2006)
			Female	872	34	59	31	32	
	1997 - 2001	24 – 74 (1 of 2)	Male	1823	60.1	57.6	34.6	24.3	(Meisinger et al., 2006)
			Female	1921	38.5	71.3	50.9	40.9	
	1997 - 2001	24 – 74 (2 of 2)	Male	2073	41.4	55	28.2	36.2	(Meisinger et al., 2006)
			Female	2151	28.6	73.6	51.3	48.1	
Italy	1993 - 1994	35 – 64	Male	651	41	38	24	45	(Antikainen et al., 2006)
			Female	666	31	43	31	14	

	1994	35 - 64	Male	685	54	45	13	13	(Antikainen et al., 2006)
			Female	689	41	48	25	31	
	1998	35 - 64	Male	8233	44.8	46.4	26.7	22.5	(Wolf-Maier et al., 2003, 2004)
			Female		30.6	57.2	37.3	32.9	
Spain	1994 - 1996	35 - 64	Male	1398	19	62	31	67	(Antikainen et al., 2006)
			Female	1211	20	83	49	48	
	2004	>18	Male	1336	31.1	42.4	65.9	34.9	(Perez-Fernandez et al., 2007)
			Female	1548	20.7	61.3	77.6	37.5	
India	1999 - 2000	40 - 60	Male	163	56.3	33.7	22.8	38.1	(Zachariah et al., 2003)
			Female	151	52.3	44.3	35.4	25	
	2001 - 2002	>30	Male	1441	33.2	22.8	22.4	15.9	(Hazarika et al., 2004)
			Female	1739	33.4	20.7	20.5	20.2	

	2001 - 2004	20 - 65>	Male	1096	23.2	36.9	28	47	(Mohan et al., 2007; Pereira et al., 2009)
			Female	1254	17.2	26.2	16.8	44.2	
China	1993	35 - 64	Male	480	38	49	19	14	(Antikainen et al., 2006)
			Female	643	36	63	31	21	
	1992 - 1994	35 - 59	Male	8840	24.1	34.9	23.3	11.8	(Wang et al., 2004)
			Female	9906	21.5	39.8	31.4	13.3	
	1999	>35	Male	4640	51.2	77	69	28	(Li et al., 2003)
			Female	5063	42.2	78	70	38	
	2000 - 2001	35 - 74	Male	7684	28.6	39.5	23.5	26.1	(Gu et al., 2002)
			Female	8154	25.8	50.8	33.8	31	

Table A.1. Summary of the prevalence, awareness, treatment and control of hypertension in worldwide studies. Hypertension prevalence rates were recorded according to the international definition of hypertension. Control rates show the proportion of control among treated hypertensive patients.

References

Abate, N., Chandalia, M., Cabo-Chan, A.V., Moe, O.W., and Sakhaee, K. (2004). The metabolic syndrome and uric acid nephrolithiasis: Novel features of renal manifestation of insulin resistance. Kidney Int. *65*, 386–392.

Adachi, M., Asakura, Y., Muroya, K., Tajima, T., Fujieda, K., Kuribayashi, E., and Uchida, S. (2010). Increased Na reabsorption via the Na–Cl cotransporter in autosomal recessive pseudohypoaldosteronism. Clin. Exp. Nephrol. *14*, 228–232.

Adu, D., Michael, J., Turney, J., and McMaster, P. (1983). Hyperkalaemia in cyclosporin-treated renal allograft recipients. The Lancet *322*, 370–372.

Affleck, J.A., Helliwell, P.A., and Kellett, G.L. (2003). Immunocytochemical Detection of GLUT2 at the Rat Intestinal Brush-border Membrane. J. Histochem. Cytochem. *51*, 1567–1574.

Ahmed, M., Salker, M.S., Elvira, B., Umbach, A.T., Fakhri, H., Saeed, A.M., Shumilina, E., Hosseinzadeh, Z., and Lang, F. (2015). SPAK Sensitive Regulation of the Epithelial Na^+ Channel ENaC. Kidney Blood Press. Res. *40*, 335–343.

Aime, P., Palouzier-Paulignan, B., Salem, R., Al Koborssy, D., Garcia, S., Duchamp, C., Romestaing, C., and Julliard, A.K. (2014). Modulation of olfactory sensitivity and glucose-sensing by the feeding state in obese Zucker rats. Front. Behav. Neurosci. *8*.

Akalin, E., Ganeshan, S.V., Winston, J., and Muntner, P. (2008). Hyperuricemia is Associated With the Development of the Composite Outcomes of New Cardiovascular Events and Chronic Allograft Nephropathy: Transplantation *86*, 652–658.

Akar, F., Skinner, E., Klein, J.D., Jena, M., Paul, R.J., and O'Neill, W.C. (1999). Vasoconstrictors and nitrovasodilators reciprocally regulate the Na+-K+-2Cl- cotransporter in rat aorta. Am. J. Physiol.-Cell Physiol. *45*, C1383–C1390.

Akar, F., Jiang, G., Paul, R.J., and O'Neill, W.C. (2001). Contractile regulation of the Na+-K+-2Cl- cotransporter in vascular smooth muscle. Am. J. Physiol.-Cell Physiol. *50*, C579–C584.

Alvarez, M.L., Khosroheidari, M., Ravi, R.K., and DiStefano, J.K. (2012). Comparison of protein, microRNA, and mRNA yields using different methods of urinary exosome isolation for the discovery of kidney disease biomarkers. Kidney Int. *82*, 1024–1032.

Ambuhl, P.M., Amemiya, M., Danczkay, M., Lotscher, M., Kaissling, B., Moe, O.W., Preisig, P.A., and Alpern, R.J. (1996). Chronic metabolic acidosis increases NHE3 protein abundance in rat kidney. Am. J. Physiol.-Ren. Physiol. *271*, F917–F925.

Ambühl, P.M., Zajicek, H.K., Wang, H., Puttaparthi, K., and Levi, M. (1998). Regulation of renal phosphate transport by acute and chronic metabolic acidosis in the rat. Kidney Int. *53*, 1288–1298.

Ambühl, P.M., Meier, D., Wolf, B., Dydak, U., Boesiger, P., and Binswanger, U. (1999). Metabolic aspects of phosphate replacement therapy for hypophosphatemia after renal transplantation: Impact on muscular phosphate content, mineral metabolism, and acid/base homeostasis. Am. J. Kidney Dis. *34*, 875–883.

Amemiya, M., Yamaji, Y., Cano, A., Moe, O.W., and Alpern, R.J. (1995). Acid incubation increases NHE-3 mRNA abundance in OKP cells. Am. J. Physiol.-Cell Physiol. *269*, C126–C133.

Andoh, T.F., Burdmann, E.A., Fransechini, N., Houghton, D.C., and Bennett, W.M. (1996). Comparison of acute rapamycin nephrotoxicity with cyclosporine and FK506. Kidney Int. *50*, 1110–1117.

Anselmo, A.N., Earnest, S., Chen, W., Juang, Y.-C., Kim, S.C., Zhao, Y., and Cobb, M.H. (2006). WNK1 and OSR1 regulate the Na+, K+, 2Cl- cotransporter in HeLa cells. Proc. Natl. Acad. Sci. *103*, 10883–10888.

Antikainen, R., Moltchanov, V., Chukwuma Sr, C., Kuulasmaa, K., Marques-Vidal, P., Sans, S., Wilhelmsen, L., Tuomilehto, J., and The WHO MONICA Project (2006). Trends in the prevalence, awareness, treatment and control of hypertension: the WHO MONICA Project. Eur. J. Cardiovasc. Prev. Rehabil. *13*, 13–29.

Apanay, D.C., Neylan, J.F., Ragab, M.S., and Sgoutas, D.S. (1994). Cyclosporine increases the oxidizability of low-density lipoproteins in renal transplant recipients. Transplantation *58*, 663–669.

Araki, M., Flechner, S.M., Ismail, H.R., Flechner, L.M., Zhou, L., Derweesh, I.H., Goldfarb, D., Modlin, C., Novick, A.C., and Faiman, C. (2006). Posttransplant Diabetes Mellitus in Kidney Transplant Recipients Receiving Calcineurin or mTOR Inhibitor Drugs: Transplantation *81*, 335–341.

Armstrong, K.A., Johnson, D.W., Campbell, S.B., Isbel, N.M., and Hawley, C.M. (2005). Does Uric Acid Have a Pathogenetic Role in Graft Dysfunction and Hypertension in Renal Transplant Recipients?: Transplantation *80*, 1565–1571.

Arroyo, J.P., Lagnaz, D., Ronzaud, C., Vazquez, N., Ko, B.S., Moddes, L., Ruffieux-Daidie, D., Hausel, P., Koesters, R., Yang, B., et al. (2011). Nedd4-2 Modulates Renal Na+-Cl- Cotransporter via the Aldosterone-SGK1-Nedd4-2 Pathway. J. Am. Soc. Nephrol. *22*, 1707–1719.

Artz, M.A., Boots, J.M.M., Ligtenberg, G., Roodnat, J.I., Christiaans, M.H.L., Vos, P.F., Blom, H.J., Sweep, F.C.G.J., Demacker, P.N.M., and Hilbrands, L.B. (2003). Improved Cardiovascular Risk Profile and Renal Function in Renal Transplant Patients after Randomized Conversion from Cyclosporine to Tacrolimus. J. Am. Soc. Nephrol. *14*, 1880–1888.

Avdonin, P.V., Cottet-Maire, F., Afanasjeva, G.V., Loktionova, S.A., Lhote, P., and Ruegg, U.T. (1999). Cyclosporine A up-regulates angiotensin II receptors and calcium responses in human vascular smooth muscle cells. Kidney Int. *55*, 2407–2414.

Bachmann, S., Koeppen-Hagemann, L., and Kriz, W. (1985). Ultrastructural localization of Tamm-Horsfall glycoprotein (THP) in rat kidney as revealed by protein A-gold immunocytochemistry. Histochemistry *83*, 531–538.

Bachmann, S., Metzger, R., and Bunnemann, B. (1990). Tamm-Horsfall protein-mRNA synthesis is localized to the thick ascending limb of Henle's loop in rat kidney. Histochemistry *94*, 517–523.

Bachmann, S., Mutig, K., Bates, J., Welker, P., Geist, B., Gross, V., Luft, F.C., Alenina, N., Bader, M., Thiele, B.J., et al. (2005). Renal effects of Tamm-Horsfall protein (uromodulin) deficiency in mice. AJP Ren. Physiol. *288*, F559–F567.

Bachmanov, A.A., Reed, D.R., Beauchamp, G.K., and Tordoff, M.G. (2002). Food intake, water intake, and drinking spout side preference of 28 mouse strains. Behav. Genet. *32*, 435–443.

Baid-Agrawal, S., Delmonico, F.L., Tolkoff-Rubin, N.E., Farrell, M., Williams, W.W., Shih, V., Auchincloss, H., Cosimi, A.B., and Pascual, M. (2004). CARDIOVASCULAR RISK PROFILE AFTER CONVERSION FROM CYCLOSPORINE A TO TACROLIMUS IN STABLE RENAL TRANSPLANT RECIPIENTS: Transplantation *77*, 1199–1202.

Bakar, F., Keven, K., Dogru, B., Aktan, F., Erturk, S., Tuzuner, A., Erbay, B., and Nebioglu, S. (2009). Low-Density Lipoprotein Oxidizability and the Alteration of Its Fatty Acid Content in Renal Transplant Recipients Treated With Cyclosporine/Tacrolimus. Transplant. Proc. *41*, 1630–1633.

Baker, W.L., Smyth, L.R., Riche, D.M., Bourret, E.M., Chamberlin, K.W., and White, W.B. (2014). Effects of sodium-glucose co-transporter 2 inhibitors on blood pressure: A systematic review and meta-analysis. J. Am. Soc. Hypertens. *8*, 262–275.e9.

Bates, J.M., Raffi, H.M., Prasadan, K., Mascarenhas, R., Laszik, Z., Maeda, N., Hultgren, S.J., and Kumar, S. (2004). Tamm-Horsfall protein knockout mice are more prone to urinary tract infection. Kidney Int. *65*, 791–797.

Beals, C.R., Clipstone, N.A., Ho, S.N., and Crabtree, G.R. (1997). Nuclear localization of NF-ATc by a calcineurin-dependent, cyclosporin-sensitive intramolecular interaction. Genes Dev. *11*, 824–834.

Beck, L., Karaplis, A.C., Amizuka, N., Hewson, S.A., Ozawa, H., and Tenenhouse, H.S. (1998). Targeted inactivation of Npt2 in mice leads to severe renal phosphate wasting, hypercalciuria, and skeletal abnormalities. Proc. Natl. Acad. Sci. U. S. A. *95*, 5372–5377.

Bergaya, S., Faure, S., Baudrie, V., Rio, M., Escoubet, B., Bonnin, P., Henrion, D., Loirand, G., Achard, J.-M., Jeunemaitre, X., et al. (2011). WNK1 Regulates Vasoconstriction and Blood Pressure Response to 1-Adrenergic Stimulation in Mice. Hypertension *58*, 439–445.

Bergwitz, C., Roslin, N.M., Tieder, M., Loredo-Osti, J.C., Bastepe, M., Abu-Zahra, H., Frappier, D., Burkett, K., Carpenter, T.O., and Anderson, D. (2006). SLC34A3 mutations in patients with hereditary hypophosphatemic rickets with hypercalciuria predict a key role for the sodium-phosphate cotransporter NaP i-IIc in maintaining phosphate homeostasis. Am. J. Hum. Genet. *78*, 179–192.

Berndt, T., Thomas, L.F., Craig, T.A., Sommer, S., Li, X., Bergstralh, E.J., and Kumar, R. (2007). Evidence for a signaling axis by which intestinal phosphate rapidly modulates renal phosphate reabsorption. Proc. Natl. Acad. Sci. *104*, 11085–11090.

Bhan, I., Shah, A., Holmes, J., Isakova, T., Gutierrez, O., Burnett, S.-A., Juppner, H., and Wolf, M. (2006). Post-transplant hypophosphatemia: Tertiary “Hyper-Phosphatoninism”? Kidney Int. *70*, 1486–1494.

Bianchi, G., Fox, U., Di Francesco, G.F., Giovanetti, A.M., and Pagetti, D. (1974). Blood pressure changes produced by kidney cross-transplantation between spontaneously hypertensive rats and normotensive rats. Clin. Sci. *47*, 435–448.

Biber, J., Stieger, B., Haase, W., and Murer, H. (1981). A high yield preparation for rat kidney brush border membranes different behaviour of lysosomal markers. Biochim. Biophys. Acta BBA-Biomembr. *647*, 169–176.

Bickel, C.A., Verbalis, J.G., Knepper, M.A., and Ecelbarger, C.A. (2001). Increased renal Na-K-ATPase, NCC, and B-ENaC abundance in obese Zucker rats. Am. J. Physiol.-Ren. Physiol. *281*, F639-48.

Bickel, C.A., Knepper, M.A., Verbalis, J.G., and Ecelbarger, C.A. (2002). Dysregulation of renal salt and water transport proteins in diabetic Zucker

rats. Kidney Int. *61*, 2099–2110.

Bielesz, B., Bacic, D., Honegger, K., Biber, J., Murer, H., and Wagner, C.A. (2006). Unchanged expression of the sodium-dependent phosphate cotransporter NaPi-IIa despite diurnal changes in renal phosphate excretion. Pflüg. Arch. - Eur. J. Physiol. *452*, 683–689.

Binger, K.J., Gebhardt, M., Heinig, M., Rintisch, C., Schroeder, A., Neuhofer, W., Hilgers, K., Manzel, A., Schwartz, C., Kleinewietfeld, M., et al. (2015). High salt reduces the activation of IL-4– and IL-13–stimulated macrophages. J. Clin. Invest. *125*, 4223–4238.

Black, B.L., Croom, J., Eisen, E.J., Petro, A.E., Edwards, C.L., and Surwit, R.S. (1998). Differential effects of fat and sucrose on body composition in A J and C57BL/6 mice. Metabolism *47*, 1354–1359.

Blank, M.E., Bode, F., Huland, E., Diedrich, D.F., and Baumann, K. (1985). Kinetic studies of D-glucose transport in renal brush-border membrane vesicles of streptozotocin-induced diabetic rats. Biochim. Biophys. Acta *844*, 314–319.

Blankenstein, K.I., Borschewski, A., Labes, R., Paliege, A., Boldt, C., McCormick, J.A., Ellison, D.H., Bader, M., Bachmann, S., and Mutig, K. (2017). Calcineurin inhibitor cyclosporine A activates renal Na-K-Cl cotransporters via local and systemic mechanisms. Am. J. Physiol. - Ren. Physiol. *312*, F489–F501.

Blazer-Yost, B.L., Liu, X., and Helman, S.I. (1998). Hormonal regulation of ENaCs: insulin and aldosterone. Am. J. Physiol.-Cell Physiol. *274*, C1373–C1379.

Bleich, M., Schlatter, E., and Greger, R. (1990). The luminal K+ channel of the thick ascending limb of Henle's loop. Pflüg. Arch. *415*, 449–460.

Blonde, L., Stenlöf, K., Fung, A., Xie, J., Canovatchel, W., and Meininger, G. (2016). Effects of canagliflozin on body weight and body composition in patients with type 2 diabetes over 104 weeks. Postgrad. Med. *128*, 371–380.

Bobulescu, I.A., Dubree, M., Zhang, J., McLeroy, P., and Moe, O.W. (2008). Effect of renal lipid accumulation on proximal tubule Na+/H+ exchange and ammonium secretion. AJP Ren. Physiol. *294*, F1315–F1322.

Bochud, M., Nussberger, J., Bovet, P., Maillard, M.R., Elston, R.C., Paccaud, F., Shamlaye, C., and Burnier, M. (2006). Plasma Aldosterone Is Independently Associated With the Metabolic Syndrome. Hypertension *48*, 239–245.

Bolinder, J., Ljunggren, Ö., Kullberg, J., Johansson, L., Wilding, J., Langkilde, A.M., Sugg, J., and Parikh, S. (2012). Effects of Dapagliflozin on

Body Weight, Total Fat Mass, and Regional Adipose Tissue Distribution in Patients with Type 2 Diabetes Mellitus with Inadequate Glycemic Control on Metformin. J. Clin. Endocrinol. Metab. *97*, 1020–1031.

Bonsnes, R.W., and Taussky, H.H. (1945). On the colorimetric determination of creatinine by the Jaffe reaction. J. Biol. Chem. *158*, 581–591.

Bookstein, C., DePaoli, A.M., Xie, Y., Niu, P., Musch, M.W., Rao, M.C., and Chang, E.B. (1994). Na+/H+ exchangers, NHE-1 and NHE-3, of rat intestine. Expression and localization. J. Clin. Invest. *93*, 106.

Boots, J.M.M., Van Duijnhoven, E.M., Christiaans, M.H.L., Wolffenbuttel, B.H.R., and Van Hooff, J.P. (2002). Glucose Metabolism in Renal Transplant Recipients on Tacrolimus: The Effect of Steroid Withdrawal and Tacrolimus Trough Level Reduction. J. Am. Soc. Nephrol. *13*, 221–227.

Borel, J.F. (1976). Comparative study of in vitro and in vivo drug effects on cell-mediated cytotoxicity. Immunology *31*, 631.

Borel, Jf. al, Feurer, C., Gubler, H.U., and Stähelin, H. (1994). Biological effects of cyclosporin A: a new antilymphocytic agent. Inflamm. Res. *43*, 179–186.

Boron, W.F., and Boulpaep, E.L. (1983a). Intracellular pH regulation in the renal proximal tubule of the salamander. Basolateral HCO3-transport. J. Gen. Physiol. *81*, 53–94.

Boron, W.F., and Boulpaep, E.L. (1983b). Intracellular pH regulation in the renal proximal tubule of the salamander. Na-H exchange. J. Gen. Physiol. *81*, 29–52.

Borschewski, A., Himmerkus, N., Boldt, C., Blankenstein, K.I., McCormick, J.A., Lazelle, R., Willnow, T.E., Jankowski, V., Plain, A., Bleich, M., et al. (2016). Calcineurin and Sorting-Related Receptor with A-Type Repeats Interact to Regulate the Renal Na+-K+-2Cl- Cotransporter. J. Am. Soc. Nephrol. *27*, 107–119.

Boudreaux, J.P., McHugh, L., Canafax, D.M., Ascher, N., Sutherland, D.E.R., Payne, W., Simmons, R.L., Najarian, J.S., and Fryd, D.S. (1987). The impact of cyclosporine and combination immunosuppression on the incidence of posttransplant diabetes in renal allograft recipients. Transplantation *44*, 376–381.

Boyden, L.M., Choi, M., Choate, K.A., Nelson-Williams, C.J., Farhi, A., Toka, H.R., Tikhonova, I.R., Bjornson, R., Mane, S.M., Colussi, G., et al. (2012). Mutations in kelch-like 3 and cullin 3 cause hypertension and electrolyte abnormalities. Nature *482*, 98–102.

Bradford, M.M. (1976). A rapid and sensitive method for the quantitation of

microgram quantities of protein utilizing the principle of protein-dye binding. Anal. Biochem. *72*, 248–254.

Brinton, E.A., Eisenberg, S., and Breslow, J.L. (1990). A low-fat diet decreases high density lipoprotein (HDL) cholesterol levels by decreasing HDL apolipoprotein transport rates. J. Clin. Invest. *85*, 144–151.

Buhl, E.S., Jessen, N., Pold, R., Ledet, T., Flyvbjerg, A., Pedersen, S.B., Pedersen, O., Schmitz, O., and Lund, S. (2002). Long-Term AICAR Administration Reduces Metabolic Disturbances and Lowers Blood Pressure in Rats Displaying Features of the Insulin Resistance Syndrome. Diabetes *51*, 2199–2206.

Bunchman, T.E., and Brookshire, C.A. (1991). Cyclosporine-induced synthesis of endothelon by cultured human endothelial cells. J. Clin. Invest. *88*, 310–314.

Burnier, M., Biollaz, J., Magnin, J.L., Bidlingmeyer, M., and Brunner, H.R. (1993). Renal sodium handling in patients with untreated hypertension and white coat hypertension. Hypertension *23*, 496–502.

Cai, H., Cebotaru, V., Wang, Y.-H., Zhang, X.-M., Cebotaru, L., Guggino, S., and Guggino, W. (2006). WNK4 kinase regulates surface expression of the human sodium chloride cotransporter in mammalian cells. Kidney Int. *69*, 2162–2170.

du Cailar, G., Ribstein, J., Grolleau, R., and Mimran, A. (1989). Influence of sodium intake on left ventricular structure in untreated essential hypertensives. J. Hypertens. *7*, S258–S259.

Calado, J., Soto, K., Clemente, C., Correia, P., and Rueff, J. (2004). Novel compound heterozygous mutations in SLC5A2 are responsible for autosomal recessive renal glucosuria. Hum. Genet. *114*, 314–316.

Cameron, M.A., Maalouf, N.M., Adams-Huet, B., Moe, O.W., and Sakhaee, K. (2006). Urine Composition in Type 2 Diabetes: Predisposition to Uric Acid Nephrolithiasis. J. Am. Soc. Nephrol. *17*, 1422–1428.

Campistol, J.M., Romero, R., Paul, J., and Gutierrez-Dalmau, A. (2004). Epidemiology of arterial hypertension in renal transplant patients: changes over the last decade. Nephrol. Dial. Transplant. *19*, iii62-iii66.

Canessa, C., Schild, L., Buell, G., Thorens, B., Gautschi, I., Horisberger, J.-D., and Rossier, B.C. (1994). Amiloride-sensitive epithelial Na+ channel is made of three homologous subunits. Nature *367*, 463–467.

Capasso, G., Unwin, R., Agulian, S., and Giebisch, G. (1991). Bicarbonate transport along the loop of Henle. I. Microperfusion studies of load and inhibitor sensitivity. J. Clin. Invest. *88*, 430.

Carey, R. (1978). Evidence for a Splanchnic Sodium Input Monitor Regulating Renal Sodium Excretion in Man. Lack of Dependence upon Aldosterone. Circ. Res. *43*, 19–23.

Carrithers, S.L., Jackson, B.A., Cai, W.Y., Greenberg, R.N., and Ott, C.E. (2002). Site-specific effects of dietary salt intake on guanylin and uroguanylin mRNA expression in rat intestine. Regul. Pept. *107*, 87–95.

Cartier, R., Dagenais, F., Hollmann, C., Cambron, H., and Buluran, J. (1994). Chronic exposure to cyclosporine affects endothelial and smooth muscle reactivity in the rat aorta. Ann. Thorac. Surg. *58*, 789–794.

Castaneda-Bueno, M., Cervantes-Perez, L.G., Vazquez, N., Uribe, N., Kantesaria, S., Morla, L., Bobadilla, N.A., Doucet, A., Alessi, D.R., and Gamba, G. (2012). Activation of the renal Na+:Cl− cotransporter by angiotensin II is a WNK4-dependent process. Proc. Natl. Acad. Sci. *109*, 7929–7934.

Cauduro, R.L., Costa, C., Lhulier, F., Garcia, R.G., Cabral, R.D., Goncalves, L.F., and Manfro, R.C. (2005). Endothelin-1 plasma levels and hypertension in cyclosporine-treated renal transplant patients. Clin. Transplant. *19*, 470–474.

Cavarape, A., Endlich, K., Feletto, F., Parekh, N., Bartoli, E., and Steinhausen, M. (1998). Contribution of endothelin receptors in renal microvessels in acute cyclosporine-mediated vasoconstriction in rats. Kidney Int. *53*, 963–969.

Chang, S.S., Gründer, S., Hanukoglu, A., Rosler, A., Matthew, P.M., Hanukoglu, I., Schild, L., Lu, Y., Shimkets, R.A., Nelson-Williams, C., et al. (1996). Mutations in subunits of the epithelial sodium channel cause salt wasting with hyperkalaemic acidosis, pseudohypoaldosteronism type 1. Nat. Genet. *12*, 248–253.

Channavajjhala, S.K., Rossato, M., Morandini, F., Castagna, A., Pizzolo, F., Bazzoni, F., and Olivieri, O. (2014). Optimizing the purification and analysis of miRNAs from urinary exosomes. Clin. Chem. Lab. Med. *52*.

Chapman, J.R., Marcen, R., Arias, M., Raine, A.E.G., Dunnill, M.S., and Morris, P.J. (1987). Hypertension after renal transplantation. A comparison of cyclosporine and conventional immunosuppression. Transplantation *43*, 860–864.

Chávez-Canales, M., Arroyo, J.P., Ko, B., Vázquez, N., Bautista, R., Castañeda-Bueno, M., Bobadilla, N.A., Hoover, R.S., and Gamba, G. (2013). Insulin increases the functional activity of the renal NaCl cotransporter: J. Hypertens. 1.

Chen, S.-Y., Bhargava, A., Mastroberardino, L., Meijer, O.C., Wang, J.,

Buse, P., Firestone, G.L., Verrey, F., and Pearce, D. (1999). Epithelial sodium channel regulated by aldosterone-induced protein sgk. Proc. Natl. Acad. Sci. U. S. A. *96*, 2514–2519.

Cheruvanky, A., Zhou, H., Pisitkun, T., Kopp, J.B., Knepper, M.A., Yuen, P.S.T., and Star, R.A. (2007). Rapid isolation of urinary exosomal biomarkers using a nanomembrane ultrafiltration concentrator. AJP Ren. Physiol. *292*, F1657–F1661.

du Cheyron, D., Daubin, C., Poggioli, J., Ramakers, M., Houillier, P., Charbonneau, P., and Paillard, M. (2003). Urinary measurement of Na+/H+ exchanger isoform 3 (NHE3) protein as new marker of tubule injury in critically ill patients with ARF. Am. J. Kidney Dis. *42*, 497–506.

Chichger, H., Cleasby, M.E., Srai, S.K., Unwin, R.J., Debnam, E.S., and Marks, J. (2016). Experimental type II diabetes and related models of impaired glucose metabolism differentially regulate glucose transporters at the proximal tubule brush border membrane: GLUT2, SGLT1 and SGLT2 in diabetes-related disease. Exp. Physiol. *101*, 731–742.

Chiga, M., Rai, T., Yang, S.-S., Ohta, A., Takizawa, T., Sasaki, S., and Uchida, S. (2008). Dietary salt regulates the phosphorylation of OSR1/ SPAK kinases and the sodium chloride cotransporter through aldosterone. Kidney Int. *74*, 1403–1409.

Chiga, M., Rafiqi, F.H., Alessi, D.R., Sohara, E., Ohta, A., Rai, T., Sasaki, S., and Uchida, S. (2011). Phenotypes of pseudohypoaldosteronism type II caused by the WNK4 D561A missense mutation are dependent on the WNK-OSR1/SPAK kinase cascade. J. Cell Sci. *124*, 1391–1395.

Chilton, R., Tikkanen, I., Cannon, C.P., Crowe, S., Woerle, H.J., Broedl, U.C., and Johansen, O.E. (2015). Effects of empagliflozin on blood pressure and markers of arterial stiffness and vascular resistance in patients with type 2 diabetes. Diabetes Obes. Metab. *17*, 1180–1193.

Chin, E., Zhou, J., and Bondy, C. (1993). Anatomical and developmental patterns of facilitative glucose transporter gene expression in the rat kidney. J. Clin. Invest. *91*, 1810.

Choate, K.A., Kahle, K.T., Wilson, F.H., Nelson-Williams, C., and Lifton, R.P. (2003). WNK1, a kinase mutated in inherited hypertension with hyperkalemia, localizes to diverse Cl--transporting epithelia. Proc. Natl. Acad. Sci. *100*, 663–668.

Chobanian, A.V., Bakris, G.L., Black, H.R., Cushman, W.C., Green, L.A., Izzo, J.L., Jones, D.W., Materson, B.J., Oparil, S., Wright, J.T., et al. (2003). Seventh Report of the Joint National Committee on Prevention, Detection, Evaluation, and Treatment of High Blood Pressure. Hypertension *42*, 1206–

1252.

Chu, P.-Y., Cheng, C.-J., Wu, Y.-C., Fang, Y.-W., Chau, T., Uchida, S., Sasaki, S., Yang, S.-S., and Lin, S.-H. (2013). SPAK Deficiency Corrects Pseudohypoaldosteronism II Caused by WNK4 Mutation. PLoS ONE *8*, e72969.

Clipstone, N.A., and Crabtree, G.R. (1992). Identification of calcineurin as a key signalling enzyme in T-lymphocyte activation. Nature *357*, 695–697.

Coleman, T.G., and Guyton, A.C. (1969). Hypertension Caused by Salt Loading in the Dog. Circ. Res. *25*, 153–160.

Coles, G.A., Jones, G.R., Crosby, D.L., Jones, J.H., and McVeigh, S. (1972). Hypertension following cadaveric renal transplantation. Postgrad. Med. J. *48*, 399–404.

Collins, J.F., and Ghishan, F.K. (1994). Molecular cloning, functional expression, tissue dstribution, and in situ hybridization of the renal sodium phosphate (Na+/Pi) transporter in the control and hypophosphatemic mouse. FASEB J. *8*, 862–868.

Cool, B., Zinker, B., Chiou, W., Kifle, L., Cao, N., Perham, M., Dickinson, R., Adler, A., Gagne, G., Iyengar, R., et al. (2006). Identification and characterization of a small molecule AMPK activator that treats key components of type 2 diabetes and the metabolic syndrome. Cell Metab. *3*, 403–416.

Corbetta, S., Raimondo, F., Tedeschi, S., Syren, M.-L., Rebora, P., Savoia, A., Baldi, L., Bettinelli, A., and Pitto, M. (2015). Urinary exosomes in the diagnosis of Gitelman and Bartter syndromes. Nephrol. Dial. Transplant. *30*, 621–630.

Cosio, F.G., Dillon, J.J., Falkenhain, M.E., Tesi, R.J., Henry, M.L., Elkhammas, E.A., Davies, E.A., Bumgardner, G.L., and Ferguson, R.M. (1995). Racial differences in renal allograft survival: The role of systemic hypertension. Kidney Int. *47*, 1136–1141.

Cosio, F.G., Falkenhain, M.E., Pesavento, T.E., Henry, M.L., Elkhammas, E.A., Davies, E.A., Bumgardner, G.L., and Ferguson, R.M. (1997). Relationships between arterial hypertension and renal allograft survival in African-American patients. Am. J. Kidney Dis. *29*, 419–427.

Cosio, F.G., Pesavento, T.E., Osei, K., Henry, M.L., and Ferguson, R.M. (2001). Post-transplant diabetes mellitus: Increasing incidence in renal allograft recipients transplanted in recent years. Kidney Int. *59*, 732–737.

Cosio, F.G., Pesavento, T.E., Kim, S., Osei, K., Henry, M.L., and Ferguson, R.M. (2002). Patient survival after renal transplantation: IV. Impact of post-

transplant diabetes. Kidney Int. *62*, 1440–1446.

Cosio, F.G., Kudva, Y., Van der Velde, M., Larson, T.S., Textor, S.C., Griffin, M.D., and Stegall, M.D. (2005). New onset hyperglycemia and diabetes are associated with increased cardiovascular risk after kidney transplantation. Kidney Int. *67*, 2415–2421.

Courivaud, C., Kazory, A., Simula-Faivre, D., Chalopin, J.-M., and Ducloux, D. (2007). Metabolic Syndrome and Atherosclerotic Events in Renal Transplant Recipients: Transplantation *83*, 1577–1581.

Crevel, R.W., Friend, J.V., Goodwin, B.F.., and Parish, W.E. (1992). High-fat diets and the immune response of C57 Bl mice. Br. J. Nutr. *67*, 17–26.

Curtis, J., Diethelm, A., Luke, R., Whelchel, J., and Jones, P. (1985b). Benefits of removal of native kidneys in hypertension after renal transplantation. The Lancet *326*, 739–742.

Curtis, J., Dubovsky, E., Whelchel, J., Luke, R., Diethelm, A., and Jones, P. (1986). Cyclosporin in therapeutic doses increases renal allograft vascular resistance. The Lancet *328*, 477–479.

Curtis, J.J., Luke, R.G., Jones, P., Diethelm, A.G., and Whelchel, J.D. (1985a). Hypertension after successful renal transplantation. Am. J. Med. *79*, 193–200.

Curtis, J.J., Luke, R.G., Jones, P., and Diethelm, A.G. (1988). Hypertension in cyclosporine-treated renal transplant recipients is sodium dependent. Am. J. Med. *85*, 134–138.

Custer, M., Lotscher, M., Biber, J., Murer, H., and Kaissling, B. (1994). Expression of Na-P (i) cotransport in rat kidney: localization by RT-PCR and immunohistochemistry. Am. J. Physiol.-Ren. Physiol. *35*, F767–F774.

Dahan, K., Devuyst, O., Smaers, M., Vertommen, D., Loute, G., Poux, J.-M., Viron, B., Jacquot, C., Gagnadoux, M.-F., Chauveau, D., et al. (2003). A Cluster of Mutations in the UMOD Gene Causes Familial Juvenile Hyperuricemic Nephropathy with Abnormal Expression of Uromodulin. J. Am. Soc. Nephrol. *14*, 2883–2893.

Dahl, L.K., and Heine, M. (1975). Primary role of renal homografts in setting chronic blood pressure levels in rats. Circ. Res. *36*, 692–696.

Dahl, L.K., Heine, M., and Thompson, K. (1974). Genetic influence of the kidneys on blood pressure. Circ. Res. *34*, 94–101.

Darman, R.B., and Forbush, B. (2002). A Regulatory Locus of Phosphorylation in the N Terminus of the Na-K-Cl Cotransporter, NKCC1. J. Biol. Chem. *277*, 37542–37550.

Daudon, M., Traxer, O., Conort, P., Lacour, B., and Jungers, P. (2006). Type 2 Diabetes Increases the Risk for Uric Acid Stones. J. Am. Soc. Nephrol. *17*, 2026–2033.

Davies, M.R., Lund, R.J., and Hruska, K.A. (2003). BMP-7 Is an Efficacious Treatment of Vascular Calcification in a Murine Model of Atherosclerosis and Chronic Renal Failure. J. Am. Soc. Nephrol. *14*, 1559–1567.

Davies, M.R., Lund, R.J., Mathew, S., and Hruska, K.A. (2005). Low Turnover Osteodystrophy and Vascular Calcification Are Amenable to Skeletal Anabolism in an Animal Model of Chronic Kidney Disease and the Metabolic Syndrome. J. Am. Soc. Nephrol. *16*, 917–928.

Debnam, E.S., Smith, M.W., Sharp, P.A., Srai, S.K.S., Turvey, A., and Keable, S.J. (1995). The effects of streptozotocin diabetes on sodium-glucose transporter (SGLT1) expression and function in rat jejunal and ileal villus-attached enterocytes. Pflugers Arch. *430*, 151–159.

Debonneville, C., Flores, S.Y., Kamynina, E., Plant, P.J., Tauxe, C., Thomas, M.A., Munster, C., Chraibi, A., Pratt, J.H., Horisberger, J.-D., et al. (2001). Phosphorylation of Nedd4-2 by Sgk1 regulates epithelial Na(+) channel cell surface expression. EMBO J. *20*, 7052–7059.

Deji, N., Kume, S., Araki, S. -i., Soumura, M., Sugimoto, T., Isshiki, K., Chin-Kanasaki, M., Sakaguchi, M., Koya, D., Haneda, M., et al. (2008). Structural and functional changes in the kidneys of high-fat diet-induced obese mice. AJP Ren. Physiol. *296*, F118–F126.

Del Castillo, D., Cruzado, J.M., Diaz, J.M., Castello, I.B., Valdemoros, R.L., Huertas, E.G., and Andres, M.D.C. (2004). The effects of hyperlipidaemia on graft and patient outcome in renal transplantation. Nephrol. Dial. Transplant. *19*, iii67-iii71.

Delpire, E., and Gagnon, K.B.E. (2007). Genome-wide analysis of SPAK/OSR1 binding motifs. Physiol. Genomics *28*, 223–231.

Delpire, E., Rauchman, M.I., Beierl, D.R., Hebert, S.C., and Gullans, S.R. (1994). Molecular cloning and chromosome localisation of a putative basolateral Na+-K+-2Cl- cotransporter from mouse inner medullary collecting duct (mIMCD-3) cells. J. Biol. Chem. *269*, 25677–25683.

Dërmaku-Sopjani, M., Almilaji, A., Pakladok, T., Munoz, C., Hosseinzadeh, Z., Blecua, M., Sopjani, M., and Lang, F. (2013). Down-Regulation of the Na+-Coupled Phosphate Transporter NaPi-IIa by AMP- Activated Protein Kinase. Kidney Blood Press. Res. *37*, 547–556.

Derst, C., Konrad, M., Kockerling, A., Karolyi, L., Deschenes, G., Daut, J., Karschin, A., and Seyberth, H.W. (1997). Mutations in the ROMK Gene in Antenatal Bartter Syndrome Are Associated with Impaired K+ Channel

Function. Biochem. Biophys. Res. Commun. *230*, 641–645.

Dickson, B.K., Blackledge, J., and Hajjar, I.M. (2006). The Impact of Lifestyle Behavior on Hypertension Awareness, Treatment, and Control in a Southeastern Population. Am. J. Med. Sci. *332*, 211–215.

Dieter, M., Palmada, M., Rajamanickam, J., Aydin, A., Busjahn, A., Boehmer, C., Luft, F.C., and Lang, F. (2004). Regulation of glucose transporter SGLT1 by ubiquitin ligase Nedd4-2 and kinases SGK1, SGK3, and PKB. Obesity *12*, 862–870.

Dominguez, J.H., Camp, K., Maianu, L., Feister, H., and Garvey, W.T. (1994). Molecular adaptations of GLUT1 and GLUT2 in renal proximal tubules of diabetic rats. Am. J. Physiol.-Ren. Fluid Electrolyte Physiol. *35*, F283–F290.

Douglas, B.H., Guyton, A.C., Langston, J.B., and Bishop, V.S. (1964). Hypertension caused by salt loading. II: Fluid volume and tissue pressure changes. Am. J. Physiol. *207*, 669–671.

Dowd, B.F.X., and Forbush, B. (2003). PASK (Proline-Alanine-rich STE20-related Kinase), a Regulatory Kinase of the Na-K-Cl Cotransporter (NKCC1). J. Biol. Chem. *278*, 27347–27353.

Drumm, K., Kress, T.R., Gassner, B., Krug, A.W., and Gekle, M. (2006). Aldosterone Stimulates Activity and Surface Expression of NHE3 in Human Primary Renal Proximal Tubule Epithelial Cells (RPTEC). Cell. Physiol. Biochem. *17*, 21–28.

Ducloux, D., Kazory, A., Simula-Faivre, D., and Chalopin, J.-M. (2005). One-Year Post-Transplant Weight Gain is a Risk Factor for Graft Loss: Post-Transplant Weight Gain and Graft Loss. Am. J. Transplant. *5*, 2922–2928.

Dunn, S.R., Qi, Z., Bottinger, E.P., Breyer, M.D., and Sharma, K. (2004). Utility of endogenous creatinine clearance as a measure of renal function in mice. Kidney Int. *65*, 1959–1967.

Ecelbarger, C.A., Terris, J., Hoyer, J.R., Nielsen, S., Wade, J.B., and Knepper, M.A. (1996). Localization and regulation of the rat renal Na+-K+-2Cl- cotransporter, BSC-1. Am. J. Physiol.-Ren. Fluid Electrolyte Physiol. *271*, F619–F628.

El-Agroudy, A.E., Wafa, E.W., Gheith, O.E., Shehab El-Dein, A.B., and Ghoneim, M.A. (2004). WEIGHT GAIN AFTER RENAL TRANSPLANTATION IS A RISK FACTOR FOR PATIENT AND GRAFT OUTCOME: Transplantation *77*, 1381–1385.

Elliot, P., Stamler, J., Nichols, R., Dyer, A.R., Stamler, R., Kesteloot, H., and Marmot, M. (1996). Intersalt revisited: further analyses of 24 hour sodium

excretion and blood pressure within and across populations. BMJ *312*, 1249–1253.

Ellison, D.H., Velazquez, H., and Wright, F.S. (1987). Thiazide-sensitive sodium chloride cotransport in early distal tubule. Am. J. Physiol.-Ren. Fluid Electrolyte Physiol. *253*, F546–F554.

Elvira, B., Blecua, M., Luo, D., Yang, W., Shumilina, E., Munoz, C., and Lang, F. (2014). SPAK-Sensitive Regulation of Glucose Transporter SGLT1. J. Membr. Biol. *247*, 1191–1197.

Emmel, E.A., Verweij, C.L., Durand, D.B., Higgins, K.M., Lacy, E., and Crabtree, G.R. (1989). Cyclosporin A specifically inhibits function of nuclear proteins involved in T cell activation. Science *246*, 1617–1620.

Engeli, S., Bohnke, J., Gorzelniak, K., Janke, J., Schling, P., Bader, M., Luft, F.C., and Sharma, A.M. (2005). Weight Loss and the Renin-Angiotensin-Aldosterone System. Hypertension *45*, 356–362.

Engevik, M.A., Aihara, E., Montrose, M.H., Shull, G.E., Hassett, D.J., and Worrell, R.T. (2013). Loss of NHE3 alters gut microbiota composition and influences Bacteroides thetaiotaomicron growth. AJP Gastrointest. Liver Physiol. *305*, G697–G711.

Engevik, M.A., Engevik, K.A., Yacyshyn, M.B., Wang, J., Hassett, D.J., Darien, B., Yacyshyn, B.R., and Worrell, R.T. (2015). Human *Clostridium difficile* infection: inhibition of NHE3 and microbiota profile. Am. J. Physiol. - Gastrointest. Liver Physiol. *308*, G497–G509.

English, J., Evan, A., Houghton, D.C., and Bennett, W.M. (1987). Cyclosporine-induced acute renal dysfunction in the rat. Transplantation *44*, 135–141.

Espinola-Klein, C., Rupprecht, H.J., Bickel, C., Post, F., Genth-Zotz, S., Lackner, K., Munzel, T., and Blankenberg, S. (2007). Impact of Metabolic Syndrome on Atherosclerotic Burden and Cardiovascular Prognosis. Am. J. Cardiol. *99*, 1623–1628.

Esteva-Font, C., Ars, E., Guillen-Gomez, E., Campistol, J.M., Sanz, L., Jimenez, W., Knepper, M.A., Torres, F., Torra, R., Ballarin, J.A., et al. (2007). Ciclosporin-induced hypertension is associated with increased sodium transporter of the loop of Henle (NKCC2). Nephrol. Dial. Transplant. *22*, 2810–2816.

Esteva-Font, C., Guillén-Gómez, E., Diaz, J.M., Guirado, L., Facundo, C., Ars, E., Ballarin, J.A., and Fernández-Llama, P. (2014). Renal Sodium Transporters Are Increased in Urinary Exosomes of Cyclosporine-Treated Kidney Transplant Patients. Am. J. Nephrol. *39*, 528–535.

Falkiewicz, K., Nahaczewska, W., Boratynska, M., Owczarek, H., Klinger, M., Kaminska, D., Wozniak, M., Szepietowski, T., and Patrzalek, D. (2003). Tacrolimus decreases tubular phosphate wasting in renal allograft recipients. Transplant. Proc. *35*, 2213–2215.

Farfel, Z., Mayan, H., Yaacov, Y., Mouallem, M., Shaharabany, M., Pauzner, R., Kerem, E., and Wilschanski, M. (2005). WNK4 regulates airway Na+ transport: study of familial hyperkalaemia and hypertension. Eur. J. Clin. Invest. *35*, 410–415.

Farrington, K., Varghese, Z., Newman, S.P., Ahmed, K.Y., Fernando, O.N., and Moorhead, J.F. (1979). Dissociation of absorptions of calcium and phosphate after successful cadaveric renal transplantation. Br. Med. J. *1*, 712–714.

Fenton, R.A., Poulsen, S.B., de la Mora Chavez, S., Soleimani, M., Rieg, J.A.D., and Rieg, T. (2017). Renal tubular NHE3 is required in the maintenance of water and sodium chloride homeostasis. Kidney Int. *92*, 397–414.

Fernandez-Fresnedo, G., Palomar, R., Escallada, R., Martin de Francisco, A.L., Cotorruelo, J.G., Zubimendi, J.A., Sanz de Castro, S., Ruiz, J.C., Rodrigo, E., and Arias, M. (2001). Hypertension and long-term renal allograft survival: effect of early glomerular filtration rate. Nephrol. Dial. Transplant. *16*, 105–109.

Fernández-Llama, P., Khositseth, S., Gonzales, P.A., Star, R.A., Pisitkun, T., and Knepper, M.A. (2010). Tamm-Horsfall protein and urinary exosome isolation. Kidney Int. *77*, 736–742.

Fezai, M., Elvira, B., Warsi, J., Ben-Attia, M., Hosseinzadeh, Z., and Lang, F. (2015). Up-Regulation of Intestinal Phosphate Transporter NaPi-IIb (SLC34A2) by the Kinases SPAK and OSR1. Kidney Blood Press. Res. *40*, 555–564.

Fields, N.G., Yuan, B., and Leenen, F.H.H. (1991). Sodium-induced cardiac hypertrophy. Cardiac sympathetic activity versus volume load. Circ. Res. *68*, 745–755.

Firsov, D., Schild, L., Gautschi, I., Merillat, A.-M., Schneeberger, E., and Rossier, B.C. (1996). Cell surface expression of the epithelial Na channel and a mutant causing Liddle syndrome: A quantitative approach. Proc. Natl. Acad. Sci. U. S. A. *93*, 15370–15375.

Flanagan, W.M., Corthesy, B., Bram, R.J., and Crabtree, G.R. (1991). Nuclear association of a T-cell transcription factor blocked by FK-506 and cyclosporin A. Nature *352*, 803–807.

Flemmer, A.W., Giménez, I., Dowd, B.F.X., Darman, R.B., and Forbush, B.

(2002). Activation of the Na-K-Cl Cotransporter NKCC1 Detected with a Phospho-specific Antibody. J. Biol. Chem. *277*, 37551–37558.

Ford, E.S., Giles, W.H., and Dietz, W.H. (2002). Prevalence of the Metabolic Syndrome Among US Adults: Findings From the Third National Health and Nutrition Examination Survey. JAMA *287*, 356–359.

Forster, I.C., Loo, D.D.F., and Eskandari, S. (1999). Stoichiometry and Na+ binding cooperativity of rat and flounder renal type II Na+-Pi cotransporters. Am. J. Physiol. - Ren. Physiol. *276*, F644–F649.

Forstner, G.G., Sabesin, S.M., and Isselbacher, K.J. (1968). Rat intestinal microvillus membranes. Purification and biochemical characterization. Biochem. J. *106*, 381–390.

Franklin, S., Gustin, W., Wong, N., Larson, M., Weber, M., Kannel, W., and Levy, D. (1997). Hemodynamic Patterns of Age-Related Changes in Blood Pressure: The Framingham Heart Study. Circulation *96*, 308–315.

Fraser, S.A., Gimenez, I., Cook, N., Jennings, I., Katerelos, M., Katsis, F., Levidiotis, V., Kemp, B.E., and Power, D.A. (2007). Regulation of the renal-specific Na^+–K^+–$2Cl^-$ co-transporter NKCC2 by AMP-activated protein kinase (AMPK). Biochem. J. *405*, 85–93.

Friedman, S.M. (1990a). The relation of cell volume, cell sodium and the transmembrane sodium gradient to blood pressure. J. Hypertens. *8*, 67–73.

Friedman, S.M., McIndoe, R.A., and Tanaka, M. (1990b). The relation of blood sodium concentration to blood pressure in the rat. J. Hypertens. *8*, 61–66.

Frohlich, E.D., Chien, Y., Sesoko, S., and Pegram, B.L. (1993). Relationship between dietary sodium intake, hemodynamics, and cardiac mass in SHR and WKY rats. Am. J. Physiol.-Regul. Integr. Comp. Physiol. *264*, R30–R34.

Fujii, N., Ho, R.C., Manabe, Y., Jessen, N., Toyoda, T., Holland, W.L., Summers, S.A., Hirshman, M.F., and Goodyear, L.J. (2008). Ablation of AMP-Activated Protein Kinase 2 Activity Exacerbates Insulin Resistance Induced by High-Fat Feeding of Mice. Diabetes *57*, 2958–2966.

Fukae, H., Kinoshita, H., Fujimoto, S., Kita, T., Nakazato, M., and Eto, T. (2002). Changes in Urinary Levels and Renal Expression of Uroguanylin on Low or High Salt Diets in Rats. Nephron *92*, 373–378.

Funayama, H., Nakamura, T., Saito, T., Yoshimura, A., Saito, M., Kawakami, M., and Ishikawa, S.-E. (2004). Urinary excretion of aquaporin-2 water channel exaggerated dependent upon vasopressin in congestive heart failure. Kidney Int. *66*, 1387–1392.

Fuster, D.G., Bobulescu, I.A., Zhang, J., Wade, J., and Moe, O.W. (2007). Characterization of the regulation of renal Na+/H+ exchanger NHE3 by insulin. AJP Ren. Physiol. *292*, F577–F585.

Gagnon, K.B.E., England, R., and Delpire, E. (2007). A Single Binding Motif is Required for SPAK Activation of the Na-K-2Cl Cotransporter. Cell. Physiol. Biochem. *20*, 131–142.

Gallou-Kabani, C., Vige, A., Gross, M.-S., Rabes, J.-P., Boileau, C., Larue-Achagiotis, C., Tome, D., Jais, J.-P., and Junien, C. (2007). C57BL/6J and A/J Mice Fed a High-Fat Diet Delineate Components of Metabolic Syndrome. Obesity *15*, 1996–2005.

Gamba, G., Saltzberg, S.N., Lombardi, M., Miyanoshita, A., Lytton, J., Hediger, M.A., Brenner, B.M., and Hebert, S.C. (1993). Primary Structure and Functional Expression of a cDNA Encoding the Thiazide-Sensitive, Electroneutral Sodium-Chloride Cotransporter. Proc. Natl. Acad. Sci. U. S. A. *90*, 2749–2753.

Gamba, G., Miyanoshita, A., Lombardi, M., Lytton, J., Lee, W.-S., Hediger, M.A., and Hebert, S.C. (1994). Molecular Cloning, Primary Structure, and Characterization of Two Members of the Mammalian Electroneutral Sodium-(Potassium)- Chloride Cotransporter Family Expressed in Kidney. J. Biol. Chem. *269*, 17713–17722.

Garg, P., Martin, C.F., Elms, S.C., Gordon, F.J., Wall, S.M., Garland, C.J., Sutliff, R.L., and O'Neill, W.C. (2007). Effect of the Na-K-2Cl cotransporter NKCC1 on systemic blood pressure and smooth muscle tone. Am. J. Physiol. - Heart Circ. Physiol. *292*, H2100–H2105.

Geibel, J., Giebisch, G., and Boron, W.F. (1990). Angiotensin II stimulates both Na(+)-H+ exchange and Na+/HCO3- cotransport in the rabbit proximal tubule. Proc. Natl. Acad. Sci. U. S. A. *87*, 7917–7920.

Gerhardt, U., Große Hüttmann, M., and Hohage, H. (1999). Influence of hyperglycemia and hyperuricemia on long-term transplant survival in kidney transplant recipients. Clin. Transplant. *13*, 375–379.

Gesek, F.A., and Schoolwerth, A.C. (1991). Insulin increases Na(+)-H+ exchange activity in proximal tubules from normotensive and hypertensive rats. Am. J. Physiol.-Ren. Fluid Electrolyte Physiol. *260*, F695–F703.

Ghisdal, L., Bouchta, N.B., Broeders, N., Crenier, L., Hoang, A.-D., Abramowicz, D., and Wissing, K.M. (2008). Conversion from tacrolimus to cyclosporine A for new-onset diabetes after transplantation: a single-centre experience in renal transplanted patients and review of the literature. Transpl. Int. *0*, 071029080703003–???

Giménez, I., and Forbush, B. (2003). Short-term Stimulation of the Renal Na-

K-Cl Cotransporter (NKCC2) by Vasopressin Involves Phosphorylation and Membrane Translocation of the Protein. J. Biol. Chem. *278*, 26946–26951.

Giménez, I., and Forbush, B. (2005). Regulatory phosphorylation sites in the NH2 terminus of the renal Na-K-Cl cotransporter (NKCC2). AJP Ren. Physiol. *289*, F1341–F1345.

Giral, H., Caldas, Y., Sutherland, E., Wilson, P., Breusegem, S., Barry, N., Blaine, J., Jiang, T., Wang, X.X., and Levi, M. (2009). Regulation of rat intestinal Na-dependent phosphate transporters by dietary phosphate. AJP Ren. Physiol. *297*, F1466–F1475.

Golub, M.S., and Berger, M.E. (1987). Direct augmentation by cyclosporin A of the vascular contractile response to nerve stimulation. Hypertension *9*, III96-III96.

Gonzales, P.A., Pisitkun, T., Hoffert, J.D., Tchapyjnikov, D., Star, R.A., Kleta, R., Wang, N.S., and Knepper, M.A. (2009). Large-Scale Proteomics and Phosphoproteomics of Urinary Exosomes. J. Am. Soc. Nephrol. *20*, 363–379.

Gonzales, P.A., Zhou, H., Pisitkun, T., Wang, N.S., Star, R.A., Knepper, M.A., and Yuen, P.S.T. (2010). Isolation and Purification of Exosomes in Urine. In The Urinary Proteome, A.J. Rai, ed. (Totowa, NJ: Humana Press), pp. 89–99.

Gorboulev, V., Schurmann, A., Vallon, V., Kipp, H., Jaschke, A., Klessen, D., Friedrich, A., Scherneck, S., Rieg, T., Cunard, R., et al. (2012). Na+-D-glucose Cotransporter SGLT1 is Pivotal for Intestinal Glucose Absorption and Glucose-Dependent Incretin Secretion. Diabetes *61*, 187–196.

Gore, J.L., Pham, P.T., Danovitch, G.M., Wilkinson, A.H., Rosenthal, J.T., Lipshutz, G.S., and Singer, J.S. (2006). Obesity and Outcome Following Renal Transplantation. Am. J. Transplant. *6*, 357–363.

Gores, P.F., Fryd, D.S., Sutherland, D.E.R., Najarian, J.S., and Simmons, R.L. (1988). Hyperuricemia after renal transplantation. Am. J. Surg. *156*, 397–400.

Grahammer, F., Henke, G., Sandu, C., Rexhepaj, R., Hussain, A., Friedrich, B., Risler, T., Metzger, M., Just, L., Skutella, T., et al. (2006). Intestinal function of gene-targeted mice lacking serum- and glucocorticoid-inducible kinase 1. AJP Gastrointest. Liver Physiol. *290*, G1114–G1123.

Greene, A.S., Yu, Z.Y., Roman, R.J., and Cowley, A.W. (1990). Role of blood volume expansion in Dahl rat model of hypertension. Am. J. Physiol. - Heart Circ. Physiol. *258*, H508–H514.

Greger, R. (1981b). Chloride reabsorption in the rabbit cortical thick

ascending limb of the loop of Henle. Pflüg. Arch. Eur. J. Physiol. *390*, 38–43.

Greger, R., and Schlatter, E. (1981a). Presence of luminal K+, a prerequisite for active NaCl transport in the cortical thick ascending limb of Henle's loop of rabbit kidney. Pflüg. Arch. Eur. J. Physiol. *392*, 92–94.

Greger, R., Schlatter, E., and Lang, F. (1983). Evidence for electroneutral sodium chloride cotransport in the cortical thick ascending limb of Henle's loop of rabbit kidney. Pflüg. Arch. *396*, 308–314.

Grichtchenko, I.I., Choi, I., Zhong, X., Bray-Ward, P., Russell, J.M., and Boron, W.F. (2001). Cloning, Characterization, and Chromosomal Mapping of a Human Electroneutral Na^+-driven Cl-HCO_3 Exchanger. J. Biol. Chem. *276*, 8358–8363.

Griffith, J.P., Kim, J.L., Kim, E.E., Sintchak, M.D., Thomson, J.A., Fitzgibbon, M.J., Fleming, M.A., Caron, P.R., Hsiao, K., and Navia, M.A. (1995). X-ray structure of calcineurin inhibited by the immunophilin-immunosuppressant FKBP12-FK506 complex. Cell *82*, 507–522.

Grimm, M., Rinaldi, M., Yonan, N.A., Arpesella, G., Arizon Del Prado, J.M., Pulpon, L.A., Villemot, J.P., Frigerio, M., Rodriguez Lambert, J.L., Crespo-Leiro, M.G., et al. (2006). Superior Prevention of Acute Rejection by Tacrolimus vs. Cyclosporine in Heart Transplant Recipients-A Large European Trial. Am. J. Transplant. *6*, 1387–1397.

Grubb, B.R., Lee, E., Pace, A.J., Koller, B.H., and Boucher, R.C. (2000). Intestinal ion transport in NKCC1-deficient mice. Am. J. Physiol. - Gastrointest. Liver Physiol. *279*, G707–G718.

Gründer, S., Firsov, D., Chang, S.S., Jaeger, N.F., Gautschi, I., Schild, L., Lifton, R.P., and Rossier, B.C. (1997). A mutation causing pseudohypoaldosteronism type 1 identifies a conserved glycine that is involved in the gating of the epithelial sodium channel. EMBO J. *16*, 899–907.

Gu, D., Reynolds, K., Wu, X., Chen, J., Duan, X., Muntner, P., Huang, G., Reynolds, R.F., Su, S., Whelton, P.K., et al. (2002). Prevalence, Awareness, Treatment, and Control of Hypertension in China. Hypertension *40*, 920–927.

Gu, J.-W., Anand, V., Shek, E.W., Moore, M.C., Brady, A.L., Kelly, W.C., and Adair, T.H. (1998). Sodium Induces Hypertrophy of Cultured Myocardial Myoblasts and Vascular Smooth Muscle Cells. Hypertension *31*, 1083–1087.

Guerrero-Romero, F., and Rodríguez-Morán, M. (2002). Low serum magnesium levels and metabolic syndrome. Acta Diabetol. *39*, 209–213.

Guerrero-Romero, F., and Rodríguez-Morán, M. (2006). Hypomagnesemia, oxidative stress, inflammation, and metabolic syndrome. Diabetes Metab.

Res. Rev. *22*, 471–476.

Guidi, E., Menghetti, D., Milani, S., Montagnino, G., Palazzi, P., and Bianchi, G. (1996). Hypertension may be transplanted with the kidney in humans: a long-term historical prospective follow-up of recipients grafted with kidneys coming from donors with or without hypertension in their families. J. Am. Soc. Nephrol. *7*, 1131–1138.

Guidi, E., Cozzi, M.G., Minetti, E., and Bianchi, G. (1998). Donor and recipient family histories of hypertension influence renal impairment and blood pressure during acute rejections. J. Am. Soc. Nephrol. *9*, 2102–2107.

Gurley, S.B., Riquier-Brison, A.D.M., Schnermann, J., Sparks, M.A., Allen, A.M., Haase, V.H., Snouwaert, J.N., Le, T.H., McDonough, A.A., Koller, B.H., et al. (2011). AT 1A Angiotensin Receptors in the Renal Proximal Tubule Regulate Blood Pressure. Cell Metab. *13*, 469–475.

Guyton, A.C., Coleman, T.G., Cowley, A.W., Scheel, K.W., Manning, R.D., and Norman, R.A. (1972). Arterial pressure regulation: Overriding dominance of the kidneys in long-term regulation and in hypertension. Am. J. Med. *52*, 584–594.

Hall, D.A., and Varney, D.M. (1980). Effect of vasopressin on electrical potential difference and chloride transport in mouse medullary thick ascending limb of Henle's loop. J. Clin. Invest. *66*, 792.

Halseth, A.E., Ensor, N.J., White, T.A., Ross, S.A., and Gulve, E.A. (2002). Acute and chronic treatment of ob/ob and db/db mice with AICAR decreases blood glucose concentrations. Biochem. Biophys. Res. Commun. *294*, 798–805.

Handschumacher, R.E., Harding, M.W., Rice, J., Drugge, R.J., and Speicher, D.W. (1984). Cyclophilin: A specific cytosolic binding protein for cyclosporin A. Science *226*, 544–547.

Harding, M.W., Galat, A., Uehling, D.E., and Schreiber, S.L. (1989). A receptor for the immunosuppressant FK506 is a cis-trans peptidyl-prolyl isomerase. Nature *341*, 758–760.

Harris, R.C., Brenner, B.M., and Seifter, J.L. (1986). Sodium-hydrogen exchange and glucose transport in renal microvillus membrane vesicles from rats with diabetes mellitus. J. Clin. Invest. *77*, 724–733.

Hart, T.C., Gorry, M.C., Woodard, A.S., Shihabi, Z., Sandhu, J., Shirts, B., Xu, L., Zhu, H., Barmada, M.M., and Bleyer, A.J. (2002). Mutations of the UMOD gene are responsible for medullary cystic kidney disease 2 and familial juvenile hyperuricaemic nephropathy. J. Med. Genet. *39*, 882–892.

Hattenhauer, O., Traebert, M., Murer, H., and Biber, J. (1999). Regulation of

small intestinal Na-Pi type IIb cotransporter by dietary phosphate intake. Am. J. Physiol. - Gastrointest. Liver Physiol. *40*, G756–G762.

Hausberg, M., Lang, D., Levers, A., Suwelack, B., Kisters, K., Tokmak, F., Barenbrock, M., and Kosch, M. (2006). Sympathetic nerve activity in renal transplant patients before and after withdrawal of cyclosporine. J. Hypertens. *24*, 957–964.

Hayek, T., Ito, Y., Azrolan, N., Verdery, R.B., Aalto-Setälä, K., Walsh, A., and Breslow, J.L. (1993). Dietary fat increases high density lipoprotein (HDL) levels both by increasing the transport rates and decreasing the fractional catabolic rates of HDL cholesterol ester and apolipoprotein (Apo) A-I. Presentation of a new animal model and mechanistic studies in human Apo A-I transgenic and control mice. J. Clin. Invest. *91*, 1665–1671.

Hazarika, N.C., Narain, K., Biswas, D., Kalita, H.C., and Mahanta, J. (2004). Hypertension in the native rural population of Assam. Natl. Med. J. India *17*, 300–304.

He, H., Liu, X., Lv, L., Liang, H., Leng, B., Zhao, D., Zhang, Y., Du, Z., Chen, X., Li, S., et al. (2014). Calcineurin suppresses AMPK-dependent cytoprotective autophagy in cardiomyocytes under oxidative stress. Cell Death Dis. *5*, e997.

Hebert, S.C., Culpepper, R.M., and Andreoli, T.E. (1981a). NaCl transport in mouse medullary thick ascending limbs. I. Functional nephron heterogeneity and ADH-stimulated NaCl cotransport. Am. J. Physiol.-Ren. Fluid Electrolyte Physiol. *241*, F412–F431.

Hebert, S.C., Culpepper, R.M., and Andreoli, T.E. (1981b). NaCl transport in mouse medullary thick ascending limbs. II. ADH enhancement of transcellular NaCl cotransport; origin of transepithelial voltage. Am. J. Physiol.-Ren. Fluid Electrolyte Physiol. *241*, F432–F442.

Hebert, S.C., Culpepper, R.M., and Andreoli, T.E. (1981c). NaCl transport in mouse medullary thick ascending limbs. III. Modulation of the ADH effect by peritubular osmolality. Am. J. Physiol.-Ren. Fluid Electrolyte Physiol. *241*, F443–F451.

Hediger, M.A., Coady, M.J., Ikeda, T.S., and Wright, E.M. (1987). Expression cloning and cDNA sequencing of the Na+/glucose co-transporter. Nature *330*, 379–381.

Heering, P.J., Kurschat, C., Vo, D.T., Klein-Vehne, N., Fehsel, K., and Ivens, K. (2004). Aldosterone resistance in kidney transplantation is in part induced by a down-regulation of mineralocorticoid receptor expression. Clin. Transplant. *18*, 186–192.

Heise, C.J., Xu, B., Deaton, S.L., Cha, S.-K., Cheng, C.-J., Earnest, S.,

Sengupta, S., Juang, Y.-C., Stippec, S., Xu, Y., et al. (2010). Serum and Glucocorticoid-induced Kinase (SGK) 1 and the Epithelial Sodium Channel Are Regulated by Multiple with No Lysine (WNK) Family Members. J. Biol. Chem. *285*, 25161–25167.

Heisel, O., Heisel, R., Balshaw, R., and Keown, P. (2004). New Onset Diabetes Mellitus in Patients Receiving Calcineurin Inhibitors: A Systematic Review and Meta-Analysis. Am. J. Transplant. *4*, 583–595.

Heit, J.J., Apelqvist, Å.A., Gu, X., Winslow, M.M., Neilson, J.R., Crabtree, G.R., and Kim, S.K. (2006). Calcineurin/NFAT signalling regulates pancreatic β-cell growth and function. Nature *443*, 345–349.

Helmchen, U., Schmidt, W.E., Siegel, E.G., and Creutzfeldt, W. (1984). Morphological and functional changes of pancreatic B cells in cyclosporin A-treated rats. Diabetologia *27*, 416–418.

Hernando, N., Myakala, K., Simona, F., Knöpfel, T., Thomas, L., Murer, H., Wagner, C.A., and Biber, J. (2015). Intestinal Depletion of NaPi-IIb/ *Slc34* a2 in Mice: Renal and Hormonal Adaptation: INTESTINAL DEPLETION OF NAPI-IIB/ *SLC34* A2 IN MICE. J. Bone Miner. Res. *30*, 1925–1937.

Heuvel, L. van den, K., A., M., W., and L., M. (2002). Autosomal recessive renal glucosuria attributable to a mutation in the sodium glucose cotransporter (SGLT2). Hum. Genet. *111*, 544–547.

Higgins, R.M., Richardson, A.J., Endre, Z.H., Frostick, S.P., and Morris, P.J. (1990). Hypophosphataemia after renal transplantation: relationship to immunosuppressive drug therapy and effects on muscle detected by 31P nuclear magnetic resonance spectroscopy. Nephrol. Dial. Transplant. *5*, 62–68.

Hildebrandt, M.A., Hoffmann, C., Sherrill–Mix, S.A., Keilbaugh, S.A., Hamady, M., Chen, Y., Knight, R., Ahima, R.S., Bushman, F., and Wu, G.D. (2009). High-Fat Diet Determines the Composition of the Murine Gut Microbiome Independently of Obesity. Gastroenterology *137*, 1716–1724.e2.

Hilfiker, H., Hattenhauer, O., Traebert, M., Forster, I., Murer, H., and Biber, J. (1998). Characterization of a murine type II sodium-phosphate cotransporter expressed in mammalian small intestine. Proc. Natl. Acad. Sci. *95*, 14564–14569.

Hirano, Y., Fujihira, S., Ohara, K., Katsuki, S., and Noguchi, H. (1992). Morphological and functional changes of islets of Langerhans in FK506-treated rats. Transplantation *53*, 889–894.

Ho, K., Nichols, C.G., Lederer, W.J., Lytton, J., Vassilev, P.M., Kanazirska, M.V., and Hebert, S.C. (1993). Cloning and expression of an inwardly rectifying ATP-regulated potassium channel. Nature *362*, 31–38.

Hoag, H.M., Martel, J., Gauthier, C., and Tenenhouse, H.S. (1999). Effects of Npt2 gene ablation and low-phosphate diet on renal Na+/phosphate cotransport and cotransporter gene expression. J. Clin. Invest. *104*, 679–686.

Hoogerwerf, W.A., Tsao, S.C., Devuyst, O., Levine, S.A., Yun, C.H., Yip, J.W., Cohen, M.E., Wilson, P.D., Lazenby, A.J., and Tse, C.-M. (1996). NHE2 and NHE3 are human and rabbit intestinal brush-border proteins. Am. J. Physiol.-Gastrointest. Liver Physiol. *270*, G29–G41.

Hoorn, E.J., Walsh, S.B., McCormick, J.A., Fürstenberg, A., Yang, C.-L., Roeschel, T., Paliege, A., Howie, A.J., Conley, J., Bachmann, S., et al. (2011). The calcineurin inhibitor tacrolimus activates the renal sodium chloride cotransporter to cause hypertension. Nat. Med. *17*, 1304–1309.

Hoskova, L., Malek, I., Kautzner, J., Honsova, E., van Dokkum, R.P.E., Huskova, Z., Vojtiskova, A., Varcabova, S., Cervenka, L., and Kopkan, L. (2014). Tacrolimus-induced hypertension and nephrotoxicity in Fawn-Hooded rats are attenuated by dual inhibition of renin–angiotensin system. Hypertens. Res. *37*, 724–732.

Hoyer, P.F., Lee, I.J., Oemar, B.S., Krohn, H.P., Offner, G., and Brodehl, J. (1988). Renal handling of uric acid under cyclosporin A treatment. Pediatr. Nephrol. *2*, 18–21.

Huang, D.Y., Boini, K.M., Osswald, H., Friedrich, B., Artunc, F., Ullrich, S., Rajamanickam, J., Palmada, M., Wulff, P., Kuhl, D., et al. (2006). Resistance of mice lacking the serum- and glucocorticoid-inducible kinase SGK1 against salt-sensitive hypertension induced by a high-fat diet. AJP Ren. Physiol. *291*, F1264–F1273.

Huggett, A.S.G., and Nixon, D.A. (1957). Use of glucose oxidase, peroxidase, and o-dianisidine in determination of blood and urinary glucose. The Lancet *273*, 368–370.

Hummel, C.S., Lu, C., Loo, D.D.F., Hirayama, B.A., Voss, A.A., and Wright, E.M. (2011). Glucose transport by human renal Na+/D-glucose cotransporters SGLT1 and SGLT2. AJP Cell Physiol. *300*, C14–C21.

Igarashi, P., Heuvel, G.V., Payne, J.A., and Forbush, B. (1995). Cloning, embryonic expression, and alternative splicing of a murine kidney-specific Na-K-Cl cotransporter. Am. J. Physiol.-Ren. Physiol. *38*, F405–F418.

Ikeda, T.S., Hwang, E.-S., Coady, M.J., Hirayama, B.A., Hediger, M.A., and Wright, E.M. (1989). Characterization of a Na+/glucose cotransporter cloned from rabbit small intestine. J. Membr. Biol. *110*, 87–95.

Inoue, S., Honma, K., Mochizuki, K., and Goda, T. (2015). Induction of histone H3K4 methylation at the promoter, enhancer, and transcribed regions

of the Si and Sglt1 genes in rat jejunum in response to a high-starch/low-fat diet. Nutrition *31*, 366–372.

Isobe, K., Mori, T., Asano, T., Kawaguchi, H., Nonoyama, S., Kumagai, N., Kamada, F., Morimoto, T., Hayashi, M., Sohara, E., et al. (2013). Development of enzyme-linked immunosorbent assays for urinary thiazide-sensitive Na-Cl cotransporter measurement. AJP Ren. Physiol. *305*, F1374–F1381.

Israni, A.K., Snyder, J.J., Skeans, M.A., Kasiske, B.L., and for the PORT Investigators (2012). Clinical diagnosis of metabolic syndrome: predicting new-onset diabetes, coronary heart disease, and allograft failure late after kidney transplant: Metabolic syndrome and new-onset diabetes after kidney transplant. Transpl. Int. *25*, 748–757.

Jacques, T., Picard, N., Miller, R.L., Riemondy, K.A., Houillier, P., Sohet, F., Ramakrishnan, S.K., Busst, C.J., Jayat, M., Corniere, N., et al. (2013). Overexpression of Pendrin in Intercalated Cells Produces Chloride-Sensitive Hypertension. J. Am. Soc. Nephrol. *24*, 1104–1113.

Jevnikar, A.M., Petric, R., Holub, B.J., Philbrick, D.-J., and Clark, W.F. (1988). Effect of cyclosporine on plasma lipids and modification with dietary fish oil. Transplantation *46*, 722–725.

Jiang, H., Guan, G., Zhang, R., Liu, G., Cheng, J., Hou, X., and Cui, Y. (2009). Identification of urinary soluble E-cadherin as a novel biomarker for diabetic nephropathy. Diabetes Metab. Res. Rev. *25*, 232–241.

Jin, J., Jin, L., Luo, K., Lim, S.W., Chung, B.H., and Yang, C.W. (2017). Effect of Empagliflozin on Tacrolimus-Induced Pancreas Islet Dysfunction and Renal Injury. Am. J. Transplant. *17*, 2601–2616.

Joffres, M., Falaschetti, E., Gillespie, C., Robitaille, C., Loustalot, F., Poulter, N., McAlister, F.A., Johansen, H., Baclic, O., and Campbell, N. (2013). Hypertension prevalence, awareness, treatment and control in national surveys from England, the USA and Canada, and correlation with stroke and ischaemic heart disease mortality: a cross-sectional study. BMJ Open *3*, e003423.

Joffres, M.R., Ghadirian, P., Fodor, J.G., Petrasovits, A., Chockalingam, A., and Hamet, P. (1997). Awareness, Treatment, and Control of Hypertension in Canada,. Am. J. Hypertens. *10*, 1097–1102.

Johann, S.V., Gibbons, J.J., and O'hara, B. (1992). GLVR1, a receptor for gibbon ape leukemia virus, is homologous to a phosphate permease of Neurospora crassa and is expressed at high levels in the brain and thymus. J. Virol. *66*, 1635–1640.

Johnston, A.M., Naselli, G., Gonez, L.J., Martin, R.M., Harrison, L.C., and

DeAizpurua, H.J. (2000). SPAK, a STE20/SPS1-related kinase that activates the p38 pathway. Oncogene *19*, 4290–4297.

Johnston, C.P., Gallagher-Lepak, S., Zhu, Y.-R., Porth, C., Kelber, S., Roza, A.M., and Adams, M.B. (1993). Factors influencing weight gain after renal transplantation. Transplantation *56*, 822–827.

Joo, K.W., Lee, J.W., Jang, H.R., Heo, N.J., Jeon, U.S., Oh, Y.K., Lim, C.S., Na, K.Y., Kim, J., Cheong, H.I., et al. (2007). Reduced Urinary Excretion of Thiazide-Sensitive Na-Cl Cotransporter in Gitelman Syndrome: Preliminary Data. Am. J. Kidney Dis. *50*, 765–773.

Kahan, B.D., Flechner, S.M., Lorber, M.I., Golden, D., Conley, S., and Van Buren, C.T. (1987). Complications of cyclosporine-prednisone immunosuppression in 402 renal allograft recipients exclusively followed at a single center for from one to five years. Transplantation *43*, 197–204.

Kalantar, E., Khalili, N., Hossieni, M.-S., Rostami, Z., and Einollahi, B. (2011). Hyperuricemia After Renal Transplantation. Transplant. Proc. *43*, 584–585.

Kamar, N., Mariat, C., Delahousse, M., Dantal, J., Al Najjar, A., Cassuto, E., Lefrancois, N., Cointault, O., Touchard, G., Villemain, F., et al. (2007). Diabetes mellitus after kidney transplantation: a French multicentre observational study. Nephrol. Dial. Transplant. *22*, 1986–1993.

Kanai, Y., Lee, W.-S., You, G., Brown, D., and Hediger, M.A. (1994). The human kidney low affinity Na+/glucose cotransporter SGLT2. Delineation of the major renal reabsorptive mechanism for D-glucose. J. Clin. Invest. *93*, 397.

Kanbay, M., Akcay, A., Huddam, B., Usluogullari, C.A., Arat, Z., Ozdemir, F.N., and Haberal, M. (2005). Influence of Cyclosporine and Tacrolimus on Serum Uric Acid Levels in Stable Kidney Transplant Recipients. Transplant. Proc. *37*, 3119–3120.

Kannel, W.B., Gordon, T., and Schwartz, M.J. (1971). Systolic versus diastolic blood pressure and risk of coronary heart disease: the Framingham study. Am. J. Cardiol. *27*, 335–346.

Kanno, K., Sasaki, S., Hirata, Y., Ishikawa, S.-E., Fushimi, K., Nakanishi, S., Bichet, D.G., and Marumo, F. (1995). Urinary excretion of aquaporin-2 in patients with diabetes insipidus. N. Engl. J. Med. *332*, 1540–1545.

Kasiske, B.L. (1987). Possible causes and consequences of hypertension in stable renal transplant patients. Transplantation *44*, 639–643.

Kasiske, B.L., Snyder, J.J., Gilbertson, D., and Matas, A.J. (2003). Diabetes Mellitus after Kidney Transplantation in the United States. Am. J. Transplant.

3, 178–185.

Kasiske, B.L., Anjum, S., Shah, R., Skogen, J., Kandaswamy, C., Danielson, B., O'Shaughnessy, E.A., Dahl, D.C., Silkensen, J.R., Sahadevan, M., et al. (2004). Hypertension after kidney transplantation. Am. J. Kidney Dis. *43*, 1071–1081.

Kavanaugh, M.P., Miller, D.G., Zhang, W., Law, W., Kozak, S.L., Kabat, D., and Miller, A.D. (1994). Cell-surface receptors for gibbon ape leukemia virus and amphotropic murine retrovirus are inducible sodium-dependent phosphate symporters. Proc. Natl. Acad. Sci. *91*, 7071–7075.

Kawasoe, S., Maruguchi, Y., Kajiya, S., Uenomachi, H., Miyata, M., Kawasoe, M., Kubozono, T., and Ohishi, M. (2017). Mechanism of the blood pressure-lowering effect of sodium-glucose cotransporter 2 inhibitors in obese patients with type 2 diabetes. BMC Pharmacol. Toxicol. *18*.

Kaye, D., Thompson, J., Jennings, G., and Esler, M. (1993). Cyclosporine therapy after cardiac transplantation causes hypertension and renal vasoconstriction without sympathetic activation. Circulation *88*, 1101–1109.

Kearney, P.M., Whelton, M., Reynolds, K., Muntner, P., Whelton, P.K., and He, J. (2005). Global burden of hypertension: analysis of worldwide data. The Lancet *365*, 217–223.

Kellett, G.L., and Helliwell, P.A. (2000). The diffusive component of intestinal glucose absorption is mediated by the glucose-induced recruitment of GLUT2 to the brush-border membrane. Biochem. J. *350*, 155–162.

Kempson, S.A., Lotscher, M., Kaissling, B., Biber, J., Murer, H., and Levi, M. (1995). Parathyroid hormone action on phosphate transporter mRNA and protein in rat renal proximal tubules. Am. J. Physiol.-Ren. Physiol. *268*, F784–F791.

Kessler, M., Acuto, O., Storelli, C., Murer, H., Müller, M., and Semenza, G. (1978). A modified procedure for the rapid preparation of efficiently transporting vesicles from small intestinal brush border membranes. Their use in investigating some properties of D-glucose and choline transport systems. Biochim. Biophys. Acta BBA-Biomembr. *506*, 136–154.

Keven, K., Ozturk, R., Sengul, S., Kutlay, S., Ergun, I., Erturk, S., and Erbay, B. (2007). Renal tubular acidosis after kidney transplantation--incidence, risk factors and clinical implications. Nephrol. Dial. Transplant. *22*, 906–910.

Kiberd, B.A. (1989). Cyclosporine-induced renal dysfunction in human renal allograft recipients. Transplantation *48*, 965–969.

Kidambi, S., Kotchen, J.M., Grim, C.E., Raff, H., Mao, J., Singh, R.J., and Kotchen, T.A. (2007). Association of Adrenal Steroids With Hypertension and

the Metabolic Syndrome in Blacks. Hypertension *49*, 704–711.

Kieferle, S., Fong, P., Bens, M., Vandewalle, A., and Jentsch, T.J. (1994). Two highly homologous members of the ClC chloride channel family in both rat and human kidney. Proc. Natl. Acad. Sci. *91*, 6943–6947.

Kim, G.-H., Ecelbarger, C.A., Mitchell, C., Packer, R.K., Wade, J.B., and Knepper, M.A. (1999). Vasopressin increases Na-K-2Cl cotransporter expression in thick ascending limb of Henle's loop. Am. J. Physiol.-Ren. Physiol. *276*, F96–F103.

Kim, H.C., Hwang, E.A., Han, S.Y., Park, S.B., Kim, H.T., and Cho, W.H. (2004). Primary immunosuppression with tacrolimus in kidney transplantation: Three-year follow-up in a single center. Transplant. Proc. *36*, 2082–2083.

Kino, T., Hatanaka, H., Hashimoto, M., Nishiyama, M., Goto, T., Okuhara, M., Kohsaka, M., Aoki, H., and Imanaka, H. (1987a). FK-506, a novel immunosuppressant isolated from a Streptomyces. I. Fermentation, isolation, and physico-chemical and biological characteristics. J. Antibiot. (Tokyo) *40*, 1256–1265.

Kino, T., Hatanaka, H., Miyata, S., Inamura, N., NISHIYAMA, M., YAJIMA, T., GOTO, T., OKUHARA, M., KOHSAKA, M., and AOKI, H. (1987b). FK-506, a novel immunosuppressant isolated from a Streptomyces. J. Antibiot. (Tokyo) *40*, 1256–1265.

Kishikawa, H., Nishimura, K., Kato, T., Kobayashi, Y., Arichi, N., Okuno, A., Fujii, N., Kyo, M., Takahara, S., and Ichikawa, Y. (2009). Prevalence of the Metabolic Syndrome in Kidney Transplantation. Transplant. Proc. *41*, 181–183.

Kissinger, C.R., Parge, H.E., Knighton, D.R., Lewis, C.T., Pelletier, L.A., Tempczyk, A., Kalish, V.J., Tucker, K.D., Showalter, R.E., Moomaw, E.W., et al. Crystal structures of human calcineurin and the human FKBP12-FK506-calcineurin complex. Nature *378*, 1995.

Klag, M.J., Whelton, P.K., Randall, B.L., Neaton, J.D., Brancati, F.L., Ford, C.E., Shulman, N.B., and Stamler, J. (1996). Blood pressure and end-stage renal disease in men. N. Engl. J. Med. *334*, 13–18.

Klein, I.H., Abrahams, A.C., van Ede, T., Oey, P.L., Ligtenberg, G., and Blankestijn, P.J. (2010). Differential effects of acute and sustained cyclosporine and tacrolimus on sympathetic nerve activity: J. Hypertens. *28*, 1928–1934.

Kleinewietfeld, M., Manzel, A., Titze, J., Kvakan, H., Yosef, N., Linker, R.A., Muller, D.N., and Hafler, D.A. (2013). Sodium chloride drives autoimmune disease by the induction of pathogenic TH17 cells. Nature *496*, 518–522.

Klisic, J., Hu, M.C., Nief, V., Reyes, L., Fuster, D., Moe, O.W., and Ambühl, P.M. (2002). Insulin activates Na^+/H^+ exchanger 3: biphasic response and glucocorticoid dependence. Am. J. Physiol. - Ren. Physiol. *283*, F532–F539.

Kobayashi, K., Monkawa, T., Hayashi, M., and Saruta, T. (2004). Expression of the Na+/H+ exchanger regulatory protein family in genetically hypertensive rats. J. Hypertens. *22*, 1723 – 1730.

Kohan, D.E., Fioretto, P., Tang, W., and List, J.F. (2014). Long-term study of patients with type 2 diabetes and moderate renal impairment shows that dapagliflozin reduces weight and blood pressure but does not improve glycemic control. Kidney Int. *85*, 962–971.

Koltsova, S.V., Kotelevtsev, S.V., Tremblay, J., Hamet, P., and Orlov, S.N. (2009). Excitation–contraction coupling in resistance mesenteric arteries: Evidence for NKCC1-mediated pathway. Biochem. Biophys. Res. Commun. *379*, 1080–1083.

Komers, R., Rogers, S., Oyama, T.T., Xu, B., Yang, C.-L., McCormick, J., and Ellison, D.H. (2012). Enhanced phosphorylation of Na^+–Cl^- co-transporter in experimental metabolic syndrome: role of insulin. Clin. Sci. *123*, 635–647.

Kopf, D., Waldherr, R., and Rettig, R. (1993). Source of kidney determines blood pressure in young renal transplanted rats. Am. J. Physiol.-Ren. Physiol. *265*, F104–F111.

Kosanović, M., and Janković, M. (2014). Isolation of urinary extracellular vesicles from Tamm- Horsfall protein–depleted urine and their application in the development of a lectin-exosome-binding assay. BioTechniques *57*.

Kovesdy, C.P., Czira, M.E., Rudas, A., Ujszaszi, A., Rosivall, L., Novak, M., Kalantar-Zadeh, K., Molnar, M.Z., and Mucsi, I. (2010). Body Mass Index, Waist Circumference and Mortality in Kidney Transplant Recipients: Obesity and Mortality in Kidney Transplant. Am. J. Transplant. *10*, 2644–2651.

Krämer, B.K., Montagnino, G., del Castillo, D., Margreiter, R., Sperschneider, H., Olbricht, C.J., Krüger, B., Ortuño, J., Köhler, H., Kunzendorf, U., et al. (2005). Efficacy and safety of tacrolimus compared with cyclosporin A microemulsion in renal transplantation: 2 year follow-up results. Nephrol. Dial. Transplant. *20*, 968–973.

Krug, A.W., Papavassiliou, F., Hopfer, U., Ullrich, K.J., and Gekle, M. (2003). Aldosterone stimulates surface expression of NHE3 in renal proximal brush borders. Pflüg. Arch. - Eur. J. Physiol. *446*, 492–496.

Kurtz, A., Della Bruna, R., and Kuhn, K. (1988). Cyclosporine A enhances renin secretion and production in isolated juxtaglomerular cells. Kidney Int. *33*, 947–953.

Laghmani, K., Borensztein, P., Ambühl, P., Froissart, M., Bichara, M., Moe, O.W., Alpern, R.J., and Paillard, M. (1997). Chronic metabolic acidosis enhances NHE-3 protein abundance and transport activity in the rat thick ascending limb by increasing NHE-3 mRNA. J. Clin. Invest. *99*, 24.

Lai, F., Orelli, B.J., Till, B.G., Godley, L.A., Fernald, A.A., Pamintuan, L., and Le Beau, M.M. (2000). Molecular Characterization of KLHL3, a Human Homologue of the Drosophila kelch Gene. Genomics *66*, 65–75.

Laine, J., and Holmberg, C. (1995). Renal and adrenal mechanisms in cyclosporine-induced hyperkalaemia after renal transplantation. Eur. J. Clin. Invest. *25*, 670–676.

Laine, J., and Holmberg, C. (1996). Mechanisms of Hyperuricemia in Cyclosporine-Treated Renal Transplanted Children. Nephron *74*, 318–323.

Lakka, T.A., Salonen, R., Kaplan, G.A., and Salonen, J.T. (1999). Blood pressure and the progression of carotid atherosclerosis in middle-aged men. Hypertension *34*, 51–56.

Lalioti, M.D., Zhang, J., Volkman, H.M., Kahle, K.T., Hoffmann, K.E., Toka, H.R., Nelson-Williams, C., Ellison, D.H., Flavell, R., Booth, C.J., et al. (2006). Wnk4 controls blood pressure and potassium homeostasis via regulation of mass and activity of the distal convoluted tubule. Nat. Genet. *38*, 1124–1132.

Lamb, F.S., and Webb, R.C. (1987). Cyclosporine augments reactivity of isolated blood vessles. Life Sci. *40*, 2571–2578.

Lanese, D.M., and Conger, J.D. (1993). Effects of endothelin receptor antagonist on cyclosporine-induced vasoconstriction in isolated rat renal arterioles. J. Clin. Invest. *91*, 2144–2149.

LaPointe, M.S., Sodhi, C., Sahai, A., and Batlle, D. (2002). Na+/H+ exchange activity and NHE-3 expression in renal tubules from the spontaneously hypertensive rat. Kidney Int. *62*, 157–165.

Larmonier, C.B., Laubitz, D., Hill, F.M., Shehab, K.W., Lipinski, L., Midura-Kiela, M.T., McFadden, R.-M.T., Ramalingam, R., Hassan, K.A., Golebiewski, M., et al. (2013). Reduced colonic microbial diversity is associated with colitis in NHE3-deficient mice. AJP Gastrointest. Liver Physiol. *305*, G667–G677.

Laubitz, D., Harrison, C.A., Midura-Kiela, M.T., Ramalingam, R., Larmonier, C.B., Chase, J.H., Caporaso, G., Besselsen, D.G., Ghishan, F.K., and Kiela, P.R. (2016). Reduced Epithelial Na+/H+ Exchange Drives Gut Microbial Dysbiosis and Promotes Inflammatory Response in T Cell-Mediated Murine Colitis. PLOS ONE *11*, e0152044.

Lawrence, M.C., Bhatt, H.S., Watterson, J.M., and Easom, R.A. (2001).

Regulation of Insulin Gene Transcription by a Ca2+- Responsive Pathway Involving Calcineurin and Nuclear Factor of Activated T Cells. Mol. Endocrinol. *15*, 1758–1767.

Lazelle, R.A., McCully, B.H., Terker, A.S., Himmerkus, N., Blankenstein, K.I., Mutig, K., Bleich, M., Bachmann, S., Yang, C.-L., and Ellison, D.H. (2016). Renal Deletion of 12 kDa FK506-Binding Protein Attenuates Tacrolimus-Induced Hypertension. J. Am. Soc. Nephrol. *27*, 1456–1464.

Lee, F.N., Oh, G., McDonough, A.A., and Youn, J.H. (2007). Evidence for gut factor in K+ homeostasis. AJP Ren. Physiol. *293*, F541–F547.

Lee, G.J., Mossa-Al Hashimi, L., Debnam, E.S., Unwin, R.J., and Marks, J. (2017). Postprandial adjustments in renal phosphate excretion do not involve a gut-derived phosphaturic factor: No evidence for an intestinal phosphatonin. Exp. Physiol. *102*, 462–474.

Lee, W.-S., Kanai, Y., Wells, R.G., and Hediger, M.A. (1994). The high affinity Na+/glucose cotransporter: Re-evaluation of function and distribution of expression. J. Biol. Chem. *269*, 12032–12039.

Leenen, F.H.H., and Yuan, B. (1998). Dietary-sodium-induced cardiac remodeling in spontaneously hypertensive rat versus Wistar–Kyoto rat. J. Hypertens. *16*, 885–892.

Lenertz, L.Y., Lee, B.-H., Min, X., Xu, B., Wedin, K., Earnest, S., Goldsmith, E.J., and Cobb, M.H. (2005). Properties of WNK1 and Implications for Other Family Members. J. Biol. Chem. *280*, 26653–26658.

Lennane, R.J., Carey, R.M., Goodwin, T.J., and Peart, W.S. (1975). A comparison of natriuresis after oral and intravenous sodium loading in sodium-depleted man: evidence for a gastrointestinal or portal monitor of sodium intake. Clin. Sci. Mol. Med. *49*, 437–440.

Leong, P.K.K., Devillez, A., Sandberg, M.B., Yang, L.E., Yip, D.K.P., Klein, J.B., and McDonough, A.A. (2006b). Effects of ACE inhibition on proximal tubule sodium transport. AJP Ren. Physiol. *290*, F854–F863.

Leong, P.K.K., Yang, L.E., Landon, C.S., McDonough, A.A., and Yip, K.-P. (2006). Phenol injury-induced hypertension stimulates proximal tubule Na+/H+ exchanger activity. AJP Ren. Physiol. *290*, F1543–F1550.

Levi, M., Lotscher, M., Sorribas, V., Custer, M., Arar, M., Kaissling, B., Murer, H., and Biber, J. (1994). Cellular mechanisms of acute and chronic adaptation of renal Pi transporter to alterations in dietary Pi. Am. J. Physiol.-Ren. Fluid Electrolyte Physiol. *36*, F900–F908.

Leviel, F., Hübner, C.A., Houillier, P., Morla, L., El Moghrabi, S., Brideau, G., Hatim, H., Parker, M.D., Kurth, I., Kougioumtzes, A., et al. (2010). The Na+-

dependent chloride-bicarbonate exchanger SLC4A8 mediates an electroneutral Na+ reabsorption process in the renal cortical collecting ducts of mice. J. Clin. Invest. *120*, 1627–1635.

Lewington, S., Clarke, R., Qizilbash, N., Peto, R., and Collins, R. (2002). Age-specific relevance of usual blood pressure to vascular mortality: a meta-analysis of individual data for one million adults in 61 prospective studies. The Lancet *360*, 1903–1913.

Li, X.C., and Zhuo, J.L. (2007). Selective knockdown of AT1 receptors by RNA interference inhibits Val5-ANG II endocytosis and NHE-3 expression in immortalized rabbit proximal tubule cells. AJP Cell Physiol. *293*, C367–C378.

Li, W., Jiang, X., Ma, H., Ignatius Yu, T., Ma, L., Puente, J.G., Tang, Y., He, X., Ma, S., Jin, S., et al. (2003). Awareness, treatment and control of hypertension in patients attending hospital clinics in China. J. Hypertens. *21*, 1191–1197.

Li, Z., Sun, F., Zhang, Y., Chen, H., He, N., Chen, H., Song, P., Wang, Y., Yan, S., and Zheng, S. (2015). Tacrolimus Induces Insulin Resistance and Increases the Glucose Absorption in the Jejunum: A Potential Mechanism of the Diabetogenic Effects. PLOS ONE *10*, e0143405.

Ligtenberg, G., Hene, R.J., Blankestijn, P.J., and Koomans, H.A. (2001). Cardiovascular Risk Factors in Renal Transplant Patients: Cyclosporin A Versus Tacrolimus. J. Am. Soc. Nephrol. *12*, 368–373.

Lim, S.S., Vos, T., Flaxman, A.D., Danaei, G., Shibuya, K., Adair-Rohani, H., AlMazroa, M.A., Amann, M., Anderson, H.R., Andrews, K.G., et al. (2012). A comparative risk assessment of burden of disease and injury attributable to 67 risk factors and risk factor clusters in 21 regions, 1990–2010: a systematic analysis for the Global Burden of Disease Study 2010. The Lancet *380*, 2224–2260.

Lima, M. de L., Cruz, T., Rodrigues, L.E., Bomfim, O., Melo, J., Correia, R., Porto, M., Cedro, A., and Vicente, E. (2009a). Serum and intracellular magnesium deficiency in patients with metabolic syndrome—Evidences for its relation to insulin resistance. Diabetes Res. Clin. Pract. *83*, 257–262.

Lima, M. de L., Cruz, T., Rodrigues, L.E., Bomfim, O., Melo, J., Correia, R., Porto, M., Cedro, A., and Vicente, E. (2009b). Serum and intracellular magnesium deficiency in patients with metabolic syndrome—Evidences for its relation to insulin resistance. Diabetes Res. Clin. Pract. *83*, 257–262.

Lin, H.-Y., Rocher, L.L., McQuillan, M.A., Schmaltz, S., Palella, T.D., and Fox, I.H. (1989). Cyclosporine-Induced Hyperuricemia and Gout. N. Engl. J. Med. *321*, 287–292.

Liu, J., Farmer, J.D., Lane, W.S., Friedman, J., Weissman, I., and Schreiber,

S.L. (1991). Calcineurin is a common target of cyclophilin-cyclosporin A and FKBP-FK506 complexes. Cell *66*, 807–815.

Liu, J., Albers, M.W., Wandless, T.J., Luan, S., Alberg, D.G., Belshaw, P.J., Cohen, P., MacKintosh, C., Klee, C.B., and Schreiber, S.L. (1992). Inhibition of T cell signaling by immunophilin-ligand complexes correlates with loss of calcineurin phosphatase activity. Biochemistry (Mosc.) *31*, 3896–3901.

Liu, Y., Wan, Q., Guan, Q., Gao, L., and Zhao, J. (2006). High-fat diet feeding impairs both the expression and activity of AMPKa in rats' skeletal muscle. Biochem. Biophys. Res. Commun. *339*, 701–707.

Loffing, J., Pietri, L., Aregger, F., Bloch-Faure, M., Ziegler, U., Meneton, P., Rossier, B.C., and Kaissling, B. (2000). Differential subcellular localization of ENaC subunits in mouse kidney in response to high-and low-Na diets. Am. J. Physiol.-Ren. Physiol. *279*, F252–F258.

Loffing, J., Loffing-Cueni, D., Valderrabano, V., Klausli, L., Hebert, S.C., Rossier, B.C., Hoenderop, J.G.J., Bindels, R.J.M., and Kaissling, B. (2001). Distribution of transcellular calcium and sodium transport pathways along mouse distal nephron. Am. J. Physiol. - Ren. Physiol. *50*, F1021 – F1027.

Loh, C., Shaw, K.T.-Y., Carew, J., Viola, J.P.B., Luo, C., Perrino, B.A., and Rao, A. (1996). Calcineurin Binds the Transcription Factor NFAT1 and Reversibly Regulates Its Activity. J. Biol. Chem. *271*, 10884–10891.

Lorenz, J.N., Schultheis, P.J., Traynor, T., Shull, G.E., and Schnermann, J. (1999). Micropuncture analysis of single-nephron function in NHE3-deficient mice. Am. J. Physiol.-Ren. Physiol. *277*, F447-53.

Lorenz, J.N., Nieman, M., Sabo, J., Sanford, L.P., Hawkins, J.A., Elitsur, N., Gawenis, L.R., Clarke, L.L., and Cohen, M.B. (2003). Uroguanylin knockout mice have increased blood pressure and impaired natriuretic response to enteral NaCl load. J. Clin. Invest. *112*, 1244–1254.

Lorenz-Depiereux, B., Benet-Pages, A., Eckstein, G., Tenenbaum-Rakover, Y., Wagenstaller, J., Tiosano, D., Gershoni-Baruch, R., Albers, N., Lichtner, P., and Schnabel, D. (2006). Hereditary hypophosphatemic rickets with hypercalciuria is caused by mutations in the sodium-phosphate cotransporter gene SLC34A3. Am. J. Hum. Genet. *78*, 193–201.

Lote, C.J., Thewles, A., Wood, J.A., and Zafar, T. (2000). The hypomagnesaemic action of FK506: urinary excretion of magnesium and calcium and the role of parathyroid hormone. Clin. Sci. *99*, 285–292.

Louis-Dit-Picard, H., Barc, J., Trujillano, D., Miserey-Lenkei, S., Bouatia-Naji, N., Pylypenko, O., Beaurain, G., Bonnefond, A., Sand, O., Simian, C., et al. (2012). KLHL3 mutations cause familial hyperkalemic hypertension by impairing ion transport in the distal nephron. Nat. Genet. *44*, 456–460.

Luan, F.L., Langewisch, E., and Ojo, A. (2010). Metabolic syndrome and new onset diabetes after transplantation in kidney transplant recipients: Metabolic syndrome and new onset diabetes mellitus. Clin. Transplant. *24*, 778–783.

van der Lubbe, N., Jansen, P.M., Salih, M., Fenton, R.A., van der Meiracker, A.H., Danser, A.H.J., Zietse, R., and Hoorn, E.J. (2012). The phosphorylated sodium chloride cotransporter in urinary exosomes is superior to prostasin as a marker for aldosteronism. Hypertension *60*, 741–748.

Lv, L.-L., Cao, Y., Liu, D., Xu, M., Liu, H., Tang, R.-N., Ma, K.-L., and Liu, B.-C. (2013). Isolation and Quantification of MicroRNAs from Urinary Exosomes/Microvesicles for Biomarker Discovery. Int. J. Biol. Sci. *9*, 1021–1031.

Lyson, T., Ermel, L.D., Belshaw, P.J., Alberg, D.G., Schreiber, S.L., and Victor, R.G. (1993). Cyclosporine- and FK506-induced sympathetic activation correlates with calcineurin-mediated inhibition of T-cell signaling. Circ. Res. *73*, 596–602.

Maalouf, N.M., Cameron, M.A., Moe, O.W., Adams-Huet, B., and Sakhaee, K. (2007). Low Urine pH: A Novel Feature of the Metabolic Syndrome. Clin. J. Am. Soc. Nephrol. *2*, 883–888.

Magagnin, S., Werner, A., Markovich, D., Sorribas, V., Stange, G., Biber, J., and Murer, H. (1993). Expression cloning of human and rat renal cortex Na/Pi cotransport. Proc. Natl. Acad. Sci. *90*, 5979–5983.

Magen, D., Sprecher, E.L.I., Zelikovic, I., and Skorecki, K. (2005). A novel missense mutation in SLC5A2 encoding SGLT2 underlies autosomal-recessive renal glucosuria and aminoaciduria. Kidney Int. *67*, 34–41.

Malheiro, J., Almeida, M., Fonseca, I., Martins, L.S., Pedroso, S., Dias, L., Henriques, A.C., and Cabrita, A. (2012). Hyperuricemia in Adult Renal Allograft Recipients: Prevalence and Predictors. Transplant. Proc. *44*, 2369–2372.

Manning, R.D., Coleman, T.G., Guyton, A.C., Norman, R.A., and McCaa, R.E. (1979a). Essential role of mean circulatory filling pressure in salt-induced hypertension. Am. J. Physiol.-Regul. Integr. Comp. Physiol. *236*, R40–R47.

Manning, R.D., Guyton, A.C., Coleman, T.G., and McCaa, R.E. (1979b). Hypertension in dogs during antidiuretic hormone and hypotonic saline infusion. Am. J. Physiol. - Heart Circ. Physiol. *236*, H314–H322.

Marcen, R., Gallego, N., Orofino, L., Sabater, J., Pascual, J., Teruel, J.L., Liano, F., and Ortuño, J. (1992). Influence of cyclosporin A (CyA) on renal handling of urate. Transpl. Int. *5*, S81–S83.

Margreiter, R. (2002). Efficacy and safety of tacrolimus compared with ciclosporin microemulsion in renal transplantation: a randomised multicentre study. The Lancet *359*, 741–46.

Marks, J., Srai, S.K., Biber, J., Murer, H., Unwin, R.J., and Debnam, E.S. (2006). Intestinal phosphate absorption and the effect of vitamin D: a comparison of rats with mice: Intestinal phosphate transport in rats and mice. Exp. Physiol. *91*, 531–537.

Marks, J., Churchill, L.J., Srai, S.K., Biber, J., Murer, H., Jaeger, P., Debnam, E.S., Unwin, R.J., and Group, C.B. (2007). Intestinal phosphate absorption in a model of chronic renal failure. Kidney Int. *72*, 166–173.

Marks, J., Churchill, L.J., Debnam, E.S., and Unwin, R.J. (2008). Matrix Extracellular Phosphoglycoprotein Inhibits Phosphate Transport. J. Am. Soc. Nephrol. *19*, 2313–2320.

Marumo, T., Nakaki, T., Hishikawa, K., Suzuki, H., Kato, R., and Saruta, T. (1995). Cyclosporin A Inhibits Nitric Oxide Synthase Induction in Vascular Smooth Muscle Cells. Hypertension *25*, 764–768.

Masilamani, S., Kim, G.-H., Mitchell, C., Wade, J.B., and Knepper, M.A. (1999). Aldosterone-mediated regulation of ENaC α, β, and γ subunit proteins in rat kidney. J. Clin. Invest. *104*, R19.

Mather, H.M., Nisbet, J.A., Burton, G.H., Poston, G.J., Bland, J.M., Bailey, P.A., and Pilkington, T.R.E. (1979). Hypomagnesaemia in diabetes. Clin. Chim. Acta *95*, 235–242.

May, A., Puoti, A., Gaeggeler, H.-P., Horisberger, J.-D., and Rossier, B.C. (1997). Early effect of aldosterone on the rate of synthesis of the epithelial sodium channel alpha subunit in A6 renal cells. J. Am. Soc. Nephrol. *8*, 1813–1822.

Mayan, H., Attar-Herzberg, D., Shaharabany, M., Holtzman, E.J., and Farfel, Z. (2008). Increased urinary Na-Cl cotransporter protein in familial hyperkalaemia and hypertension. Nephrol. Dial. Transplant. *23*, 492–496.

McCormick, J.A., Nelson, J.H., Yang, C.-L., Curry, J.N., and Ellison, D.H. (2011). Overexpression of the Sodium Chloride Cotransporter Is Not Sufficient to Cause Familial Hyperkalemic Hypertension. Hypertension *58*, 888–894.

McCune, T.R., Thacker II, L.R., Peters, T.G., Mulloy, L., Rohr, M.S., Adams, P.A., Yium, J., Light, J.A., Pruett, T., Gaber, A.O., et al. (1998). Effects of Tacrolimus on hyperlipidemia after successful renal transplantation: A Southeastern Organ Procurement Foundation Multicenter Clinical Study. Transplantation *65*, 87–92.

McDiarmid, S.V., Colonna II, J.O., Shaked, A., Ament, M.E., and Busuttil, R.W. (1993). A comparison of renal function in cyclosporine- and FK-506-treated patients after primary orthotopic liver transplantation. Transplantation *56*, 847–853.

McKee, J.A., Kumar, S., Ecelbarger, C.A., Fernández-Llama, P., Terris, J., and Knepper, M.A. (2000). Detection of Na(+) transporter proteins in urine. J. Am. Soc. Nephrol. *11*, 2128–2132.

Meier-Kriesche, H.-U., Arndorfer, J.A., and Kaplan, B. (2002). The impact of body mass index on renal transplant outcomes: a significant independent risk factor for graft failure and patient death. Transplantation *73*, 70–74.

Meisinger, C., Heier, M., Volzke, H., Lowel, H., Mitusch, R., Hense, H.-W., and Ludemann, J. (2006). Regional disparities of hypertension prevalence and management within Germany. J. Hypertens. *24*, 293–299.

Mell, B., Jala, V.R., Mathew, A.V., Byun, J., Waghulde, H., Zhang, Y., Haribabu, B., Vijay-Kumar, M., Pennathur, S., and Joe, B. (2015). Evidence for a link between gut microbiota and hypertension in the Dahl rat. Physiol. Genomics *47*, 187–197.

Melnikov, S., Mayan, H., Uchida, S., Holtzman, E.J., and Farfel, Z. (2011). Cyclosporine metabolic side effects: association with the WNK4 system: CYCLOSPORINE SIDE EFFECTS AND WNK4. Eur. J. Clin. Invest. *41*, 1113–1120.

Merchant, M.L., Powell, D.W., Wilkey, D.W., Cummins, T.D., Deegens, J.K., Rood, I.M., McAfee, K.J., Fleischer, C., Klein, E., and Klein, J.B. (2010). Microfiltration isolation of human urinary exosomes for characterization by MS. PROTEOMICS - Clin. Appl. *4*, 84–96.

Meyer, J.W., Flagella, M., Sutliff, R.L., Lorenz, J.N., Nieman, M.L., Weber, C.S., Paul, R.J., and Shull, G.E. (2002). Decreased blood pressure and vascular smooth muscle tone in mice lacking basolateral Na^+-K^+-$2Cl^-$ cotransporter. Am. J. Physiol. - Heart Circ. Physiol. *283*, H1846–H1855.

Meyer, M.H., Meyer, R.A., Gray, R.W., and Irwin, R.L. (1985). Picric acid methods greatly overestimate serum creatinine in mice: more accurate results with high-performance liquid chromatography. Anal. Biochem. *144*, 285–290.

Miller, D.G., Edwards, R.H., and Miller, A.D. (1994). Cloning of the cellular receptor for amphotropic murine retroviruses reveals homology to that for gibbon ape leukemia virus. Proc. Natl. Acad. Sci. U. S. A. *91*, 78–82.

Min, X., Lee, B.-H., Cobb, M.H., and Goldsmith, E.J. (2004). Crystal Structure of the Kinase Domain of WNK1, a Kinase that Causes a Hereditary Form of Hypertension. Structure *12*, 1303–1311.

Miranda, K.C., Bond, D.T., McKee, M., Skog, J., Paunescu, T.G., Da Silva, N., Brown, D., and Russo, L. (2010). Nucleic acids within urinary exosomes/microvesicles are potential biomarkers for renal disease. Kidney Int. *78*, 191–199.

Miyamoto, K., Segawa, H., Morita, K., NII, T., Tatsumi, S., Taketani, Y., and Takeda, E. (1997). Relative contributions of Na+-dependent phosphate co-transporters to phosphate transport in mouse kidney: RNase H-mediated hybrid depletion analysis. Biochem. J. *327*, 735–739.

Mohan, V., Deepa, M., Farooq, S., Datta, M., and Deepa, R. (2007). Prevalence, Awareness and Control of Hypertension in Chennai - The Chennai Urban Rural Epidemiology Study (CURES – 52). J. Assoc. Physicians India *55*, 326–332.

Mohebbi, N., Mihailova, M., and Wagner, C.A. (2009). The calcineurin inhibitor FK506 (tacrolimus) is associated with transient metabolic acidosis and altered expression of renal acid-base transport proteins. AJP Ren. Physiol. *297*, F499–F509.

Molkentin, J.D., Lu, J.-R., Antos, C.L., Markham, B., Richardson, J., Robbins, J., Grant, S.R., and Olson, E.N. (1998). A calcineurin-dependent transcriptional pathway for cardiac hypertrophy. Cell *93*, 215–228.

Moorhead, J.F., Ahmed, K.Y., Varghese, Z., Wills, M.R., Baillod, R.A., and Tatler, G.L. (1974). Hypophosphataemic osteomalacia after cadaveric renal transplantation. The Lancet *1*, 693–694.

Morgan, B.J., Lyson, T., Scherrer, U., and Victor, R.G. (1991). Cyclosporine Causes Sympathetically Mediated Elevations in Arterial Pressure in Rats. Hypertension *18*, 458–466.

Mori, Y., Wakabayashi, M., Mori, T., Araki, Y., Sohara, E., Rai, T., Sasaki, S., and Uchida, S. (2013). Decrease of WNK4 ubiquitination by disease-causing mutations of KLHL3 through different molecular mechanisms. Biochem. Biophys. Res. Commun. *439*, 30–34.

Moriguchi, T., Urushiyama, S., Hisamoto, N., Iemura, S., Uchida, S., Natsume, T., Matsumoto, K., and Shibuya, H. (2005). WNK1 Regulates Phosphorylation of Cation-Chloride-coupled Cotransporters via the STE20-related Kinases, SPAK and OSR1. J. Biol. Chem. *280*, 42685–42693.

Morris, S.T.W., McMurray, J.J.V., Rodger, R.S.C., Farmer, R., and Jardine, A.G. (2000). Endothelial dysfunction in renal transplant recipients maintained on cyclosporine. Kidney Int. *57*, 1100–1106.

Moss, N.G., Powell, S.L., and Falk, R.J. (1985). Intravenous cyclosporine activates afferent and efferent renal nerves and causes sodium retention in innervated kidneys in rats. Proc. Natl. Acad. Sci. U. S. A. *82*, 8222–8226.

Moz, Y., Levi, R., Lavi-Moshayoff, V., Cox, K.B., Molkentin, J.D., Silver, J., and Naveh-Many, T. (2004). Calcineurin A Is Central to the Expression of the Renal Type II Na/Pi Co-transporter Gene and to the Regulation of Renal Phosphate Transport. J. Am. Soc. Nephrol. *15*, 2972–2980.

Mu, J.Y., Hansson, G.C., Bergstrom, G., and Lundgren, O. (1995). Renal sodium excretion after oral or intravenous sodium loading in sodium-deprived normotensive and spontaneously hypertensive rats. Acta Physiol. Scand. *153*, 169–177.

Murer, H., Hopfer, U., and Kinne, R. (1976). Sodium/proton antiport in brush-border-membrane vesicles isolated from rat small intestine and kidney. Biochem. J. *154*, 597–604.

Murray, B.M., Paller, M.S., and Ferris, T.F. (1985). Effect of cyclosporine administration on renal hemodynamics in conscious rats. Kidney Int. *28*, 767–774.

Mutig, K., Saritas, T., Uchida, S., Kahl, T., Borowski, T., Paliege, A., Bohlick, A., Bleich, M., Shan, Q., and Bachmann, S. (2010). Short-term stimulation of the thiazide-sensitive Na+-Cl- cotransporter by vasopressin involves phosphorylation and membrane translocation. AJP Ren. Physiol. *298*, F502–F509.

Nagase, M., Yoshida, S., Shibata, S., Nagase, T., Gotoda, T., Ando, K., and Fujita, T. (2006). Enhanced Aldosterone Signaling in the Early Nephropathy of Rats with Metabolic Syndrome: Possible Contribution of Fat-Derived Factors. J. Am. Soc. Nephrol. *17*, 3438–3446.

Nasser, S.A., Sabra, R., Elmallah, A.I., El-Din, M.M.M., Khedr, M.M., and El-Mas, M.M. (2016). Facilitation by the renin-angiotensin system of cyclosporine-evoked hypertension in rats: Role of arterial baroreflexes and vasoreactivity. Life Sci. *163*, 1–10.

National Cholesterol Education Program (NCEP) (2012). Third Report of the National Cholesterol Education Program (NCEP) Expert Panel on Detection, Evaluation, and Treatment of High Blood Cholesterol in Adults (Adult Treatment Panel III). National Heart, Lung, and Blood Institute.

National Institute for Health and Care Excellence (NICE) (2011). Hypertension in adults: diagnosis and management. Hypertension.

Nickenig, G., Strehlow, K., Roeling, J., Zolk, O., Knorr, A., and Bohm, M. (1998). Salt Induces Vascular AT1 Receptor Overexpression In Vitro and In Vivo. Hypertension *31*, 1272–1277.

Nielsen, S., Maunsbach, A.B., Ecelbarger, C.A., and Knepper, M.A. (1998). Ultrastructural localization of Na-K-2Cl cotransporter in thick ascending limb and macula densa of rat kidney. Am. J. Physiol. - Ren. Physiol. *44*, F885 –

F893.

Nijenhuis, T., Hoenderop, J.G.J., and Bindels, R.J.M. (2004). Downregulation of Ca2+ and Mg2+ Transport Proteins in the Kidney Explains Tacrolimus (FK506)-Induced Hypercalciuria and Hypomagnesemia. J. Am. Soc. Nephrol. *15*, 549–557.

Nishida, H., Sohara, E., Nomura, N., Chiga, M., Alessi, D.R., Rai, T., Sasaki, S., and Uchida, S. (2012). Phosphatidylinositol 3-Kinase/Akt Signaling Pathway Activates the WNK-OSR1/SPAK-NCC Phosphorylation Cascade in Hyperinsulinemic db/db Mice * Novelty and Significance. Hypertension *60*, 981–990.

Noonan, W.T., Woo, A.L., Nieman, M.L., Prasad, V., Schultheis, P.J., Shull, G.E., and Lorenz, J.N. (2005). Blood pressure maintenance in NHE3-deficient mice with transgenic expression of NHE3 in small intestine. AJP Regul. Integr. Comp. Physiol. *288*, R685–R691.

Norman, R.A., Coleman, T.G., Wiley, T.L., Manning, R.D., and Guyton, A.C. (1975). Separate roles of sodium ion concentration and fluid volumes in salt-loading hypertension in sheep. Am. J. Physiol. *229*, 1068–1072.

Nozue, T., Kobayashi, A., Kodama, T., Uemasu, F., Endoh, H., Sako, A., and Takagi, Y. (1992). Clinical and laboratory observations. Pathogenesis of cyclosporine-induced hypomagnesemia. J. Pediatr. *120*, 638–640.

Obermüller, N., Kunchaparty, S., Ellison, D.H., and Bachmann, S. (1996). Expression of the Na-K-2Cl Cotransporter by Macula Densa and Thick Ascending Limb Cells of Rat and Rabbit Nephron. J. Clin. Invest. *98*, 635–640.

O'Hara, B., Johann, S.V., Klinger, H.P., Blair, D.G., Rubinson, H., Dunn, K.J., Sass, P., Vitek, S.M., and Robins, T. (1990). Characterisation of a human gene conferring sensitivity to infection by Gibbon Ape Leukemia Virus. Cell Growth Differ. *1*, 119–127.

Ohi, A., Hanabusa, E., Ueda, O., Segawa, H., Horiba, N., Kaneko, I., Kuwahara, S., Mukai, T., Sasaki, S., Tominaga, R., et al. (2011). Inorganic phosphate homeostasis in sodium-dependent phosphate cotransporter Npt2b+/- mice. AJP Ren. Physiol. *301*, F1105–F1113.

Ohkido, I., Segawa, H., Yanagida, R., Nakamura, M., and Miyamoto, K. (2003). Cloning, gene structure and dietary regulation of the type-IIc Na/Pi cotransporter in the mouse kidney. Pflüg. Arch. - Eur. J. Physiol. *446*, 106–115.

Ohta, A., Rai, T., Yui, N., Chiga, M., Yang, S.-S., Lin, S.-H., Sohara, E., Sasaki, S., and Uchida, S. (2009). Targeted disruption of the Wnk4 gene decreases phosphorylation of Na-Cl cotransporter, increases Na excretion

and lowers blood pressure. Hum. Mol. Genet. *18*, 3978–3986.

Ohta, A., Schumacher, F.-R., Mehellou, Y., Johnson, C., Knebel, A., Macartney, T.J., Wood, N.T., Alessi, D.R., and Kurz, T. (2013). The CUL3–KLHL3 E3 ligase complex mutated in Gordon's hypertension syndrome interacts with and ubiquitylates WNK isoforms: disease-causing mutations in KLHL3 and WNK4 disrupt interaction. Biochem. J. *451*, 111–122.

Olah, Z., Lehel, C., Anderson, W.B., Eiden, M.V., and Wilson, C.A. (1994). The cellular receptor for gibbon ape leukemia virus is a novel high affinity sodium-dependent phosphate transporter. J. Biol. Chem. *269*, 25426–25431.

Ong, C.S., Pollock, C.A., Caterson, R.J., Mahony, J.F., Waugh, D.A., and Ibels, L.S. (1994). Hyperlipidemia in renal transplant recipients: Natural history and response to treatment. Medicine (Baltimore) *73*, 215–223.

Oosthuyzen, W., Sime, N.E.L., Ivy, J.R., Turtle, E.J., Street, J.M., Pound, J., Bath, L.E., Webb, D.J., Gregory, C.D., Bailey, M.A., et al. (2013). Quantification of human urinary exosomes by nanoparticle tracking analysis: Nanoparticle tracking analysis and exosomes. J. Physiol. *591*, 5833–5842.

Opelz, G., Wujciak, T., and Ritz, E. (1998). Association of chronic kidney graft failure with recipient blood pressure. Kidney Int. *53*, 217–222.

Opelz, G., Dohler, B., and for the Collaborative Transplant Study (2005). Improved Long-Term Outcomes After Renal Transplantation Associated with Blood Pressure Control. Am. J. Transplant. *5*, 2725–2731.

Oriji, G.K., and Keiser, H.R. (1998). Role of Nitric Oxide in Cyclosporine A–Induced Hypertension. Hypertension *32*, 849–855.

Pacha, J., Frindt, G., Antonian, L., Silver, R.B., and Palmer, L.G. (1993). Regulation of Na channels of the rat cortical collecting tubule by aldosterone. J. Gen. Physiol. *102*, 25–42.

Pacheco-Alvarez, D., Cristóbal, P.S., Meade, P., Moreno, E., Vazquez, N., Muñoz, E., Díaz, A., Juárez, M.E., Giménez, I., and Gamba, G. (2006). The Na+:Cl- Cotransporter Is Activated and Phosphorylated at the Amino-terminal Domain upon Intracellular Chloride Depletion. J. Biol. Chem. *281*, 28755–28763.

Paigen, B., Morrow, A., Brandon, C., Mitchell, D., and Holmes, P. (1985). Variation in susceptibility to atherosclerosis among inbred strains of mice. Atherosclerosis *57*, 65–73.

Palm, M., and Lundblad, A. (2005). Creatinine concentration in plasma from dog, rat, and mouse: a comparison of 3 different methods. Vet. Clin. Pathol. *34*, 232–236.

Palmada, M. (2004). Regulation of intestinal phosphate cotransporter NaPi IIb by ubiquitin ligase Nedd4-2 and by serum- and glucocorticoid-dependent kinase 1. AJP Gastrointest. Liver Physiol. *287*, G143–G150.

Paredes, A., Plata, C., Rivera, M., Moreno, E., Vazquez, N., Munoz-Clares, R., Hebert, S.C., and Gamba, G. (2006). Activity of the renal Na+-K+-2Cl- cotransporter is reduced by mutagenesis of N-glycosylation sites: role for protein surface charge in Cl- transport. AJP Ren. Physiol. *290*, F1094–F1102.

Park, H.G., Yi, H., Kim, S.H., Yu, H.S., Ahn, Y.M., Lee, Y.H., Roh, M.-S., and Kim, Y.S. (2011). The effect of cyclosporine A on the phosphorylation of the AMPK pathway in the rat hippocampus. Prog. Neuropsychopharmacol. Biol. Psychiatry *35*, 1933–1937.

Pasham, V., Pathare, G., Fajol, A., Rexhepaj, R., Michael, D., Pakladok, T., Alesutan, I., Rotte, A., Foller, M., and Lang, F. (2012). OSR1-sensitive small intestinal Na+ transport. AJP Gastrointest. Liver Physiol. *303*, G1212–G1219.

Pathare, G., Föller, M., Daryadel, A., Mutig, K., Bogatikov, E., Fajol, A., Almilaji, A., Michael, D., Stange, G., Voelkl, J., et al. (2012a). OSR1-Sensitive Renal Tubular Phosphate Reabsorption. Kidney Blood Press. Res. *36*, 149–161.

Pathare, G., Tutakhel, O.A.Z., van der Wel, M.C., Shelton, L.M., Deinum, J., Lenders, J.W.M., Hoenderop, J.G.J., and Bindels, R.J.M. (2017). Hydrochlorothiazide treatment increases the abundance of the NaCl cotransporter in urinary extracellular vesicles of essential hypertensive patients. Am. J. Physiol. - Ren. Physiol. *312*, F1063–F1072.

Payne, J.A., and Forbush, B. (1994). Alternatively spliced isoforms of the putative renal Na-K-Cl cotransporter are differentially distributed within the rabbit kidney. Proc. Natl. Acad. Sci. *91*, 4544–4548.

Payne, J.A., Xu, J.-C., Haas, M., Lytle, C., Ward, D., and Forbush, B. (1995). Primary structure, functional expression, and chromosomal localization of the bumetanide-sensitive Na-K-Cl cotransporter in human colon. J. Biol. Chem. *270*, 17977–17985.

Pedersen, N.B., Hofmeister, M.V., Rosenbaek, L.L., Nielsen, J., and Fenton, R.A. (2010). Vasopressin induces phosphorylation of the thiazide-sensitive sodium chloride cotransporter in the distal convoluted tubule. Kidney Int. *78*, 160–169.

Pedrollo, E.F., Corrêa, C., Nicoletto, B.B., Manfro, R.C., Leitão, C.B., Souza, G.C., and Gonçalves, L.F.S. (2016). Effects of metabolic syndrome on kidney transplantation outcomes: a systematic review and meta-analysis. Transpl. Int. *29*, 1059–1066.

Pereira, M., Lunet, N., Azevedo, A., and Barros, H. (2009). Differences in prevalence, awareness, treatment and control of hypertension between developing and developed countries: J. Hypertens. *27*, 963–975.

Perez-Fernandez, R., Marino, A.F., Cadarso-Suarez, C., Botana, M.A., Tome, M.A., Solache, I., Rego-Iraeta, A., and Mato, A.J. (2007). Prevalence, awareness, treatment and control of hypertension in Galicia (Spain) and association with related diseases. J. Hum. Hypertens. *21*, 366–373.

Piechotta, K., Lu, J., and Delpire, E. (2002). Cation Chloride Cotransporters Interact with the Stress-related Kinases Ste20-related Proline-Alanine-rich Kinase (SPAK) and Oxidative Stress Response 1 (OSR1). J. Biol. Chem. *277*, 50812–50819.

Piechotta, K., Garbarini, N., England, R., and Delpire, E. (2003). Characterization of the Interaction of the Stress Kinase SPAK with the Na^+-K^+-$2Cl^-$ Cotransporter in the Nervous System: EVIDENCE FOR A SCAFFOLDING ROLE OF THE KINASE. J. Biol. Chem. *278*, 52848–52856.

Pinto, V., Pinho, M.J., Hopfer, U., Jose, P.A., and Soares-da-Silva, P. (2008). Oxidative stress and the genomic regulation of aldosterone-stimulated NHE1 activity in SHR renal proximal tubular cells. Mol. Cell. Biochem. *310*, 191–201.

Pirsch, J.D., Miller, J., Deierhoi, M.H., Vincenti, F., and Filo, R.S. (1997). A comparison of Tacrolimus (FK506) and Cyclosporine for immunosuppression after cadaveric renal transplantation. Transplantation *63*, 977–983.

Pisitkun, T., Shen, R.-F., and Knepper, M.A. (2004). Identification and proteomic profiling of exosomes in human urine. Proc. Natl. Acad. Sci. U. S. A. *101*, 13368–13373.

Pisitkun, T., Gandolfo, M.T., Das, S., Knepper, M.A., and Bagnasco, S.M. (2012). Application of systems biology principles to protein biomarker discovery: Urinary exosomal proteome in renal transplantation. PROTEOMICS - Clin. Appl. *6*, 268–278.

Plotkin, M.D., Kaplan, M.R., Verlander, J.W., Lee, W.-S., Brown, D., Poch, E., Gullans, S.R., and Hebert, S.C. (1996). Localization of the thiazide sensitive Na-Cl cotransporter, rTSC1, in the rat kidney. Kidney Int. *50*, 174–183.

Ponce-Coria, J., San-Cristobal, P., Kahle, K.T., Vazquez, N., Pacheco-Alvarez, D., de los Heros, P., Juárez, P., Muñoz, E., Michel, G., and Bobadilla, N.A. (2008). Regulation of NKCC2 by a chloride-sensing mechanism involving the WNK3 and SPAK kinases. Proc. Natl. Acad. Sci. *105*, 8458–8463.

Ponticelli, C., Montagnino, G., Aroldi, A., Angelini, C., Braga, M., and

Tarantino, A. (1993). Hypertension after renal transplantation. Am. J. Kidney Dis. *21*, 73–78.

Porrini, E., Moreno, J.M., Osuna, A., Benitez, R., Lampreabe, I., Diaz, J.M., Silva, I., Domínguez, R., Gonzalez-Cotorruelo, J., Bayes, B., et al. (2008a). Prediabetes in Patients Receiving Tacrolimus in the First Year After Kidney Transplantation: A Prospective and Multicenter Study: Transplantation *85*, 1133–1138.

Porrini, E., Delgado, P., Alvarez, A., Cobo, M., Perez, L., Gonzalez-Posada, J.M., Hortal, L., Gallego, R., Garcia, J.J., Checa, M., et al. (2008b). The combined effect of pre-transplant triglyceride levels and the type of calcineurin inhibitor in predicting the risk of new onset diabetes after renal transplantation. Nephrol. Dial. Transplant. *23*, 1436–1441.

Porrini, E., Delgado, P., Bigo, C., Alvarez, A., Cobo, M., Checa, M.D., Hortal, L., Fernández, A., García, J.J., Velázquez, S., et al. (2006). Impact of Metabolic Syndrome on Graft Function and Survival After Cadaveric Renal Transplantation. Am. J. Kidney Dis. *48*, 134–142.

Powell, D.R., DaCosta, C.M., Gay, J., Ding, Z.-M., Smith, M., Greer, J., Doree, D., Jeter-Jones, S., Mseeh, F., Rodriguez, L.A., et al. (2013). Improved glycemic control in mice lacking Sglt1 and Sglt2. AJP Endocrinol. Metab. *304*, E117–E130.

Pradervand, S., Barker, P.M., Wang, Q., Ernst, S.A., Beermann, F., Grubb, B.R., Burnier, M., Schmidt, A., Bindels, R.J.M., Gatzy, J.T., et al. (1999a). Salt restriction induces pseudohypoaldosteronism type 1 in mice expressing low levels of the B-subunit of the amiloride-sensitive epithelial sodium channel. Proc. Natl. Acad. Sci. U. S. A. *96*, 1732–1737.

Pradervand, S., Wang, Q., Burnier, M., Beermann, F., Horisberger, J.-D., Hummler, E., and Rossier, B.C. (1999b). A Mouse Model for Liddle's Syndrome. J. Am. Soc. Nephrol. *10*, 2527–2533.

Primatesta, P., and Poulter, N.R. (2006). Improvement in hypertension management in England: results from the Health Survey for England 2003. J. Hypertens. *24*, 1187–1192.

Primatesta, P., Brookes, M., and Poulter, N.R. (2001). Improved Hypertension Management and Control: Results From the Health Survey for England 1998. Hypertension *38*, 827–832.

Rabinowitz, L., Green, D.M., Sarason, R.L., and Yamauchi, H. (1988). Homeostatic potassium excretion in fed and fasted sheep. Am. J. Physiol.-Regul. Integr. Comp. Physiol. *254*, R357–R380.

Radanovic, T., Wagner, C.A., Murer, H., and Biber, J. (2005). Regulation of Intestinal Phosphate Transport I. Segmental expression and adaptation to

low-Pi diet of the type IIb Na+-Pi cotransporter in mouse small intestine. AJP Gastrointest. Liver Physiol. *288*, G496–G500.

Rafiqi, F.H., Zuber, A.M., Glover, M., Richardson, C., Fleming, S., Jovanović, S., Jovanović, A., O'Shaughnessy, K.M., and Alessi, D.R. (2010). Role of the WNK-activated SPAK kinase in regulating blood pressure: Control of blood pressure by SPAK kinase. EMBO Mol. Med. *2*, 63–75.

Rahmoune, H., Thompson, P.W., Ward, J.M., Smith, C.D., Hong, G., and Brown, J. (2005). Glucose transporters in human renal proximal tubular cells isolated from the urine of patients with non–insulin-dependent diabetes. Diabetes *54*, 3427–3434.

Raj, D.A.A., Fiume, I., Capasso, G., and Pocsfalvi, G. (2012). A multiplex quantitative proteomics strategy for protein biomarker studies in urinary exosomes. Kidney Int. *81*, 1263–1272.

Rampoldi, L., Caridi, G., Santon, D., Boaretto, F., Bernascone, I., Lamorte, G., Tardanico, R., Dagnino, M., Colussi, G., Scolari, F., et al. (2003). Allelism of MCKD, FJHN and GCKD caused by impairment of uromodulin export dynamics. Hum. Mol. Genet. *12*, 3369–3384.

Ranger, A.M., Grusby, M.J., Hodge, M.R., Gravallese, E.M., de La Brousse, F.C., Hoey, T., Mickanin, C., Baldwin, H.S., and Glimcher, L.H. (1998). The transcription factor NF-ATc is essential for cardiac valve formation. Nature *392*, 186–190.

Rasch, R., Torffvit, O., Jensen, P.K., and Jacobsen, N.O. (1995). Tamm-Horsfall glycoprotein in streptozotocin diabetic rats: a study of kidney in situ hybridization, immunohistochemistry, and urinary excretion. Diabetologia *38*, 525–535.

Raya, A.I., Rios, R., Pineda, C., Rodriguez-Ortiz, M.E., Diez, E., Almaden, Y., Muñoz-Castañeda, J.R., Rodriguez, M., Aguilera-Tejero, E., and Lopez, I. (2016). Energy-dense diets increase FGF23, lead to phosphorus retention and promote vascular calcifications in rats. Sci. Rep. *6*.

Rayyes, O.A., Wallmark, A., and Floren, C.-H. (1996). Cyclosporine inhibits catabolism of low-density lipoproteins in HepG2 cells by about 25%. Hepatology *24*, 613–619.

Redmon, J.B., Olson, L.K., Armstrong, M.B., Greene, M.J., and Robertson, R.P. (1996). Effects of Tacrolimus (FK506) on Human Insulin Gene Expression, Insulin mRNA Levels, and Insulin Secretion in HIT-T15 Cells. J. Clin. Invest. *98*, 2786–2793.

Rettig, R., Folberth, C.G., Stauss, H., Kopf, D., Waldherr, R., Baldauf, G., and Unger, T. (1990b). Hypertension in rats induced by renal grafts from renovascular hypertensive donors. Hypertension *15*, 429–435.

Rettig, R., Folberth, C., Stauss, H., Kopf, D., Waldherr, R., and Unger, T. (1990a). Role of the kidney in primary hypertension: a renal transplantation study in rats. Am. J. Physiol.-Ren. Physiol. *258*, F606–F611.

Rettig, R., Stauss, H., Folberth, C., Ganten, D., Waldherr, B., and Unger, T. (1989). Hypertension transmitted by kidneys from stroke-prone spontaneously hypertensive rats. Am. J. Physiol.-Ren. Physiol. *257*, F197–F203.

Riazi, S., Khan, O., Tiwari, S., Hu, X., and Ecelbarger, C.A. (2006). Rosiglitazone Regulates ENaC and Na-K-2Cl Cotransporter ($NKCC_2$) Abundance in the Obese Zucker Rat. Am. J. Nephrol. *26*, 245–257.

Richards, N.T., Poston, L., and Hilton, P.J. (1989). Cyclosporine A inhibits relaxation but does not induce vasoconstriction in human subcutaneous resistance vessels. J. Hypertens. *7*, 1–3.

Richardson, C., Rafiqi, F.H., Karlsson, H.K.R., Moleleki, N., Vandewalle, A., Campbell, D.G., Morrice, N.A., and Alessi, D.R. (2008). Activation of the thiazide-sensitive Na+-Cl- cotransporter by the WNK-regulated kinases SPAK and OSR1. J. Cell Sci. *121*, 675–684.

Richardson, C., Sakamoto, K., de los Heros, P., Deak, M., Campbell, D.G., Prescott, A.R., and Alessi, D.R. (2011). Regulation of the NKCC2 ion cotransporter by SPAK-OSR1-dependent and -independent pathways. J. Cell Sci. *124*, 789–800.

Rieg, T., Masuda, T., Gerasimova, M., Mayoux, E., Platt, K., Powell, D.R., Thomson, S.C., Koepsell, H., and Vallon, V. (2014). Increase in SGLT1-mediated transport explains renal glucose reabsorption during genetic and pharmacological SGLT2 inhibition in euglycemia. AJP Ren. Physiol. *306*, F188–F193.

Rinehart, J., Kahle, K.T., de los Heros, P., Vazquez, N., Meade, P., Wilson, F.H., Hebert, S.C., Gimenez, I., Gamba, G., and Lifton, R.P. (2005). WNK3 kinase is a positive regulator of NKCC2 and NCC, renal cation-Cl- cotransporters required for normal blood pressure homeostasis. Proc. Natl. Acad. Sci. U. S. A. *102*, 16777–16782.

Ring, A.M., Cheng, S.X., Leng, Q., Kahle, K.T., Rinehart, J., Lalioti, M.D., Volkman, H.M., Wilson, F.H., Hebert, S.C., and Lifton, R.P. (2007a). WNK4 regulates activity of the epithelial Na+ channel in vitro and in vivo. Proc. Natl. Acad. Sci. *104*, 4020–4024.

Ring, A.M., Leng, Q., Rinehart, J., Wilson, F.H., Kahle, K.T., Hebert, S.C., and Lifton, R.P. (2007b). An SGK1 site in WNK4 regulates Na+ channel and K+ channel activity and has implications for aldosterone signaling and K+ homeostasis. Proc. Natl. Acad. Sci. *104*, 4025–4029.

Riquier-Brison, A.D.M., Leong, P.K.K., Pihakaski-Maunsbach, K., and McDonough, A.A. (2010). Angiotensin II stimulates trafficking of NHE3, NaPi2, and associated proteins into the proximal tubule microvilli. AJP Ren. Physiol. *298*, F177–F186.

Roden, M., Weng, J., Eilbracht, J., Delafont, B., Kim, G., Woerle, H.J., and Broedl, U.C. (2013). Empagliflozin monotherapy with sitagliptin as an active comparator in patients with type 2 diabetes: a randomised, double-blind, placebo-controlled, phase 3 trial. Lancet Diabetes Endocrinol. *1*, 208–219.

Rodriguez-Rodriguez, A.E., Triñanes, J., Velazquez-Garcia, S., Porrini, E., Vega-Prieto, M.J., Diez Fuentes, M.L., Arevalo, M., Salido Ruiz, E., and Torres, A. (2013). The Higher Diabetogenic Risk of Tacrolimus Depends on Pre-Existing Insulin Resistance. A Study in Obese and Lean Zucker Rats. Am. J. Transplant. *13*, 1665–1675.

Rodríguez-Rodríguez, A.E., Triñanes, J., Porrini, E., Velázquez-García, S., Fumero, C., Vega-Prieto, M.J., Díez-Fuentes, M.L., Luis Lima, S., Salido, E., and Torres, A. (2015). Cambios en la homeostasis de la glucosa y la proliferación de la célula beta pancreática tras el cambio a ciclosporina en la diabetes inducida por tacrolimus. Nefrología *35*, 264–272.

Rojas-Vega, L., Jimenez, A.R., Bazua-Valenti, S., Arroyo-Garza, I., Jimenez, J.V., Gomez-Ocadiz, R., Carrillo-Perez, D.L., Moreno, E., Morales-Buenrostro, L.E., Alberú, J., et al. (2015). Increased phosphorylation of the renal Na+-Cl- cotransporter in male kidney transplant recipient patients with hypertension: a prospective cohort. Am. J. Physiol. - Ren. Physiol. *309*, F836-42.

Roland, M., Gatault, P., Doute, C., Büchler, M., Al-Najjar, A., Barbet, C., Chatelet, V., Marlière, J.-F., Nivet, H., Lebranchu, Y., et al. (2008). Immunosuppressive medications, clinical and metabolic parameters in new-onset diabetes mellitus after kidney transplantation. Transpl. Int. *21*, 523–530.

Romero, M.F., Hediger, M.A., Boulpaep, E.L., and Boron, W.F. (1997). Expression cloning and characterisation of a renal electrogenic Na+/HCO3- cotransporter. Nature *387*, 409–413.

Ronzaud, C., Loffing-Cueni, D., Hausel, P., Debonneville, A., Malsure, S.R., Fowler-Jaeger, N., Boase, N.A., Perrier, R., Maillard, M., Yang, B., et al. (2013). Renal tubular NEDD4-2 deficiency causes NCC-mediated salt-dependent hypertension. J. Clin. Invest. *123*, 657–665.

Rood, I.M., Deegens, J.K., Merchant, M.L., Tamboer, W.P.M., Wilkey, D.W., Wetzels, J.F.M., and Klein, J.B. (2010). Comparison of three methods for isolation of urinary microvesicles to identify biomarkers of nephrotic syndrome. Kidney Int. *78*, 810–816.

Rose, G., Stamler, J., Stamler, R., Elliot, P., Marmot, M., Pyorala, K., Kesteloot, H., Joossens, J., Hansson, L., Mancia, G., et al. (1988). Intersalt: An international study of electrolyte excretion and blood pressure. Results for 24 hour urinary sodium and potassium excretion. BMJ *297*, 319–328.

Roth, D., Milgrom, M., Esquenazi, V., Fuller, L., Burke, G., and Miller, J. (1989). Posttransplant hyperglycemia. Increased incidence in cyclosporine-treated renal allograft recipients. Transplantation *47*, 278–281.

Roullet, J.-B., Xue, H., McCarron, D.A., Holcomb, S., and Bennett, W.M. (1994). Vascular mechanisms of cyclosporin-induced hypertension in the rat. J. Clin. Invest. *93*, 2244–2250.

Royaux, I.E., Wall, S.M., Karniski, L.P., Everett, L.A., Suzuki, K., Knepper, M.A., and Green, E.D. (2001). Pendrin, encoded by the Pendred syndrome gene, resides in the apical region of renal intercalated cells and mediates bicarbonate secretion. Proc. Natl. Acad. Sci. *98*, 4221–4226.

Rozansky, D.J., Cornwall, T., Subramanya, A.R., Rogers, S., Yang, Y.-F., David, L.L., Zhu, X., Yang, C.-L., and Ellison, D.H. (2009). Aldosterone mediates activation of the thiazide-sensitive Na-Cl cotransporter through an SGK1 and WNK4 signaling pathway. J. Clin. Invest. *119*, 2601–2612.

Ruan, X., Wagner, C., Chatziantoniou, C., Kurtz, A., and Arendshorst, W.J. (1997). Regulation of angiotensin II receptor AT1 subtypes in renal afferent arterioles during chronic changes in sodium diet. J. Clin. Invest. *99*, 1072–1081.

Sabbagh, Y., O'Brien, S.P., Song, W., Boulanger, J.H., Stockmann, A., Arbeeny, C., and Schiavi, S.C. (2009). Intestinal Npt2b Plays a Major Role in Phosphate Absorption and Homeostasis. J. Am. Soc. Nephrol. *20*, 2348–2358.

Sacks, F.M., Svetkey, L.P., Vollmer, W.M., Appel, L.J., Bray, G.A., Harsha, D., Obarzanek, E., Conlin, P.R., Miller III, E.R., Simons-Morton, D.G., et al. (2001). Effects on Blood Pressure of Reduced Dietary Sodium and the Dietary Approaches to Stop Hypertension (DASH) Diet. N. Engl. J. Med. *344*, 3–10.

Sakhaee, K., Adams-Huet, B., Moe, O.W., and Pak, C.Y.C. (2002). Pathophysiologic basis for normouricosuric uric acid nephrolithiasis. Kidney Int. *62*, 971–979.

San-Cristobal, P., Pacheco-Alvarez, D., Richardson, C., Ring, A.M., Vazquez, N., Rafiqi, F.H., Chari, D., Kahle, K.T., Leng, Q., Bobadilla, N.A., et al. (2009). Angiotensin II signaling increases activity of the renal Na-Cl cotransporter through a WNK4-SPAK-dependent pathway. Proc. Natl. Acad. Sci. *106*, 4384–4389.

Sandberg, M.B., Maunsbach, A.B., and McDonough, A.A. (2006). Redistribution of distal tubule Na+-Cl- cotransporter (NCC) in response to a high-salt diet. AJP Ren. Physiol. *291*, F503–F508.

Santer, R., Kinner, M., Lassen, C.L., Schneppenheim, R., Eggert, P., Bald, M., Brodehl, J., Daschner, M., Enhrich, J.H.H., Kemper, M., et al. (2003). Molecular Analysis of the SGLT2 Gene in Patients with Renal Glucosuria. J. Am. Soc. Nephrol. *14*, 2873–2882.

Santisteban, M.M., Qi, Y., Zubcevic, J., Kim, S., Yang, T., Shenoy, V., Cole-Jeffrey, C.T., Lobaton, G.O., Stewart, D.C., Rubiano, A., et al. (2017). Hypertension-Linked Pathophysiological Alterations in the Gut. Circ. Res. *120*, 312–323.

Sasaki, S., and Imai, M. (1980). Effects of vasopressin on water and NaCl transport across the in vitro perfused medullary thick ascending limb of Henle's loop of mouse, rat, and rabbit kidneys. Pflüg. Arch. *383*, 215–221.

Sato, T., Inagaki, A., Uchida, K., Ueki, T., Goto, N., Matsuoka, S., Katayama, A., Haba, T., Tominaga, Y., Okajima, Y., et al. (2003). Diabetes mellitus after transplant: relationship to pretransplant glucose metabolism and tacrolimus or cyclosporine A-based therapy: Transplantation *76*, 1320–1326.

Scherrer, U., Vissing, S.F., Morgan, B.J., Rollins, J.A., Tindall, R.S.A., Ring, S., Hanson, P., Mohanty, P.K., and Victor, R.G. (1990). Cyclosporine-induced sympathetic activation and hypertension after heart transplantation. N. Engl. J. Med. *323*, 693–699.

Schiavi, S.C., Tang, W., Bracken, C., O'Brien, S.P., Song, W., Boulanger, J., Ryan, S., Phillips, L., Liu, S., Arbeeny, C., et al. (2012). Npt2b Deletion Attenuates Hyperphosphatemia Associated with CKD. J. Am. Soc. Nephrol. *23*, 1691–1700.

Schmitt, B.M., Biemesderfer, D., Romero, M.F., Boulpaep, E.L., and Boron, W.F. (1999a). Immunolocalization of the electrogenic Na+-HCO 3-cotransporter in mammalian and amphibian kidney. Am. J. Physiol.-Ren. Physiol. *45*, F27–F38.

Schmitt, R., Ellison, D.H., Farman, N., Rossier, B.C., Reilly, R.F., Reeves, B., Oberbaumer, I., Tapp, R., and Bachmann, S. (1999b). Developmental expression of sodium entry pathways in rat nephron. Am. J. Physiol.-Ren. Physiol. *45*, F367–F381.

Schnermann, J., Wright, F.S., Davis, J.M., Stackelberg, W. v, and Grill, G. (1970). Regulation of superficial nephron filtration rate by tubulo-glomerular feedback. Pflüg. Arch. Eur. J. Physiol. *318*, 147–175.

Schorn, T.F., Kliem, V., Bojanovski, M., Bojanovski, D., Repp, H., Bunzendahl, H., and Frei, U. (1991). Impact of long-term immunosuppression

with cyclosporin A on serum lipids in stable renal transplant recipients. Transpl. Int. *4*, 92–95.

Schreyer, S.A., Wilson, D.L., and LeBoeuf, R.C. (1998). C57BL/6 mice fed high fat diets as models for diabetes-accelerated atherosclerosis. Atherosclerosis *136*, 17–24.

Schroter, J., Timmermans, G., Seyberth, H.W., Greven, J., and Bachmann, S. (1993). Marked reduction of Tamm-Horsfall protein synthesis in hyperprostaglandin E-syndrome. Kidney Int. *44*, 401–410.

Schultheis, P.J., Clarke, L.L., Meneton, P., Miller, M.L., Soleimani, M., Gawenis, L.R., Riddle, T.M., Duffy, J.J., Doetschman, T., and Wang, T. (1998a). Renal and intestinal absorptive defects in mice lacking the NHE3 Na+/H+ exchanger. Nat. Genet. *19*, 282–285.

Schultheis, P.J., Lorenz, J.N., Meneton, P., Nieman, M.L., Riddle, T.M., Flagella, M., Duffy, J.J., Doetschman, T., Miller, M.L., and Shull, G.E. (1998b). Phenotype Resembling Gitelman's Syndrome in Mice Lacking the Apical Na+-Cl- Cotransporter of the Distal Convoluted Tubule. J. Biol. Chem. *273*, 29150–29155.

Schwarz, C., Benesch, T., Kodras, K., Oberbauer, R., and Haas, M. (2006). Complete renal tubular acidosis late after kidney transplantation. Nephrol. Dial. Transplant. *21*, 2615–2620.

Segawa, H., Kaneko, I., Takahashi, A., Kuwahata, M., Ito, M., Ohkido, I., Tatsumi, S., and Miyamoto, K. (2002). Growth-related Renal Type II Na/Pi Cotransporter. J. Biol. Chem. *277*, 19665–19672.

Shaw, J.-P., Utz, P.J., Durand, D.B., Toole, J.J., Emmel, E.A., and Crabtree, G.R. (1988). Identification of a putative regulator of early T cell activation genes. Science *241*, 202–205.

Shaw, K.T., Ho, A.M., Raghavan, A., Kim, J., Jain, J., Park, J., Sharma, S., Rao, A., and Hogan, P.G. (1995). Immunosuppressive drugs prevent a rapid dephosphorylation of transcription factor NFAT1 in stimulated immune cells. Proc. Natl. Acad. Sci. *92*, 11205–11209.

Shi, P.P., Cao, X.R., Sweezer, E.M., Kinney, T.S., Williams, N.R., Husted, R.F., Nair, R., Weiss, R.M., Williamson, R.A., Sigmund, C.D., et al. (2008). Salt-sensitive hypertension and cardiac hypertrophy in mice deficient in the ubiquitin ligase Nedd4-2. AJP Ren. Physiol. *295*, F462–F470.

Shibata, S., Zhang, J., Puthumana, J., Stone, K.L., and Lifton, R.P. (2013). Kelch-like 3 and Cullin 3 regulate electrolyte homeostasis via ubiquitination and degradation of WNK4. Proc. Natl. Acad. Sci. *110*, 7838–7843.

Shimkets, R.A., Warnock, D.G., Bositis, C.M., Nelson-Williams, C., Hansson,

J.H., Schambelan, M., Gill, J.R., Ulick, S., Milora, R.V., and Findling, J.W. (1994). Liddle's syndrome: heritable human hypertension caused by mutations in the β subunit of the epithelial sodium channel. Cell *79*, 407–414.

Shoda, W., Nomura, N., Ando, F., Mori, Y., Mori, T., Sohara, E., Rai, T., and Uchida, S. (2017). Calcineurin inhibitors block sodium-chloride cotransporter dephosphorylation in response to high potassium intake. Kidney Int. *91*, 402–411.

Shojaiefard, M., Strutz-Seebohm, N., Tavaré, J.M., Seebohm, G., and Lang, F. (2007). Regulation of the Na+, glucose cotransporter by PIKfyve and the serum and glucocorticoid inducible kinase SGK1. Biochem. Biophys. Res. Commun. *359*, 843–847.

Simon, G., and Illyes, G. (2001). Structural vascular changes in hypertension: role of angiotensin II, dietary sodium supplementation, and sympathetic stimulation, alone and in combination in rats. Hypertension *37*, 255–260.

Simon, D.B., Karet, F.E., Hamdan, J.M., Di Pietro, A., Sanjad, S.A., and Lifton, R.P. (1996a). Bartter's syndrome, hypokalaemic alkalosis with hypercalciuria, is caused by mutations in the Na-K-2Cl cotransporter NKCC2. Nat. Genet. *13*, 183–188.

Simon, D.B., Karet, F.E., Rodriguez-Soriano, J., Hamdan, J.M., DiPietro, A., Trachtman, H., Sanjad, S.A., and Lifton, R.P. (1996b). Genetic heterogeneity of Bartter's syndrome revealed by mutations in the K+ channel, ROMK. Nat. Genet. *14*, 152–156.

Simon, D.B., Nelson-Williams, C., Johnston Bia, M., Ellison, D.H., Karet, F.E., Morey Molina, A., Vaara, I., Iwata, F., Cushner, H.M., Koolen, M., et al. (1996c). Gitelman's variant of Bartter's syndrome, inherited hypokalaemic alkalosis, is caused by mutations in the thiazide-sensitive Na-Cl cotransporter. Nat. Genet. *12*, 24–30.

Simon, D.B., Bindra, R.S., Mansfield, T.A., Nelson-Williams, C., Mendonca, E., Stone, R., Schurman, S., Nayir, A., Alpay, H., Bakkaloglu, A., et al. (1997). Mutations in the chloride channel gene, CLCNKB, cause Bartter's syndrome type III. Nat. Genet. *17*, 171–178.

Sinangil, A., Celik, V., Barlas, S., Sakaci, T., Koc, Y., Basturk, T., Akin, E.B., and Ecder, T. (2016). New-Onset Diabetes After Kidney Transplantation and Pretransplant Hypomagnesemia. Prog. Transplant. *26*, 55–61.

Skou, J.C. (1957). The influence of some cations on an adenosine triphosphatase from peripheral nerves. Biochim. Biophys. Acta *23*, 394–401.

Skou, J.C. (1962). Preparation from mammallian brain and kidney of the enzyme system involved in active transport of Na+ and K+. Biochim.

Biophys. Acta *58*, 314–325.

Snyder, P.M., Price, M.P., McDonald, F.J., Adams, C.M., Volk, K.A., Zeiher, B.G., Stokes, J.B., and Welsh, M.J. (1995). Mechanism by Which Liddle's Syndrome Mutations Increase Activity of a Human Epithelial Na+ Channel. Cell *83*, 969–978.

Snyder, P.M., Olson, D.R., and Thomas, B.C. (2002). Serum and Glucocorticoid-regulated Kinase Modulates Nedd4-2-mediated Inhibition of the Epithelial Na $^{+}$ Channel. J. Biol. Chem. *277*, 5–8.

Snyder, P.M., Olson, D.R., Kabra, R., Zhou, R., and Steines, J.C. (2004). cAMP and Serum and Glucocorticoid-inducible Kinase (SGK) Regulate the Epithelial Na $^{+}$ Channel through Convergent Phosphorylation of Nedd4-2. J. Biol. Chem. *279*, 45753–45758.

Sohara, E., Rai, T., Yang, S.-S., Ohta, A., Naito, S., Chiga, M., Nomura, N., Lin, S.-H., Vandewalle, A., Ohta, E., et al. (2011). Acute Insulin Stimulation Induces Phosphorylation of the Na-Cl Cotransporter in Cultured Distal mpkDCT Cells and Mouse Kidney. PLoS ONE *6*, e24277.

Soleimani, M., Bizal, G.L., McKinney, T.D., and Hattabaugh, Y.J. (1992). Effect of in vitro metabolic acidosis on luminal Na+/H+ exchange and basolateral Na+:HCO3- cotransport in rabbit kidney proximal tubules. J. Clin. Invest. *90*, 211–218.

Soleimani, M., Greeley, T., Petrovic, S., Wang, Z., Amlal, H., Kopp, P., and Burnham, C.E. (2001). Pendrin: an apical Cl-/OH-/HCO 3- exchanger in the kidney cortex. Am. J. Physiol.-Ren. Physiol. *280*, F356–F364.

Song, X.M., Fiedler, M., Galuska, D., Ryder, J.W., Fernstrom, M., Chibalin, A.V., Wallberg-Henriksson, H., and Zierath, J.R. (2002). 5-Aminoimidazole-4-carboxamide ribonucleoside treatment improves glucose homeostasis in insulin-resistant diabetic (ob/ob) mice. Diabetologia *45*, 56–65.

Sonoda, H., Yokota-Ikeda, N., Oshikawa, S., Kanno, Y., Yoshinaga, K., Uchida, K., Ueda, Y., Kimiya, K., Uezono, S., Ueda, A., et al. (2009). Decreased abundance of urinary exosomal aquaporin-1 in renal ischemia-reperfusion injury. AJP Ren. Physiol. *297*, F1006–F1016.

Sopjani, M., Bhavsar, S.K., Fraser, S., Kemp, B.E., Föller, M., and Lang, F. (2010). Regulation of Na $^{+}$ -coupled glucose carrier SGLT1 by AMP-activated protein kinase. Mol. Membr. Biol. *27*, 137–144.

Spartà, G., Kemper, M.J., and Neuhaus, T.J. (2006). Hyperuricemia and gout following pediatric renal transplantation. Pediatr. Nephrol. *21*, 1884–1888.

Stauber, A., Radanoiv, T., Stange, G., Murer, H., Wagner, C.A., and Biber, J. (2005). Regulation of Intestinal Phosphate Transport II. Metabolic acidosis

stimulates Na+-dependent phosphate absorption and expression of the Na+-Pi cotransporter NaPi-IIb in small intestine. AJP Gastrointest. Liver Physiol. *288*, G501–G506.

Stein, M., He, H., Pincus, T., and Wood, A.J.. (1995). Cyclosporine Impairs Vasodilation Without Increased Sympathetic Activity in Humans. Hypertension *26*, 705–710.

Stemmer, P.M., and Klee, C.B. (1994). Dual calcium ion regulation of calcineurin by calmodulin and calcineurin B. Biochemistry (Mosc.) *33*, 6859–6866.

Stenlof, K., Cefalu, W.T., Kim, K.-A., Alba, M., Usiskin, K., Tong, C., Canovatchel, W., and Meininger, G. (2013). Efficacy and safety of canagliflozin monotherapy in subjects with type 2 diabetes mellitus inadequately controlled with diet and exercise. Diabetes Obes. Metab. *15*, 372–382.

Stokes, J. 3rd, Kannel, W.B., Wolf, P.A., D'agostino, R.B., and Cupples, L.A. (1989). Blood pressure as a risk factor for cardiovascular disease. The Framingham Study–30 years of follow-up. Hypertension *13*, I13.

Surwit, R.S., Kuhn, C.M., Cochrane, C., McCubbin, J.A., and Feinglos, M.N. (1988). Diet-Induced Type II Diabetes in C57BL/6J Mice. Diabetes *37*, 1163–1167.

Surwit, R.S., Feinglos, M.N., Rodin, J., Sutherland, A., Petro, A.E., Opara, E.C., Kuhn, C.M., and Rebuffe-Scrive, M. (1995). Differential effects of fat and sucrose on the development of obesity and diabetes in C57BL/6J and mice. Metabolism *44*, 645–651.

Susa, K., Kita, S., Iwamoto, T., Yang, S.-S., Lin, S.-H., Ohta, A., Sohara, E., Rai, T., Sasaki, S., Alessi, D.R., et al. (2012). Effect of heterozygous deletion of WNK1 on the WNK-OSR1/SPAK-NCC/NKCC1/NKCC2 signal cascade in the kidney and blood vessels. Clin. Exp. Nephrol. *16*, 530–538.

Susa, K., Sohara, E., Rai, T., Zeniya, M., Mori, Y., Mori, T., Chiga, M., Nomura, N., Nishida, H., Takahashi, D., et al. (2014). Impaired degradation of WNK1 and WNK4 kinases causes PHAII in mutant KLHL3 knock-in mice. Hum. Mol. Genet. *23*, 5052–5060.

Takahashi, D., Mori, T., Nomura, N., Khan, M.Z.H., Araki, Y., Zeniya, M., Sohara, E., Rai, T., Sasaki, S., and Uchida, S. (2014). WNK4 is the major WNK positively regulating NCC in the mouse kidney. Biosci. Rep. *34*, 195–205.

Takeda, Y., Miyamori, I., Yoneda, T., and Takeda, R. (1992). Endothelin-1 release from the mesenteric arteries of cyclosporine-treated rats. Eur. J. Pharmacol. *213*, 445–447.

Takeda, Y., Miyamori, I., Wu, P., Yoneda, T., Furukawa, K., and Takeda, R. (1995). Effects of an Endothelin Receptor Antagonist in Rats With Cyclosporine-Induced Hypertension. Hypertension *26*, 932–936.

Takeda, Y., Miyamori, I., Furukawa, K., Inaba, S., and Mabuchi, H. (1999). Mechanisms of FK 506 Induced Hypertension in the Rat. Hypertension *33*, 130–136.

Talati, G., Ohta, A., Rai, T., Sohara, E., Naito, S., Vandewalle, A., Sasaki, S., and Uchida, S. (2010). Effect of angiotensin II on the WNK-OSR1/SPAK-NCC phosphorylation cascade in cultured mpkDCT cells and in vivo mouse kidney. Biochem. Biophys. Res. Commun. *393*, 844–848.

Tamari, M., Daigo, Y., and Nakamura, Y. (1999). Isolation and characterization of a novel serine threonine kinase gene on chromosome 3p22-21.3. J. Hum. Genet. *44*, 116–120.

Tamura, K., Fujimura, T., Tsutsumi, T., Nakamura, K., Ogawa, T., Atumaru, C., Hirano, Y., Ohara, K., Ohtsuka, K., Shimomura, K., et al. (1995). Transcriptional inhibition of insulin by FK506 and possible involvement of FK506 binding protein-12 in pancreatic B-cell. Transplantation *59*, 1606–1613.

Tenenhouse, H.S., Roy, S., Martel, J., and Gauthier, C. (1998). Differential expression, abundance, and regulation of Na+-phosphate cotransporter genes in murine kidney. Am. J. Physiol.-Ren. Physiol. *44*, F527–F534.

Tenenhouse, H.S., Martel, J., Gauthier, C., Segawa, H., and Miyamoto, K. (2003). Differential effects of Npt2a gene ablation and X-linked Hyp mutation on renal expression of Npt2c. Am. J. Physiol. - Ren. Physiol. *54*, F1271–F1278.

Thastrup, J.O., Rafiqi, F.H., Vitari, A.C., Pozo-Guisado, E., Deak, M., Mehellou, Y., and Alessi, D.R. (2012). SPAK/OSR1 regulate NKCC1 and WNK activity: analysis of WNK isoform interactions and activation by T-loop trans-autophosphorylation. Biochem. J. *441*, 325–337.

Thomas, L., Bettoni, C., Knöpfel, T., Hernando, N., Biber, J., and Wagner, C.A. (2017). Acute Adaption to Oral or Intravenous Phosphate Requires Parathyroid Hormone. J. Am. Soc. Nephrol. *28*, 903–914.

Thorens, B., Sarkar, H.K., Kaback, H.R., and Lodish, H.F. (1988). Cloning and functional expression in bacteria of a novel glucose transporter present in liver, intestine, kidney, and B-pancreatic islet cells. Cell *55*, 281–290.

Timmerman, L.A., Clipstone, N.A., Ho, S.N., Northrop, J.P., and Crabtree, G.R. (1996). Rapid shuttling of NF-AT in discrimination of Ca2+ signals and immunosuppression. Nature *383*, 837–840.

Toora, B.D., and Rajagopal, G. (2002). Measurement of creatinine by Jaffe's reaction - Determination of concentration of sodium hydroxide required for maximum color development in standard, urine and protein free filtrate of serum. Indian J. Exp. Biol. *40*, 352–354.

Tory, R., Sachs-Barrable, K., Goshko, C.-B., Hill, J.S., and Wasan, K.M. (2009). Tacrolimus-Induced Elevation in Plasma Triglyceride Concentrations After Administration to Renal Transplant Patients Is Partially Due to a Decrease in Lipoprotein Lipase Activity and Plasma Concentrations: Transplantation *88*, 62–68.

Triñanes, J., Rodriguez-Rodriguez, A.E., Brito-Casillas, Y., Wagner, A., De Vries, A.P.J., Cuesto, G., Acebes, A., Salido, E., Torres, A., and Porrini, E. (2017). Deciphering Tacrolimus-Induced Toxicity in Pancreatic β Cells. Am. J. Transplant.

Tsai, C.-Y., Wu, T.-H., Yu, C.-L., Yu, J.-Y., and Tsai, Y.-Y. (2000). Increased Excretions of β2-Microglobulin, IL-6, and IL-8 and Decreased Excretion of Tamm-Horsfall Glycoprotein in Urine of Patients with Active Lupus nephritis. Nephron *85*, 207–214.

Tse, C.-M., Brant, S.R., Walker, S., Pouyssegur, J., and Donowitz, M. (1992). Cloning and sequencing of a rabbit cDNA encoding an intestinal and kidney-specific Na+/H+ exchanger isoform (NHE-3). J. Biol. Chem. *267*, 9340–9346.

Tse, K.-C., Lam, M.-F., Yip, P.-S., Li, F.-K., Lai, K.-N., and Chan, T.-M. (2004). A long-term study on hyperlipidemia in stable renal transplant recipients. Clin. Transplant. *18*, 274–280.

Tuck, M.L., Sowers, J., Dornfeld, L., Kledzik, G., and Maxwell, M. (1981). The effect of weight reduction on blood pressure, plasma renin activity, and plasma aldosterone levels in obese patients. N. Engl. J. Med. *304*, 930–933.

Turnbaugh, P.J., Ley, R.E., Mahowald, M.A., Magrini, V., Mardis, E.R., and Gordon, J.I. (2006). An obesity-associated gut microbiome with increased capacity for energy harvest. Nature *444*, 1027–1131.

Turnbaugh, P.J., Bäckhed, F., Fulton, L., and Gordon, J.I. (2008). Diet-Induced Obesity Is Linked to Marked but Reversible Alterations in the Mouse Distal Gut Microbiome. Cell Host Microbe *3*, 213–223.

Turner, R.J., and Moran, A. (1982). Heterogeneity of sodium-dependent D-glucose transport sites along the proximal tubule: evidence from vesicle studies. Am. J. Physiol.-Ren. Physiol. *242*, F406–F414.

Tutakhel, O.A.Z., Jeleń, S., Valdez-Flores, M., Dimke, H., Piersma, S.R., Jimenez, C.R., Deinum, J., Lenders, J.W., Hoenderop, J.G.J., and Bindels, R.J.M. (2016). Alternative splice variant of the thiazide-sensitive NaCl cotransporter: a novel player in renal salt handling. Am. J. Physiol. - Ren.

Physiol. *310*, F204–F216.

Tutakhel, O.A.Z., Moes, A.D., Valdez-Flores, M., Kortenoeven, M.L.A., Vrie, M. v.D., Jeleń, S., Fenton, R.A., Zietse, R., Hoenderop, J.G.J., Hoorn, E.J., et al. (2017). NaCl cotransporter abundance in urinary vesicles is increased by calcineurin inhibitors and predicts thiazide sensitivity. PLOS ONE *12*, e0176220.

Ushiro, H., Tsutsumi, T., Suzuki, K., Kayahara, T., and Nakano, K. (1998). Molecular Cloning and Characterization of a Novel Ste20-Related Protein Kinase Enriched in Neurons and Transporting Epithelia. Arch. Biochem. Biophys. *355*, 233–240.

Valadi, H., Ekström, K., Bossios, A., Sjöstrand, M., Lee, J.J., and Lötvall, J.O. (2007). Exosome-mediated transfer of mRNAs and microRNAs is a novel mechanism of genetic exchange between cells. Nat. Cell Biol. *9*, 654–659.

Vallon, V., Schroth, J., Lang, F., Kuhl, D., and Uchida, S. (2009). Expression and phosphorylation of the Na+-Cl- cotransporter NCC in vivo is regulated by dietary salt, potassium, and SGK1. AJP Ren. Physiol. *297*, F704–F712.

Vallon, V., Platt, K.A., Cunard, R., Schroth, J., Whaley, J., Thomson, S.C., Koepsell, H., and Rieg, T. (2011). SGLT2 Mediates Glucose Reabsorption in the Early Proximal Tubule. J. Am. Soc. Nephrol. *22*, 104–112.

Vallon, V., Rose, M., Gerasimova, M., Satriano, J., Platt, K.A., Koepsell, H., Cunard, R., Sharma, K., Thomson, S.C., and Rieg, T. (2013). Knockout of Na-glucose transporter SGLT2 attenuates hyperglycemia and glomerular hyperfiltration but not kidney growth or injury in diabetes mellitus. AJP Ren. Physiol. *304*, F156–F167.

Van Laecke, S., Van Biesen, W., Verbeke, F., De Bacquer, D., Peeters, P., and Vanholder, R. (2009). Posttransplantation Hypomagnesemia and Its Relation with Immunosuppression as Predictors of New-Onset Diabetes after Transplantation. Am. J. Transplant. *9*, 2140–2149.

Vasan, R.S., Larson, M.G., Leip, E.P., Evans, J.C., O'Donnell, C.J., Kannel, W.B., and Levy, D. (2001). Impact of high-normal blood pressure on the risk of cardiovascular disease. N. Engl. J. Med. *345*, 1291–1297.

Vasilakou, D., Karagiannis, T., Athanasiadou, E., Mainou, M., Liakos, A., Bekiari, E., Sarigianni, M., Matthews, D.R., and Tsapas, A. (2013). Sodium–Glucose Cotransporter 2 Inhibitors for Type 2 Diabetes: A Systematic Review and Meta-analysis. Ann. Intern. Med. *159*, 262–274.

Verissimo, F., and Jordan, P. (2001). WNK kinases, a novel protein kinase subfamily in multi-cellular organisms. Oncogene *20*, 5562–5569.

Vestri, S., Okamoto, M.M., de Freitas, H.S., Aparecida dos Santos, R.,

Nunes, M.T., Morimatsu, M., Heimann, J.C., and Machado, U.F. (2001). Changes in Sodium or Glucose Filtration Rate Modulate Expression of Glucose Transporters in Renal Proximal Tubular Cells of Rat. J. Membr. Biol. *182*, 105–112.

Vidal-Petiot, E., Elvira-Matelot, E., Mutig, K., Soukaseum, C., Baudrie, V., Wu, S., Cheval, L., Huc, E., Cambillau, M., Bachmann, S., et al. (2013). WNK1-related Familial Hyperkalemic Hypertension results from an increased expression of L-WNK1 specifically in the distal nephron. Proc. Natl. Acad. Sci. *110*, 14366–14371.

Vijay-Kumar, M., Aitken, J.D., Carvalho, F.A., Cullender, T.C., Mwangi, S., Srinivasan, S., Sitaraman, S.V., Knight, R., Ley, R.E., and Gewirtz, A.T. (2010). Metabolic Syndrome and Altered Gut Microbiota in Mice Lacking Toll-Like Receptor 5. Science *328*, 228–231.

Villa-Bellosta, R., Ravera, S., Sorribas, V., Stange, G., Levi, M., Murer, H., Biber, J., and Forster, I.C. (2009). The Na+-Pi cotransporter PiT-2 (SLC20A2) is expressed in the apical membrane of rat renal proximal tubules and regulated by dietary Pi. AJP Ren. Physiol. *296*, F691–F699.

Villamil, M.F., Amorena, C., Ponce-Hornos, J., Muller, A., and Taquini, A. (1982). Role of extracellular volume expansion in the development of DOC-salt hypertension in the rat. Hypertension *4*, 620–624.

Vincenti, F., Jensik, S.C., Filo, R.S., Miller, J., and Pirsch, J.D. (2002). A long-term comparison of tacrolimus (FK506) and cyclosporine in kidney transplantation: evidence for improved allograft survival at five years. Transplantation *73*, 775–782.

Vincenti, F., Friman, S., Scheuermann, E., Rostaing, L., Jenssen, T., Campistol, J.M., Uchida, K., Pescovitz, M.D., Marchetti, P., Tuncer, M., et al. (2007). Results of an International, Randomized Trial Comparing Glucose Metabolism Disorders and Outcome with Cyclosporine Versus Tacrolimus. Am. J. Transplant. *7*, 1506–1514.

Vitari, A.C., Deak, M., Morrice, N.A., and Alessi, D.R. (2005). The WNK1 and WNK4 protein kinases that are mutated in Gordon's hypertension syndrome phosphorylate and activate SPAK and OSR1 protein kinases. Biochem. J. *391*, 17–24.

Vitari, A.C., Thastrup, J., Rafiqi, F.H., Deak, M., Morrice, N.A., Karlsson, H.K.R., and Alessi, D.R. (2006). Functional interactions of the SPAK/OSR1 kinases with their upstream activator WNK1 and downstream substrate NKCC1. Biochem. J. *397*, 223–231.

de Vries, A.P.J., Bakker, S.J.L., van Son, W.J., van der Heide, J.J.H., Ploeg, R.J., The, H.T., de Jong, P.E., and Gans, R.O.B. (2004). Metabolic

Syndrome Is Associated with Impaired Long-term Renal Allograft Function; Not All Component criteria Contribute Equally. Am. J. Transplant. *4*, 1675–1683.

Wakabayashi, M., Mori, T., Isobe, K., Sohara, E., Susa, K., Araki, Y., Chiga, M., Kikuchi, E., Nomura, N., Mori, Y., et al. (2013). Impaired KLHL3-Mediated Ubiquitination of WNK4 Causes Human Hypertension. Cell Rep. *3*, 858–868.

Walling, M.W. (1977). Intestinal Ca and phosphate transport: differential responses to vitamin D3 metabolites. Am. J. Physiol.-Gastrointest. Liver Physiol. *233*, G488–G494.

Walton, J., and Gray, T.K. (1979). Absorption of inorganic phosphate in the human small intestine. Clin. Sci. *56*, 407–412.

Wang, J., Zhang, Z.-R., Chou, C.-F., Liang, Y.-Y., Gu, Y., and Ma, H.-P. (2009). Cyclosporine stimulates the renal epithelial sodium channel by elevating cholesterol. AJP Ren. Physiol. *296*, F284–F290.

Wang, Z., Wu, Y., Zhao, L., Li, Y., Yang, J., and Zhou, B. (2004). Trends in Prevalence, Awareness, Treatment and Control of Hypertension in the Middle-Aged Population of China, 1992–1998. Hypertens. Res. *27*, 703–709.

Webster, A.C., Woodroffe, R.C., Taylor, R.S., Chapman, J.R., and Craig, J.C. (2005). Tacrolimus versus ciclosporin as primary immunosuppression for kidney transplant recipients: meta-analysis and meta-regression of randomised trial data. BMJ *331*, 810–0.

Webster, M.K., Goya, L., Ge, Y., Maiyar, A.C., and Firestone, G.L. (1993). Characterization of sgk, a novel member of the serine/threonine protein kinase gene family which is transcriptionally induced by glucocorticoids and serum. Mol. Cell. Biol. *13*, 2031–2040.

Weder, A.B. (1986). Red-Cell Lithium-Sodium Countertransport and Renal Lithium Clearance in Hypertension. N. Engl. J. Med. *314*, 198–201.

West, K.M., and Kalbfleisch, J.M. (1971). Influence of nutritional factors on prevalence of diabetes. Diabetes *20*, 99–108.

West, D.B., Boozer, C.N., Moody, D.L., and Atkinson, R.L. (1992). Dietary obesity in nine inbred mouse strains. Am. J. Physiol.-Regul. Integr. Comp. Physiol. *262*, R1025–R1032.

Wilson, F.H., Disse-Nicodeme, S., Choate, K.A., Ishikawa, K., Nelson-Williams, C., Desitter, I., Gunel, M., Milford, D.V., Lipkin, G.W., Achard, J.-M., et al. (2001). Human Hypertension Caused by Mutations in WNK Kinases. Science *293*, 1107–1112.

Wilson, F.H., Kahle, K.T., Sabath, E., Lalioti, M.D., Rapson, A.K., Hoover,

R.S., Hebert, S.C., Gamba, G., and Lifton, R.P. (2003). Molecular pathogenesis of inherited hypertension with hyperkalemia: the Na–Cl cotransporter is inhibited by wild-type but not mutant WNK4. Proc. Natl. Acad. Sci. *100*, 680–684.

Winzell, M.S., and Ahren, B. (2004). The High-Fat Diet–Fed Mouse A Model for Studying Mechanisms and Treatment of Impaired Glucose Tolerance and Type 2 Diabetes. Diabetes *53*, S215-219.

Wiśniewski, J.R., Friedrich, A., Keller, T., Mann, M., and Koepsell, H. (2015). The Impact of High-Fat Diet on Metabolism and Immune Defense in Small Intestine Mucosa. J. Proteome Res. *14*, 353–365.

Wissing, K.M., Abramowicz, D., Broeders, N., and Vereerstraeten, P. (2000). Hypercholesterolemia is associated with increased kidney graft loss caused by chronic rejection in male patients with previous acute rejection. Transplantation *70*, 464–472.

Wolf, M.T.F., Mucha, B.E., Attanasio, M., Zalewski, I., Karle, S.M., Neumann, H.P.H., Rahman, N., Bader, B., Baldamus, C.A., Otto, E., et al. (2003). Mutations of the Uromodulin gene in MCKD type 2 patients cluster in exon 4, which encodes three EGF-like domains. Kidney Int. *64*, 1580–1587.

Wolf-Maier, K., Cooper, R.S., Banegas, J.R., Giampaoli, S., Hense, H.-W., Joffres, M.R., Kastarinen, M., Poulter, N., Primatesta, P., Rodríguez-Artalejo, F., et al. (2003). Hypertension prevalence and blood pressure levels in 6 European countries, Canada, and the United States. JAMA *289*, 2363–2369.

Wolf-Maier, K., Cooper, R.S., Kramer, H., Banegas, J.R., Giampaoli, S., Joffres, M.R., Poulter, N., Primatesta, P., Stegmayr, B., and Thamm, M. (2004). Hypertension Treatment and Control in Five European Countries, Canada, and the United States. Hypertension *43*, 10–17.

Wolley, M.J., Wu, A., Xu, S., Gordon, R.D., Fenton, R.A., and Stowasser, M. (2017). In Primary Aldosteronism, Mineralocorticoids Influence Exosomal Sodium-Chloride Cotransporter Abundance. J. Am. Soc. Nephrol. *28*, 56–63.

Woods, S.C., Seeley, R.J., Rushing, P.A., Alessio, D.D., and Tso, P. (2003). A controlled high-fat diet induces an obese syndrome in rats. J. Nutr. *133*, 1081–1087.

Woodward, R.S., Schnitzler, M.A., Baty, J., Lowell, J.A., Lopez-Rocafort, L., Haider, S., Woodworth, T.G., and Brennan, D.C. (2003). Incidence and Cost of New Onset Diabetes Mellitus Among U.S. Wait-Listed and Transplanted Renal Allograft Recipients. Am. J. Transplant. *3*, 590–598.

Wu, G., and Peng, J.-B. (2013). Disease-causing mutations in KLHL3 impair its effect on WNK4 degradation. FEBS Lett. *587*, 1717–1722.

Wu, C., Yosef, N., Thalhamer, T., Zhu, C., Xiao, S., Kishi, Y., Regev, A., and Kuchroo, V.K. (2013). Induction of pathogenic TH17 cells by inducible salt-sensing kinase SGK1. Nature *496*, 513–517.

Wu, M.-S., Biemesderfer, D., Giebisch, G., and Aronson, P.S. (1996). Role of NHE3 in Mediating Renal Brush Border Na+-H+ Exchange ADAPTATION TO METABOLIC ACIDOSIS. J. Biol. Chem. *271*, 32749–32752.

Xu, B., English, J.M., Wilsbacher, J.L., Stippec, S., Goldsmith, E.J., and Cobb, M.H. (2000). WNK1, a Novel Mammalian Serine/Threonine Protein Kinase Lacking the Catalytic Lysine in Subdomain II. J. Biol. Chem. *275*, 16795–16801.

Xu, B., Min, X., Stippec, S., Lee, B.-H., Goldsmith, E.J., and Cobb, M.H. (2002). Regulation of WNK1 by an Autoinhibitory Domain and Autophosphorylation. J. Biol. Chem. *277*, 48456–48462.

Xu, B., Stippec, S., Chu, P.-Y., Lazrak, A., Li, X.-J., Lee, B.-H., English, J.M., Ortega, B., Huang, C.-L., and Cobb, M.H. (2005). WNK1 activates SGK1 to regulate the epithelial sodium channel. Proc. Natl. Acad. Sci. U. S. A. *102*, 10315–10320.

Xu, H., Uno, J.K., Inouye, M., Xu, L., Drees, J.B., Collins, J.F., and Ghishan, F.K. (2003). Regulation of intestinal NaPi-IIb cotransporter gene expression by estrogen. Am. J. Physiol. - Gastrointest. Liver Physiol. *285*, G1317–G1324.

Xu, J.-C., Lytle, C., Zhu, T.T., Payne, J.A., Benz, E., and Forbush, B. (1994). Molecular cloning and functional expression of the bumetanide-sensitive Na-K-Cl cotransporter. Proc. Natl. Acad. Sci. *91*, 2201–2205.

Xu, L., Dixit, M.P., Nullmeyer, K.D., Xu, H., Kiela, P.R., Lynch, R.M., and Ghishan, F.K. (2006). Regulation of Na+/H+ exchanger-NHE3 by angiotensin-II in OKP cells. Biochim. Biophys. Acta BBA - Biomembr. *1758*, 519–526.

Xue, H., Bukoski, R.D., McCarron, D.A., and Bennett, W.M. (1987). Induction of contraction in isolated rat aorta by cyclosporine. Transplantation *43*, 715–718.

Yanchar, N.L., Riegel, T.M., Martin, G., Fedorak, R.N., Kneteman, N., and Sigalet, D.L. (1996). Tacrolimus (FK506)-Its effects on intestinal glucose transporter. Transplantation *61*, 630–634.

Yang, C.-L., Angell, J., Mitchell, R., and Ellison, D.H. (2003). WNK kinases regulate thiazide-sensitive Na-Cl cotransport. J. Clin. Invest. *111*, 1039–1045.

Yang, C.-L., Zhu, X., Wang, Z., Subramanya, A.R., and Ellison, D.H. (2005).

Mechanisms of WNK1 and WNK4 interaction in the regulation of thiazide-sensitive NaCl cotransport. J. Clin. Invest. *115*, 1379–1387.

Yang, S.-S., Hsu, Y.-J., Chiga, M., Rai, T., Sasaki, S., Uchida, S., and Lin, S.-H. (2010a). Mechanisms for Hypercalciuria in Pseudohypoaldosteronism Type II-Causing WNK4 Knock-In Mice. Endocrinology *151*, 1829–1836.

Yang, S.-S., Lo, Y.-F., Wu, C.-C., Lin, S.-W., Yeh, C.-J., Chu, P., Sytwu, H.-K., Uchida, S., Sasaki, S., and Lin, S.-H. (2010b). SPAK-Knockout Mice Manifest Gitelman Syndrome and Impaired Vasoconstriction. J. Am. Soc. Nephrol. *21*, 1868–1877.

Yang, S.-S., Morimoto, T., Rai, T., Chiga, M., Sohara, E., Ohno, M., Uchida, K., Lin, S.-H., Moriguchi, T., Shibuya, H., et al. (2007). Molecular Pathogenesis of Pseudohypoaldosteronism Type II: Generation and Analysis of a Wnk4D561A/+ Knockin Mouse Model. Cell Metab. *5*, 331–344.

Yang, S.-S., Fang, Y.-W., Tseng, M.-H., Chu, P.-Y., Yu, I.-S., Wu, H.-C., Lin, S.-W., Chau, T., Uchida, S., Sasaki, S., et al. (2013). Phosphorylation Regulates NCC Stability and Transporter Activity In Vivo. J. Am. Soc. Nephrol. *24*, 1587–1597.

Yang, T., Santisteban, M.M., Rodriguez, V., Li, E., Ahmari, N., Carvajal, J.M., Zadeh, M., Gong, M., Qi, Y., Zubcevic, J., et al. (2015). Gut Dysbiosis Is Linked to Hypertension. Hypertension *65*, 1331–1340.

Yasuda, H., Kurokawa, T., Fujii, Y., Yamashita, A., and Ishibashi, S. (1990). Decreased D-glucose transport across renal brush-border membrane vesicles from streptozotocin-induced diabetic rats. Biochim. Biophys. Acta *1021*, 114–118.

Yasutake, H., Goda, T., and Takase, S. (1995). Dietary regulation of sucrase-isomaltase gene expression in rat jejunum. Biochim. Biophys. Acta *1243*, 270–276.

Yi, B., Titze, J., Rykova, M., Feuerecker, M., Vassilieva, G., Nichiporuk, I., Schelling, G., Morukov, B., and Choukèr, A. (2015). Effects of dietary salt levels on monocytic cells and immune responses in healthy human subjects: a longitudinal study. Transl. Res. *166*, 103–110.

Yoda, K., Imanishi, Y., Yoda, M., Mishima, T., Ichii, M., Yamada, S., Mori, K., Emoto, M., and Inaba, M. (2012). Impaired Response of FGF-23 to Oral Phosphate in Patients with Type 2 Diabetes: A Possible Mechanism of Atherosclerosis. J. Clin. Endocrinol. Metab. *97*, E2036–E2043.

Yoshikawa, T., Inoue, R., Matsumoto, M., Yajima, T., Ushida, K., and Iwanaga, T. (2011). Comparative expression of hexose transporters (SGLT1, GLUT1, GLUT2 and GLUT5) throughout the mouse gastrointestinal tract. Histochem. Cell Biol. *135*, 183–194.

Yoshitomi, K., Burckhardt, B.-C., and Frömter, E. (1985). Rheogenic sodium-bicarbonate cotransport in the peritubular cell membrane of rat renal proximal tubule. Pflüg. Arch. *405*, 360–366.

You, G., Lee, W.-S., Barros, E.J., Kanai, Y., Huo, T.-L., Khawaja, S., Wells, R.G., Nigam, S.K., and Hediger, M.A. (1995). Molecular Characteristics of Na+-coupled Glucose Transporters in Adult and Embryonic Rat Kidney. J. Biol. Chem. *270*, 29365–29371.

Yu, H.C.M., Burrell, L.M., Black, M.J., Wu, L.L., Dilley, R.J., Cooper, M.E., and Johnson, C.I. (1998). Salt Induces Myocardial and Renal Fibrosis in Normotensive and Hypertensive Rats. Circulation *98*, 2621–2628.

Yue, G., Edinger, R.S., Bao, H.-F., Johnson, J.P., and Eaton, D.C. (2000). The effect of rapamycin on single ENaC channel activity and phosphorylation in A6 cells. Am. J. Physiol.-Cell Physiol. *279*, C81–C88.

Zachariah, M.G., Thankappan, K., Alex, S.C., Sarma, P., and Vasan, R. (2003). Prevalence, correlates, awareness, treatment, and control of hypertension in a middle-aged urban population in Kerala. Indian Heart J. *55*, 245–251.

Zagórska, A., Pozo-Guisado, E., Boudeau, J., Vitari, A.C., Rafiqi, F.H., Thastrup, J., Deak, M., Campbell, D.G., Morrice, N.A., Prescott, A.R., et al. (2007). Regulation of activity and localization of the WNK1 protein kinase by hyperosmotic stress. J. Cell Biol. *176*, 89–100.

Zeniya, M., Sohara, E., Kita, S., Iwamoto, T., Susa, K., Mori, T., Oi, K., Chiga, M., Takahashi, D., Yang, S.-S., et al. (2013). Dietary Salt Intake Regulates WNK3-SPAK-NKCC1 Phosphorylation Cascade in Mouse Aorta Through Angiotensin II. Hypertension *62*, 872–878.

Zhang, W., and Victor, R.G. (2000a). Calcineurin Inhibitors Cause Renal Afferent Activation in Rats: A Novel Mechanism of Cyclosporine-Induced Hypertension. Am. J. Hypertens. *13*, 999–1004.

Zhang, J., Siew, K., Macartney, T., O'Shaughnessy, K.M., and Alessi, D.R. (2015). Critical role of the SPAK protein kinase CCT domain in controlling blood pressure. Hum. Mol. Genet. *24*, 4545–4558.

Zhang, W., Li, J.-L., Hosaka, M., Janz, R., Shelton, J.M., Albright, G.M., Richardson, J.A., Südhof, T.C., and Victor, R.G. (2000b). Cyclosporine A-induced hypertension involves synapsin in renal sensory nerve endings. Proc. Natl. Acad. Sci. U. S. A. *97*, 9765–9770.

Zhou, H., Yuen, P.S.T., Pisitkun, T., Gonzales, P.A., Yasuda, H., Dear, J.W., Gross, P., Knepper, M.A., and Star, R.A. (2006a). Collection, storage, preservation, and normalization of human urinary exosomes for biomarker discovery. Kidney Int. *69*, 1471–1476.

Zhou, H., Pisitkun, T., Aponte, A., Yuen, P.S.T., Hoffert, J.D., Yasuda, H., Hu, X., Chawla, L., Shen, R.-F., Knepper, M.A., et al. (2006b). Exosomal Fetuin-A identified by proteomics: A novel urinary biomarker for detecting acute kidney injury. Kidney Int. *70*, 1847–1857.

Zhou, H., Cheruvanky, A., Hu, X., Matsumoto, T., Hiramatsu, N., Cho, M.E., Berger, A., Leelahavanichkul, A., Doi, K., Chawla, L.S., et al. (2008). Urinary exosomal transcription factors, a new class of biomarkers for renal disease. Kidney Int. *74*, 613–621.

Zimmerhackl, L.B. (1993). Evaluation of nephrotoxicity with renal antigens in children: role of Tamm-Horsfall protein. Eur. J. Clin. Pharmacol. *44*, S39–S42.

Zurcher, R.M., Bock, H.A., and Thiel, G. (1996). Hyperuricaemia in cyclosporin-treated patients: a GFR-related effect. Nephrol. Dial. Transplant. *11*, 153–158.